

**University of Strathclyde  
Department of Bioengineering**

**Designing a comprehensive system for analysis of handwriting biomechanics  
in relation to neuromotor control of handwriting**

**by**

**Rutger C. Zietsma**

**A thesis presented in partial fulfilment of the requirements for the degree of  
Doctor of Philosophy from the Bioengineering Unit, University of Strathclyde,  
Glasgow, 2010**

This thesis is the result of the author's original research. It has been composed by the author and has not been previously submitted for examination which has led to the award of a degree.

The copyright of this thesis belongs to the author under the terms of the United Kingdom Copyright Acts as qualified by University of Strathclyde Regulation 3.50. Due acknowledgement must always be made of the use of any material contained in, or derived from, this thesis.

## **Acknowledgements**

My sincerest thanks go to Professor S. Nicol and Professor B.A.Conway for giving me the opportunity to undertake this research project in the Bioengineering Unit and for the effort that was put into the application for the faculty PhD studentship. I am grateful to the Faculty of Engineering for awarding the scholarship, which has enabled me to start the work.

I wish to thank my supervisor, Professor Conway, for his support and thoroughness. I would also like to thank Mr. J.MacLean for accurately manufacturing the electronics and mounting the strain gauge system and Mr. D.Robb and Mr. R.Hay for the manufacturing of the mechanical parts of the system that I developed. My thanks also go to Mr. D. Smith and Mr. S.Solomonidis for their help with the aluminium tensile testing.

I would also like to thank Mr. S. Solomonidis for his availability to discuss the biomechanical issues related to handwriting and motion control.

I am grateful to my family and friends for their general support and encouragement and especially to Anita for her advice on motion analysis and biomechanics and for telling me when it was time to take a break.

# Contents

1	Introduction .....	1
2	Background .....	2
2.1	Introduction .....	2
2.2	Handwriting and pen grip mechanics .....	3
2.2.1	Pen hand interaction .....	3
2.2.2	Grip force modulation .....	5
2.2.3	Pen grip measurement .....	13
2.3	Motor control in handwriting .....	17
2.3.1	Introduction .....	17
2.3.2	Neuromuscular and biophysical models .....	19
2.3.3	Learning and cognitive models .....	24
2.3.4	Neurological and biomechanics issues .....	27
2.4	Evaluation: writing tools .....	34
2.5	Conclusion: including biomechanics into handwriting research .....	34
2.6	Objectives .....	38
3	Transducer design .....	41
3.1	Introduction .....	41
3.2	Pen grip mechanics: a model .....	41
3.2.1	Description of the model .....	42
3.2.2	Conclusion for transducer development .....	46
3.3	Design procedure .....	47
3.4	Definition phase .....	47
3.4.1	Requirement specification .....	47
3.4.2	Function analysis .....	54
3.5	Conceptual phase .....	55
3.5.1	Prototype concept .....	55
3.5.2	Rejection of hypothetical concept considerations .....	57
3.6	Design phase .....	59
3.7	Calibration .....	64
3.7.1	Equipment .....	64
3.7.2	Procedure .....	64
3.7.3	Results .....	66
4	Methodology .....	70
4.1	Introduction .....	70
4.2	System overview .....	70
4.2.1	Test set up .....	70
4.2.2	Definition global frame of reference .....	73
4.3	Recording techniques .....	74
4.3.1	Introduction .....	74
4.3.2	Script recording .....	74
4.3.3	Pen grip force measurement .....	76
4.3.4	Motion capture with Vicon .....	77
4.3.4.1	Recording of handwriting motion: introduction and overview .....	77
4.3.4.2	Vicon system .....	78
4.3.4.3	System calibration .....	79
4.3.4.4	Bone embedded anatomical axis frames .....	80
4.3.4.5	Marker set and anatomical point calibration .....	85
4.3.4.5.1	Trunk marker set .....	85
4.3.4.5.2	Upper- and forearm segment marker set .....	87
4.3.4.5.3	Hand and pen marker set .....	89

4.3.4.6	Vicon camera setup .....	91
4.3.5	Synchronisation of script, grip force and Vicon data.....	92
4.4	Data analysis techniques .....	95
4.4.1	Development programs for script, grip force and joint motion analysis. ....	95
4.4.2	Power Spectral Density .....	98
4.4.3	Root Mean Square measures .....	98
4.4.4	Linear regression .....	99
4.4.4.1	Statistics for linear regression .....	99
4.4.4.2	Linear regression and normalisation .....	103
5	Subject testing: Line drawing .....	107
5.1	Subjects .....	107
5.2	Activities .....	108
5.3	Data collection and processing .....	109
5.4	Results .....	109
5.4.1	Line curvature and time duration. ....	110
5.4.2	Comprehensive description of line drawing features subjects 1 and 2.....	112
5.4.2.1	Pen Tip X,Y-,Z-coordinates at 50% cycle length subject 1 and 2.....	114
5.4.2.2	Subject 1: description of line drawing mechanics .....	124
5.4.2.3	Subject 2: description of line drawing mechanics .....	149
5.4.3	Comparing line drawing features for subjects 1 and 2.....	169
5.4.4	Further discussion on coordination of line drawing.....	172
6	Subject testing: Writing activity .....	175
6.1	Subjects .....	175
6.2	Activities .....	175
6.3	Data collection and processing .....	177
6.4	Results: Comparison pen grip for writing the whole sentence.....	178
6.4.1	Introduction .....	178
6.4.2	Description of pen grip features for subject 1 .....	179
6.4.3	Comparison of pen grip for all 4 subjects.....	184
6.5	Results: Variations in measures of repeated word writing.....	199
6.5.1	Introduction .....	199
6.5.2	Subject 1: Writing 'great' twice in 4 tablet positions .....	200
6.5.2.1	Subject 1: Comparing writing features of '1st great' in 4 positions. ....	200
6.5.2.2	Comparing writing features for 1st and 2nd 'great' for subject 1.....	204
6.5.3	Subject 2: Writing 'great' twice in 4 tablet positions .....	207
6.5.3.1	Comparing writing features of 1st 'great' in 4 positions .....	207
6.5.3.2	Comparing writing features for 1st and 2nd 'great' for subject 2.....	211
6.5.4	Subject 5: Writing 'great' twice in 4 tablet positions .....	215
6.5.4.1	Comparing writing features of 4 positions for subject 5 .....	215
6.5.4.2	Comparing writing features for 1st and 2nd 'great' for subject 5.....	222
6.5.5	Comparison subjects 1, 2 and 5 and conclusion. ....	226
7	Spiral Drawing .....	228
7.1	Background .....	228
7.2	Activities .....	231
7.3	Data collection and processing .....	233
7.4	Subjects .....	236
7.5	Results .....	236
7.5.1	Spiral drawing by subject 1 .....	237
7.5.2	Spiral drawing by subject 2 .....	254
7.5.3	Discussion: spiral drawing by subjects 1 and 2 .....	264
7.5.4	Conclusion .....	266
8	Handwriting and signature verification .....	268
8.1	Introduction .....	268
8.2	Subjects .....	268

8.3	Part I - Script comparison: methods for data analysis .....	269
8.3.1	Activity: comparing x,y- and z-coordinates .....	269
8.3.2	Data analysis: comparing x,y- and z-coordinates .....	270
8.3.2.1	Comparison of signatures produced by one subject.....	271
8.3.2.2	Comparison of counterfeited to original signatures .....	280
8.4	Part II - Grip force comparison: methods for data analysis.....	285
8.4.1	Activity: comparing grip force.....	285
8.4.2	Data analysis: comparing grip force signals .....	285
8.4.2.1	Pen grip characteristics: comparing signatures by one subject.....	285
8.4.2.2	Summary: need for data analysis for grip force assessment.....	293
8.4.2.3	Development data analysis techniques for comparing grip patterns ...	294
8.4.2.4	Comparison of authentic and counterfeited signatures .....	300
8.5	Conclusion .....	302
9	Conclusion and discussion .....	304
9.1	System limitations and recommendations .....	304
9.1.1	System evaluation.....	305
9.1.2	Recommendations for further system development .....	309
9.2	Research outcomes .....	314
9.2.1	Proximal and distal muscle control: Fingers enables vertical (y-)motion.....	314
9.2.2	Control of wrist rotation during horizontal line drawing .....	315
9.2.3	Anticipatory grip actions .....	316
9.2.4	Redundancy and flexibility of continuous neuromuscular control.....	317
9.2.5	Pen grip and signature verification.....	317
9.3	Recommendations for further research .....	318
9.3.1	Line drawing - Chapter 5.....	318
9.3.2	Writing activity - Chapter 6 .....	321
9.3.3	Spiral drawing - Chapter 7 .....	323
9.3.4	Handwriting and signature verification Chapter 8 .....	324
	Bibliography .....	226
	Appendix 1 Pen design .....	345
	Appendix 1A Lower pen part.....	345
	Appendix 1B Upper pen part.....	346
	Appendix 2 Properties HE30.....	347
	Appendix 2A Properties HE30: Specification sheet.....	347
	Appendix 2B Properties HE30: Tensile test.....	348
	Appendix 3 Transducer beam dimensioning .....	351
	Appendix 4 MC Sili-E0.15 wire specifications.....	352

## Figures

Fig.2.1: Tripod pen grip. ....	5
Fig.3.1: Free body diagram of pen grip during handwriting: .....	45
Fig.3.1: Tripod pen grip: See text for details.....	50
Fig.3.2: Schematic representation of transducer sub-functions.....	54
Fig. 3.3: Full Wheatstone's bridge arrangement for each cantilever beam.....	56
Fig 3.4: Model grip force transducer pen core.....	59
Fig 3.5: Model grip force measuring ring-beam construction.....	60
Fig 3.6a: Grip force digitising pen prototype 1 and 2; Fig 3.6b: Grip force digitising pen prototype 3....	62
Fig.3.7: Calibration set up.....	65
Fig. 3.7: Calibration results for beam 1.....	67
Fig. 3.8: Calibration results for beam 2.....	68
Fig. 3.9: Calibration results for beam 3.....	69
Fig. 4.1.: System components.....	71
Fig. 4.2.: Global axis system of the test setup.....	73
Fig. 4.3: Grip force digitiser pen, strain gauge amplifier and CED1401 ADC.....	77
Fig. 4.4.: Vicon camera setup for handwriting motion capture.....	78
Fig.4.5: Trunk anatomical axis frame: .....	81
Fig.4.6: Right arm anatomical axis frame in anterior view: .....	82
Fig.4.7: Right hand anatomical axis frame in posterior view: .....	83
Fig.4.8: Right index finger proximal phalange anatomical axis frame in sagittal view: .....	84
Fig.4.9: Marker set.....	86
Fig.4.10. Technical axis frame of the upper arm .....	88
Fig. 4.11: Pen markers.....	90
Fig.4.12: Vicon motion capture result: anatomical points that are captured or calculated.....	91
Fig. 4.13: Arrangement of 8 CCD cameras for Vicon motion capture for handwriting.....	92
Fig.4.14: Synchronisation Spike2, Vicon and ScriptAlyzer.....	93
Fig.4.15: Phase difference between Vicon and ScriptAlyzer pen tip coordinates.....	94
Fig. 4.16: x,y-Coordinates of spiral drawing activity: sampling numbers showing time dimension.....	97
Fig. 4.17: Drawing of a straight line from coordinates (0,0) to (0,100).....	102
Fig. 4.19: Line drawing for target 12 o'clock by subject 1: y-coordinates.....	105
Fig. 4.20: Line drawing for target 12 o'clock by subject 1: x,y-coordinates.....	105
Fig. 4.21: linear regression of line drawing for target 12 o'clock by subject 1.....	106
Fig. 4.22: linear regression of line drawing for target 12 o'clock by subject 1 after normalisation.....	106
Fig 5.1: Line drawing activity: start and end targets for each set of lines to be drawn.....	108
Fig 5.2: Duration of line drawing tasks (5 cycles) for different target directions for all four subjects....	110
a: x,y-coordinates subject 1.....	111
b: x,y-coordinates subject 2.....	111
c: x,y-coordinates subject 3.....	111
Fig.5.4: Defining the latitude.....	113
Fig.5.5: Line length of 50% cycle (out of 5 cycles) for subject 1: mean and standard deviation.....	115
Fig.5.6: Latitude perpendicular to ideal straight line (50% cycle out of 5 cycles) for subject 1.....	115
Fig.5.7: Line length of 50% cycle (out of 5 cycles) for subject 2: mean and standard deviation.....	116
Fig.5.8: Latitude perpendicular to ideal straight line (50% cycle out of 5 cycles) for subject 2.....	116
Fig.5.9: The latitude is defined as the maximum deviation from the line towards the target .....	120
Fig.5.10: x,y- and z-coordinates for target direction 9 o'clock by subject 1 .....	123

Fig.5.11: Recording for 12 o'clock target by subject 1.....	129
a: Finger forces for target direction 12 o'clock for subject 1.....	129
b: y-coordinates for target direction 12 o'clock for subject 1.....	129
c: Resultant grip force vector for target direction 12 o'clock for subject 1.....	129
Fig.5.12: Recording for the 4th cycle of the 12 o'clock target by subject 1.....	130
a: Finger forces for target direction 12 o'clock for subject 1.....	130
b: y-coordinates for target direction 12 o'clock for subject 1.....	130
c: Resultant grip force vector for target direction 12 o'clock for subject 1.....	130
Fig.5.13: Recorded trajectories for 12 o'clock target by subject 1.....	131
Fig.5.14: Recorded pen tip and wrist joint trajectories in 3 dimensions: linear motion.....	131
Fig.5.15 Recorded elbow joint trajectories in 3 dimensions: linear motion.....	132
Fig.5.16: Recorded shoulder joint trajectories in 3 dimensions. Rotational motion is seen.....	132
Fig.5.17: Recorded trajectories in 3 dimensions for 12 o'clock target by subject 1.....	133
Fig.5.18: Recorded trajectories in 3 dimensions (connection lines): 12 o'clock target by subject 1.....	133
Fig.5.19: Right arm anatomical axis frame in anterior view (copy Fig.4.6):.....	134
Z-axis: The common line perpendicular to the Xf- and Yf-axis, pointing to the left.....	134
Fig.5.20: Recording for 3 o'clock target by subject 1.....	137
a: Finger forces for target direction 3 o'clock for subject 1.....	137
b: y-coordinates for target direction 3 o'clock for subject 1.....	137
c: Resultant grip force vector for target direction 3 o'clock for subject 1.....	137
d: Resultant grip force vector for target direction 3 o'clock for subject 1.....	137
Fig.5.21: Recording for 3 o'clock target by subject 1:Trajectories for target direction 3.....	138
Fig.5.22: Recording for 3 o'clock target by subject 1:Trajectories for target direction 3.....	138
Fig.4.23: Right arm anatomical axis frame in anterior view (copy Fig.4.6):.....	139
Z-axis: The common line perpendicular to the Xf- and Yf-axis, pointing to the left.....	139
Fig.5.24: Recording for 6 o'clock target by subject 1.....	142
a: Finger forces for target direction 6 o'clock for subject 1.....	142
b: y-coordinates for target direction 6 o'clock for subject 1.....	142
c: Resultant grip force vector for target direction 6 o'clock for subject 1.....	142
Fig.5.25: Recording of pen tip limb and joint trajectories for 6 o'clock target by subject 1.....	143
Fig.5.26: Recording of pen tip and limb and joint trajectories for 6 o'clock target by subject 1.....	144
Fig.5.27: Recording for 9 o'clock target by subject 1.....	146
a: Finger forces for target direction 9 o'clock for subject 1.....	146
b: y-coordinates for target direction 9 o'clock for subject 1.....	146
c: Resultant grip force vector for target direction 9 o'clock for subject 1.....	146
Fig.5.28: Recording for 9 o'clock target by subject 1:Trajectories for target direction 9.....	147
Fig.5.29: Recording of pen tip and limb joint trajectories for 9 o'clock target by subject 1.....	148
Fig.5.30: Recording for 12 o'clock target by subject 2.....	151
a: Finger forces for target direction 12 o'clock for subject 2.....	151
b: y-coordinates for target direction 12 o'clock for subject 2.....	151
c: Resultant grip force vector for target direction 12 o'clock for subject 2.....	151
Fig.5.31: Recording for 12 o'clock target by subject 2: Trajectories.....	152
Fig.5.32: Recording for 12 o'clock target by subject 2: Trajectories.....	153
Fig.5.33: Recording for 3 o'clock target by subject 2.....	156
Fig.5.34: Recording for 3 o'clock target by subject 2: Trajectories.....	157
Fig.5.35: Recording for 3 o'clock target by subject 2: Trajectories.....	158
Fig.5.36: Recording for 6 o'clock target by subject 2.....	160
a: Finger forces for target direction 6 o'clock for subject 2.....	160
b: y-coordinates for target direction 6 o'clock for subject 2.....	160
c: Resultant grip force vector for target direction 6 o'clock for subject 2.....	160
Fig.5.37: Recording for 6 o'clock target by subject 2: Trajectories.....	162
Fig.5.38: Recording for 6 o'clock target by subject 2: Trajectories.....	162
Fig.5.39: Recording for 9 o'clock target by subject 2.....	165

Fig.5.40: Recording for 9 o'clock target by subject 2: Trajectories. ....	166
Fig.5.41: Recording for 9 o'clock target by subject 2: Trajectories. ....	167
Fig 6.1: Writing task in four quadrants: "She sells great sea shells by the great sea shore." .....	176
Fig.6.2: Sum of force values for subject 1. ....	182
Fig. 6.3: Root Mean Square (RMS) values (4 writing positions for each of 4 trials). ....	183
Fig.6.4: Total and maximum band power within the 0-10Hz band (4 writing positions for 4 trials). ....	184
Fig.6.5: Sum of force values during the whole trial (4 writing positions for 4 trials) for subject 1. ....	188
Fig. 6.6: Root Mean Square (RMS) values (4 writing positions for each of 4 trials) for subject 2. ....	189
Fig. 6.7: Total and maximum power spectral density (4 writing positions for 4 trials) for subject 2. ....	190
Fig.6.8: Sum of force values during the whole trial (4 writing positions for 4 repetitions): subject 3. ....	192
Fig. 6.9: Root Mean Square (RMS) values (4 writing positions for each of 4 trials) for subject 3. ....	193
Fig. 6.10: Total and maximum power spectral density (4 writing positions for 4 trials) for subject 3. ....	194
Fig.6.11: Sum of force values during the whole trial (4 writing positions for 4 repetitions): subject 4. ....	196
Fig. 6.12: Root Mean Square (RMS) values (4 writing positions for each of 4 trials) for subject 4. ....	197
Fig. 6.13: Total and maximum power spectral density (4 writing positions for 4 trials) for subject 4. ....	198
Fig.6.14: Script of writing the 1st 'great' in the four tablet positions .....	200
Fig.6.15: Trajectories while writing the 1st 'great' in the four tablet positions .....	201
Fig. 6.16: Thumb, Middle and Index finger forces while writing 1st 'great' in four tablet positions .....	202
Fig. 6.17: Resultant pen grip forces while writing the 1st 'great' in the four tablet positions .....	203
Fig.6.18: Script of writing the 1st 'great' in the four tablet positions .....	205
Fig.6.19: Script of writing the 2nd 'great' in the four tablet positions .....	205
Fig.6.20: Trajectories while writing the 1st 'great' in the four tablet positions. ....	206
Fig.6.21: Trajectories while writing the 2nd 'great' in the four tablet positions .....	206
Fig.6.22: Script of writing the 1st 'great' in the four tablet positions .....	207
Fig.6.23: Trajectories while writing the 1st 'great' in the four tablet positions .....	208
Fig. 6.24: Thumb, Middle and Index finger forces while writing 1st 'great' in four tablet positions .....	209
Fig. 6.25: Resultant pen grip forces while writing the 1st 'great' in the four tablet positions: .....	210
Fig.6.26: Script of writing the 1st 'great' in the four tablet positions .....	211
Fig.6.27: Script of writing the 2nd 'great' in the four tablet positions .....	211
Fig. 6.28: Resultant pen grip forces while writing the 1st 'great' in the four tablet positions .....	213
Fig. 6.29: Resultant pen grip forces while writing the 2nd 'great' in the four tablet positions .....	213
Fig.6.30: Trajectories while writing 1st 'great' in four tablet positions .....	214
Fig.6.31: Trajectories while writing 1st 'great' in four tablet positions .....	214
Fig.6.32: Script of writing the 1st 'great' in the four tablet positions .....	215
Fig.6.33: Trajectories while writing the 1st 'great' in four tablet positions: .....	216
Fig. 6.34: Thumb, Middle and Index finger forces while writing 1st 'great' in four tablet positions .....	218
Fig. 6.35: Resultant pen grip forces while writing 1st 'great' in four tablet positions .....	219
Fig.6.36: Tablet position I: a.: Finger forces and b.: y-coordinates .....	220
Fig.6.37: Tablet position II: a.: Finger forces and b.: y-coordinates .....	221
Fig.6.38: Script of writing the 1st 'great' in the four tablet positions by subject 5 .....	222
Fig.6.39: Script of writing the 2nd 'great' in the four tablet positions by subject 5 .....	222
Fig. 6.40: Resultant pen grip forces while writing 1st 'great' in four tablet positions by subject 5 .....	224
Fig. 6.41: Resultant pen grip forces while writing 2nd 'great' in four tablet positions by subject 5 .....	224
Fig.6.42: Trajectories while writing 1st 'great' in four tablet positions by subject 5 .....	225
Fig.6.43: Trajectories while writing 2nd 'great' in four tablet positions by subject 5 .....	225
Fig 7.1: spiral drawing activity: drawing clockwise from inside to outside .....	232
Fig 7.2: circle drawing activity: drawing cycles clockwise with outer diameter d=120mm. ....	232
Fig 7.3.: Power Spectral Density without (a) and with DC-removal (b) for grip force during spiral. ....	235
Fig.7.4: Spiral drawing result: x,y-coordinates by subject 1 .....	238
Fig.7.5: Spiral drawing kinematics: x-coordinates by subject 1. ....	239
Fig.7.6: Spiral drawing kinematics: y-coordinates by subject 1. ....	240

Fig.7.7: Pen tip and joint trajectories in the x- and y-frame for subject 1.....	240
Fig.7.8: Pen tip and joint trajectories in three dimensions for subject 1.....	241
Fig.7.9: Radius of angular motion of the pen tip for subject 1. ....	241
Fig.7.10: Radius of angular motion of the wrist joint for subject 1. ....	242
Fig.7.11: Radius of angular motion of the elbow joint for subject 1. ....	242
Fig.7.12: Radius of angular motion of the shoulder joint for subject 1.....	243
Fig.7.13: Pen tip x- and y-coordinates for subject 1. ....	245
Fig.7.14: Thumb, Middle and Index finger pen grip force for subject 1.....	245
Fig.7.15: Pen grip force: Thumb, Middle and Index finger force for subject 1. ....	245
Fig.7.16: Pen tip force (in z-direction) for subject 1. ....	246
Fig.7.17: Power spectral Density for Thumb, Index, Middle finger for spiral drawing by subject 1. ....	250
Fig.7.18: x,y-coordinates for circle drawing (10 turns with d=12mm) by subject 1. ....	251
Fig.7.19: Power Spectral density (dB/Hz) for pen grip force during circle drawing (10 turns):.....	252
Fig.7.20: Spiral drawing result: x,y-coordinates by subject 2.....	255
Fig.7.21: Spiral drawing kinematics: x-coordinates by subject 2. ....	256
Fig.7.22: Spiral drawing kinematics: y-coordinates by subject 2. ....	256
Fig.7.23: Pen tip and joint trajectories for subject 2.....	257
Fig.7.24: Pen tip and joint trajectories in three dimensions for subject 2.....	257
Fig.7.25: Radius of angular motion of the pen tip for subject 2. ....	258
Fig.7.26: Radius of angular motion of the wrist joint for subject 2. ....	258
Fig.7.27: Radius of angular motion of the elbow joint for subject 2. ....	258
Fig.7.28: Radius of angular motion of the shoulder joint for subject 2. ....	259
Fig.7.29: Pen tip x- and y-coordinates for spiral drawing by subject 2.....	261
Fig.7.30: Pen tip finger forces for spiral drawing by subject 2. ....	261
Fig.7.31: Resultant pen grip force for spiral drawing by subject 2. ....	261
Fig.7.32: Power spectral Density for Thumb, Index, Middle finger for spiral drawing by subject 2. ....	263
Fig.8.1: x-and y-coordinates of signature by subject 1: tablet orientation 0 ° (a.) 90 °.....	270
Fig.8.2: x-and y-coordinates of signature: recorded (a.) after rotation and translation (b.). ....	271
Fig.8.3a: Rotation and translation of signatures written with incline angle of 0 - 40° by subject .....	273
Fig.8.3b: Rotation and translation of signatures written with incline angle of 50 - 90° by subject 1. ....	274
Fig.8.4a: Rotation and translation of signatures written with incline angle of 10 -40° by subject 2. ....	275
Fig.8.4b: Rotation and translation of signatures written with incline angle of 50 -90° by subject 2. ....	276
Fig.8.5a: Rotation and translation of signatures written with incline angle of 10 -40° by subject 4. ....	277
Fig.8.5b: Rotation and translation of signatures written with incline angle of 50 -90° by subject 4. ....	278
Fig.8.6: x,y-Coordinates: .....	280
Fig.8.7: Pen tip velocity profiles:.....	282
Fig.8.8: Pen tip velocity profiles for subject 1's signature and attempt to counterfeit by subject 4 .....	284
Fig.8.9a: Pen grip forces for signatures by subject 4: trials 1 to 6. ....	287
Fig.8.9b: Pen grip forces for signatures by subject 4: trials 7 to 12. ....	288
Fig. 8.10: Thumb, Index and Middle finger force during trials 6 and 7 of signature by subject 1. ....	292
Fig. 8.11: Thumb, Index and Middle finger force during trials 7 and 9 of signature by subject 4. ....	293
Fig. 8.12: Thumb, Index and Middle finger force during trials 3 and 11 of signature by subject 3. ....	295
Fig. 8.13: Thumb force patterns during trial 1 and trial 2 of signature writing by subject 4. ....	297
Fig. 8.14: Pen tip velocity during two signature writing trials by subject 1 .....	299
Fig. 8.15: Thumb force patterns during two trials of signature writing .....	301

*To Ed&Roelie*

## Abstract

A comprehensive system for investigation of biomechanical and neuromuscular processes involved with producing handwriting and drawing was developed. The system included a pen-like grip measuring device that enabled the variations of finger grip force associated with writing and drawing to be measured while holding the pen in tripod grip. The pen was integrated with a digitiser tablet for recording x,y-coordinates and pressure of the nib and a motion analysis system for recording the limb and hand kinematics.

It was observed that for line drawing in the y-direction of the tablet, finger forces were directly related to pen tip movement and finger forces were modulated in a repeatable and predictable fashion, while this was not the case for line drawing in the x-direction. This was evidence for longstanding assumptions. Wrist rotation was required for production of lines in the x-direction without excessive deviation.

For writing tasks, it was observed that no two tasks performed by one subject share an identical writing process, not even when the writing results are (nearly) identical. The neuromuscular control apparatus is highly flexible and works in a coordinated fashion that allows production of nearly equal end-results by means of different mechanical and therefore neuromuscular processes.

For spiral drawing, tremor that originates from the fingers, hand and arm was quantified with the transducer pen. Limb joint kinematics were displayed in three dimensions with colour coding of coordinate sample numbers. This method can reveal the origin of some forms of limb tremor.

Pen grip force patterns during signature writing were found to be characteristic for subjects, which relate to their individual pen-hand interaction, resulting from fine control of distal joints. Variation between trials of the same subject was observed, revealing adaptations of the computational processes during writing. The potential for signature verification by means of finger force recording was explored.

# 1 Introduction

Handwriting is firstly a communication tool that all people are expected to be able to master. Importantly, handwriting and the production of a signature remains a necessary consent for official and personal documents.

Handwriting is an example of a learned motor skill that is of considerable functional importance and which is an activity that depends on the integrity of both the nervous system and biomechanical plant formed by the arm and the hand. Deficits in brain function or in the musculoskeletal system due to disease or trauma will cause deterioration in handwriting ability. Accordingly, the study of biomechanics of handwriting is of interest to scientists and clinicians interested in motor learning and the effects of ageing or disease on motor skills. In addition, the study of handwriting finds important applications for biometric purposes, such as signature verification and forensic research.

At present, little is known about the pen-hand interaction and pen grip force control during writing tasks. Consequently, control of pen grip force has not been included in theories on handwriting as yet.

The aim of this project was to develop a comprehensive system for the investigation of the biomechanical and neuromuscular processes involved in producing handwriting or drawing. This includes study of forces applied by the fingers to the pen. To achieve this, a pen-like grip measuring device was developed that enables the variations of finger grip force associated with writing and drawing tasks to be measured while holding the pen in tripod grip. This measurement system was integrated with a script digitiser and motion analysis system.

The background, problem definition and objectives are expounded in chapter 2, with the transducer design being reviewed in chapter 3. Chapter 4 describes the integration of various methodologies associated with motion analysis, script digitising and synchronisation with the grip force transducer pen.

The potential of the system was assessed in a four different pilot experiments, exploring different forms of writing and drawing tasks. The results of these experiments are presented in chapters 5 to 8. Chapter 9 finally gives the conclusion and recommendations of this study.

## **2 Background**

### **2.1 Introduction**

Handwriting is a learned motor skill that is of considerable functional importance as a communication tool. The study of handwriting and drawing has been known as graphonomics since the early 1980s. This multi-disciplinary science aims to uncover the relationship between the planning and generation of drawing and handwriting movements with the neural processes that control and regulate this type of motor activity. By improved understanding of the handwriting process many technologies associated with script recognition could become established.

Scientists involved in graphonomics recognised in 1982 that their science would have both scientific and practical benefits (Meulenbroek et al, 1998). As a practical benefit, graphonomic research was expected to speed up automatic processing, interpretation and recognition of both static script and digitally recorded pen-tip displacements. Analysis of static script could be used in biometrics, such as forensic research and for signature-verification purposes. Pen-tip recordings would find their application as user-friendly reliable interfaces in computers as is the case with digitising tablets and palm top devices. Research benefits of graphonomics would provide information about specifics of various motor control processes (Meulenbroek, 2003). Furthermore, practical and scientific applications of graphonomics are now to be realised for diagnosis and rehabilitation purposes. An example is computer-assisted training, where the subject receives feedback of a specific movement characteristic.

During the last ten years a variety of input/output devices have become available for handwriting and drawing assessment (e.g. Wacom and Calcomp digitisers). These devices are used with a PC and allow digitising of the positions of the tip of a stylus and graphical display, which can be quantified using software for handwriting assessment (e.g. ScriptAlyzer). These devices allow accurate recording and automatic processing of movement patterns.

The following sections deal with the specific details of studying motor control of handwriting and the biomechanical aspects of pen-hand interaction. Firstly, the mechanics of pen grip and pen motion and control of grip are described in 2.2. Paragraph 2.3 continues with an overview of theories on motor control for general

tasks involving the limb and hand coordination (e.g., point to point movements) and specifically handwriting, including neuromuscular and biophysical models, learning and cognitive models and issues of neurology and biomechanics that limit handwriting ability. A section on writing tools follows in 2.4. Section 2.5 summarises the outcomes of the literature review and gives conclusions that lead to the objectives of the research that are given in 2.6.

## **2.2 Handwriting and pen grip mechanics**

Pen hand grip mechanics and control will be discussed in three sections. The mechanical interaction between pen and hand will be described in 2.2.1. Control strategies for finger tip actions in multi-digit grip tasks during a variety of loading conditions other than handwriting are summarised in 2.2.2. Section 2.2.3 evaluates four systems for measuring grip force during handwriting activities.

### **2.2.1 Pen hand interaction**

The most common pen grip is the so called tripod grip (Fig.2.1). The pen is held with thumb in opposition to index and middle finger in such a way to make contacts with the hand at four sites. Namely, with a proximal portion of the hand (between metacarpophalangeal MCP joints of the thumb and the index finger or at the proximal phalange of the index finger), with the tips of the thumb, the index finger and the lateral surface of the distal phalanx of the middle finger (Latash et al, 2003). During handwriting the fingers modulate the grip force applied to the pen. The force experienced by the pen at each of the usual four contact areas, can be distinguished as an axial (shear) force component in the longitudinal pen direction and a force normal the surface of contact. The free body diagram, showing the active forces acting on the pen, is described in section 3.2 and shown in Fig.3.1 of the next chapter.

These days children are taught at school to write while holding the pen in tripod grip and often triangular shaped pens are used to aid stability. From a pilot study (Zietsma, 2003), it was concluded that subjects show a variety in the exact positioning of the fingers in tripod grip and that positioning can be manipulated by use of different pen shapes and sizes. The use of a triangular pen model is seen to

decrease the variation in the exact positioning (Zietsma, 2003). A study on how the type of pencil grip affects (four-finger pencil grips, the triple and quad grips) the speed and legibility of fourth-grade high school student's handwriting concluded that all grips to be equally functional (Koziatek and Powell, 2003). This highlights that the production of good script is highly adaptive and can be independent of the pen design.

The basic features of the mechanics of pen motion were described by Latash et al (2003). During tripod grip, at each of the four contact sites that were described above, normally a three dimensional vector  $F$  is applied to the pen. As the contact sites are soft, no point contacts exist, but the forces are distributed over a contact area. According to Latash et al (2003), the non-point contact induces a moment  $M$  with respect to a nominal point of contact and this moment vector is normal to the surface of contact if the pen does not stick to the skin. However, the author of this thesis does not agree with Latash et al (2003) on this point. A moment vector can only develop if the pen is fixed to the skin. Valero-Cuevas et al (1997) describes this principal rightly for the contact force produced by the distal phalange of the index finger to a surface. According to Valero-Cuevas et al (1997), in the sagittal plane, the distal phalanx of the finger can exert both a force and a couple on the environment. However, to exert a couple, two equal and opposite forces should act in opposite direction; hence, two contacting surfaces should adhere to each other (Valero-Cuevas et al, 1997).

Normally, when lifting an object using two or three finger grip, the force distribution by the fingers is controlled and creates force equilibrium to ensure a stable grip. Following, the laws of mechanics, one of these forces could be transferred if a moment was induced and only then the equilibrium would only be maintained. However, as the fingers do not stick to the object, such a moment cannot exist. It can be concluded that during gripping of an object, it is required to balance the grip force to maintain a stable grip and moments cannot be exerted. One could test this by lifting an object (e.g a coin using two finger grip between thumb and index finger) and try to move the position of one of the two fingers without losing balance. As soon as one finger slides along the object, the balance is lost as no moment is induced and the object will drop.

It is assumed that the basic grip of the pen does not change in the process of handwriting, i.e. the positions of the three digits are fixed, while the site of the more proximal contact can change because of the sliding motion of the pen.



*Fig.2.1: Tripod pen grip.*

Any set of forces and moments acting on a rigid body in three dimensions can be uniquely represented by a wrench, i.e. a combination of a force vector and a moment vector both acting on the object along the same or parallel axis (Zatsiorsky, 2002). Each of the four contact sites acting on a pen (fingertips and proximal contact site) produces a wrench acting on the object along a certain axis. Four individual wrenches always form a redundant system set since they cannot act along four orthogonal directions. That implies that a force/moment generated at one site can be counterbalanced by another force/moment along the same wrench axis. It can be concluded that producing an adequate grip of the pen in the process of handwriting is a typical example of controlling a redundant system, when analyzed at the level of the production of forces and moment at each contact site.

### 2.2.2 Grip force modulation

Writing requires small movement of the pen nib that are organised in time and position on a page. Currently, there is very limited research on how grip force modulation during hand writing tasks contributes to the writing process. The existing literature on grip force is predominantly related to object lifting and placing. All grip actions are based on predictions of the consequences of self-generated actions. When humans lift and place objects, predictive feed forward neural control mechanisms are essential and are considered to depend on internal presentation of

object properties. One reason for this is the neuromechanical delays that exist and curtail the usefulness of closed-loop feedback control (Hogan et al, 1987; Johansson and Cole, 1994; Johansson, 1998).

Predictive feed forward control mechanisms are therefore required during both proactive tasks (self induced) and reactive tasks (in response to a change in load or object orientation).

Examples of predictions will first of all be discussed below for specifically *reactive* tasks during manipulation involving restraint of *active* objects, which exert unpredictable changes in loading forces. In the next section, predictions for proactive or self-induced tasks will be mentioned. It is expected that during normal handwriting both self induced and reactive actions (e.g. in response to inertia effects during pen acceleration) are present, for which predictive control mechanisms are required and in the concluding section of this paragraph reference will be made to pen grip modulation.

Control of finger tip actions in two-digit grip tasks have been investigated during a variety of loading conditions, including lifting and moving hand-held objects under viscous, inertial and elastic loads (Flanagan and Wing 1993, 1997a,b; Johansson and Westling 1984a, 1988a, b; others as mentioned see below). The findings suggest that subjects attempt to minimise fingertip forces, while at the same time ensuring that the grasp stability is preserved during lifting and transport of an object. In two finger manipulatory tasks with different friction at two contacting sites, subjects attempt to distribute the load between digits in a manner that decreases the normal force required to maintain grasp stability (Burstedt et al, 1997a, b, Edin et al, 1992).

Control of finger tip actions in multi-digit tasks in which subjects lifted an object using unimanual and bimanual grasps, engaging the tips of the thumb and two fingers was examined by Flanagan et al in 1999. From these experiments it was seen that principles for control of forces demonstrated for two-digit grasping also apply for various three digit grasps. These principles agree with the construct that fingertip grip force is minimised without compromising grasp stability.

Grip force is modulated in phase with fluctuations in load force in both precision grip (Flanagan et al, 1993; Augurelle et al, 2002) and other grips including one- and two-handed grips and inverted grips (Flanagan and Tresilian, 1994). The tight temporal coupling between grip and load force was seen in fluctuations in load force induced

by both arm movement and during whole-body jumping while the arm's joint angles were fixed. The results reflect a general control strategy, which is not specific to any particular grip or mode of transport. Blakemore et al (1998) demonstrated that only when load force is generated by the hand holding the object, grip force is modulated in parallel with load force. The fact that the subject generates the load, in itself is not sufficient to produce precise predictive grip force modulation and delays in adapting grip force will occur without receiving feedback from cutaneous afferents from the load generating hand.

Importantly, feedback from cutaneous afferents are also required for setting and maintaining the background level of the grip force in addition to their phasic slip-detection function and their role in adapting the grip force/load force ratio to the friction on initial contact with an object. Grip force is modulated using sensory information related to the loading forces of active objects: an increased safety margin against slip is presented when tangential load is expected to increase (Johansson and Westling, 1988b; Johansson et al, 1992a,b; Cole and Johansson, 1993; Winstein et al 1999). Automatic normal force responses are also triggered by cutaneous receptors in the fingertips (Johansson et al., 1992b,c; Macefield et al, 1996) as a mechanism to predict future behaviour of active objects by scaling the responses by early cues about the rate of the load force changes (Cole and Abbs, 1988; Johansson et al, 1992b and friction (Cole and Johansson, 1993, Birznieks et al, 1998). It is believed that cutaneous afferents play a role in correcting and maintaining an internal model of the physical properties of hand-held objects (Augurelle et al, 2002). The predicted physical properties of objects control fingertip forces during manipulative tasks. Specifically, the automatic reactive responses reflect predictions at the level of individual digits as to the mechanical linkage of items contacted by the fingertips in manipulations (Ohki et al, 2002).

When holding an object, potentially destabilising loads include time-varying linear forces and also torque loads tangential to the grip surfaces. Torque loads develop in manipulation of objects whose centre of mass does not lie on the grip axis.

In precision grip, the grip axis is the axis between the centres of the grip surfaces of the thumb and the index finger. The grip force required to prevent rotational slips increase linearly with the torque load with a slope that depends on the friction of the grasp (Kinoshita et al.1997). Subjects reflexly modulate the grip force respectively to changes in torque load (Goodwin et al 1998; Johansson et al. 1999; Wing and

Lederman 1998), just as was seen for changes in linear loads (Flanagan and Wing 1993; Johansson and Westling 1984a).

Grasp stability was examined for the thumb, index and middle finger, for lifting a cylindrical object with diameter of 30mm from above by Burstedt et al (1999), which may reveal something of finger grip modulation during lifting a pen, although not being exactly representative for lifting a pen and no reference was made to pen lifting. The three dimensional forces and torques applied by each of the digits and the contact positions were measured along with the position and orientation of the subject. It was seen that the distribution of forces among the digits strongly reflected constraints imposed by geometric relationship between the object's centre of mass and the contact surfaces. A change in force coordinations was seen to be related to changes in the combination of surface materials as well, e.g. object covered with rayon or sandpaper for one or more of the finger contact points. During the load phase the surface combination influenced the slope of the relationship between normal force and load at the individual digits, whereas the parallel change in normal force and load remained regardless of surface combination (Burstedt et al, 1999). From all the above findings the idea was accepted that reducing fingertip forces represents one general role in dexterous manipulation.

When grasping an object with five digits, a cumulative force of the four fingers equal and opposite to the thumb force is required to maintain static equilibrium and a balance of forces and moments as an object is lifted and held. However, how the four fingers share the force is indeterminate (Santello, 2000). Several studies suggest that the four fingers opposite the thumb parcel force in the following systematic way (Rearick, 2002; Reilmann, 2001; Santello, 2000). First of all, a 'finger force rank order' (force sharing pattern) exists, which indicates least to greatest contribution of each finger to overall force application and which is related to the object's centre of mass. Second, a common mechanism exists for force development and maintenance, which is shown by a significant co variation across all digits during the force-rise, lift and hold phases. Last, across a large band of force frequency range (0-10Hz), a strong in-phase coupling exists among all five digits, regardless of object properties, e.g. centre of mass (Santello, 2000) and handedness (Rearick, 2002).

For curved surfaces it was demonstrated that under linear forces the curvature has modest effect on the grip force requirements, whereas the effects are profound under torque loads. Adaptation of finger tip forces to surface curvature for grasp

stability under torque load is achieved by parametric adjustment of the balance between the grip force and the fingertip load. For a given torque load, subjects scale the grip force to curvature, keeping an adequate safety margin against rotational slip (Goodwin et al 1998). These findings agreed with established principles concerning the adaptation of fingertip forces to other object properties as shape, surface friction and weight (Johansson 1996, 1998). Furthermore when the torque load develops, tactile information related to localized rotational slips may update memory systems for parametric control of force-torque coordination. This process is similar to the adaptation process of the linear grip-load force modulation by use of tactile information (Johansson et al 1984, 1987; Johansson, 1998).

For relatively fast force production tasks, involving three digits, there is preferential stabilization of moment. For such tasks, forces can only be stabilised when applied above a certain value. For tasks in unstable conditions, using three fingers with an explicit requirement to stabilise the total force and implicit requirement of not losing balance, stabilising moments is also preferential by the CNS. An example is drinking from a glass of water: The total force only needs to be above the slipping threshold, but below the crushing level; at the same time accurately stabilising moments is required to prevent spilling contents of the glass.

Apart from rotational slips, torsional viscoelasticity of the fingertip pulps tends to destabilise precision grips in tasks that involve tangential torque load. The fingertip properties show viscoelastic properties both when compressed (Pawluk and Howe 1999; Serina et al 1997, 1998; Srinivasan 1989, Srinivasan and Dandekar 1996) and when subjected to tangential shear forces (Nakazawa et al 2000).

Jenmalm et al (2000) observed subjects grasping an elongated object at one end using a precision grip when lifting it while instructed to keep it level. The principal load of the grasp was tangential torque as a result of the location of the center of mass of the object, relative to the horizontal grip axis between the centers of the opposing grasp surfaces.

The curvature strongly influenced the grip force required to prevent rotational slips and the rotational yield of the grasp that developed under the tangential torque load due to the viscoelastic properties of the fingertip pulps. It was seen that subjects twisted the grasp around the grip axis by a radial flexion of the wrist to keep the desired object orientation despite the rotational yield. In addition to Goodwin's findings in 1998, it was concluded that humans use both visual and tactile sensibility for feed forward parametric adaptation of grip forces and grasp kinematics to

curvature (Jenmalm et al. 2000). Normal control of radial flexion of the wrist requires digital afferent input, whereas digital anaesthesia caused little impairment of grip force control. When subjects had vision available, but no tactile sensibility, the twist of the wrist became delayed, whereas grip force control was normal. In addition, visual cues about the form of the grasp surface obtained before contact was also used to scale grip force, whereas the scaling of the radial flexion of the wrist are dependent on visual cues related to object movement (Jenmalm et al. 2000). This lead to the conclusion that different visuomotor mechanisms support the control of the grasp twist and the grip force.

Objects that have tapered flat surfaces may be particularly suitable for forward control based on visual geometric cues because the surface angle directly relates to the required coordination of grip and load forces (Jenmalm and Johanssen, 1997).

Examples of predictions were reported so far for *reactive* tasks during manipulation involving restraint of *active* objects, which exert unpredictable changes in loading forces. The reactive grip actions in response to object's actions were based on predictions of the consequences of self-generated actions. Different from *reactive* grip force modulation tasks are *proactive* grip force modulation tasks, which primarily depend on feed forward, predictive neural control mechanisms that depend on internal representations of the physical properties of the objects. During bi-manual proactive tasks, predictive modulation requires not only that the movement is self-generated, but also that the efference copy (internal representation of object) and sensory feedback are consistent with a specific context, e.g. the manipulation of a single object (Blakemore et al, 1998). This implies that the expression of anticipatory grip actions depend on whether a test apparatus behaves like one or two physical objects.

As already mentioned in the introduction of this section, it is expected that for finger grip modulation during normal handwriting both pro-active (initiated small pen tip movement executed by fingers) and reactive grip force modulation tasks (e.g. respond to inertia effect) are crucial and therefore feed forward predictive neural control mechanisms are essential, but no reference to pro-active and reactive phenomena exist regarding specifically handwriting in current literature. As predicted physical properties of objects do not only control fingertip forces during proactive but also in reactive manipulative tasks (Ohki et al, 2002) as mentioned above, one may

conclude that during handwriting internal representations of the physical properties of the pen, such as mass, centre of gravity of the pen and distance between pen-hand contact and pen tip are crucial.

Latash et al (2003) touched on this issue in a description of pen tip movement:

"Three variables, the distance from the tip of the pen to the proximal contact (between metacarpophalangeal MCP joints of the thumb and the index finger or at the proximal phalange of the index finger) and two angles vary. These motions need to be coordinated to preserve the grip coordination and are constrained by the geometry of the hand. Motion of the pen with respect to three involved digits results from motions in the MCP and interphalangeal joints of the digits (Latash, 2003)."

Latash et al studied two- and three-finger synergies (movement patterns) during object manipulation (2003). For relatively fast force production tasks, involving three digits, there is preferential stabilization of moment. For such tasks, forces can only be stabilised when applied above a certain value. For tasks in unstable conditions, using three fingers with an explicit requirement to stabilise the total force and implicit requirement of not losing balance, the central nervous system gives priority to stabilising the total moments produced by the fingers with respect to a midpoint between the two most lateral fingers. An example is drinking from a glass of water: The total force only needs to be above the slipping threshold to grip the glass, but below the crushing level; at the same time accurately stabilising moments are required to prevent spilling contents of the glass.

Initial study on two-finger oscillatory movements in which subjects were asked to control total force, subjects showed strong tendency to stabilise moments, while forces were destabilised, particularly at low moderate forces. A more recent study by Latash (2003) on two-finger discrete (ramp) and oscillatory movements, revealed a strong tendency to control the force amplitude, but a limitation of the central nervous system to organise a two-finger synergy to compensate for errors in timing of force-related control signals (force profiles of individual levels) by an interaction at the synergy level. It is concluded that multi-finger synergies seem to function better with respect to an explicit task of total force-control during slow rates of force change. During the production of quickly changing forces, the CNS tends to use a "fork strategy", according to Latash. The fork strategy ensures that a constant sharing pattern is kept among the fingers, which leads to predominantly positive co-variations among individual finger forces and to stabilisation of moment with respect to a point located between the most lateral finger.

Normal handwriting is a relative fast task with motions of pen tip over 2 Hz. (Kunesch et al, 1989; Siebner et al, 2001), according to Latash et al (2003). Therefore, a 'fork strategy' as described above is likely to dominate. If assumed that the subject is writing with only three points of contact between pen and hand (at pads of thumb, index and middle finger), according to Latash (2003), the oscillatory pen tip movement might be viewed as produced by time varying moment applied by two fingers with respect of thumb contact point that is in between other two contact points (major simplification). A "fork strategy" is efficient in stabilising a time pattern of this moment. If a person has a motor program, responsible for his or her individual natural handwriting, the fork strategy will effectively stabilise it against possible perturbations, either intrinsic or extrinsic.

During relatively slow handwriting movements, the above expound on finger synergies, suggests that the total force applied by the two fingers is likely to become stabilised, while the moment may become destabilised. This will require constant monitoring of the action and its explicit corrections in cases of spontaneous occurring errors. Handwriting will turn into a drawing pattern resembling handwriting. This is likely to happen when script is traced or copied.

Latash' suggestion (2003) that the oscillatory pen tip movement might be viewed as produced by time varying moments applied by two fingers with respect of thumb contact point that is in between other two contact points seems invalid. The mechanical system gripping the pen was simplified by assuming that only three points of contact between pen and hand exist (at pads of thumb, index and middle finger), However, first of all, it is both in statics and dynamics not justifiable to choose the axis for moment calculation through the third point of contact at the thumb as this eliminates the force applied by the thumb and consequently manipulates the force system. Secondly, in the same manner as in the example of balancing the glass of water while drinking (see previous discussion on two- and three-finger synergies), the moments applied by the fingers to the pen have to act around an axis through the centre of gravity in order to stabilise the pen.

Besides requiring to balance the weight of the pen during pen tip acceleration, it is also required that same moments applied at pen contact points also act on an axis through the centre of the pen to prevent rotation of the pen. Whether this might influence the moment stabilisation is unknown. It is expected that the friction at a fourth point of contact between the proximal phalange of index finger and MCP joints of thumb and index finger plays a role in maintaining this balance.

Latash' research suggests that natural handwriting depends crucially on the stability of one's individual multi-digit synergies. The limitation to substantiate these speculations were technological: a tool, that allows measurement of forces and moments in multi-finger synergies during handwriting, did not exist.

### 2.2.3 Pen grip measurement

As a continuation of work done by Harris and Rarick (1959), who measured pen tip pressure in relation to legibility of handwriting, a study by Herrick and Otto (1961) focused on the methodology of examining tip pressure and grip pressure phenomena in handwriting.

A table equipped with a pressure sensing plate and grip pressure transducer pen formed the basis of the study. The pen was developed by the Experimental Process Lab of the Parker Pen Company, Janesville, Wisconsin for the Committee for Research in Basic Skills. The pen grip pressure was sensed by strain gauges on barrels and the pressure variations were recorded by an 8-channel polygraph on standard EEG paper. The system allowed variations in applied pressure by the three fingers to be measured by manually measuring the distance between baseline of the pressure graph (before applying any pressure) and values recorded while performing a writing task. The authors do not comment on the accuracy of the measurements.

The barrels were calibrated by applying weights on the barrel at one particular (to the reader unknown) point on the beam and measuring the deviation from the polygraph's baseline. This does not seem an accurate method for three reasons. First of all, the author's state that the pressure was measured in grams of pressure. However, the term force may be more appropriate than pressure as the applied weights could be directly related to force by gravity, whereas in order to relate the measured grams to pressure, the contact area between pen barrel and finger tip needs to be known. The contact area of was not taken into account and in fact varies for each subject and varies for one subject even during a trial.

Secondly, the measuring technique is not accurate also, because the exact pressure or force values could not be measured as the centre of contact area between barrel and finger tip will not coincide with the point of weight application during calibration. Thirdly, manually measuring deviation of pressure from the baseline will only provide limited resolution and could involve significant error.

The lack of a digital representation of the data also restricts the scope for signal processing to be carried out. The analysis focused on the relationship between pen grip pressure and pen tip pressure, pressure variations between fingers of one subject and pressure variations between subjects. High pen tip pressure values were found to be accompanied by high pen grip pressure.

Chau et al (2006) instrumented a digitising pen with F-Socket (Tekscan Inc.) 9811 pressure sensors and F-scan electronics to study force distribution over the shaft of the pen, permitting to obtain correlations between normal and grip force and differences between subjects with and without handwriting difficulties.

The F-Socket pressure sensors were arranged in 6 strips of 16 sensors by the manufacturer. Chau et al (2006) used 4 strips of sensors on the digitising pen. The pen was used along with a pressure sensitive liquid crystal display writing surface and a desktop computer.

Also here, there are accuracy issues. The F-scan system uses force sensitive resistors. Force sensitive resistors are in general prone to inaccuracies due to drift, hysteresis and non-linearity. Tekscan specifies that the sensor operate best over a pressure range of 15:1, which means that in the pressure range of 6.9-172kPa=0.69-17N/cm<sup>2</sup>, pressure above 172/15=11.5kPa=1.15N/cm<sup>2</sup> cannot not be measured accurately.

The pen grip pressure for normal handwriting will not exceed 10N/cm<sup>2</sup>. Therefore, only 60% of the total sensor pressure range is used. Working with a limited portion of output range results in increased errors due to limited resolution (Luo et al,1998). For F-scan inaccuracies up to 62% have been reported by Sih (2001) and even higher inaccuracies were reported by Fergenbaum et al (2003) during static and dynamic testing on flat and curved surfaces using pressure testing equipment. According to Morin et al (2000) calibration should be performed under conditions that are as close as possible to test conditions. However, the grip pressure study by Chau (2006) only calibrated the sensors on a flat surface before mounting them on a round pen shaft. Nicolopoulos et al (2000) also found that the accuracy of the system was highly dependent on calibration. More over hysteresis effects, preconditioning, bending and the shear and temperature effects strongly influence the output of the F-scan system (Nicolopoulos et al, 2000). Woodburn et al (1996) state that it is unrealistic to compare clinical data from sensors measured at different times using F-scan (generally; not discussed specifically for handwriting).

The system by Chau et al (2006) derived total grip force by summing up the individual F-socket sensor outputs. However, according to Morin et al (2000), different calibration methods during which the same pressure is applied, give different calibration slopes and during normal use different sensors tend to give a different output to the same applied pressure (Morin et al, 2000). Therefore, it can be concluded that measuring total force as sum of individual sensors is not reliable. Consequently, it can be concluded that using F-socket sensors with the F-scan system is not a reliable method for comparing pen grip force distributions and its relation to script production and investigating pressure ranges, though it may allow to compare hand function and different types of pen grip between subjects if the measurements are taken within a close approximation of time. Further analysis of grip force modulation was not carried out.

Calibration of tip pressure was attempted using a plunger and cylinder that relates normal forces applied by calibration weights to sampled sensor output. This method is only valid in static situations where there is no pen incline. As soon as the pen is held at an angle away from the vertical, the measured tip force is a component (ground reaction force times cosine of inclination angle) of the normal force. Secondly, during dynamic conditions (normal writing) the pen is accelerated continuously (positive/negative) in the horizontal plane. As a result of pen movement there is friction force acting on the pen tip, which has a component that increases/decreases (dependent on acceleration direction) the pen tip force. A free body diagram of pen-hand system is shown in section 2.2.1. Both incline and pen acceleration thus affect the measured pen tip pressure, which makes the suggested calibration method unreliable.

The results of the work by Chau et al show correlation between grip force and normal force and normal force appears to lag the grip force. In addition, quantitative differences between writers with and without handwriting difficulties were seen.

Proficient writers tended to hold the pen closer to the pen nib. Writers suffering from cerebral palsy had weaker and less adaptive grasps (Chau et al, 2006).

Despite of the accuracy issues with the device by Chau et al (2006) described above, a study by Fernandes et (2008) al used the device to further investigate grip measurement during handwriting and drawing in adults and children. The characteristics of grip force during handwriting and timing of writing were described by means of fractal dimensioning. From observing subjects attempting to synchronise their drawing with a metronome, it was found that found that

independent processes control the variations in pacing and grip force. It is stated that the 10-40% of the variance in grip force for any participant could be explained by a linear regression against spatial and kinematic observables, but no evidence was provided.

Baur et al (2006) instrumented a pen with an off-the-shelf sensor matrix to study the effects of modified pen grip and handwriting training on writers cramp (WC), a form of dystonia. The sensor used in the project was the Novel S2060 pen sensor combined with the Novel pliance X system. The system measured the force distribution around the pen by means of eighty-eight force sensors with a surface area of 1 square centimeter. The mean pen force was calculated for comparison between trials. The individual finger forces could not be determined and the maximum sampling frequency was 50Hz. Consequently, the system was not suitable for investigating the finger force control during handwriting as is described in this thesis. The authors do not evaluate the technology and do not comment on the accuracy of the system. However, accuracy issues are to be expected similar as with the F-scan system related to drift, hysteresis, non-linearity and repeatability, especially due to wrapping the sensor around the shaft of the pen. The reasons behind the inaccuracies are explained in more detail in the evaluation of the F-scan system used by Chau et al (2006).

WC patients were seen to exert more pen grip pressure and pen tip pressure than healthy controls. The modified pen grip with the pen being gripped between index and middle finger and supported by the thumb, led to a decrease in grip and tip pressure in both groups, but WC patients still had higher pen grip values. Training of patients in handwriting movements, following a method prescribed by Mai et al, was seen to decrease pen grip during writing for both the conventional and adapted pen grip. There were no significant changes during follow-up, but there was a trend for re-increase of writing pressure.

Hooke et al (2008) published a short paper that describes the development of a pen that measures six-component force and torque at the four individual pen-hand contact points during handwriting. The costly sensors enabled high accuracy force measurement (sensor inaccuracy 0.01%-0.96%). The pen was slightly larger than a normal ball point of fountain pen. The synchronisation of recordings at the start of each letter was carried out by a force plate, but no comments on the accuracy of synchronisation were included. No script recording was incorporated, which makes it

difficult to study the relationship between script and pen grip mechanics. In addition, no further analysis of finger force application was carried out that enable to explain the process of coordinating pen motion.

It can be concluded that grip force during handwriting activities is relatively poorly studied and no single system has achieved accuracy and reliability for good extended series of investigations.

## **2.3 Motor control in handwriting**

### 2.3.1 Introduction

In order to control the overall writing trajectory, the pen tip movement with respect to the hand co-coordinates have to be controlled by modulating the proximal joint forces for processing the grip force, while at the same time modulating the arm joint forces to steer the hand movement with respect to an external reference frame.

The Russian physiologist Bernstein (1967) defined coordination as a problem of mastering the very many degrees of freedom involved in a particular movement. His outlook was that coordination is the organisation of the control of the motor apparatus. Inertia, reactive forces and initial posture conditions combine with active muscle forces in producing movement. Bernstein ruled out any straightforward, unambiguous relation between the nervous impulses innervating movements and the movements themselves. He underscored the formative and steering roles of the information available to perceptual systems. More specifically, he saw the basic problem of coordination as that of mastering the many degrees of freedom involved in a particular movement - of reducing the number of independent variables to be controlled (Bernstein, 1967; Turvey, 1990, Meulenbroek et al, 1996).

At one extreme, coordination can be considered as a problem in organisation, with each part behaving in a well-defined way according to instructions from an outside source (Turvey, 1990), in an analogue fashion to a marionette being hand-controlled.

At the other extreme, coordination can be considered as a problem in self-organisation without external instruction. The parts cooperate through some kind of mutual understanding in achieving a common goal. It conveys the idea that a self-organising system of very many interacting degrees may be governable by principles described in few dimensions.

Handwriting is an activity that depends on the integrity of the peripheral and central nervous system (Meulenbroek et al, 1998; Van den Heuvel et al, 1998; Van Galen and Weber, 1998; Van Galen and Morasso, 1998). For example, the choice for a specific way of holding the pen may have led to the establishment of preferences to move in certain directions rather than in others and such preferences may constrain higher order processes, e.g., the selection of starting points in planning sequences of strokes (Van Sommers, 1984, Schillings et al, 1998). Edelman and Flash (1987) proposed a model of handwriting, that suggested that the central nervous systems is able to learn, store and modify motor action plans for performing peripheral joint control in a efficient manner. In addition, Bullock et al (1993) developed a neural network model that interacts with a trajectory generator that moves a hand with redundant degrees of freedom.

The smoothness of handwriting partly originates peripheral from segmental reflexes and dynamic muscle interactions (Van den Heuvel et al, 1998) and the importance of peripheral aspects of motor control became apparent when exploring the geometric features of work space and joint-space (Lacquaniti et al, 1987; Cruse et al, 1987; Klein Breteler et al, 1998; Schillings et al, 1998). Fine movement patterns are executed and sensed by the peripheral sensori motor apparatus (Van den Heuvel et al, 1998; Thomassen et al, 1998; Meulenbroek et al, 1998), but nothing happens without the drive and supervision of the central nervous system. The central nervous system has to be involved with providing the timing structure of muscle commands so as to adjust output for example with increases in writing speed. (Sanguineti et al, 1998).

The principles and models in motor control during handwriting activities are reported below in three main sections (as suggested by van Galen and Weber, 1998) each focussing on a particular theme. Neuromuscular and biophysical models in 2.3.2 initially deal with the kinetics and kinematics of handwriting production, while 2.3.3 focuses on learning and cognitive models and the planning of the motor function. Section 2.3.4 reports on neuropsychological issues associated with changes in the normal motor processing due to deficits and impairments.

### 2.3.2 Neuromuscular and biophysical models

Hollerbach (1981) suggested considering handwriting as a superposition of two movements, a translation of the pen and an oscillatory motion of the pen tip. Singer and Tishby (1994) considered handwriting as a modulation of a simple cycloidal pen motion, described by two coupled oscillations, with a constant linear drift along the line of writing. The movement of pen tip gets contributions from at least two components: hand movement with respect to the external reference frame and pen movement with respect to the hand. The relative contributions of these two motions to kinematics of pen tip can vary and it is assumed that during normal handwriting both components contribute to the trajectory of the pen on the paper (Lacquaniti et al, 1987; Meulenbroek et al, 1998; Dounska et al, 2000).

It is known that selection and sequencing of movement trajectories in handwriting and drawing and other space orientated movement are governed by abstract grammars and cognitive goals, similar to the so called higher processes of linguistic and lexical nature (Van Galen and Morasso, 1998). The more peripheral kinematic aspects of joint movements have been investigated with respect to their ruling principles. One of these principles is the relationship between movements in work plane and the direction of the joint movement. This issue was investigated by Klein Breteler et al (1998) by analysing geometric features of work space and joint-space paths of three-dimensional point to point reaching movements. The findings make an important contribution to the discussion on the role of optimisation principles in trajectory-formation models. It was found that in reaching movements optimisation processes in both workspace and joint path space jointly determine the trajectory formation process: a trade-off between path curvature in workspace and joint space was present. Fingertip path curvature was found to increase with increasing speed. In addition, subjects tend to produce 3D reaching movements by means of curved trajectories that are restricted to two dimensions, i.e. to a plane, both in workspace and in joint space (Klein Breteler et al, 1998).

Schillings et al (1998) assessed functional properties of graphic workspace by means of simulation with a 10 degrees of freedom kinematic model of the distal part of the writing arm. The effective workspace is analysed in terms of the effort required to reach the various locations in it. Effort is in this context defined in terms of the joint angles adopted by the wrist and fingers to reach each location. The

results show agreements between the distribution of required effort over the workspace and known stroke-direction preferences in drawing.

To discover how the very complex handwriting movement patterns are implemented in a dynamic neuromuscular apparatus, which at the most central levels of the psychomotor system are represented by their spatial features, the dynamic coordination between the different joint and muscle systems that are involved have been examined. The coordination of arm and hand motion and relative contributions of limb segments was studied in tasks involving handwriting and drawing movements of different amplitudes by Lacquaniti et al in 1987. It was found that the amplitude of shoulder and elbow angular motions scale roughly with the size of figure or script, whereas the size of finger and wrist motion is small, independent of size. Consequently, the smaller the script or figure, the greater the contribution by the motion at distal joints relative to that at proximal joints. The angular motion at the wrist and the linear motion at the fingertips are very small and indeed smaller than biomechanical limits of elbow and wrist joint angles as reported by Andrews et al in 1979. Furthermore, while shoulder and elbow motions are tightly coupled (constant phase relations), motions at distal joints are loosely coupled to those at the proximal joints (variable phase relation). Motion at distal joints increases accuracy of the movement as was indicated by smaller variability of pen trajectories compared to that of wrist trajectories (Lacquaniti et al, 1987).

The stability of pen-joint and inter-joint coordination in loop writing was examined by Meulenbroek et al (1998). The study focused on kinetic invariance of joint motion (coordination stability) of 15 pairs of 6 mechanical degrees of freedom of the pen-arm effector systems as a means to find the locus of coordination control. Pen-joint coordination between horizontal pen-tip displacement and wrist excursions was found to be most stable; that between vertical pen-tip displacement and finger excursions was considerably less stable. Inter-joint coordination was generally less stable than pen-joint coordination and most stable between the wrist and elbow. Surprisingly, it is the elbow which in loop writing is more closely coupled to horizontal and vertical pen-tip displacements than the index finger (Meulenbroek et al, 1998). In contrast with usual assumptions of older computational models that letter forms are represented and produced by fixed phase relationships, at least for loop writing very dynamic relationships between the motor system and the degrees of freedom of the hand-arms system exist, as was seen from the Meulenbroek et al (1998) study.

Thomassen and Meulenbroek (1998) studied the phase relations between wrist and finger-joint rotations during a repetitive graphic task (long words consisting of letter 'e'). Low frequency periodicity of 1 Hz was observed, which reflects adjustments of wrist and finger-joint coordination pattern about once per second. Word length and word position were found to affect this periodicity in a predictable manner (Thomassen et al, 1998).

For a long time, the kinematics regularity of script has inspired the search for the fundamental laws of movement production. The  $2/3$  power law, which states that the kinematics of handwriting (angular velocity) varies with the two-thirds power of the movement trajectory (curvature) (Lacquaniti et al, 1983), lead the field, attracting theoretical and experimental challenges (Van Galen and Morasso et al, 1998). Plamondon et al (1998) present the origin of some reported observations that link to the  $2/3$  power law. The paper states that from both handwriting experiments and simulation, it was seen that for non-oscillatory movements the power law does not hold for the major parts of the trajectory. However, it can be observed, that for some roughly elliptical parts of handwriting, the law can be valid (Plamondon, 1998). Computer simulations show that elliptical portions of trajectories will occur more frequently for simple patterns than for more complex patterns, which involve multiple strokes and discontinuity points. It can be concluded that in order to further understand how complex handwriting script originates from joint movements, it is required to extend the search for fundamental laws and models that could be combined with the power law (Plamondon et al, 1998).

One of the most persistent problems in understanding motor control is the selection of particular trajectories among the large number of possibilities. These computation principles and associated neural representations for motor planning and executions have attempted to be explained by models of multi-joint movement. The computational models described below allow quantitative description of both the mechanical actions of muscles and the neural commands activating them. The models can be used to explore the implications of different control hypotheses, which can be compared with experimental observations.

Many of the insights in non-linear muscle dynamics were incorporated into a neuromusculoskeletal model of the human arm by Stroeve (1998), which contains both feed forward and feedback control and thereby accounts for motor control of fast movements such as handwriting as well as interaction with external forces. The

feed forward control component forms an approximate representation of the inverse dynamics of the arm and its interaction with the environment. The feedback control component compensates for errors in the representation of the inverse dynamics and for unexpected forces acting on the arm (Stroeve, 1998).

Flash et al (2001) reported a series of computational processes for multi-joint arm movement in, which originates from three hierarchical levels. A schematic diagram of the process is shown in Fig. 2 of Flash et al (2001). First a trajectory is planned in hand co-ordinates. These processes involve internal representations of the target and limb positions and co-ordinate transformations between different internal reference frames. Optimisation models assume that the brain selects trajectories that maximise the smoothness by optimising a movement cost function.

Second, the hand trajectory is transformed into joint trajectories by solving the inverse kinematics problem. Inverse kinematics are suggested to be solved by Donders' law of the eye. Donders' law states that the eye has a unique orientation in three dimensions for any gaze direction and that the amount of ocular tension is a unique function of the gaze direction. (Flash et al, 2000). Though the suggestion that Donders' law may have a role in solving the inverse kinematics problem may be valid for many reaching tasks. However, handwriting and other tasks can be performed with the eyes closed. The author challenges the reader to write a phrase while keeping the eyes closed. Literature reports the following on the question whether Donders' law explains how the inverse kinematics problem is solved. A fully extended arm obeys Donders' law, according to Gielen et al (1997), but for arm-pointing movements, involving both shoulder and forearm rotations the law is not always valid (Soechting et al, 1995). In addition, when a target moves position during a reaching task, the final arm posture is neither more variable nor different from the one in the absence of such a target shift (Grea et al, 2000).

When the joint trajectories are known, the inverse dynamics problem is the transformation of the planned limb movement into the appropriate set of motor commands by calculating the joint torques. This problem can be explained by the direct inverse modelling approach. This theory states that the limb creates and updates internal models of limb dynamics. This proposes that the brain does not explicitly compute the required joint torques, but controls posture and movement. The posture is controlled by defining a stable equilibrium position for the limb and the movement is achieved by gradually shifting the equilibrium position along a desired trajectory.

Bernstein illustrated his famous problem of motor redundancy - mastering the many degrees of freedom involved in a particular movement by reducing the number of independent variables to be controlled - (also Turvey, 1990; Latash, 1996) by considering the task of producing a required trajectory of the fingertip in space. Three major joints of the arm, wrist, elbow and shoulder, have the total of seven major axes of rotation. This set of seven variables is redundant in a sense that no unique combination of joint angles can be computed based for one instantaneous position of the endpoint in space, which is defined by only three coordinates. Producing hand motion during handwriting is a typical example of control of a redundant system when analyzed at the level of coordinated joint angle rotations (Problem of inverse kinematics, Mussa Ivaldi, Morasso and Zaccaria, 1989; Zatsiorsky, 1999).

Within the general concept of motor redundancy handwriting has its own specificity. All multi-finger grasps combine serial and parallel mechanisms. Individual digits act as serial mechanisms, which are under-constraint (redundant) in kinematics and over-constrained in statics. In contrast, several digits grasping an object represent a parallel mechanism that is over-constrained in kinematics (movement of one finger causes movement of another finger) and is under-constrained (redundant) in statics (Burstedt, Flanagan, Johansson, 1999).

As mentioned in section 2.2.2 on grip modulation, motion of the pen with respect to three involved digits results from motions in the MCP and interphalangeal joints of the digits. Three variables, the distance from the tip of the pen to the proximal contact (between metacarpophalangeal MCP joints of the thumb and the index finger or at the proximal phalange of the index finger) and two angles vary. These motions need to be coordinated to preserve the grip coordination and are constrained by the geometry of the hand. Under these conditions (over-constrained parallel mechanism) the system does not seem to possess redundancy as it seems to be impossible to move a pen tip back and forth over a piece of paper without changing the lateral tilt of the pen in different ways (Latash et al, 2003). However, because of redundancy in endpoint of the movement, the overall kinematic system involved in handwriting is considered to be redundant. This redundancy during handwriting comes from three sources (Latash et al, 2003). Firstly, individual wrenches and their combinations can cancel each other out, i.e. a force/moment generated by one digit can be counterbalanced by another force/moment along the same wrench axis. Secondly, three digits plus the additional proximal contact are

redundant for a task that can be performed by a smaller number of digits (contacts). The third statement of redundancy is that the number of kinematic degrees of freedom of the contacting digits (seven axes of rotation) is redundant for a task that has not more than three degrees of freedom.

Based on the above description of the kinematic system involved in handwriting, Latash et al (2003) studied the organisation of the central nervous system in two- and three-finger synergies to control total force and stabilise moments for object manipulation. The results were reported in paragraph 2.2.2 on grip force modulation. Latash' research (2003) suggests that natural handwriting depends crucially on the stability of one's individual multi-digit synergies. The limitation to substantiate these speculations and incorporate these ideas into neuromuscular and biophysical models of handwriting were technological: a tool, that allows measurement of forces and moments in multi-finger synergies during handwriting, did not exist.

### 2.3.3 Learning and cognitive models

In motor control, the associated neural structures and networks must be highly adaptive and versatile in order to integrate online sensory information with knowledge acquired through experience and learning and at the same time perform highly complex sensory information processing, sensorimotor transformation and motor planning (Flash et al, 2001). A general acceptance has existed of prestructured motor plans or programs as an organising principle of motor behaviour for many years. However, what the exact nature of such generalised motor programs is and what is specified in such motorplans has been unclear and has therefore been investigated intensively over the last decades (Van Galen and Weber, 1998; Van Galen and Morasso et al, 1998).

In the early days of studying motor programs the open loop prestructured nature has been emphasised, which originated from the field of handwriting research that rise to acceptance of central and generalised motor patterns, programmed independently of afferent on line control. The often striking similarity of an individual's writing by different hands or even feet and mouth and the consistency of form across writing sizes has been supposed to be justifying these theories (Merton 1972, Raibert 1977). The view was that motor programs should be conceived of as discrete sets of prestructured specifications for muscle contractions that are stored in a long term

motor memory and are available on command and the executed movements only need to scale in size (Lashley, 1952; Keele and Summers, 1976; Van Galen and Weber, 1998; Van Galen and Morasso et al, 1998).

However, Since the 80's the availability of electronic equipment increased, which made it possible to study motor behaviour as it is realised in time. It was observed that during handwriting the form of letter strokes was significantly influenced by the form and size features of surrounding strokes and letter strokes (Thomassen and Schomakker, 1993; Van Galen and Weber, 1998). Wright observed from spatial and chronometric measures of handwriting by different hands and under different instructed sizes and instructed speeds, which many variations of form as aspect ratio and timing occur across renditions of the same subject by different effectors and/or sizes (Wright, 1990, 1993). The more continuous and dynamical view was accepted that the motor planning is open to influence of local spatial constraints. Since then both the more abstract view of prestructured motor programs (Keele, 1981) and their independence with feed back processing and on line processed spatial and temporal constraints were accepted (Arbib, 1990; Van Galen and Weber, 1998; Van Galen and Morasso et al, 1998).

Invariants in handwriting, particularly the role of time, were further explored by Thomassen et al (1985) and also Teulings et al (1993). It was concluded that motor output, although constant in its overall spatial form, is continuously modified by local contextual influences of the motor system such as force, impulse duration, timing of agonists and antagonists muscles (Wing, 1980) and other features like pen pressure and limb stiffness (Van den Heuvel et al, 1998). Thomassen et al (1993) demonstrated that even when assumed that motor programs for writing are centrally presented by abstract effector independent timing structures, the parameters of a model, representing such a system (e.g. oscillator model of Hollerbach, 1981), cannot be changed without changing other features of the model. Hollerbach's (1981) model assumes that coupled oscillations in horizontal and vertical directions produce letter forms that are superimposed on an independent horizontal (rightward) sweep of constant velocity. The parameters of the model are defined as follows:  $a$  = maximum velocity of the small horizontal oscillations;  $b$  = maximum velocity of the small vertical oscillations; and  $c$  = velocity of the constant rightward sweep. The Thomassen et al study (1993) was based on a writing task that was performed under nine different conditions, for which Hollerbach's parameters  $a$ ,  $b$  and  $c$  were

analysed and according to this study, with variations of horizontal progression velocity, nearly all other kinematic variables of script change as well. In addition, Teulings et al (1993) found that when movement patterns are executed at another size or speed, some parameters need to be intentionally rescaled. These findings do not support the view of a constant motor program, but rather of a constant intention.

The current well-recognised view on handwriting is that the handwriting motor processing is a multilevel process of which the final static outcome (cursive script) is the result of numerous concerted actions of the cognitive and motor system (Van Galen, 1991; Schomaker and Van Galen, 1996). The older literature however mainly describes chronometric effects of processing lexical and motor demands in handwriting tasks as results of examining reaction time and movement time data (see summation above). With improved equipment that was capable of investigating real time realisation of script and improved understanding, including advanced models of handwriting, it became clear, that these results on timing are not always satisfying means to obtain a better understanding of real time implementation of writing patterns in neuromuscular commands. The general current question is posed how chronometric effects such as handwriting delays arise in a task with so many biomechanical and neuromuscular processes involved. Presently, it is accepted that movement time variations are only a limited aspect of handwriting and other features such as stiffness control, as reflected by pen nib (axial) force variations, may be revealing as well. This outlook also bridges the gap between the formerly discrimination between so called central and peripheral models of the control of handwriting movements (Van Galen et al, 1998).

Investigations in pen tip (axial) pressure have shown that increased axial pressure can smooth the pattern. If a sudden change in normal handwriting occurs, for example by changing slant or size, the visual feedback information needs rescaling and becomes more complex and will increase the processing demands to the neuromotor system (Van den Heuvel, 1998). Signal to noise ratio (SNR) is defined as the ratio of the standard deviation of the average pattern (modulation of a feature across different strokes of script) and the standard deviation of the noisy deviation (Teulings et al, 1986). The sudden increased processing demands lead to less fluent movements, due to increased signal to noise ratio (SNR) in the motor system. However, increased stiffening of the limb and applying more axial pressure functions as noise filtering and the deterioration disappears (van den Heuvel et al, 1998). The

results of this study strongly suggests that biomechanical aspects should be included in theories of psychomotor control.

The discrete nature of motor programs was studied further by van Galen et al (1998) after being inspired by the work of Abbs and Winstein in (1990), which suggested a more flexible concept of motor program, existing of movement execution with feedback process. Van Galen et al (1998) more specifically examined adaptation of writing size due to local spatial changes as an instantaneously changed length of the baseline of writing during normal handwriting. Twelve subjects wrote nonsense words of a length of nine letters that were recorded with a digitiser tablet and computer program. Halfway the task word, the computer program presented the target writing space for that word, which was either normal, shortened or extended by 7%. Trajectory length of up and down strokes and horizontal and vertical displacements were seen to be adapted to local changes in writing space. Upstrokes were earlier affected than down strokes and adaptation of horizontal progression was earlier affected and more pronounced than changes of vertical displacement. The results support the concept of continuous motor programming rather than the idea of a discrete set of instructions that is insensitive to the biomechanical and psychological context of the task (Van Galen et al, 1998).

#### 2.3.4 Neurological and biomechanics issues

Deficits in brain function or in the musculoskeletal system due to disease or trauma will cause a deterioration in hand writing ability. Accordingly, the study of handwriting is of interest to scientists and clinicians interested in motor learning, rehabilitation and the effects of ageing or disease on motor skills. Recent investigations have shown that studies on biomechanics of handwriting may reveal deeper insights into the underlying neuromuscular processes involved (Walton et al, 1979; Van Galen and Morasso et al, 1998; Van den Heuvel, 1998; Latash et al, 2003; Rosenblum et al, 2003; Wang et al, 2005).

Movement disorders severely degrade a person's ability to write. Common movement disorders include Essential Tremor (ET) and Parkinson's disease. Essential Tremor is a tremor disorder affecting people in later life, which is characterised by postural and kinetic tremor and maximally affects the hands

(Panicker, Pal, 2003). Primary Writing Tremor (PWT) has often been classified as a focal form of ET, but the pathophysiology is still unknown (Modugno et al, 2002).

Multiple Sclerosis (MS) is an idiopathic inflammatory disease of the central nervous system, characterised by demyelination and subsequent axonal degeneration (Clabresi et al, 2004). MS is the most common disabling neuromotor disease in young adults and affects twice as many women as men. Common presenting symptoms include numbness, weakness, visual impairment, loss of balance, dizziness, urinary bladder urgency, fatigue and depression (Clabresi et al, 2004; Murray, 2006). Upper limb tremor is often seen. Haddow et al (1997) reported moderate and severe tremor respectively of 32% and 6%. In addition, upper limb tremor was reported in 55 out of 100 randomly selected patients and was disabling in one of these (Alusi et al, 2000).

Parkinson's disease (PD), with a prevalence of 2 per 1000 in the elderly is one of the most common neurological disorders. It is primarily a disease of the elderly and middle-aged, but can occur in all age groups. A patient can be diagnosed as having Parkinson's disease, if two out of three cardinal signs are seen. First of all patients often show rigidity, muscular stiffness throughout the range of passive movement in a limb segment. The second and most disabling manifestation is akinesia. Akinesia includes a large variety of motor deficits, which also include bradykinesia in both gross and fine motor tasks. Bradykinesia is characterised as slow execution of voluntary movements. Other forms of akinesia are slowness of movement initiation (Delwaide and Gonce, 1998), difficulty controlling multiple limb segments and reaching a target with a single continuous movement (Alberts, 1998; Invarsson et al, 1997; Teulings, 1997; Delwaide and Gonce, 1998), rapid fatigue and inability to execute simultaneous or sequential actions at normal speeds (Benecke, 1986; Stelmach, 1992; Delwaide and Gonce, 1998).

Tremor (Action tremor/postural tremor) at rest, a rhythmical oscillatory movement of a body part, is a cardinal sign of Parkinson's disease (Forssberg et al, 2000; Vaillancourt et al, 2000, 2001). Tremor activity is usually suppressed by voluntary activity, sleep and relaxation of the axial postural muscles (Forssberg et al, 2000; Vaillancourt et al, 2000; Delwaide et al, 1998). The tremor amplitude increases with stress and anxiety. These exaggerated responses can often be controlled by drugs, such as L-DOPA, which acts to supplement the loss of dopamine produced by the

substance nigra of PD patients. (Delwaide et al, 1998; Kimber et al, 1998; Delong et al, 1985).

Jankovic et al (2001) found in a three year follow-up study evidence for variable course of progression of the different PD symptoms, which implies different biochemical or degenerative mechanisms for the various clinical features associated with PD (Jankovic et al, 2001).

The consequences of tremor, rigidity and bradykinesia significantly affects the motor capabilities of PD patients to perform even the simplest of voluntary everyday motor tasks. The symptoms of Parkinson's disease are often recognised in the handwriting. Many years before PD is diagnosed, the handwriting of pre-morbid PD patients already present some specific spatial features, such as less round strokes and more abrupt changes of direction (Vinter et al, 1998). Walton (1997) and Vinter et al (1998) reported about handwriting changes due to aging and Parkinson's disease. Fourteen handwriting characteristics were examined in both Parkinson's patients and a healthy control group. The outcome of characteristics of the Parkinson patients are summarized below.

*Micrographia* was seen in one out of six early onset Parkinson patients. This writing is mainly produced by the fingers, often with hand and arm movement separating the words. The larger the requested size, the larger the size reduction (Vinter et al, 1998; Van Gemmert et al, 1999). PD patients did not reduce writing sizes as result of a high level of mental load, which suggests that writing in an automated fashion does not result in micrographia (Van Gemmert et al, 1998).

*Alternating bursts of strength and loss of control* are other characteristics of Parkinson's disease. Half of the patients were seen to write with "on-off" pen pressure. Uniformly moderate pen pressure was alternated with consistently heavy pressure in writing a single word or string of words. In addition, movement amplitude was seen to depend on type of pattern drawing. While tracing models, obtuse patterns (two lines with an angle of 135°) were reproduced with significantly shorter sizes than acute patterns (two lines with an angle of 45°) by PD patients (Vinter et al, 1998). This was expected, based on results from the Meulenbroek et al study (1993): pauses at angles were seen for drawing of obtuse patterns, whereas no pauses were seen for drawing of acute angles. Obtuse patterns involve drawing in a more or less constant direction, which brings the effector joint close to the limits of its functional range of motion. Moreover, for PD patients, a deficit in force production seems responsible for the reduction in movement amplitude. Healthy test subjects

display a perfect bell-shaped velocity profile, whereas PD patients show several EMG bursts for the execution of one movement (Eichhorn et al, 1994). On the contrary, Gemmert et al (1999) suggest that PD patients may have reduced capability to maintain a given force level as result the decreased stroke size in micrographia.

Parkinson patients showed half the amount of *tapers* on their beginning and ending strokes of words than control subjects. Uniformly heavy pen pressure was seen here as well. This together with paucity of tapers indicates that the writing of PD patients was *slower* than for control subjects.

The frequency of *pen lifts* by patients with a mean age of 53 was twice that of the controls of similar age. Sometimes *pen drag* was used to connect words or words to dots above 'i' or 'j' or to interconnect dots.

Handwriting specimens prepared by one-third of the Parkinson's patients contained *erratic movements*, words either preceded by and/or followed by weak and meandering ends on some of their stroke or fine short lines which appeared to represent modified tapers oriented at right angles or acute angles to the main strokes.

Some patients wrote with *curved strokes*. Mostly it was seen as a mixture of curved and angular strokes, or squarish flattened strokes, to connect and form the various characters. It was most prevalent in older patients and in handwriting containing moderate to widespread tremor.

Most test sentences produced by patients had poor *rhythm*, which refers to size of letters, spacing of words and letters and slope of writing. About two-thirds of these subjects wrote with irregular-sized letters and more than half of them exhibited irregularity in the slope of their writing.

One-fourth of the patients showed *variability in character forms and spacing*. The subjects, writing on two occasions, had test sentences with characters formed differently from each other. This trait was particularly seen in the late-onset subjects. Also, irregular spacing between the words affected two-thirds of the patients and irregular spacing between letters in the words occurred in one-third of them.

Half of all Parkinson patients showed *slurring*. Patients wrote with *poorly-formed characters* and one-fourth omitted whole characters or parts of characters.

Many Parkinson's patients *spelled words incorrectly or capitalised inappropriately*, but this was not found to be differently from the elderly control group.

*Tremor* appeared either in the form of *waver* (“out-in movement”), a sudden movement away from and return to the line of writing or as a *rhythmic oscillation*. Slightly less than a half of the patients exhibited only one instance of waver somewhere in the sentence. About the same number had moderate to frequent waver or rhythmic tremor which affected several parts or much of the sentence. The location where tremor was likely to occur along the length of the sentence was unpredictable. Waver was mainly found on long down strokes. Due to this waver, many of the patients appeared to have difficulty forming straight down strokes, such as the stem of the ‘z’. Intermittent wavers and rhythmic tremor were mainly found on curved strokes in the middle zone of handwriting.

*Poor line quality*, evident as abrupt change in curvature, was seen in two-thirds of these specimens and uneven stroke thickness was characteristic of more than half of them.

Word alignment is seldom straight in Parkinson patient’s handwriting. The most frequent pattern involves an undulating line of word positioned around the imaginary baseline of the sentence. With respect to margins, one-third of the subjects wrote with an upward slope and another one-third wrote with a downward slope. Slopes were especially pronounced in elderly Parkinson patients, whose neurological deterioration may also include disturbance in spatial perception.

Walton also examined the disease progression by repeating the study after a time interval of 5 years. The results showed progressively deterioration as the handwriting specimens could be characterised as being larger and more deteriorated. The number of malformed letters and the degree of that had increased. More angular connecting strokes, more overwriting and tremor were seen. The line quality had decreased and the rhythm was disrupted. The later specimen were also written slower with fewer tapers and heavy pressure in some places.

Research on precision grip in PD shows several general impairments in function, including a slowing of the pre-loading phase and a stepwise development of grip force (Ingvarsson, 1997; Fellows, 1998). In addition, Fellows reported that PD patients tend to produce excessive forces in both static and peak force application. Ingvarsson, however reported no difference in peak force amplitude between PD subjects and controls. Methodological differences might have caused different observations. In Fellows’ experiment the grip force transducer was located on a low-

friction track, which only allowed movement in vertical plane, while Ingvarsson's grip device was free to move in any direction.

Despite the above described impairments in grip control of Parkinsonians, the coupling of grip and load forces, as described earlier, are preserved, regardless of changes in an object's weight, friction coefficient (Ingvarsson et al, 1997) or anticipation of changes in load (Gordon et al, 1997).

Coordination and control of forces during multi-fingered grasping in PD was investigated by Rearick et al in 2002. It was found that PD patients coordinated and controlled five-digit forces comparable to that of age-matched controls, which is systematically as was reported for healthy subjects (Rearick et al, 2002; Reilmann et al, 2001; Santello et al, 2000, mentioned above). Both groups developed the same force amplitudes and force sharing patterns across all grasping phases. PD patients also demonstrated similar levels of variability both within and across trials. However, in the frequency domain, some differences were observed across groups, especially in PD patients exhibiting obvious action tremor (AT) at a single modal frequency. These subjects showed a systematic disruption from force synchronisation patterns normally observed between digits, a shift of phase-differences away from  $\sim 0^\circ$  (in-phase), which typically occurred at and around the AT frequency, while at many other frequencies synchronisation patterns were still maintained. As the disruption is very specific and focal and patients make no quantifiable attempt to compensate for the lack of force synchronisation at AT frequencies, e.g. by increasing total force output, it was believed that this lack of force synchronisation at the digits does not contribute to the lack of manual dexterity often observed in PD patients (Rearick et al, 2002).

Tremor severity measurement and recording takes an important place in the process of movement disorder diagnosing and treatment. The methods that are currently available will be discussed in chapter 7 on spiral drawing.

The usefulness of surgery was assessed by pre- and post-operatively spiral tracing by Zirh, Reich, Dougherty and Lenz in 1998. The effectiveness of thalamotomy (creating a lesions to the thalamus) for essential tremor of the upper extremity by use of a blinded measure of outcome was reported and a comparison with the effectiveness of high frequency stimulation of the thalamic nucleus ventralis intermedius (Vim-HFS) for treatment of tremor was made. The results show that disability from working and writing significantly improved by surgery. On average,

patients had moderately abnormal writing and multiple crosses of the line during spiral drawing before surgery and zero to mild abnormality after surgery. Scores for postural and action tremor in target side were significantly higher pre-operatively than three and twelve months after surgery. These results are comparable with results reported for Vim-HFS.

Another treatment for Parkinson's disease is deep brain stimulation or DBS (Polak et al, 1998). In DBS electrodes are inserted into the subthalamic nucleus to relieve tremor. Instead of then creating a lesion the electrode is merely tuned to emit a high frequency signal (100-300Hz) that's effect is to inhibit or blocks the symptoms of the disease. It has been hypothesized that the high frequency stimulation acts as a form of neuro-inhibition (Polak et al, 1998).

Rheumatoid arthritis (RA) is an inflammatory condition that affects about 2.5% of the adult population and which severally affects patients' neuromuscular system.

Rheumatoid arthritis particularly damages the articular cartilages and consequently there is decreased joint mobility (Gottschalk et al, 1950; Martini et al, 1989).

Rheumatoid arthritis in the hand severally deteriorates patients' handwriting ability.

Allergies, bacteria, viruses and genetic factors have all been proposed as contributing to or triggering the destructive inflammation. Some cases develop as autoimmune responses, in which the body attack its own tissues. Regular exercise, physical therapy and drugs that reduce the inflammation, such as aspirin, can slow down the progress of arthritis (Martini et al, 1989). For optimal management of RA, detection in the early phase of RA is crucial (Emery, 1994). During that time the number of swollen joints is maximal and the rate of appearance of erosion is at its greatest (Sharp et al, 1991).

Routine diagnostic screening involves erythrocyte, sedimentation rate (ESR), C-reactive protein (CRP), haematological screening, liver enzymes, renal function, rheumatoid factor (RF) and antinuclear antibodies (ANA), (Van der Horst-Bruinsma, 1998).

Gottschalk et al (1949) investigated the effects of arthritis on handwriting. Larger variations of pen tip pressure and frequency, amplitude and wave-form in the writing of a wave pattern were observed for arthritis patients compared to healthy subjects. However, similar large variations of frequency, amplitude and wave-form that were seen in the wave pattern writing of arthritis patients, were also observed for patients suffering from hypertension (Gottschalk et al, 1949).

Writer's cramp is primarily defined by the appearance of involuntary muscle contractions soon after the subjects start to write. Odergren et al (1996) investigated precision grip in writers cramp. Isometric grip and load forces were sampled with an instrumented grip object by Johansson et al (1988a). The sensory perception and force output according to memory presentations of weight and friction of the object were intact. However, impaired grip force coordination during lifting was observed. The results indicated an impaired capacity in writer's cramp subjects to integrate sensory information in motor programming and force regulation during precision grip tasks (Odergren et al, 1996).

## **2.4 Evaluation: writing tools**

Very little research has been carried out on the functionality and ease of handling of the different pen types available. Gross et al (1996) compared thenar muscle activity (EMG), three-dimensional wrist position, wrist velocity and acceleration for five different pens. The preferred pen was a larger model with an ergonomic designed gripping area. The pen was preferred because of larger diameter, larger length, its comfortable grip texture and observed higher writing velocity. Although less preferred, a smaller and more traditional pen model scored better on ease of writing as a result of rapid ink flow and consequent low friction between pen and paper.

## **2.5 Conclusion: including biomechanics into handwriting research**

The references cited in the previous sections, highlight the importance of including biomechanical aspects into future research in handwriting. This will be summarised below.

### ***The problem of coordinating handwriting***

Bernstein's problem - mastering the many degrees of freedom involved in a particular movement by reducing the number of independent variables to be controlled - was initially conducted largely in terms of how a device of very many independent variables might be regulated without ascribing excessive responsibility

to an executive subsystem. It was concluded that the control of the complex kinematic system involving inertia, reactive forces and initial postural conditions, combined with muscle forces, cannot be directly related to nervous impulses and that no models developed yet can adequately explain coordination (Bernstein, 1967; Turvey, 1990). It became evident that more advanced insights were required regarding which of the many measurable aspects of handwriting production mentioned above are relevant and revealing in order to decide what should be measured in order to develop further conclusions and theories (Turvey, 1990). A second approach to the problem is directed at an explanation of coordination in terms of very general laws and principles. Foundations of the second round are the subdisciplines of physical biology and ecological psychology. In an ecological approach to psychology, perceiving is defined as the means by which an individual maintains contact with his or her environment. Intentions function as exceptional boundary conditions on natural law. Understanding how they do so is a major challenge (Turvey, 1990). Physical biology would attempt an account of coordination in terms of laws and circumstances. (Laws identify real possibilities and when circumstances - boundary conditions/constraints - are appended, actual events result). Novel methods of observation and measurement of physical biology - including biomechanics, together with creative applications of established strategies, are required to reveal them (Turvey, 1990). This approach can be summarised as a *systems approach to coordination*. According to Van Galen et al (1998), this approach will fill the gap between the former biomechanical/ biophysical and cognitive/psychomotor models and will lead to integrated psychophysical models.

Psychophysical studies of handwriting and drawing (Morasso, 1981, 1986) have shown that the spatial trajectory is more variant than the joint rotations or than force-time patterns (Teulings et al., 1986). Based on these findings, models for script generation have been proposed (Edelman and Flash, 1987; Schomaker et al, 1989; Plamondon, 1989, 1992; Dooijes, 1983) that assume planning in two-dimensional or three-dimensional space, with continuous mapping from this space into the joint space that controls motor execution (Bullock et al, 1993). It can be concluded that kinematic biomechanical aspects are highly important in understanding and modeling handwriting production.

Biomechanical research of handwriting also leads to an understanding of motor programming as a continuous process that includes feedback processing rather

than the idea of a discrete set of instructions that is insensitive to the biomechanical context of the task (Van Galen G.P., 1990; Van Galen G.P., Weber J.F., 1998). Flash et al (2001) reported a series of computational processes, which highlight the importance of both kinematic mechanical aspects and joint mechanics, for multi-joint arm movement, originating from three hierarchical levels, involving hand coordinates, joint trajectories and joint torques to control posture and movement. Flash's theories suggests that recording both limb and posture kinematics along with measuring force and moment output of the neuromuscular system could be revealing (Flash, 2001).

Latash' research (2003) suggests that natural handwriting depends crucially on the stability of one's individual multi-digit synergies. The limitation to substantiate these speculations were technological: no tool, allowing measurement of forces and moments in multi-finger synergies during handwriting, exists (Latash, 2003). Axial tip pressure increases with increased processing demands for stiffness control (Van den Heuvel et al, 1998). This suggests that measuring forces and moments produced by the hand along with kinematics might help to explain how handwriting can be so accurately performed and will lead to integrated psychophysical models, covering both the pshychomotor and biophysical aspects.

In addition, as already reported, difficulty in controlling axial tip pressure during handwriting is observed in PD patients (Walton et al, 1997) and RA patients compared to healthy controls (Gottschalk et al, 1949). Moreover, PD patients show a deficit in some force production during tasks other than handwriting (Eichhorn et al, 1994; Van Gemmert, 1998; Van Gemmert et al, 1999). In addition, poor movement control due to a deficit in contolling distal muscle force was observed for poor handwriters (Van Galen et al, 1993). Although attempts were made to measure Pen-hand grip force (Herrick et al, 1961; Chau et al, 2006; Hooke et al, 2008 and Baur et al, 2009), it has never been accurately assessed for handwriting in healthy subjects or those with impairments. According to Rosenblum et al (2003), pressure measures while writing supplies important information about the degree of handwriting proficiency. PD patients also have difficulty to create drawing patterns in specific directions (Meulenbroek et al, 1993; Vinter et al, 1998).

As a skilled movement is characterised by precise organisation in time and space, as well as by appropriate force regulation, it is expected that measuring forces and moments produced by the hand along with kinematics will help to assess

handwriting deficits, which may lead to novel diagnostic tools and new insights in development and deterioration of handwriting ability. Measuring pen-hand grip force control therefore is a crucial step from which a multitude of advances and applications may emerge.

### ***Conclusion***

From the review above it can be concluded that a more thorough assessment of biomechanical aspects of handwriting may lead to more insightful and integrated theories on handwriting motor control. Such an overall assessment of handwriting or drawing should include the following biomechanical aspects that vary with time:

- script kinematics (x- and y-coordinates) and derivatives;
- pen tip pressure;
- pen-hand interaction, including pen grip force;
- limb and upper body kinematics.

At present little is known about the pen-hand interaction during writing tasks. The pen-hand interaction can be measured as *grip force*. Many successful attempts of grip force measurement from instrumented objects during daily living tasks, other than handwriting with pen like devices, have been made. Although previous studies have attempted to measure the variations in grip force associated with writing tasks (Herrick et al, 1961; Chau et al, 2006; Hooke et al, 2008 and Baur et al, 2009), none of these included measurement of kinematic biomechanical aspects of handwriting and therefore did not provide a platform for extended development of theories on biomechanics and motor control in handwriting. The ideal system incorporates pen grip force measurement at all four contact points with the pen: tip of the thumb, tip of the index finger, lateral surface of the distal phalanx of the middle finger and proximal portion of the hand (between metacarpophalangeal MCP joints of the thumb and the index finger or at the proximal phalange of the index finger) and allows measurement of both forces and moments in finger synergies, as suggested by Latash et al (2003).

## 2.6 Objectives

In section 2.5 it was concluded that a more thorough assessment of biomechanical aspects of handwriting is expected to lead to more insightful and integrated theories on handwriting motor control. In this PhD project, the first step towards this is taken by means of developing a novel system for recording biomechanical aspects of handwriting. The project aim and objectives are detailed below.

### ***Overall project aim:***

The overall project aim is to develop a system for recording biomechanical aspects associated with handwriting and assess its usefulness for investigating the biomechanics of handwriting in relation to study of human coordination of motion.

### ***Objectives of the current study:***

- A) to develop a novel *pen-like grip force measurement device*, combined with a *script digitiser* and *motion analysis system*. Grip force measurement in *tripod grip* - holding pen with thumb in opposition to index and middle finger - will be focussed on as this is the most common pen grip and children are taught to write, holding the pen in tripod grip. The pen grip measurement device should enable measurement of individual *thumb, index* and *middle finger pressure*. Measurement of pressure at the fourth contact point will not be incorporated at this stage. This set of equipment will fill the current measurement device deficiency and will contribute to gaining better understanding of the overall neuromuscular and biomechanical processes involved in producing handwriting or drawing.
- B) Utilise the above system to obtain pilot data on four different tasks (detailed in chapters 5, 6, 7 and 8) that illustrate the usefulness of the system:
- ***Line drawing task (chapter 5):***  
Illustrate that the developed system allows future study of the neuromuscular control apparatus, involved with drawing of lines.

- **Writing task (chapter 6)**

Firstly, illustrate that the developed system allows future study of the neuromuscular control apparatus, involved with writing tasks. Secondly, illustrate that the comprehensive set of measurements allows investigating the flexibility of the neuromuscular control apparatus in writing: among trials a very similar output can be produced by a very different process of multi joint coordination. Therefore the arm joint kinematics along with finger forces that control the fine pen movements and consequent pen tip movement will be investigated.

- **Spiral drawing (chapter 7)**

Illustrate that the developed system allows future study of the neuromuscular control apparatus, involving drawing complex shapes, such as Archimedes spirals, which is a method for assessing tremor in impairments such as Parkinson's disease (PD), Multiple Sclerosis (MS) and Essential tremor (ET), by combining the recording of pen tip kinematics with assessment of finger tremor frequencies. The potential for diagnostic purpose and study of disease progression will be assessed.

- **Signature verification (chapter 8)**

Illustrate that the developed system can explore the process of signature writing and assess whether the pen-hand interaction, measured as grip force by thumb, index and middle finger, possesses characteristics that allow to use the system for biometric signature verification.

C) General assessment of the functionality of the novel system:

Quantify the capabilities and accuracy of the system and the comprehensive set of sampled data. The data set includes: force applied by thumb, index and middle finger to the pen; pen tip pressure; pen and limb kinematics, which can be presented and analysed with developed Matlab scripts. The analysis includes:

- Calculation of resultant pen grip force exerted by thumb, index and middle finger;
- Power Spectral Density (PSD) analysis to assess the

frequencies of force modulation;

- Root Mean Square (RMS) values of forces;
- Basic statistics of force and kinematic signals (mean, max, standard deviation, sum etc.);
- Calculate and visualise trajectories of shoulder, elbow and wrist joint and pen tip in 3D and include the time aspect of the movement along with x,y,z-joint-coordinates.
- Phase characteristics between wrist, elbow and shoulder joints.

## **3 Transducer design**

### **3.1 Introduction**

The first objective, described in the previous chapter, is the development of a pen-like grip force measurement device that can be combined with a digitiser tablet for sampling script and a motion capture system for sampling limb and upper body kinematics. This chapter describes the design procedure for the grip measuring transducer, which has been designed to incorporate the stylus electronics of a Wacom Intuos2 digitiser tablet. The Wacom Intuos2 digitiser tablet and software provides an established method for pen tip pressure and coordinate measurement via commercial software (ScriptAlyzer) and will be described in chapter 4 together with the Vicon motion capture system.

Firstly, the pen grip mechanics will be described in 3.2 and a model is proposed that explains which forces are active on the pen and how pen motion is exerted. The transducer design starts in 3.3 with the methodology first of all being explained in 3.3. The sections 3.4, 3.5 and 3.6 report about the three design phases: definition, conceptual and design phase. The calibration procedure in 3.7 closes the chapter.

### **3.2 Pen grip mechanics: a model**

The pen shaped transducer will be designed to study handwriting for subjects holding the pen in tripod grip, which is the most common pen grip (Fig.2.1). A model is proposed that shows the relations between forces that act on the pen, the pen motion and which forces can be derived. This gave insights into the potential of the transducer that was going to be development. It also revealed some desires to be included with the requirement specifications and gave some direction to the development as reported in section 3.2.2.

### 3.2.1 Description of the model

During tripod grip the pen is held by thumb and (in opposition to) index and middle finger. The pen makes contacts with the hand at four sites (Latash et al, 2003):

- a proximal portion of the hand (between metacarpophalangeal MCP joints of the thumb and the index finger or at the proximal phalange of the index finger);
- the tips of the thumb;
- the tip of the index finger;
- the lateral surface of the distal phalanx of the middle finger.

During handwriting the fingers modulate the grip force applied to the pen. The force experienced by the pen at each of the usual four contact areas, can be distinguished as an axial (shear) force component in the longitudinal pen direction and a force normal the surface of contact. The free body diagram in Fig.3.1a to Fig.3.1f shows the forces that are applied to the pen and consequent reaction forces and the forces that can be derived from the pen orientation, pen motion and the applied forces. If all these forces are drawn, the number of forces shown at one point in the diagram is larger than the three x,y and z- components of one resultant force that normally act on one point. All reaction forces and components of resultant forces are shown in Fig. 3.1b, whereas Fig. 3.1a is a simplified version of Fig.3.1b, for clarity only showing the applied and resulting forces. However, Fig.3.1a can only be understood from interpreting Fig.3.1b to Fig.3.1e as described below.

The free body diagrams in Fig.3.1a and b shows the resultant grip force (composed of the four finger contact forces) at one point of the pen at a single time instant as a horizontal and vertical component and their combined shear component in the axial direction. The pen grip forces applied at the gripping area are transferred by the rigid pen body to the pen tip.

Grip force is exerted in the horizontal direction to overcome friction encountered by the pen tip and inertia effects and to exert the desired acceleration and directional changes (Fig.3.1:  $F_{\text{result},xz} = F_{\text{tip,kinetic},xz} - F_{\text{friction},xz} - F_{\text{inert}}$ ). The friction that the pen experiences ( $F_{\text{friction},xz}$ ) depends on the applied axial force and the friction caused by the pen tip mechanism in combination with the friction of the writing surface. The experienced friction force could be expressed as a factor, related to the pen-paper combination, which is multiplied by the normal reaction force ( $F_{\text{tip},y}$ ) to the pen tip ( $F_{\text{friction},xz} = \mu \times F_{\text{tip},y}$ ), where the normal reaction force equals the vertical component

of the applied grip force ( $F_{grip,y}$ ). Modern pen implementations usually flow more freely than the traditional fountain pen, causing less friction.

Vertical pen grip force will be exerted, either for lifting the pen to overcome gravity and exert acceleration or to press the pen down onto the paper. Gravity and inertia reaction forces are also shown in Fig.3.1.

The axial pen tip force will be derived below. It should be taken into consideration that the axial force experienced by the pen tip depends on the pen orientation and incline. Therefore, a plane in which the pen lies needs to be defined. In Fig. 3.1, this is the x'y-plane.

The exerted axial pen grip force ( $F_{grip,axial}$ ) does not equal the axial pen tip force ( $F_{tip,axial}$ ). Despite of the forces acting in opposite direction along a line that has an incline compared to the horizontal (Fig.3.1), the components of the resultant finger grip force ( $F_{grip,result}$ ) and resultant pen tip force ( $F_{result}$ ), that work along that line, differ for three reasons.

First of all, the resultant axial grip force and axial tip force differ due to the effects of friction and inertia as follows. The resultant pen tip force in the horizontal plane ( $F_{result,xz}$ ), does not equal the resultant pen grip force in the horizontal direction ( $F_{grip,xz}$ ). The value of the resultant pen tip force in the horizontal plane ( $F_{result,xz}$ ) is lower due to friction and inertia effects:  $F_{result,xz} = F_{tip,kinetic,xz} - F_{friction,xz} - F_{inert}$ .

Secondly, as the resultant horizontal pen tip force ( $F_{result,x,z}$ ) and consequent pen acceleration vector  $\mathbf{a}$  do not lie in the same plane as in which the pen is orientated, the force experienced by the pen tip in the horizontal (x,z) plane ( $F_{tip,x'}$ ) is lower than the resultant pen tip force in the horizontal plane ( $F_{result,xz}$ ). The direction of the pen tip force vector in the horizontal plane is through the x'-axis and therefore, a component of resultant horizontal pen tip force,  $F_{result,xz} \times \cos\alpha$ , affects the pen tip in the horizontal plane as may be seen in Fig.3.1a, b and d.

Thirdly, dependent on the pen orientation, the kinetic, friction and inertia forces ( $F_{kinetic}$  and  $F_{friction,xz}$  and  $F_{inert}$ ) have an either positive or negative effect on the axial pen tip force. During movement of the pen tip over the paper with a pen incline angle between  $0^\circ$  and  $90^\circ$  relative to the direction of motion (acceleration vector  $\mathbf{a}$ ) as seen in Fig.3.1a, b and d, the forces acting in the horizontal plane in the positive x'-direction increase the axial pen tip force. This was described above and can be seen in Fig.3.1d. The axial pen tip force becomes larger than the vertical pen tip force. The axial component of applied resultant grip force ( $F_{grip,axial}$ ) is larger than the axial tip pressure ( $F_{tip,axial}$ ).

However, during movement of the pen tip over the paper with a pen incline angle between  $90^\circ$  and  $180^\circ$  relative to the movement/acceleration direction, the friction and inertia forces ( $F_{\text{kinetic}}$  and  $F_{\text{frictionxz}}$  and  $F_{\text{inert}}$ ) decreases the axial pen tip force (and the axial pen tip force becomes smaller than the vertical pen tip force).

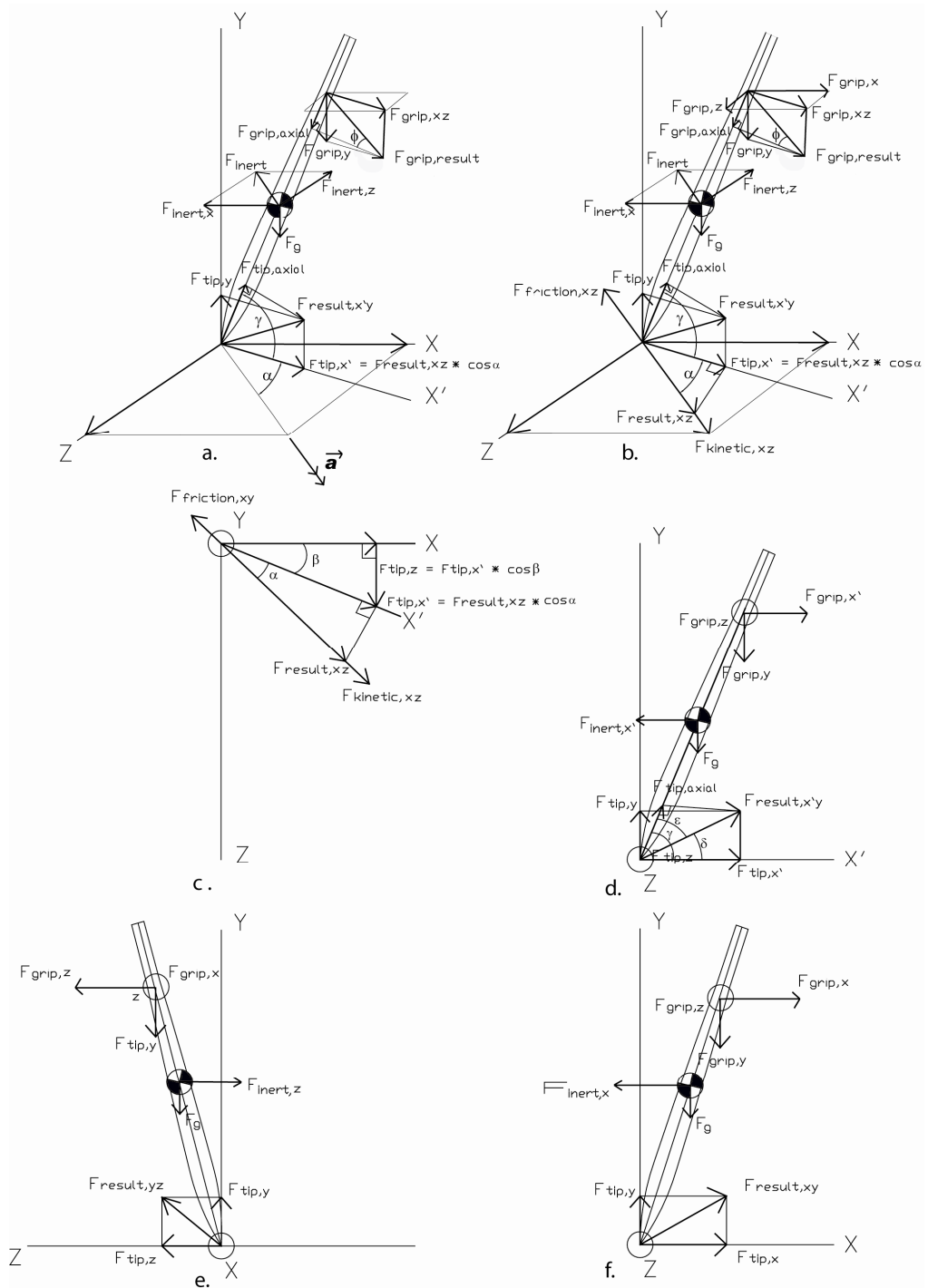


**Fig.3.1: Free body diagram of pen grip during handwriting:**  
a) x,y,z-frame in three dimensions, for clarity simplified compared to Fig.2.1b. The pen acceleration is indicated by vector  $\mathbf{a}$  (parallel to  $F_{grip,xz}$ ). The pen is orientated in plane  $x'y'$ .  
b) x,y,z-frame in three dimensions;  
c) x,z-plane, showing the movement direction and pen orientation in the plane through the origin and y-axis and  $x'$ -axis.  
d)  $x',y'$ -plane in which the pen is positioned.  
e) y,z-plane  
f) x,y-plane

In Fig.3.1 the following relationships exist:

$$\begin{aligned}
 F_{\text{friction,xz}} &= \mu \times F_{\text{tip,y}} \\
 F_{\text{result,xz}} &= F_{\text{kinetic,zx}} - F_{\text{friction,xz}} - F_{\text{inert}} \\
 F_{\text{tip,x'}} &= F_{\text{result,xz}} \times \cos\alpha \\
 F_{\text{tip,z}} &= F_{\text{tip,x'}} \times \cos\beta \\
 F_{\text{tip,y}} &= F_{\text{grip,y}} + F_{\text{g}} \\
 F_{\text{result,x'y}} &= \sqrt{((F_{\text{result,xz}} \times \cos\alpha)^2 + (F_{\text{grip,y}} + F_{\text{g}})^2)} \\
 F_{\text{tip,axial}} &= F_{\text{result,x'y}} \times \cos\varepsilon; \text{ with } \varepsilon = \gamma - \delta \text{ and } \delta = \tan^{-1}(F_{\text{tip,y}} / F_{\text{tip,x'}}) \\
 F_{\text{grip,axial}} &= F_{\text{grip,result}} \times \cos\Phi
 \end{aligned}$$

### 3.2.2 Conclusion for transducer development

The following conclusions can be drawn from the description of the model above (section 3.2.1). Ideally, pen contact force would be recorded at all four contact sites (thumb, index and middle finger and a proximal portion of the hand (between metacarpophalangeal MCP joints of the thumb and the index finger or at the proximal phalange of the index finger).

Ideally, both shear forces and normal forces to the pen tip are recorded by the system that will be developed. This would enable to perform complete analysis of the exerted forces.

The axial pen tip pressure could be measured with most standard script digitising tablets, but these are uncalibrated and give unquantified pressure levels rather than force values. In order to derive the exact axial pen tip force, it is required to know the two pen inclination angles: projections in the vertical (y,z-plane) and horizontal (x,z) plane pen and vertical reaction force at the pen tip. Pen inclination angles could be derived from a motion analysis system, using a special marker set on the pen. The forces acting on the pen tip in the horizontal (x,z) plane are affected by the friction force, which is determined by the combination of the pen nib and paper, inertia forces and applied grip force to the pen.

At this stage friction, inertia and grip force are unknown. Ideally the transducer system would enable to measure grip force in the two orthogonal directions of the horizontal orientated plane. The inertia force is relatively small and because of the erratic motions involved with handwriting and continuously changing magnitude and direction, it may be neglected. Ideally, a second system would be developed to measure friction force between pen and paper.

### **3.3 Design procedure**

As guide for the design procedure the methods prescribed by van den Kroonenberg and Siers, 1998 and Roozenburg and Eekels, 1995 were used. The applied procedure is made up of three phases.

The first phase is the design problem definition, which aims to make the objectives clear. This involves setting up the requirement specification and doing a function analysis of the individual functions and sub-functions of the device to be developed. In the conceptual phase physical principles are furnished as solutions to the functions to be performed by the device. Design concepts are all suitable combinations of principle functions that were found.

At the outset, the design concepts do not have a physical shape, but are rather abstract descriptions of functions. On arriving at the best concept, the actual design phase is started, which will provide a physical design that can be manufactured as a prototype.

### **3.4 Definition phase**

#### **3.4.1 Requirement specification**

The requirements, desires and constraints of the design regarding technical functioning and manufacturing are listed in table 3.1a and 3.1b. The requirement specifications were expanded from preliminary investigations and results of a pilot study (R.C.Zietsma, 2003, Grip force during handwriting, MSc thesis, Bioengineering Unit, University of Strathclyde) and a detailed literature search on grip force transducer designs for handwriting activities, summarised in 2.2.3.

The desired requirements can be divided into firm requirements, which must be fulfilled and variable requirements, which have to be fulfilled within a certain range. Desires are aspects that could influence the decision making, since they will give more value to the product when included. Constraints will limit the number of suitable technical principles to fulfil the desired functions of the design or the abilities to realise it.

A separation is made into criteria that must match with the technical functioning for the desired purpose and criteria that must match the ability to realise the design into

a working device. A motivation for the design criteria specifications (tabel 3.1) and literature study is given below. The numbers between brackets correspond to the numbers in the table.

<b>Technical Functioning</b>			
<b>Requirements</b>	1	Grip force transducer output in data sheet format; electronic graphical representation for processing	
	2	Force measurement on thumb, index and middle finger (see desires below: beam contact)	
	3	Pen shape: triangular shaped pen grip area	
	4	Grip force transducer integrated with WACOM digitiser stylus	
	5	Synchronisation of digitiser, (x,y and z-coordinates), grip force transducer and vicon movement data	
	6	Lenght (l)	$110 < l < 140$ mm
	7	Transducer beam width (for pen grip ergonomics)	6mm
	8	Rigid pen 'feel': maximum transducer beam deflection $\delta_{max}$	$\delta_{max} < 1$ mm
	9	Diameter (d) of circle surrounding triangular gripper	$d \leq 20$ mm
	10	Minimum measurable force range (F) on each beam:	$0 < F < 10$ N
	11	Resolution	0.05 N
	12	Sampling frequency (f): Digitiser (x,y and z-coordinates) Grip force measurement Vicon movement data	$f_{sampling, d} \geq 100$ Hz $f_{sampling, force} \geq 1000$ Hz $f_{sampling, vicon} \geq 120$ Hz
<b>Desires</b>	13	No beam contact at proximal portion of the hand	
	14	Shape of transducer beams: Flat triangular arranged grip pads	
	15	Optimal weight distribution to minimise inertial and gravitational torque development	
	16	High friction coefficient between fingers and pen: no smooth surface of grip pads	
	17	Concentric movement transducer grippads;	
	18	Monolithic transducer beam construction; No mechanical energy loss due to two-piece transducer beam construction.	
	19	Beam fixation 100% locking to ensure linear response.	
	20	Measure force application at all four contact points between pen and hand	

	21	Measure shear forces and moments applied to the pen in addition to grip force normal to the pen surface	
	22	Measure pen nib force	
	23	Record pen inclination angles: projections in horizontal and vertical plane	
	24	Measure friction force and coefficient between pen nib and paper	
<b>Constraints</b>	/		

Table 3.1a: Design requirements, desires and constraints regarding technical functioning.

<b>Manufacturing</b>			
<b>Requirements</b>	/		
<b>Desires</b>	/		
<b>Constraints</b>	20	Time limit: realisation within 4 months	
	21	Material and manufacturing costs	Max. £ 300,-

Table 3.1b: Design requirements, desires and constraints regarding manufacturing.

### Pen shape (3)

People most commonly write while holding the pen in tripod grip with the thumb in opposition to the index and middle finger (Fig.3.1). The pen makes contact with the hand at four sites: a proximal portion of the hand (between metacarpophalangeal MCP joints of the thumb and the index finger or at the proximal phalange of the index finger), with the tips of the thumb, the index finger and the lateral surface of the distal phalanx of the middle finger (Latash et al, 2003).

From a pilot study (Zietsma, 2003) it was concluded that subjects show significant variation in the positioning of the fingers in a tripod grip and that positioning can be influenced by use of different pen shapes and sizes. The use of a triangular pen model is seen to decrease the variability of positioning. Children are usually taught to learn to write while holding the pen in tripod grip and often triangular shaped pens are used.



*Fig.3.1: Tripod pen grip: See text for details.*

A study on how the type of pencil grip affects (four-finger pencil grips, the triple and quad grips) the speed and legibility of fourth-grade high school student's handwriting concluded that all grips to be equally functional (Koziatek and Powell, 2003).

However, the tripod grip is the most common grip, the pen design aims at its measurement. Accordingly, the prototype to be developed is required to have a triangular gripping area, allowing pen interaction to be studied with pen grip as natural as possible.

A triangular shaped gripping area may also enhance the pen-hand interaction as steering the pen by the fingers positioned at three flat grip surfaces may decrease the motor processing demands compared to curved surfaces. An elaboration on this follows under *Shape transducer beams (14)* and *Weight distribution (15)*.

#### *Transducer beam width (7)*

The transducer beams should provide sufficient grip area, but nevertheless be small to contribute to the right 'pen feel' and not make the pen bulky. A beam width of 6mm would be appropriate. See also transducer beam shapes (14).

#### *Transducer beam deflection (8)*

The transducer beam deflection should be kept as small as possible, but also be sufficient to allow sensitivity in force measurement. It was concluded that  $\delta_{\max}$  should not exceed 1mm to give a rigid pen feel.

### *Pinch force range (10)*

Literature does not report on handwriting grip force ranges, but reports about maximum force applications during a variety of other object manipulations. The average maximum tip pinch force applied from thumb tip and index finger tip as found by Mathiowetz et al (1984) was 80 N for male adults and 50 N for female adults. The average maximum pinch force applied from the pads of the thumb and index finger for males and females are respectively 85 and 63 N as found by Crosby et al (1994). Chao et al found for both pinch forces applied from the tips and pads of the thumb and index finger values of 60 N and 50 N for males and females respectively.

The average maximum pinch force applied from thumb pad and middle finger pad is 70 N for male adults and 45 N for female adults (Imrhan et al, 1989).

The average maximum palmar pinch force applied from thumb in opposition to index and middle finger tips is 111 N for males and 76 N for females (Mathiowetz et al). After the age of 55-59 years old, the strength gradually decreases (Mathiowetz et al).

An intuitive test during the pilot study as approximation of grip force values during normal handwriting lead to a prototype design with a measurable force range of 0 - 2N on thumb, index and middle finger and very high resolution measurement. However, the variations in grip force during handwriting among people is large and such a small sensor range was too restrictive. Accordingly, to avoid saturation effects, the transducer should enable to measure forces up to 10N on each finger and be capable of measuring grip force for all healthy subjects with normal hand anatomy.

### *Sampling frequency (12)*

Strain gauge force measurement at frequencies of 1000Hz is required in order to obtain sufficient frequency resolution to perform Power Spectral Density analysis. In addition, as handwriting movements are fast and potentially erratic, finger tip forces on the pen were expected to change at high frequencies and therefore, a sampling frequency of 1000Hz is required to avoid aliasing effects.

Basing the design around the Wacom stylus and digitiser tablet introduces constraints to available sampling frequencies and communication with the host computer for sampling of script, related to Wacom digitiser and (Wintab) drivers and recording software. However, based on the requirements of such a system as

reported by Teulings et al (1984), it was concluded that sampling frequencies between 100 Hz and 200Hz, which are enabled with Wacom tablets, were sufficient for recording script. Paragraph 3.3.1 explains more about the required sampling frequencies for script.

#### *Beam contact (13)*

Normally, the pen makes contact with the hand at four points (see: *Pen shape (3)*). Each of three transducer beams should only receive pressure from the pad of thumb, pad of index finger or lateral surface of the distal phalanx of the middle finger. The fourth contact point with the pen (between metacarpophalangeal MCP joints of the thumb and the index finger or at the proximal phalange of the index finger) should not apply pressure to any of the beams.

#### *Shape of transducer beams (14)*

In order to keep the gripping area of the pen as small as possible while still providing an ergonomic grip area, the gripping areas on each beam were designed to be flat.

#### *Weight distribution (15)*

Humans use both visual and tactile senses for feed forward parametric adaptation of fingertip forces and grasp kinematics to object properties as shape, surface friction and weight (Johansson 1996, 1998; Goodwin et al, 1998; Jenhalm et al. 2000). An adequate safety margin is kept against rotational slip (Goodwin et al 1998) and when the torque load develops, tactile information related to localized rotational slips may update memory systems for parametric control of force-torque coordination. A pen design should minimise torque development due to inertial and gravitational effects by optimal weight distribution. The centre of gravity should be aimed to lie in between the pen-fingertip contact areas and fourth contact point, the lateral surface of the distal phalanx of the middle finger.

#### *Transducer beam construction (18)*

The transducer beams need to be monolithic - machined in one piece from a solid billet - in order to ensure freedom from hysteresis and non-linearity. This approach also aids to improve repeatability (Perry et al, 1992). In the pilot study hysteresis was observed as a result of a two-piece beam construction (which was required to avoid interference of the beam with the Wacom pen induction coil).

Ordinarily, the natural frequency of the beam should be as high as it can be made consistent with the specified sensitivity and other operating requirements for the transducer. This normally calls for a rigid, low-compliance design, without unnecessary mass (Perry et al, 1992).

*Measure forces at all four contact points (20)*

The pen makes contact with the hand at four points as described in 3.2.1 and requirement of pen shape (3) above. However, the fine motion of the pen tip is enabled by the biomechanical plant formed by the hand, mainly by excursion of finger tip motion. Therefore, it is firstly required to measure forces applied by thumb, index and middle finger forces to investigate pen control. For calculation of the total force applied to the pen to establish pen motion, it is desired to also measure the force applied by the fourth contact point (as described in 3.2.1).

*Measure shear forces and moments in addition to grip force (21)*

To understand the complete mechanical interaction between pen and hand (as described in 3.2.1), it is required to also include the shear forces that are applied to the pen as well as the moments around the centre of gravity that are required to balance the pen. However, as previously stated, it is the excursion of finger tip motion that mainly controls the fine motion of the pen tip.

*Measure pen nib force (22)*

The pen tip force should be considered when studying the overall force system acting on the pen as described in section 3.2.1. Standard digitiser tablets do not enable accurate measurement and a separate transducer could be incorporated into the pen tip or a writing surface could be used that is pressure sensitive.

*Record pen inclination angles: projections in horizontal and vertical plane (23)*

The pen inclination angles should be measured if the axial pen tip force was to be calculated from the recorded vertical pen tip force or vice versa.

*Measure friction force and coefficient between pen nib and paper (24)*

Both the exerted forces on the pen and the friction between tablet and pen tip affect the resulting acceleration. The friction should be taken into account when analysing the complete force system as described in section 3.2.1 and calculating axial and

vertical pen tip force. The friction coefficient for the pen-paper combination could be derived and the friction force can then be calculated from the normal force and the friction coefficient ( $F_{\text{friction},xz} = \mu \times F_{\text{tip},y}$ ).

### 3.4.2 Function analysis

The two main functions of the device to be developed are: 1) measuring grip force, while at the same time 2) carrying out digitising of handwriting with the input stylus of a digitiser tablet. In figure 3.2 a schematic representation is given of the subfunctions for the design in order to perform both digitising and grip force measurement.

The physical principle, used for fulfilling the function of conversion of the applied mechanical work to an electric signal is the major concern in development of the transducer. This solution will give direction to solutions for fulfilling the functions of attaching the force sensor to the digitiser stylus and providing contact between finger pads and sensor. Attachment of the transducer onto the digitiser stylus is linked to the functions supplied by the original housing of the Wacom stylus, namely protecting and handling.

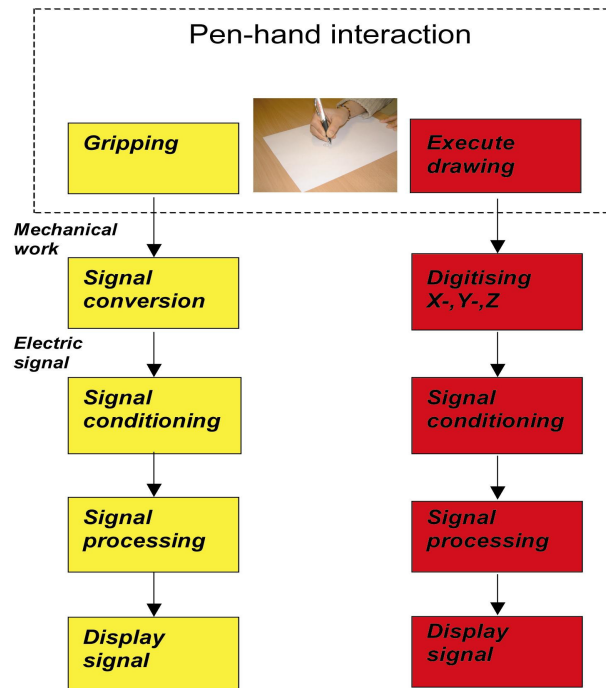


Fig.3.2: Schematic representation of transducer sub-functions.

### 3.5 Conceptual phase

Firstly the prototype concept that was chosen is described in 3.5.1. Alternative solutions that could have been deployed to fulfill some of the functions are described in 3.5.2 with reasons for rejecting these options.

#### 3.5.1 Prototype concept

The prototype concept integrates the above functions into a pen, equipped with barrel (cantilever beam) grip force transducer, which houses the digitising electronics. Contemplations leading to this prototype concept, including transducer design, literature review and decision making on physical principles to carry out individual device functions can be found in: R.C.Zietsma, 2003, Grip force during handwriting, MSc thesis, Bioengineering Unit, University of Strathclyde, pp 23.

A triple set of strain gauged cantilever beams, arranged in a triangular shape, measures grip force applied by thumb, index and middle finger in triple grip. The strain gauges on each beam convert the mechanical strain (which corresponds to the bending moment that results from force applied by the finger) into an electric signal. This principle enables low cost force measurements to be obtained with a high level of accuracy.

Ideally, the *exact* force applied to the barrels would be measured. Therefore, bending moments need to be measured at two locations along the beams, which are at known distance from each other. The bending moments  $M_a$  and  $M_b$  are experienced by the gauges at distances of respectively  $a$  and  $b$  from the point of application. Whereas:

$$M_a = Fx_a \text{ and } M_b = Fx_b \quad \Rightarrow \quad M_a - M_b = F(a-b)$$

Since the distance  $(a-b)$  between the gages is known, the force  $F$  on each beam can be derived. As two strain gauge bridges are required for each beam and each bridge uses 4 wires, a total of 24 wires are required for a pen with three beams. However, a total of 24 wires will lead to a size problem as the pen needs to become large enough to internally house both the 24 wires and a 24-pin connector that connects the pen to the external wires that are fed to the strain gauge amplifier. Moreover, the weight of the 24 wires and their connector to the amplifier could constrain pen movement.

Therefore, it was decided to use one bridge per beam, requiring three bridges and thus a total of 12 wires for the pen. This smaller pen has more potential use as a research tool as the smaller size will give a more natural pen 'feel' and enables to investigate characteristics of grip force modulation equally well. The output of the strain gauge measurement obtained when using one full bridge to measure bending moment at one location only, will not be a direct relation between strain and finger force, but a relation between strain and moment. Nevertheless, as the point of force application can be approximated for each subject, the finger force can be approximated, but with accuracy lower than when calculating finger forces directly with two bridges per beam because of the contact between pen and beam not being a point contact, but a contact area with a nominal point (centre point) of contact that may change over the writing trajectory. Nevertheless, measuring the beam's response to bending moment allows comparison between force modulations in different trials for several subjects, which at this stage of development is considered more important than the exact force value. As part of the transducer beam design considerations on page 62, comments are made on the likely inaccuracies that may result from using only one bridge per beam instead of two bridges per beam to derive the exact force value.

Mounting pairs of gages on both upper and lower side of the cantilever beam and using them in a full bridge arrangement (using four gauges) increases the sensitivity and compensates for temperature effects. Therefore, a full bridge is desired. The full bridge arrangement with gauges R1 to R4 is shown in figure 4.2.

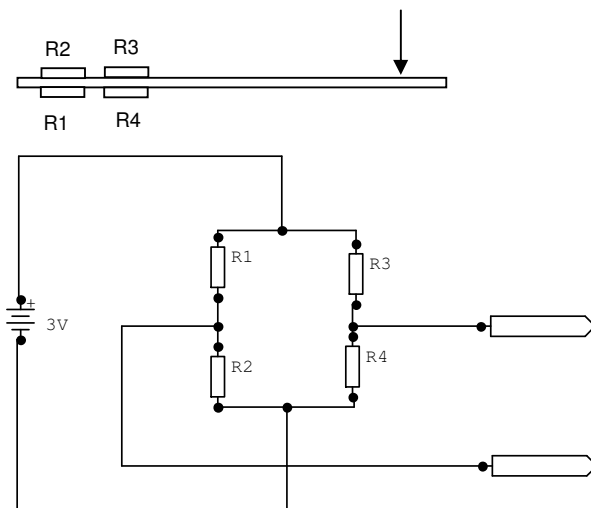


Fig. 3.3: Full Wheatstone's bridge arrangement for each cantilever beam.

### 3.5.2 Rejection of hypothetical concept considerations

#### *Alternative sensor technology*

Alternative to the strain gauge sensor technology, a number of off the shelf sensors could have been implemented. A number of miniature force sensors were identified as suitable, including Entran ELFS series and ATI load cells. However, the high cost price and bulkiness of the sensors that would make the transducer pen unnecessarily large, made them less suitable than developing a custom strain gauge grip sensor system.

#### *Incorporating force recordings at fourth contact point*

It was considered to include a fourth force sensor in addition to sensors that record forces from thumb, index and middle finger. However, this increased the number of wires from the pen to the recording equipment. As the small pen tip excursion originates from the fingers, it was decided to only measure these in the prototype.

#### *Incorporating recording of moments exerted to balance the pen*

It was considered to include sensors that enabled recording of moments that are required to balance the pen. However, this increased the number of wires from the pen to the recording equipment if strain gauge sensor systems were used. In addition, if off the shelf sensors were used, this would make the pen too bulky to be comparable to normal pens and this would increase the cost price. As the main modulation of fine pen tip motion originates from the fingers, it was decided to only measure these in the prototype.

#### *Alternative strain gauge transducer beam width*

Dummy transducer pens were machined with a different transducer beam widths. It was concluded that both transducer beams with width lower than 6mm and larger than 6mm that were arranged in a triangular arrangement were found uncomfortable to handle.

### *Alternative pen body shape*

To assess pen ergonomics, a number of dummy transducer pens were machined from POM (poly-oxymethylene, also known as Acetal). Models with a constant pen diameter, with same size as the strain gauge transducer, were found to be too bulky. Tapering the pen width from the grip sensor upwards was found easier to handle.

### *Wireless data transfer between pen recording computer/software*

It was considered to set up a wireless data connection between the pen and computer, using blue tooth or zigbee modules. However, this required using microcontrollers and printed circuit board design and the pcb and communication modules would make the pen unnecessarily large.

### *Recording of pen inclination angles*

It was considered to derive the pen orientation in three dimensions: the projected angles in horizontal and vertical plane. This is possible using light reflecting markers on the pen that reveal the pen orientation (e.g. using markers on shafts with different lengths for each of the three orthogonal axes).

The pen inclination angles would be required if the axial pen tip force was to be calculated from the recorded vertical pen tip force or vice versa. However, this would complicate the design, ease of handling and it at current stage, pen inclination angles and vertical pen tip force would not contribute to the aims of the project.

### 3.6 Design phase

A short expound of the design phase will be given here, which is the elaboration of the conceptual design (as described in 3.5) to the final design.

The CAD design drawings, developed with Autocad software are shown in appendix 1. The design of the pen has two parts, which make up the housing. Fig.3.4 shows a 3D-model of the upper and lower pen part, developed with Pro-engineer software and Fig.3.5 shows the ring-beam construction. The final manufactured prototype pen that was used for data collection is shown in fig 3.6b, together with two prototypes from earlier stages of the pen development in 3.6a.

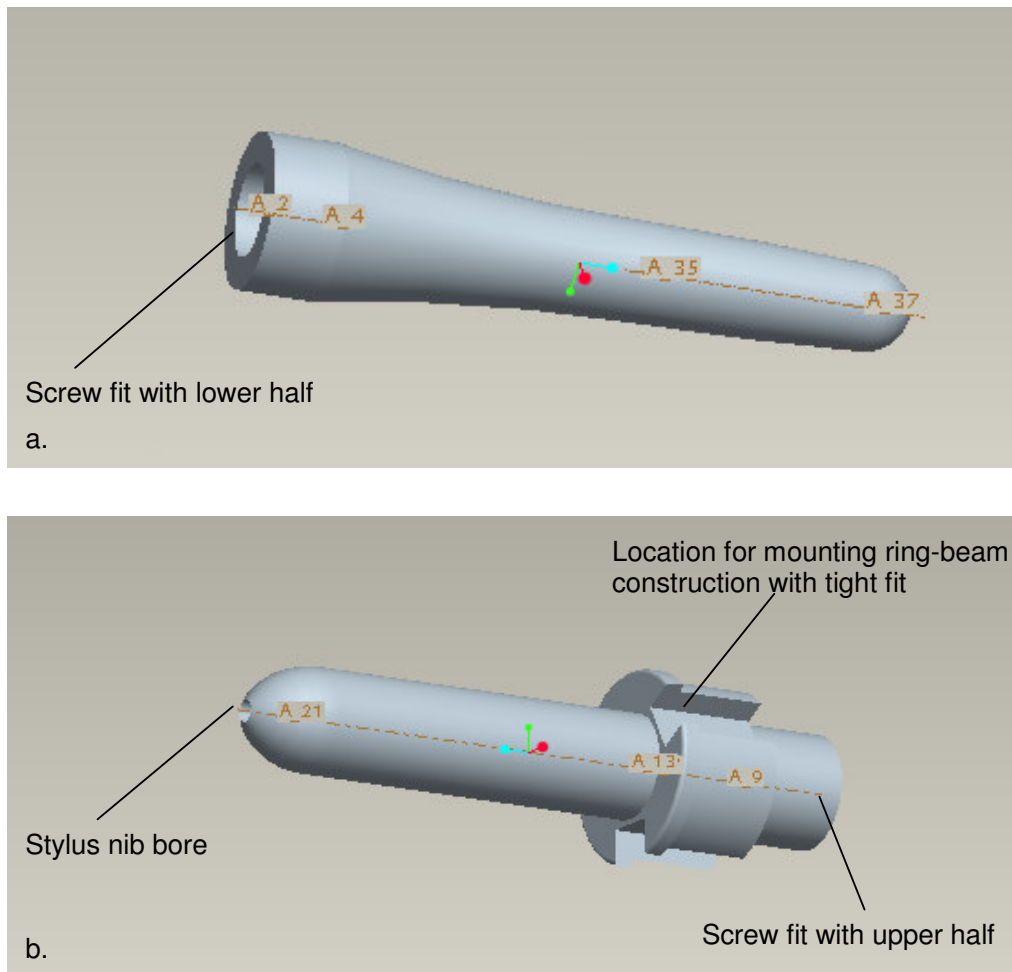


Fig 3.4: Model grip force transducer pen core.

a: upper half

b: lower half

### ***Pen housing design***

The housing of the pen (Fig.3.4) was built up from two parts, connected with a screw fit that makes the pen service-able. The pen was built up from Polyoxymethylene (POM), also known as Acetal, which is relatively light, has good machining properties (for ease of manufacturing and good surface quality can be obtained) and has sufficient rigidity. Internal space was accurately machined for exact positioning of Wacom electric print plate and all electric wiring.

### ***Beam-ring design considerations***

#### *Geometry*

The transducer beams and ring for positioning the beams were designed as one-piece construction for ease of positioning and moreover to avoid energy loss due to mechanical hysteresis in the connection of components, which would lead to a non-linear transducer response. Fig.3.5 shows the grip measuring element, developed with Pro-engineer software. The beam-ring is mounted with a tight fit over the pen housing. The geometry of the parts ensures locking in all directions, again to avoid any mechanical hysteresis and non-linearity of the transducer due to displacement of the parts.

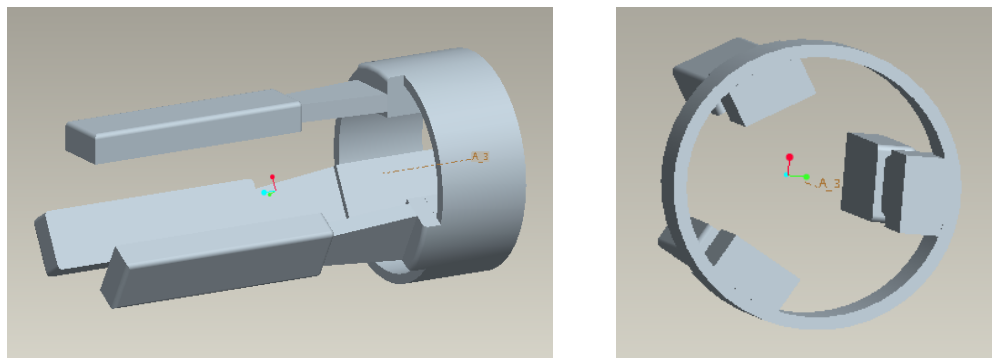


*Fig 3.5: Model grip force measuring ring-beam construction.*

#### *Material*

The ideal transducer beam material is aluminium, which has relatively low mass, though sufficient rigidity, has good properties for mounting strain gauges at high temperature and is creep resistive for the application. Interference with the induction

coil of the digitiser pen was not found to be a problem as long as the beam is placed at least 18 mm away from the stylus tip. The beams were machined from HE30 (AlSi1MgMn). The HE30 properties as specified by supplier Richard Austin are shown in appendix 2A. In addition, a tensile test was carried out and results are shown in appendix 2B. Linear elastic behaviour occurs up to at least stresses of  $\sigma=250\text{Mpa}$  and therefore the maximum allowable stress is  $\sigma=250\text{Mpa}$ .

#### *Beam geometry: gauging area thin and tapered*

The deflection of the transducer beams was largely concentrated in the gauge area by locally decreasing the thickness. The tapered shape of the gauge area gives a uniform strain distribution over the length of the area. Without tapering the gauge area, the strain would decrease linearly from the maximum at the fixed end.

#### *Limiting beam deflection*

To keep the diameter surrounding the gripping small and to give a natural (rigid) pen feel, the beam deflection was kept as low as possible and was limited to  $\delta_{\text{max}}=0.46\text{mm}$  when a force of  $P=10\text{N}$  is applied. High sensitivity was established by using a full strain (four) gauge bridge on each beam as explained below.

The transducer beams should both provide a gripping area for ergonomic pen-hand interaction and highly accurate and robust force measurement. Safety calculations for stress in the beams and strain on the gauges were carried out iteratively to derive the exact dimensions of the bending beams. Macros were written for the safety calculations and safety checks for the final dimensions are given in appendix 3.

#### *Transducer output and safety calculations*

The nominal point of force application is 30 mm away from the top of the gauging area. Force application at nominal point of contact was limited by geometry of pen (which function as limiter for the beam deflection) to  $P=10\text{N}$ . The maximum allowable force is  $P_{\text{allowable}}=15.8\text{N}$ , so as not to exceed the allowable stress,  $\sigma_{\text{max}}=250\text{Mpa}$ , in the transducer beams when a safety margin of 30% is taken into account.

The maximum strain ( $\epsilon_{\text{max}}$ ) for  $P=10\text{N}$  does not exceed  $1500\mu\epsilon$ , which theoretically gives endless lifetime of the gauges.

The strain gauges used (Shown Measuring Instruments N11-MA-2-120-23: resistance = 120.3  $\Omega$ ; gauge factor K = 2.15; gauge length=2mm) with a four gauge fully active bridge will produce an output signal of 2.15 mV/V bridge excitation at nominal strain  $\epsilon_{\max}$ =1000 micro strain. With amplification G=200 and bridge excitation  $V_{in}$ =3V, an output voltage  $V_{out}$ =1.3V will be measured at nominal strain  $\epsilon_{\max}$ =1000 micro strain.

#### *Likely inaccuracies*

The finger positioning on the transducer beams is not fixed. It is generally assumed that during normal handwriting the finger positioning does not change (Latash et al, 2003). However, it is not difficult to imagine slight variation of pen grip during pen motion. Consequently, finger motion will induce inaccuracies as the bending moment around the gauging area will vary. With the nominal point of force application being 30 mm away from the top of the gauging area and the assumption that the variation of finger positioning is not larger than +/-3mm, inaccuracies up to 10% may occur.

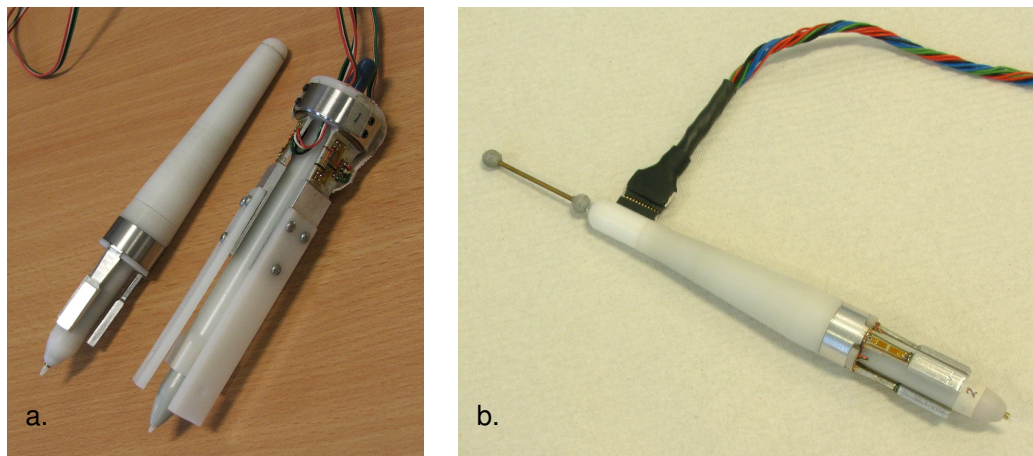


*Fig 3.6a: Grip force digitising pen prototype 1 and 2; Fig 3.6b: Grip force digitising pen prototype 3.*

### *Manufacturing and assembly*

The ring-beam construction was cnc-manufactured from the pro-engineer model by an external contractor. The lower pen half was manually manufactured by the external contractor and the top half of the pen was manufactured in the Strathclyde Bioengineering Unit.

All the strain gauge wiring and connecting plates were placed within the pen to give it a neat appearance. The pen was connected to the three strain gauge amplifiers by 12 highly flexible and light weight silicon covered wires: Multi-Contact type SILI-E 0.15, with nominal cross section  $A_{\text{nominal}}=0.15\text{mm}$  and cover outer diameter  $d_{\text{outer}}=1\text{mm}$  (specification sheet in appendix 4, which were plaited together. The connecting wires were made detachable by a miniature connector to aid servicing if required (See Fig.3.6b).

The light reflecting markers for use with the Vicon motion analysis system were screwed and glued to a brass rod that was fitted into the top cap of the pen body. The centre of gravity of the fully assembled pen was 80 mm from the bottom of the lower pen half, which is just above the ring of the grip measuring element.

## 3.7 Calibration

A calibration was performed in loading and unloading of the three transducer beams. Test equipment, procedure and results are detailed respectively in the sections 3.7.1., 3.7.2 and 3.7.3.

### 3.7.1 Equipment

The loads to the grip force transducer beams were applied by an Instron strength testing machine (Fig.3.7), which both measured applied force and resultant beam deflection. The grip force transducer was held in place on the Instron machine by a clamp that was secured by a magnet onto the machine (Fig.3.7a). Each beam was supplied with a dimple to carry a ball bearing that allowed point application of the load (Fig.3.7b). The output voltages of the transducer were measured from the strain gauge amplifier (described under methods in 4.3.3) with a multi-meter (3.7c).

### 3.7.2 Procedure

Each transducer beam was tested separately. Increasing loads were applied to the beam from zero to the maximum with manually adjusted increments. The increment size varied, but was approximately 0.25 N. The load was then reduced in analogue fashion to zero again. This procedure was repeated three times for each beam.



*Fig.3.7: Calibration set up.*

*a: Clamping the grip force transducer on the Instron machine;*

*b: Point force application by dimple and ball bearing;*

*c: Reading out the output voltage from the transducer.*

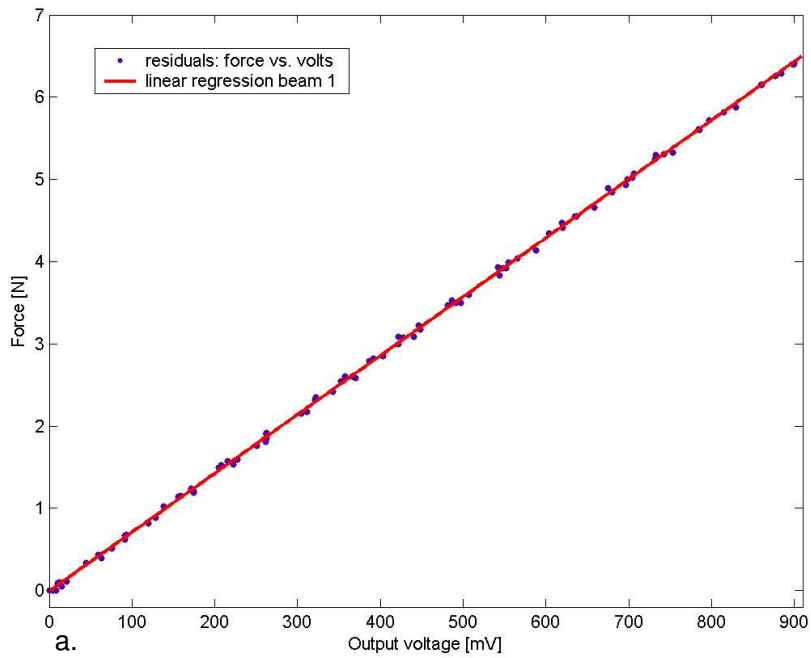
### 3.7.3 Results

A linear regression analysis gave calibration factors for each beam. Results can be found in Fig 3.7, 3.8 and 3.9.

The maximum applicable load to the beams should not exceed 10N as the beams should be stopped at maximum deflection  $\delta_{\max}=0.46\text{mm}$ . However, due to manufacturing inaccuracies of the lower pen half, the maximum applicable force varied for the three beams. The maximum stop loads for each beam that end the linear range of the calibration curve were as following. Beam 1 stopped at 6.4N; beam 2 stopped at 10.35N and beam 3 stopped at 7.5N.

The R-square and adjusted R-Square values higher than 0.999 show that the linear model fits the data well. RMSE values lower than 0.1 is another proof for a good fit of the linear model for each of the beams. No hysteresis can be seen.

Predicted force values with the linear regression model with a 95% confidence differed only +/-1% from the actual measured nominal force value (+/-0.05 N at 5N load). No cross talk was seen.



**Linear model:**

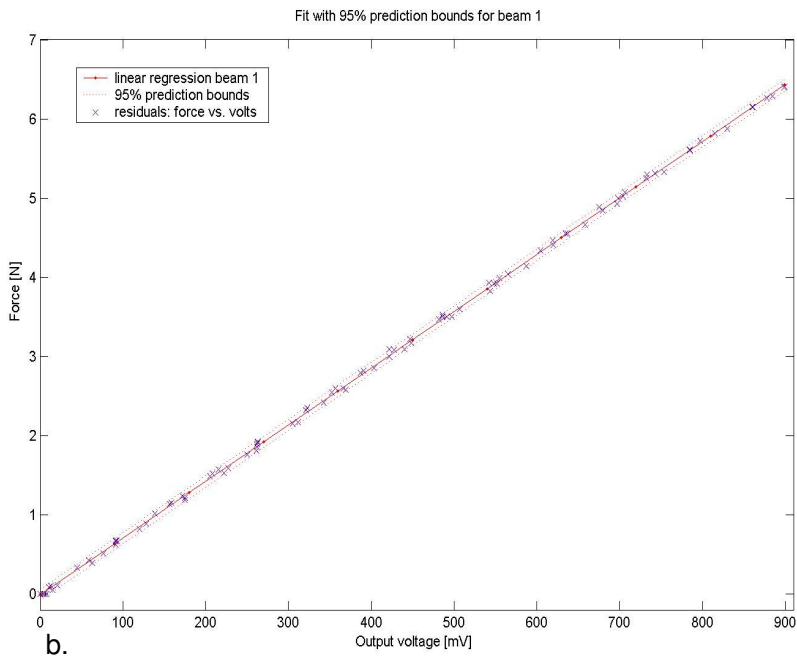
$$f(x) = p1 * x + p2$$

**Coefficients:**

p1 =  
0.007158  
p2 = -  
0.009047

**Goodness of fit:**

SSE: 0.1124  
R-square:  
0.9997  
Adjusted R-  
square: 0.9997  
RMSE:  
0.03496



**Coefficients for f(x) with 95% confidence bounds:**

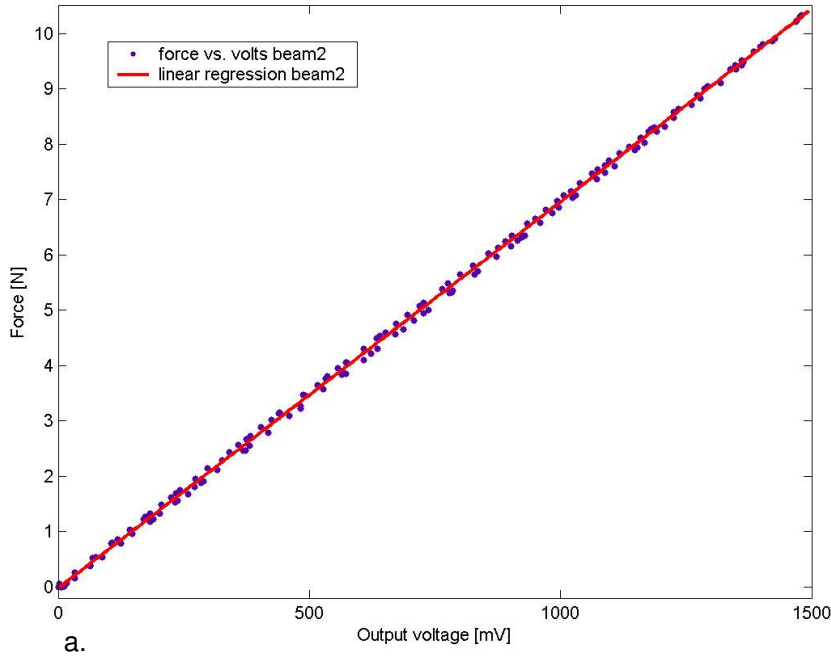
p1 =  
0.007158  
(0.007131,  
0.007184)

p2 = -  
0.009047  
(-0.0221,  
0.00401)

Fig. 3.7: Calibration results for beam 1.

a: linear regression;

b: 95% confidence interval



**Linear model:**

$$f(x) = p1 * x + p2$$

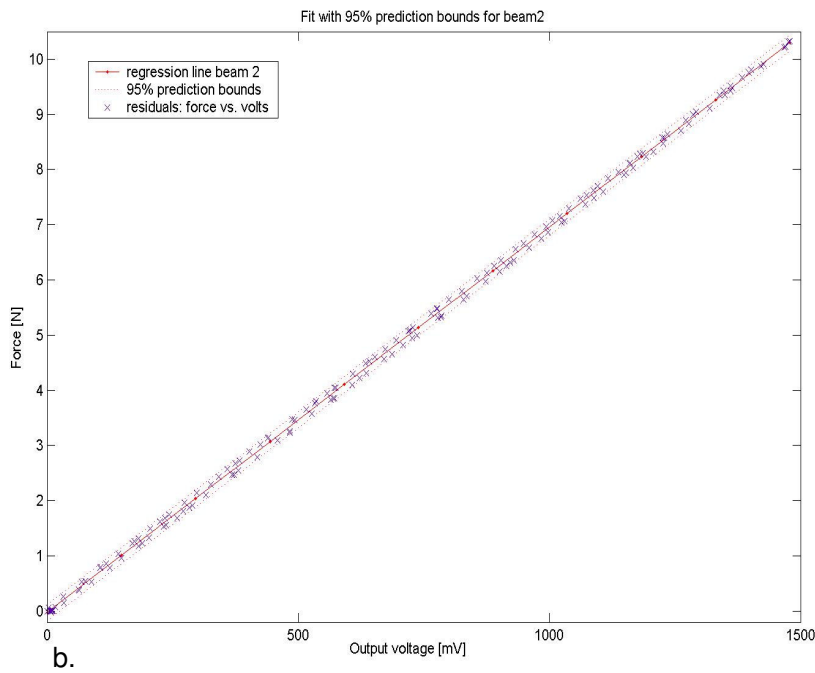
**Coefficients:**

p1 =  
0.006979  
p2 = -  
0.02494

**Goodness of fit:**

SSE: 0.9026  
R-square:  
0.9994  
Adjusted R-  
square: 0.9994  
RMSE:  
0.07464

a.



**Coefficients for f(x) with 95% confidence bounds:**

p1 =  
0.006979  
(0.006953,  
0.007005)

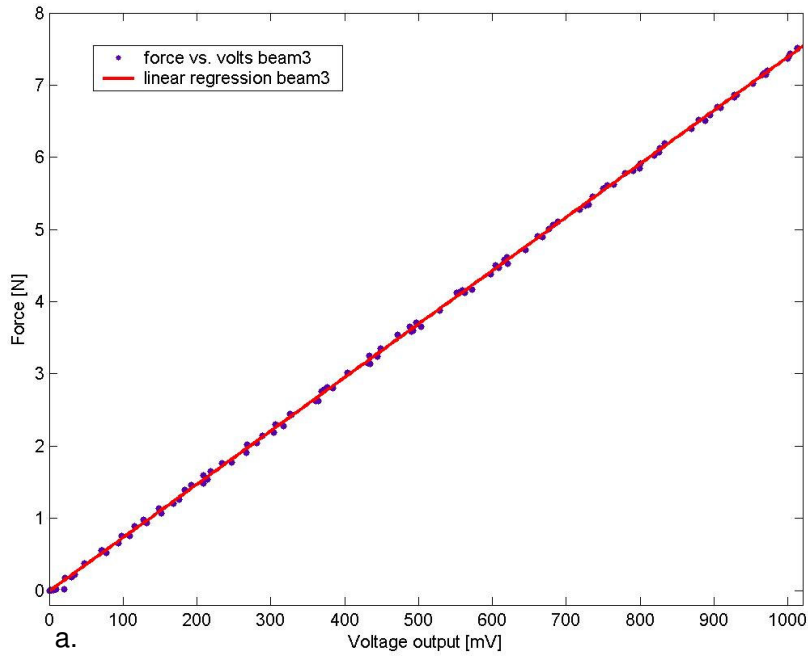
p2 = -  
0.02494  
(-0.04629, -  
0.003585)

b.

Fig. 3.8: Calibration results for beam 2.

a: linear regression;

b: 95% confidence interval



**Linear model:**

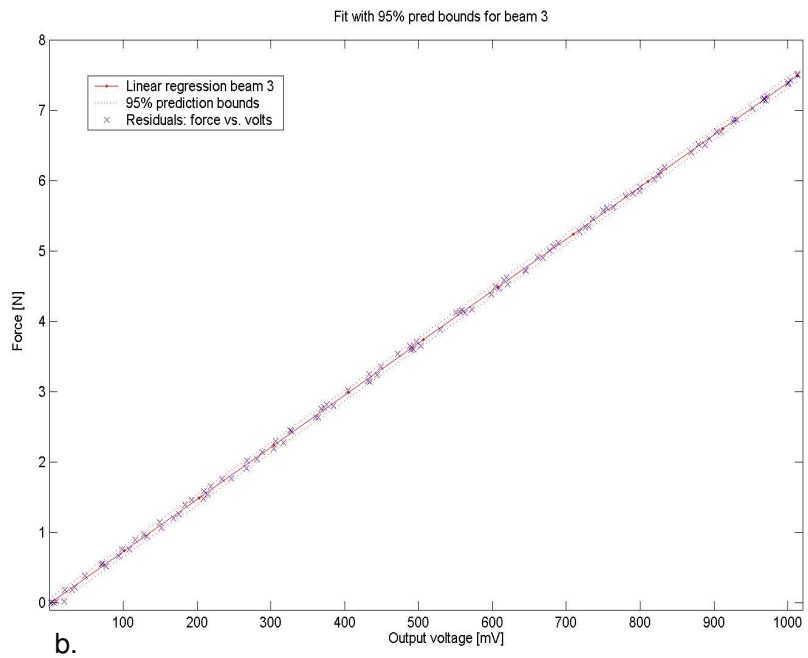
$$f(x) = p1 \cdot x + p2$$

**Coefficients:**

p1 =  
0.007398  
p2 = -  
0.01096

**Goodness of fit:**

SSE: 0.1562  
R-square:  
0.9997  
Adjusted R-  
square: 0.9997  
RMSE:  
0.03717



**Coefficients for f(x) with 95% confidence bounds:**

p1 =  
0.007398  
(0.007377,  
0.00742)  
  
p2 = -  
0.01096  
(-  
0.02371, 0.001  
788)

Fig. 3.9: Calibration results for beam 3.

a: linear regression;

b: 95% confidence interval

## **4 Methodology**

### **4.1 Introduction**

The previous chapter described the development of the grip force transducer that was used to house the Wacom Intuos2 digitiser stylus electronics. This chapter describes both the other building blocks of the system and the data analysis techniques.

First of all, section 4.2 gives an overview of the test system and its building blocks. Section 4.3 describes the recording techniques for grip force, script and motion capture in detail. The data analysis techniques are described in 4.4.

### **4.2 System overview**

The set up, test procedure and potential hazards are described in 4.2.1. The axis frame for the setup is shown in section 4.2.2.

#### **4.2.1 Test set up**

##### **Set up**

The following safety approved electronic system components are used for the testing (also shown in the blockdiagram in Fig.4.1):

Sampling script kinematics:

- Wacom Intuos2 script digitiser;
- desktop computer with a commercial software package (ScriptAlyzer) for sampling handwriting coordinates;

Sampling pen grip force:

- grip measuring digitiser pen;
- strain gauge amplifier;
- CED analogue to digital converter;
- laptop computer with Spike software and CED ADC for sampling grip force.

Motion capture and analysis:

- CCD cameras;

- Vicon workstation;
- host desktop computer, providing user interface by means of workstation software and bodybuilder software for analysis and development of scripts for analysis.

The setup in the Vicon lab is shown in Fig.4.2. The handwriting digitiser tablet is placed on a small black table. The grip force pen is connected to the strain gauge amplifier and the connecting cable is supported by a stand that is mounted on the table. The strain gauge amplifier and CED are placed on a trolley next to the table, which is two meters away from the subject.

The desktop computer for sampling handwriting coordinates and laptop with software for sampling of grip force are placed on the operator table. Wires between digitiser and desktop computer and between stain gauge amplifier, CED and laptop are routed behind the desk for safety.

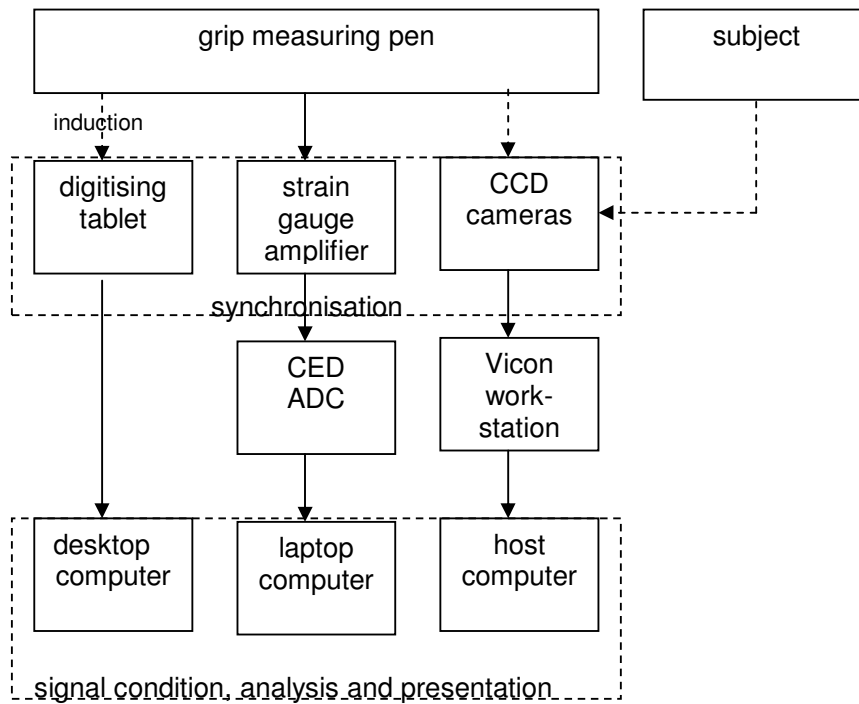


Fig. 4.1.: System components

## **Testing procedure**

The equipment was set up as described above. The subject was sitting on a chair behind the large table and was asked to hold the pen with the thumb, index and middle finger on respectively transducer beams 1, 2 and 3. The test procedure was then explained to the subject. Experimental protocols are described elsewhere. Data collection was initiated when the subject was instructed to contact the pen tip with a square target marked on the tablet surface. At this point grip force and x,y- and z-data collection became synchronized via Spike2 and MovAlyzer software respectively. The technical functioning of the synchronisation is described on page 92.

## **Hazards**

*Hazards associated with this test procedures at location:*

1. Vicon camera cabling on lab floor has potential to cause trips;
2. Subject should not be able to touch any non-isolated electronically powered recording devices.

*Procedure to eliminate risks:*

1. Keeping a clear route to the experimental set up. The subject will be led to the seating position by the experimenter who will also highlight any trip/fall hazards to the subject.
2. All electronically powered equipment is located 2 meters away from the subject and out of their normal reach.

#### 4.2.2 Definition global frame of reference

The global axis system for the test set up in the lab is shown in Fig.4.2. The positive x-direction is in the horizontal writing direction, to the right of the subject and the positive y-direction points upwards, away from the subject. The numbering of the 8 camera positions is related to the numbering of the connection points in the lab.

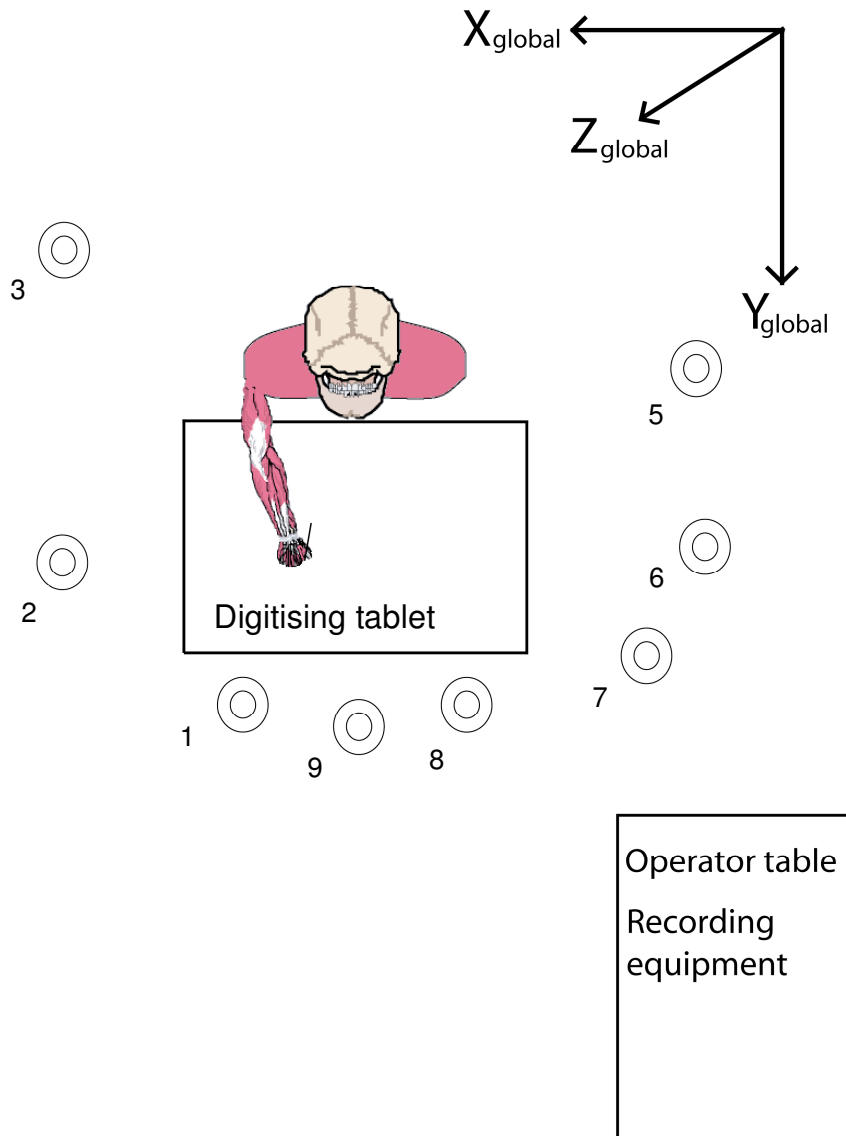


*Fig. 4.2.: Global axis system of the test setup with subject table, operator table and positioning of eight cameras.*

## 4.3 Recording techniques

### 4.3.1 Introduction

The following recording techniques are described: Script recording in 4.3.2, pen grip force measurement in 4.3.3 and motion capture with Vicon in 4.3.4.

### 4.3.2 Script recording

#### ***Script digitiser***

Modern digitiser tablets can readily be used to provide a means of recording handwriting in a digital form. In this study handwriting script was digitised with a Wacom Intuos2 A4 oversized tablet with serial port connection. This tablet allowed sampling script with high accuracy and good script quality, suitable for input into data processing applications and also allowed sampling of tip force with a resolution of 1024 pressure levels. The Wacom Intuos version 2 tablet had been previously tested extensively with both ScriptAlyzer software, a commercial software package for recording that was used in this study and Wintab drivers for accuracy. The A4 oversized format allowed easy mapping of sampled script to screen with ratio 1:1. Its large size (30:30cm active area) felt comfortable and less constraining than the smaller tablets that were tried earlier. The larger size also enabled motions involving large hand and arm movements, such as spiral drawing to be measured.

<b>Wacom Intuos2 A4 oversize digitiser tablet specifications</b>	
Dimensions	444x435.5x37mm
Active area	304.8X316.8 mm
Pressure levels	1024
Accuracy	+/- 0.50 mm
Resolution	100 lines/mm
Maximum sampling frequency	200 Hz

*Table 4.1: Wacom Intuos2 A4 oversize digitiser tablet specifications.*

The Wacom tablet and stylus communicate by the principle of electromagnetic induction. The tablet is composed of a covered grid of wires. The grid of wires alternates between transmit and receive mode with a frequency of 50 Hz (every 20 microseconds). The transmitted signal is received by a transmission/receive coil in the pen, which is part of a capacitor resonant circuit. The received signal is then attenuated through a modulator into a microchip. Two other signals are fed into the chip as well, emanating from the pressure sensitive tip and a switch.

The pressure sensitive tip is part of a capacitive sensing element in an a.c. bridge. The bridge output voltage changes corresponding to changes in tip pressure. The switch on the side of the stylus functions has three positions and can be pressed down on either the lower or upper side, which both results in activating one out of two micro-switches. The stylus is designed to also function as a mouse that signals receives in a relative co-ordinates system on the tablet. The side switch can be configured to function as mouse buttons. These switch facilities were not used in the present setup.

The three signals originating from the induction coil, the pressure sensitive tip and the switch are sent from the chip into the modulator, from where one signal is sent back to the stylus induction coil. The coil induces a current in the tablet, which is converted by the computer into three pieces of information, which are the pen location (or a signal that the pen is not touching the tablet), the applied pressure and the side switch status.

### ***ScriptAlyzer software***

Script was recorded from the Wacom digitiser using ScriptAlyzer software, purchased from Neuroscript ([www.neuroscript.net](http://www.neuroscript.net)). Although some data analysis features are included into the program, these were not used and all analysis were carried out with Matlab scripts that were written for processing and analysis of the recordings.

ScriptAlyzer software provided a convenient interface with the Wacom tablet, allowing script sampling at frequencies up to 200Hz, the maximum sampling frequency of the digitiser. Teulings et al (1984), who is one of the founders of Neuroscript, reported on requirements for high sampling frequencies for sampling of script, based on the presence of white noise (i.e., with zero mean, some specific standard deviation and uncorrelated over time) and quantisation noise (rounding-off

errors due to the finite spatial quantization-step size of the digitiser - between 0.01 and 0.3mm). Due to these noise sources, it is necessary to choose high sampling frequencies. The disadvantage of higher sampling frequencies is increased amount of data and computing requirements. However, as previously mentioned, with modern systems this is not a limitation. Sampling frequencies between 100 and 200 Hz are used for script, which seem to form a reasonable compromise between signal-to-noise ratio on the one hand, the band width of the script signal and the computing capacity needed for data storage and processing.

ScriptAlyzer starts counting and recording only when there is pen-tablet contact, which had consequences for synchronisation with grip force measurement. A trigger pulse on start-recording-signal from ScriptAlyzer (through parallel port) was not useful. Synchronisation required trigger pulses from ScriptAlyzer on both first contact (to start sampling) and second tablet contact (to mark the start of writing tasks). This is explained in detail in paragraph 4.3.4.

#### 4.3.3 Pen grip force measurement

Pen grip force was measured by a pen-like grip force transducer that uses strain gauge technology to independently sense force application by Thumb, Index and Middle fingers and which was integrated with the Wacom Intuos2 digitiser stylus. (Fig.4.3). The pen design procedure and final design concept that was used for data collection is detailed in chapter 3 and a close up of the prototype pen used for data collection is shown in Fig.3.5.

The three transducer force channels were connected to a strain gauge amplifier (built in the Bioengineering electronics workshop around circuits purchased from R.S. Components) and the signals were digitised, using a CED1401 analogue to digital converter, controlled by Spike2 software on a Windows based computer (See system overview in Fig.4.1 and setup in Fig. 4.3). Spike2 and the CED ADC allow sampling at high frequencies up to 30 kHz per channel. In this set-up the sampling rate was set at a rate of 1 kHz per channel, which ensures the frequency resolution that is required for signal processing techniques as Power Spectral Density analysis etcetera. Although a sampling frequencies of 1 kHz can be regarded as oversampling, down sampling can be performed. Graphical presentation of the data during and after sampling and a number of data processing and analysis techniques could be performed in Spike2, which were useful to assess the quality of the data.

Final analyses were carried out with scripts written in Matlab on data exported from the Spike2 environment.

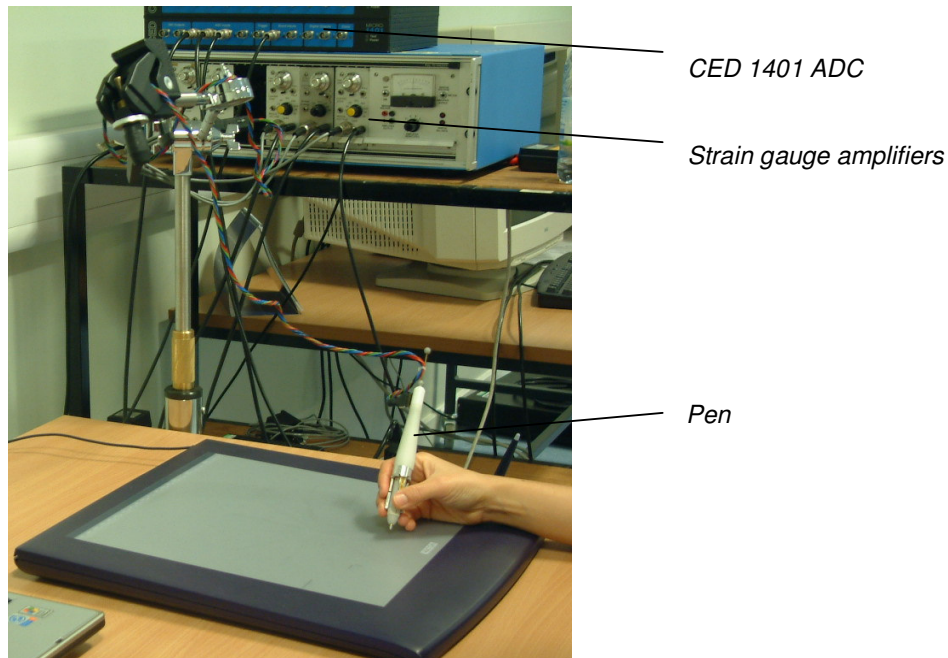


Fig. 4.3: Grip force digitiser pen, strain gauge amplifier and CED1401 ADC.

#### 4.3.4 Motion capture with Vicon

##### 4.3.4.1 Recording of handwriting motion: introduction and overview

Kinematics of the limb and upper body were sampled with the Oxford Metrics Vicon motion capture system. The system consist of a data station and eight Charge-Coupled Device (CCD) cameras, which are connected to a Windows based host computer that together with the Vicon workstation software provides the user interface (See system overview in Fig 4.1). The system samples pulsed infrared light that is reflected from markers, placed on the subject. The camera arrangements are shown in Fig. 4.2. and in Fig. 4.4.

In order to study control of the neuromuscular system involved with handwriting, it was required to record kinematics of the following segments:

- trunk;
- upper arm (positions of shoulder and elbow joint);
- forearm (positions of elbow and wrist joint);

- hand;
- segments of the thumb, index and middle finger.

For these segments (embedded) anatomical axes frames were defined, that are embedded with the bony anatomy.



*Fig. 4.4.: Vicon camera setup for handwriting motion capture.*

Section 4.3.3.2 gives a more detailed explanation of the working principles of the Vicon system, which is followed by the calibration procedure in 4.3.3.3. The embedded anatomical axes frames, that were defined for the segments that were recorded, are given in 4.3.3.4. The set of surface fixed markers, that are related to the underlying bony anatomy and defined anatomical axis frames of the segments, are described in 4.3.3.5. As the camera setup is largely determined by the marker set and axis frames that were defined, the camera arrangement will be discussed last in section 4.3.3.6.

#### 4.3.4.2 Vicon system

The Oxford Metrics Vicon motion capture system uses eight Charge-Coupled Device (CCD) cameras, which are connected to a data station that is controlled by the user from a Windows based host computer.

The principle working of the system is based on sampling reflections of pulsed infrared light from reflecting markers, placed on the subject. The CCD cameras emit pulsed infrared light at a frequency of 50Hz from an array of Light Emitting Diodes (LEDs) around the lens, which is reflected back from the markers on the subject to

the camera. From the two-dimensional image detected by the camera the centre of the marker is determined. Combining the images of two or more cameras allows reconstruction of the marker in three dimensions.

As the reflected light is pulsed, the system samples frames of marker positions and the consecutive frames need to be connected to form a continuous trajectory for each marker. Although, the Vicon workstation software performs this process automatically, it is crucial to manually set the reconstruction parameters to the appropriate value to ensure that markers are assigned to the right trajectory.

In order to label the visualized 3D-trajectories and to draw connecting lines between markers in the visualisation, a *marker file* is required that contains the names of markers and anatomical landmarks and describes the limb segments. The Vicon workstation software enables a link between the names of markers and anatomical landmarks in the marker file to be related to the visualised trajectories. The labeling results in a stick-figure representation of the limb for every frame. The marker file, (Handwriting.mkr) and model file, (Handwriting.mod), are respectively shown in appendix 5A and 5B.

#### 4.3.4.3 System calibration

Calibration is the process of determining where the cameras are and in which direction they are pointing and determining the global axis frame for one test session. Handwriting kinematics of particularly the finger and pen tip are relatively fast and potentially erratic. As both upper body, limb and finger phalanges trajectories are recorded, the eight cameras need to be divided over these areas and some areas will therefore only be seen by only two cameras. In addition, some of the smaller markers on the finger phalanges are often obscured by the hand. Therefore, it was a challenge to obtain the ideal arrangement of the eight cameras for handwriting tasks and to obtain a successful calibration that enables recording of all the markers.

The calibration process for the Vicon system is known as DYNACAL and consists of two phases. During the static calibration, an L-shaped frame with markers is used to obtain the positions and the directions of the axis of the global coordinates system in which the 3D measurements are made. The output is a number of parameters for each camera that will result in an accurate 3D reconstruction.

During the dynamic calibration, a wand, which is a rod with two markers with a known separation, was waved within the entire measurement volume. Over the period during which the wand is waved, a cloud containing many of 3D point-pairs, distributed throughout the entire measurement volume, is built up. A pair of cameras with the best distribution of overlapping wand marker observations are then selected and an initial "seed" calibration is generated for this pair. The calibration is then "propagated" from the seed camera pair by including uncalibrated cameras whose observations overlap with calibrated cameras. The coordinates of all observed wand marker samples are calculated and the average length of the wand is found. Finally, the camera calibrations are adjusted until the average length is equal to the true length of the wand, read from a separate file (user-set.cro). The accuracy of the dynamic calibration is determined by inspection of residuals calculated. The calibration residual (calibration units, normally millimetres) is the angular error (radians, by which a ray from the calibrated camera misses the reference marker) multiplied by mean distance from camera to the reference markers. Every time the system was set up, the cameras were rearranged until an average calibration residual value lower than 0.200 was obtained. The average residual was 0.184, corresponding to the average distance between a reconstructed point and the rays used for its reconstruction of 0.362mm.

#### 4.3.4.4 Bone embedded anatomical axis frames

In this paragraph the anatomical axis frames are given for the trunk, humerus (upper arm), forearm, hand and finger segments. The axes are embedded within the bony anatomy. A clear definition of embedded anatomical axis frames is highly important as the surface markers are linked to these axis frames, which allows determining the exact orientation of the segments over time. The anatomical frames for trunk (Fig.4.5.), following the ISB (International Society of Biomechanics) recommendations (Wu et al, 2005) and humerus and forearm (Fig.4.6.) are shown in anterior view. The hand (Fig.4.7) and finger segments (Fig.4.8) are shown in posterior view as this exposes the back of the hand on which the markers are mounted.

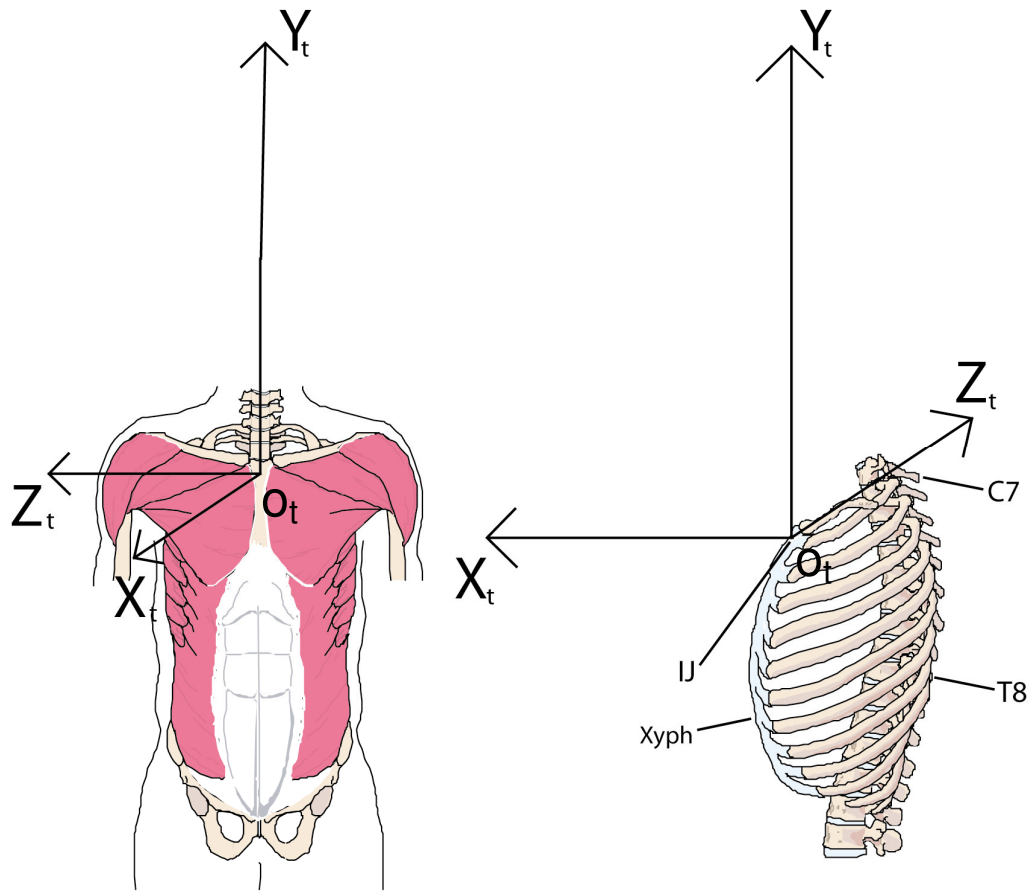


**Fig.4.5: Trunk anatomical axis frame:**

**a) Anterior view**

**b) Lateral view**

$O_t$ : origin coincident with Incisura Jugularis (IJ);

$Y_t$ -axis: The line connecting midpoint between Xyph and T8 and the midpoint between IJ and C7, pointing upward;

$Z_t$ -axis: The line perpendicular to the plane formed by IJ, C7 and the midpoint between Xyph and T8, pointing to the left.

$X_t$ -axis: The common line perpendicular to the  $Z_t$ - and  $Y_t$ -axes, pointing forwards.

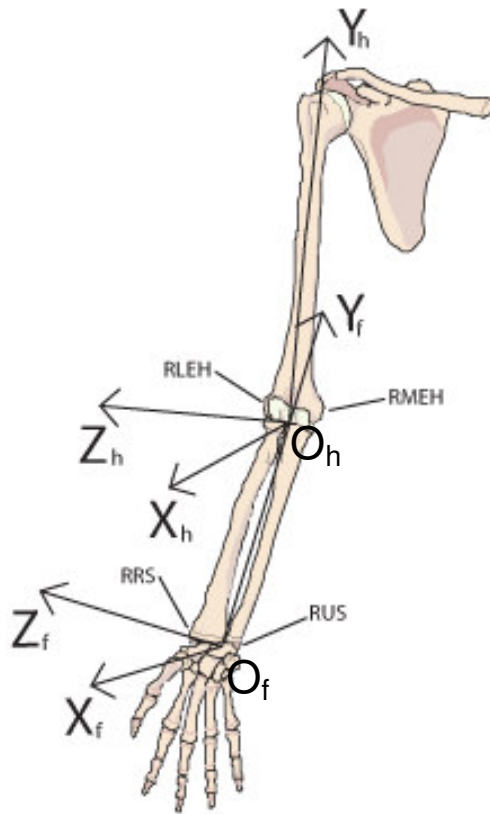


**Fig.4.6: Right arm anatomical axis frame in anterior view:**

**Humerus:**

$O_h$ : origin coincident with elbow joint centre (E) between RMEH and RLEH;

$Y_h$ -axis: The line connecting the right shoulder joint centre (RSJC) to the midpoint between RMEH and RLEH, pointing upward;

$X_h$ -axis: The line perpendicular to the plane formed by RMEH, RLEH and RSJC, pointing forward.

$Z_h$ -axis: The common line perpendicular to the  $X_h$ - and  $Y_h$ -axes, pointing to the left.

**Forearm:**

$O_f$ : origin coincident with wrist joint centre (W) between RUS and RRS;

$Y_f$ -axis: The line connecting midpoint between RUS and RRS and the midpoint between RMEH and RLEH, pointing upward;

$X_f$ -axis: The line perpendicular to the plane formed by RUS, RRS and the midpoint between RMEH and RLEH, pointing forward.

$Z_f$ -axis: The common line perpendicular to the  $X_f$ - and  $Y_f$ -axes, pointing to the left.

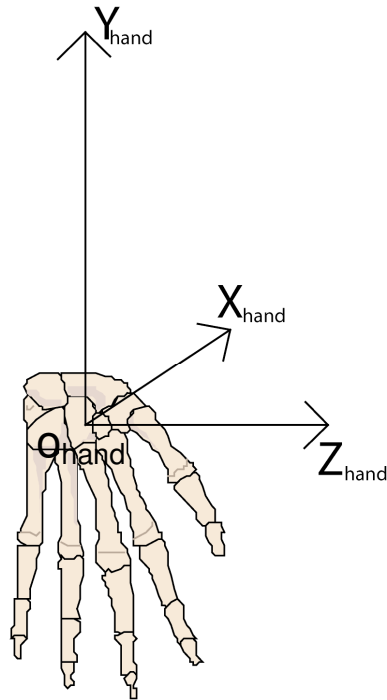


**Fig.4.7: Right hand anatomical axis frame in posterior view:**

$O_{hand}$ : origin coincident with right hand origin (RHO), the midpoint between RCMP3p and RMCP3d;

$Y_{hand}$ -axis: The line connecting RMCP3p and RMCP3d, pointing upward;

$X_{hand}$ -axis: The line perpendicular to the plane formed by the RMCP3d and RMCP3p and RMCP5d, pointing backwards.

$Z_{hand}$ -axis: The common line perpendicular to the  $Y_{hand}$ - and  $X_{hand}$ -axes, pointing to the right.

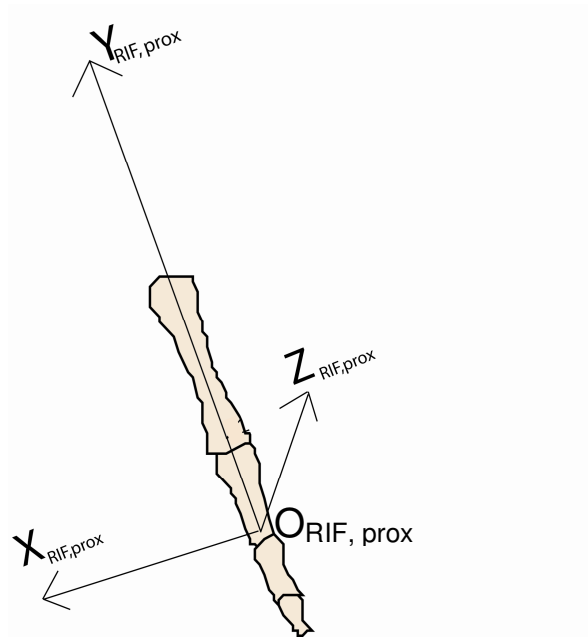


**Fig.4.8: Right index finger proximal phalange anatomical axis frame in sagittal view:**

$O_{RIF,prox}$ : origin coincident with proximal interphalangeal joint of the index finger (RIF1);

$Y_{RIF,prox}$ -axis: The line connecting proximal interphalangeal joint and the head of the second metacarpal (MCP2d), pointing upward (proximally);

$Z_{RIF,prox}$ -axis: The line perpendicular to the plane formed by the proximal interphalangeal joint and the head of the second metacarpal (MCP2d) and the distal interphalangeal joint of the index finger, pointing backwards.

$X_{RIF,prox}$ -axis: The common line perpendicular to the  $Z_{RIF,prox}$ - and  $Y_{RIF,prox}$ -axis, pointing to the left.

#### 4.3.4.5 Marker set and anatomical point calibration

The marker system that was used to record kinematics of the biomechanical plant that enables pen tip motion is described below for trunk, arm, hand and fingers. The surface markers are linked to the anatomical axis frames, described in 4.3.3.3, which allows to determine the exact orientation of the segments over time.

Fig. 4.9 shows the marker setup, which will be commented on for trunk in 4.3.3.5.1, upper and forearm in 4.3.3.5.2 and pen and hand in 4.3.3.5.3.

##### 4.3.4.5.1 Trunk marker set

For positioning of markers on the trunk, the ISB recommendations by Wu et al (2005) for shoulder motion were followed. This requires five (single) markers with a diameter of 14mm to be placed on the following anatomical landmarks of the trunk (Fig.4.5 and Fig.4.9a):

RACR Right acromion

C7 Processus Spinosus (spinous process) of the 7th cervical vertebra

T8 Processus Spinosus (spinal process) of the 8th thoracic vertebra

IJ Deepest point of the Incisura Jugularis (suprasternal notch)

Xyph Processus Xiphoideus (xiphoid process), most caudal point on the sternum

The Right Shoulder Joint Centre (RSJC) is determined from the right acromion (RACR). Following Wang (1996), the RSJC is located 37mm inferior, 14mm lateral and 8mm anterior to RACR.

In order to define the thorax system all four markers (C7, T8, IJ and Xyph) need to be included for every trial. To compensate for one of the markers missing out during recording of dynamics, static calibration trials are recorded for C7, IJ and XYPH that relate the positions of each of these markers relative to the other three markers. This allows to calculate the coordinates of a marker C7, IJ or XYPH in case they have not been recorded over the full length of the trial.

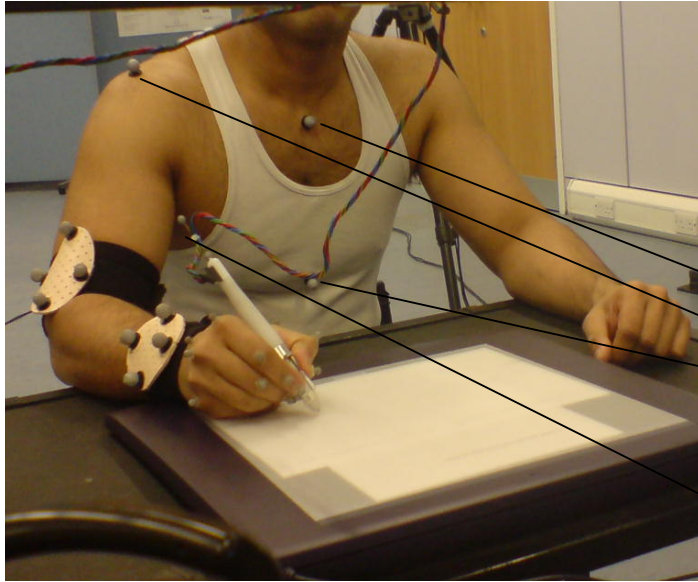
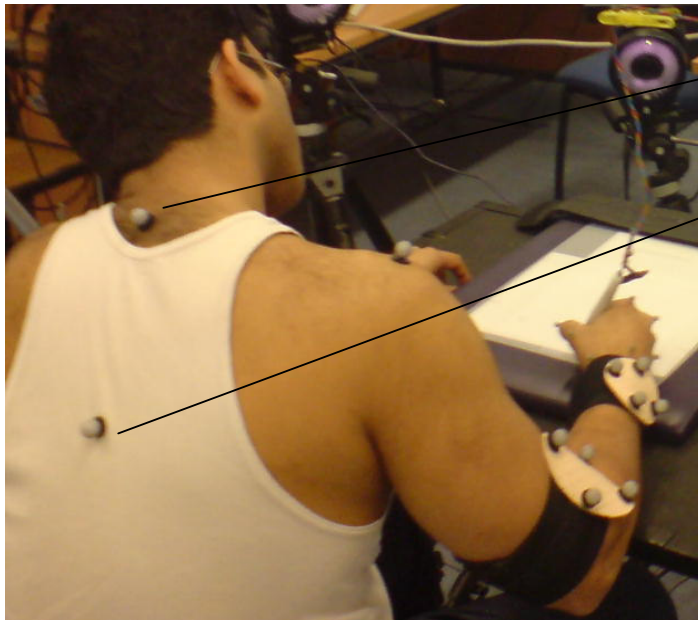


Fig.4.9: Marker set.

a:  
Upper and fore arm marker clusters;

Incisura Jugularis (IJ);  
Right Acromion (RACR);  
Processus Xiphoideus (Xyph);

Two pen markers attached with shaft on top of the pen;



b:  
Processus Spinosus of the 7th cervical vertebra (C7);

Processus Spinosus of the 8th thoracic vertebra (T8)

c:  
For thumb:  
Thumb CMC joint  
Thumb MCP joint line  
Thumb IP joint line  
Tip of thumb

For middle finger (idem other fingers):

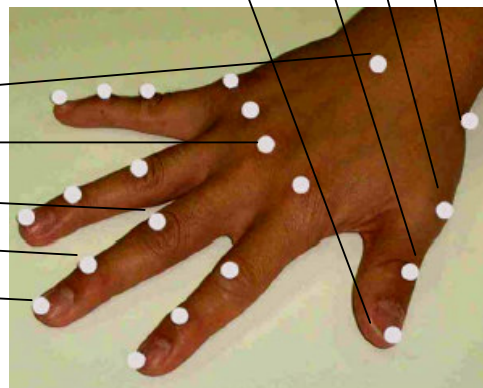
Base 3rd metacarpal (RMCP3d)

Head 3rd metacarpal (RMCP3p)

PIP joint (RTF1)

DIP joint (RTF2)

Tip (RTF3)



#### 4.3.4.5.2 Upper- and forearm segment marker set

##### ***Marker clusters***

For upper limb motion analysis, it is common practice to mount a rigid cluster of markers on the arm segments by positioning them on cuffs, strapped to the arm segments, as suggested by Cappozzo et al (1995) and Schmidt et al (1999) instead of mounting markers directly onto the skin (Fig.4.9a). This avoids problems of skin movement, particularly with regard to forearm pronation/ supination.

In order to fully describe the motion of any rigid body in three dimensions, it is required to track motion of at least three points on the body and therefore a minimum of three markers were required within a cluster on a cuff. A fourth point on the rigid body is useful as this allows to substitute for any missing marker that may be obscured by other body segments or due to movement that occurs outside the workspace. Cuffs with four markers (diameter of 14mm) were used on both upper arm and forearm. The forearm cuff was strapped as close to the wrist as possible in order to record most of the pro-/supination movement.

##### ***Technical axis frame and anatomical point calibration***

As the position of the marker clusters strapped to the upper and forearm are chosen for convenience during testing only, the technical axis frame for the markers may be arbitrary and in non-repeatable geometric relationship to the bony arm anatomy. Fig.4.10 illustrates the technical axis frame of the upper arm segment with four markers on a rigid plate that is attached to the strap. The frame origin is marker 2 with the z-axis going through marker 1. However, the orientation of the axis frame is arbitrary and in non-repeatable geometric relationship to the anatomy of the humerus. An anatomical point calibration (static trial) is required to relate the technical axis frame of a particular marker cluster to two anatomical landmarks on the arm segment (medial epicondyle of humerus and lateral epicondyle of humerus). During calibration, a pointer is held against anatomical points while the arm segment is rested. Static data is then sampled that allows parameters to be added to the parameter file that relate the anatomical points to the technical axis frame of the marker cluster. During dynamic trials, the parameters are used to calculate the anatomical landmarks from the marker cluster coordinates in the global reference frame of the lab. From the anatomical landmarks in the global frame, a bone embedded anatomical axis frame is constructed for both the upper and forearm as

described in paragraph 3.1.3.3. Fig.4.6 shows the anatomical frame of the upper arm.

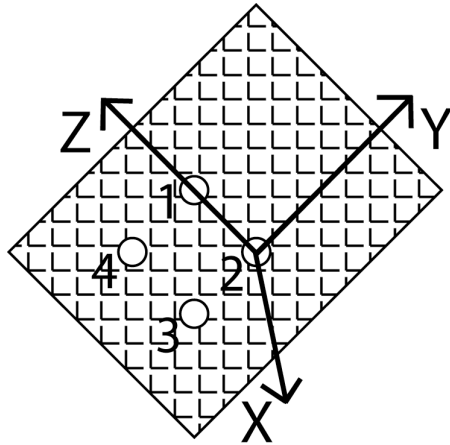


*Fig.4.10. Technical axis frame of the upper arm: orientation of axis frame shown is determined by orientation of the marker cluster, which does not have a geometric relationship to the bony anatomy of the upper arm (humerus). An anatomical point calibration is required to relate the axis frame of the marker cluster to the bony anatomy of the humerus.*

The anatomical landmarks and four markers on each cluster that relate to the anatomical landmarks were labeled in the Vicon model as following.

Upper arm cluster labels:

Right upper arm proximal	RUA1
Right upper arm anterior	RUA2
Right upper arm distal	RUA3
Right upper arm posterior	RUA4

Upper arm anatomical landmarks:

Right medial epicondyle of humerus	RMEH
Right lateral epicondyle of humerus	RLEH
Right elbow joint centre	REJC

Forearm cluster labels:

Right forearm proximal	RFA1
Right forearm radial side	RFA2
Right forearm distal	RFA3
Right forearm ulnar side	RFA4

Forearm anatomical landmarks:

Right Ulnar Styloid	RUS
Right Radial Styloid	RRS
Right Wrist Joint Centre	RWJC

Calibration parameters that refer in dynamic trials to anatomical calibration points:

Calibration ref for right medial epicondyle of humerus	CalRMEH
Calibration ref for right lateral epicondyle of humerus	CalRLEH
Calibration ref for right ulnar styloid	CalRUS
Calibration ref for right radial styloid	CalRRS
Pointer1	POI1
Pointer2	POI2

#### 4.3.4.5.3 Hand and pen marker set

For motion capture of the thumb, index and middle finger segments, markers were placed directly onto the skin over the following anatomical landmarks of each digit: head of metacarpals, proximal and distal interphalangeal joints, recommended by Zhang et al (2003) and Lee et al (2004). As the finger movement is minimal during handwriting compared to other activities, excessive skin motion was not expected. In addition, the pen was equipped with two markers that extend from the top of the pen from which the pen tip coordinates in space were calculated (Fig.4.11). All markers had a diameter of 7mm.

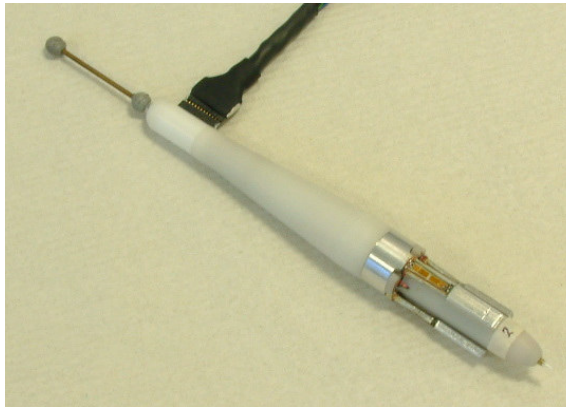


*Fig. 4.11: Pen markers.*

The anatomical landmarks and pen markers were labeled in the Vicon model as following.

Hand and fingers anatomical landmarks:

Thumb CMC joint	RTH0
Thumb MCP joint line	RTH1
Thumb IP joint line	RTH2
Tip of thumb	RTH3
Base of second metacarpal	RMCP2p
PIPjt index finger	RIF1
DIPjt index finger	RIF2
Tip of index finger	RIF3
Base of third metacarpal	RMCP3p
Head of third metacarpal	RMCP3d
PIPjt third finger	RTF1
DIPjt third finger	RTF2
Tip of third finger	RTF3
Head of fifth metacarpal	RMCP5d
Original Right Hand	RHandO

Pen markers:

Pen1 (marker closest to pen tip)  
Pen2  
Pen tip

Pen1  
Pen2  
Tip

#### 4.3.4.6 Vicon camera setup

The camera arrangement was already shown in both fig. 4.4 and the global axis system of the overall system setup in Fig. 4.2 and is shown in more detail in Fig.4.13. The camera setup is determined by both the marker set and the writing and drawing tasks that are recorded. Together they determine the marker movement and the volume in which it takes place. An example of resulting motion capture is shown in Fig.4.12. Each marker must be tracked by at least two cameras in order to construct a three dimensional motion from the two dimensional motion captures from each camera.

Four cameras were required to record the hand and finger segments. Three of these cameras (Fig.4.13: cameras 1,2,3) were positioned just 5 centimeters above and in front of the table in order to record the distal markers that get easily obscured by the fingers and lower half of the pen. The fourth camera (Fig.4.13: camera 4) for recording hand and finger segments is placed on the right side of the table, slightly higher than the other three. The same four cameras record the two pen markers.

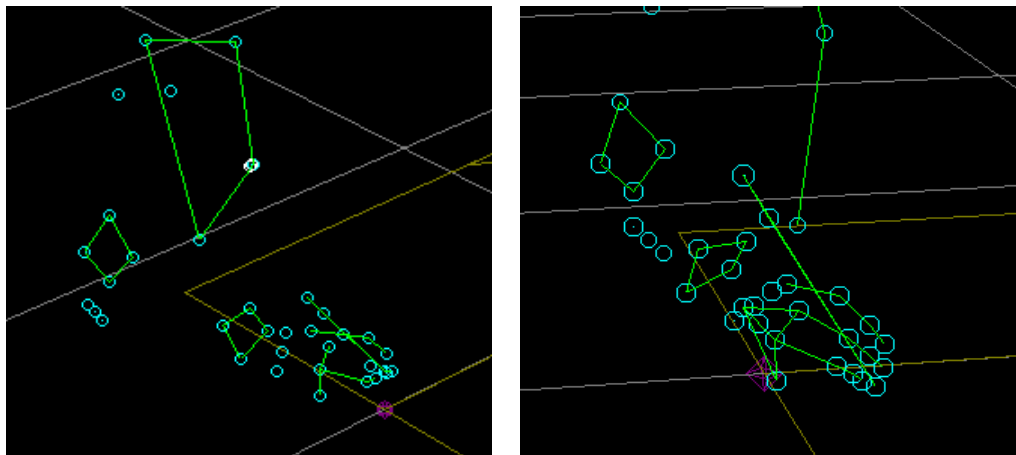


*Fig.4.12: Vicon motion capture result: anatomical points that are captured or calculated.*



Fig. 4.13: Arrangement of 8 CCD cameras for Vicon motion capture for handwriting.

The upper and forearm marker clusters are recorded by cameras 1,2,3,4,5 and 8. The RACR single marker was recorded by two cameras (Fig.4.12: camera 7 and 8). The thorax markers C7 and T8 were recorded by cameras 6 and 7 and markers IJ and Xyph were recorded by cameras 1,2,3,4 and 8.

#### 4.3.5 Synchronisation of script, grip force and Vicon data

ScriptAlyzer was synchronised with Spike2 by a synchronisation pulse on pen-tablet contact from Script (through parallel port) to Spike2 (through CED ADC). To avoid any failed triggers at the start of a trial, on command of the investigator, the subject firstly pressed the pen down in a square located in the bottom left corner of the tablet. This initiated data recording. Then on second command of the investigator, the subject started the writing trial. On the instant of first pen-tablet contact and the instant that marks the start of the writing task, pulses (M1 and M2) were sent to

Spike2, which appeared as marker events. Both markers were also recorded as audio output from Spike2. Fig.4.14 shows the markers M1 and M2 in Spike2 on first and second contact moment between pen and tablet.

Spike2 was started manually first and was already running when ScripAlyzer became active (Fig.4.14). Vicon was synchronised with Spike2 by a start signal concurrently with the start of Spike2.

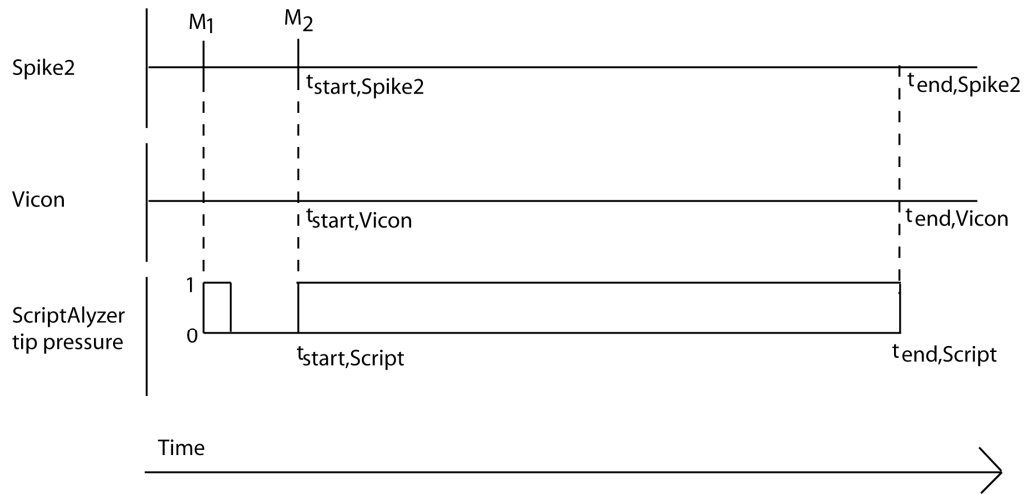


Fig.4.14: Synchronisation Spike2, Vicon and ScriptAlyzer.

The synchronization procedures as described above and shown in Fig.4.14 look as follows in formula form. The writing x,y,z-coordinates sampled with ScriptAlyzer were analyzed from  $t_{start,Script}$  until  $t_{end,Script}$ . If  $n$  is the number of samples between  $t_{start,Script}$  and  $t_{end,Script}$  and the sampling frequencies of the three systems are:

$$f_{Spike2}=1000\text{Hz}$$

$$f_{Vicon}=120\text{Hz}$$

$$f_{ScripAlyzer}=100\text{Hz}$$

and M2 as the time in seconds that marks the start of the task;

Then the Spike2 force data and Vicon joint coordinates were analyzed between:

$$t_{start,Spike2}=M2 * f_{Spike2}$$

$$t_{stop,Spike2}=t_{start,Spike2} + (n / f_{ScripAlyzer} * f_{Spike2})$$

$$t_{start,Vicon}=M2 * f_{Vicon}$$

$$t_{stop,Vicon}=t_{start,Spike2} + (n / f_{ScripAlyzer} * f_{Vicon})$$

It was observed that Spike2 and Vicon were always synchronised and both systems are known to have an accurate internal timer. However, variations were observed in the timing of the ScriptAlyzer program, which is dependent on the Windows operating system of the host computer. The time between  $t_0$  and  $t_{\text{start,Script}}$  in the ScriptAlyzer data was not always equal to the time between  $M1$  and  $M2$ . Moreover, sampled x,y-coordinates in both system, although equal in value, were seen to be out of phase over part of the trajectory on some occasions (an example can be found in Fig.4.15). Therefore, for every trial the sampled ScriptAlyzer x,y- and z-coordinates were compared to the Vicon coordinates and if required, the ScriptAlyzer coordinates were shifted to compensate for phase lag between  $M2$  and  $t_{\text{start,Script}}$  to ensure that the start and stop of both signals were always synchronised. After synchronising the start signal, the ScriptAlyzer and Vicon recordings were on some occasions observed to be out of phase with a difference up to 0.2 seconds over part of the trajectory due to varying sampling rate of ScriptAlyzer and Wacom digitizer under Windows control.

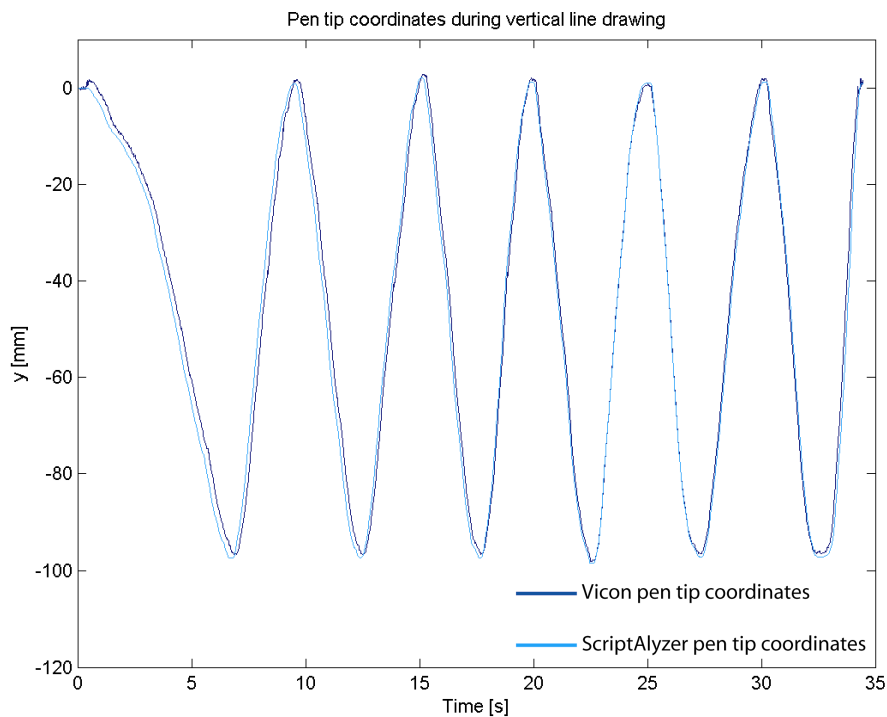


Fig.4.15: Phase difference between Vicon and ScriptAlyzer pen tip coordinates.

## 4.4 Data analysis techniques

### 4.4.1 Development programs for script, grip force and joint motion analysis.

Matlab scripts were written for both analysis and graphical presentation of recorded script, pen grip force and 3D joint motion. The final programs firstly import the test data files for handwriting script, grip forces and limb kinematics and synchronise the data file, based on start and stop marker events as explained in 4.3.5 (Fig.4.15).

Per data set the following tasks may be performed for the analysis:

#### ***Script - derived from ScriptAlyzer files***

Calculations:

- derive velocity and acceleration of individual pen tip x-coordinates and y-coordinates over time and script x,y-coordinates;
- derive angular tip motion, velocity and radius.

Plotting:

- plot the x-coordinates of pen tip over time;
- plot the y-coordinates of pen tip over time;
- plot the script x,y-coordinates;
- plot the z-coordinates (pen tip pressure) of script over time;
- plot the pen tip velocity and acceleration over time;
- plot the radius of circular motion over time;

### ***Pen grip force - derived from Spike2 files***

Calculations:

- Calculate resultant pen grip force that is exerted by thumb, index and middle finger to the pen. Firstly, for each sample of the forces applied to the transducer beams (for thumb, index and middle finger), its components in forward (x) direction and up- and downward direction (y) direction are calculated, using trigonometry. The sum of the force components, applied by all three fingers are calculated in x- and y-direction. The resultant of the total force, applied to the pen by all fingers, in x- and y-direction is then calculated, using Pythagoras theorem. A matlab script was written to enable computation of the force magnitude and direction for every sample. The resultant grip force is determined by the pen orientation angle in the plane through the longitudinal pen axis. This is because this orientation angle determines the direction and magnitude of force components that act in x- and y-direction. This is described on p.126 and examples are shown.
- Filtering: DC-term removal / smoothing.

Plotting:

- plot Thumb, Index and Middle finger forces with and without DC-removal;
- plot the resultant grip force vector.

Quantifying data was possible by using the following techniques:

- Power Spectral Density (PSD) of pen grip signal for each finger, explained in 4.4.2;
- Root Mean Square (RMS) values of pen grip measurements for each finger, explained in paragraph 4.4.3;
- Basic statistics of pen grip measurement for each finger, including mean, maximum, standard deviation and sum of forces, explained in 4.4.4.

### ***3D joint kinematics - derived from Vicon files***

Calculations:

- Conversion of the Vicon global axis system into the global axis system of the lab setup;
- Fill up gaps in the data by interpolation;
- Make up stick figure models of the x,y,z-joint kinematics.
- A script was written that allows visualisation of the trajectories of Shoulder, Elbow and Wrist joint and pen Tip in three dimensions. The color of the

plotted 3D joint coordinate samples is related to sample number. This creates a method of including the time aspect of the movement along with x,y,z-joint-coordinates (Fig.4.16). The x,y,z-coordinate samples vary in color over the trajectory in the range from dark blue (first sample) to red (last sample). The joints are connected by lines to make up a stick figure of the limb. By changing the camera position in the 3D plot during visualisation, a 2D representation of the x,y-plane can be created as shown in Fig.4.16.

Plotting:

- Plotting the trajectories of shoulder, elbow and wrist joint and pen tip over time in 3D, where the timing of the motion is presented by color changes over the trajectory as shown in Fig.4.16. The Matlab script that was developed to create these graphs, accommodated for the different sampling frequencies for pen recordings (100Hz) and limb recordings (120Hz) by resampling the both data sets at 100Hz.

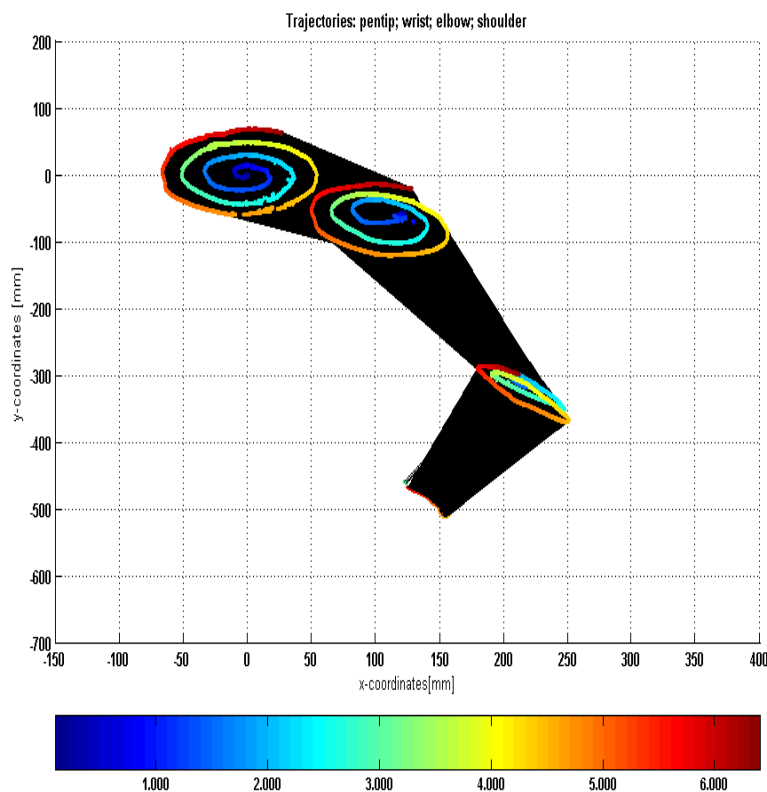


Fig. 4.16: x,y-Coordinates of spiral drawing activity (z not shown in 2D view) along with sampling numbers showing the time dimension (first sample is dark blue; last sample is dark red). The sampling frequency is 100 Hz.

#### 4.4.2 Power Spectral Density

The basic operation to transform a continuous time signal to the frequency domain is the Fourier Transform. It is used on a stationary, non-periodic time signal to give its continuous frequency spectrum. Stationary means here, that both mean value and variance do not change over time. Most practical applications of this theory use numerical procedures and take advantage of digital computing. The Discrete Fourier Transform (DFT) is the most appropriate mathematical tool as digital applications sample data, originating from an analogue source, into discrete data points. Any results displayed digitally are discrete in nature also.

The power spectral density analysis is one of the main tools used allowing the frequency components of the waveform contained in a physiological signal and the relative power at each frequency to be viewed. Visually this can be easier to follow than structures in the time domain. The simplest method is the periodogram, a non-parametric in which the PSD is derived directly from the signal itself. Practically, the estimation of the periodogram translates to the simple calculation of the DFT of the finite set of samples of the process and taking the magnitude squared as a result. Coherence is defined as the cross spectra of both signals divided by the product of each signals' auto-spectra. Auto-spectra are calculated by dividing the data into discrete segments, or bins, of equal length and applying a Discrete Fourier Transform (DFT) over each segment. The final Auto-spectra estimate is calculated by averaging across each discrete bin. Cross spectra are calculated in a similar way but use both waveforms as inputs to the calculations.

This process can be automated by Matlab functions. The output of the DFT calculations is a matrix that can be used by other functions to calculate the auto and cross spectra, and therefore the coherence estimate, and produce graphical outputs of the results.

#### 4.4.3 Root Mean Square measures

Root mean square (RMS), also known as the quadratic mean, is a statistical measure of the magnitude of a varying quantity. RMS is useful when variates are positive and negative, e.g. waves.

It can be calculated for a series of discrete values or for a continuously varying function. The name comes from the fact that it is the square root of the mean of the squares of the values. It is a power mean with the power  $p = 2$ .

The RMS for  $n$  samples  $\{x_1, x_2, \dots, x_n\}$  is defined as:

$$x_{\text{rms}} = \sqrt{\frac{1}{n} \sum_{i=1}^n x_i^2} = \sqrt{\frac{x_1^2 + x_2^2 + \dots + x_n^2}{n}}$$

For a continuous function  $f(t)$  defined over the interval  $T_1 \leq t \leq T_2$ , RMS is defined as:

$$f_{\text{rms}} = \sqrt{\frac{1}{T_2 - T_1} \int_{T_1}^{T_2} [f(t)]^2 dt}$$

The rms of a periodic function is equal to the rms of one period of the function. The rms value of a continuous function or signal can be approximated by taking the rms value of a series of equally spaced samples.

If  $\bar{x}$  is the arithmetic mean and  $\sigma_x$  is the standard deviation of a population, then:

$$x_{\text{rms}}^2 = \bar{x}^2 + \sigma_x^2.$$

RMS therefore is always equal or greater than the average and can be expressed for an entire record or for segments of a time series.

#### 4.4.4 Linear regression

##### 4.4.4.1 Statistics for linear regression

For statistical evaluation of goodness of fit for linear regression, the following statistics are calculated: Sum of Squares Due to Error (SSE) and Root Mean Squared Error (RMSE) to assess the deviation from the ideal straight line and also R-Squares ( $R^2$ ) and Adjusted R-square to assess how well the linear model fits the data.

**Sum of Squares Due to Error (SSE)** measures the total deviation of the response values from the fit to the response values and is also called the summed square of residuals. A value closer to 0 indicates a better fit.

$$SSE = \sum_{i=1}^n w_i (y_i - \hat{y}_i)^2$$

**Root Mean Squared Error (RMSE)** is also known as the fit standard error and the standard error of the regression where MSE is the mean square error or the residual mean square. A RMSE value closer to 0 indicates a better fit.

$$RMSE = s = \sqrt{MSE}$$

$$MSE = \frac{SSE}{v}$$

The residual degrees of freedom  $v$  is defined as the number of response values  $n$  minus the number of fitted coefficients  $m$  estimated from the response values. The residual degrees of freedom  $v$  indicates the number of independent pieces of information involving the  $n$  data points that are required to calculate the sum of squares.

$$v = n - m$$

### **R-Squares ( $R^2$ ) and Adjusted R-square**

R-square value of a linear regression is the square of the correlation between the response values and the predicted response values and therefore represents how well the linear model explains the variation of the data. The R-square statistics can take values between 0 and 1 with 1 indicating a closer fit.

Adjusted R-square uses the R-square value and adjusts it based on the residuals degree of freedom. The residual degrees of freedom  $v$  is defined as the number of response values  $n$  minus the number of fitted coefficients  $m$  estimated from the response values. The residual degrees of freedom  $v$  indicates the number of independent pieces of information involving the  $n$  data points that are required to calculate the sum of squares.

$$v = n - m$$

For an ideal straight line, Fig. 4.16 illustrates the y-coordinates as function of time and the linear regression fit to the drawn line with residuals. For an ideal straight line the linear fit gives an R-square value of  $R^2=1$  and Sum of Squares Due to Error of  $SSE=0$  and Root Mean Squared Error of  $RMSE=0$  (Fig.4.17).

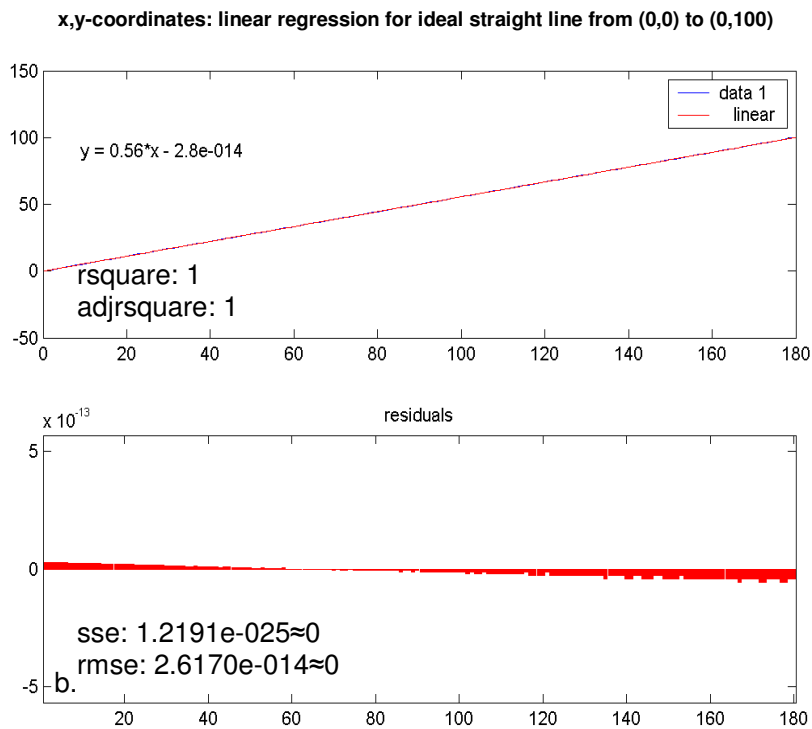
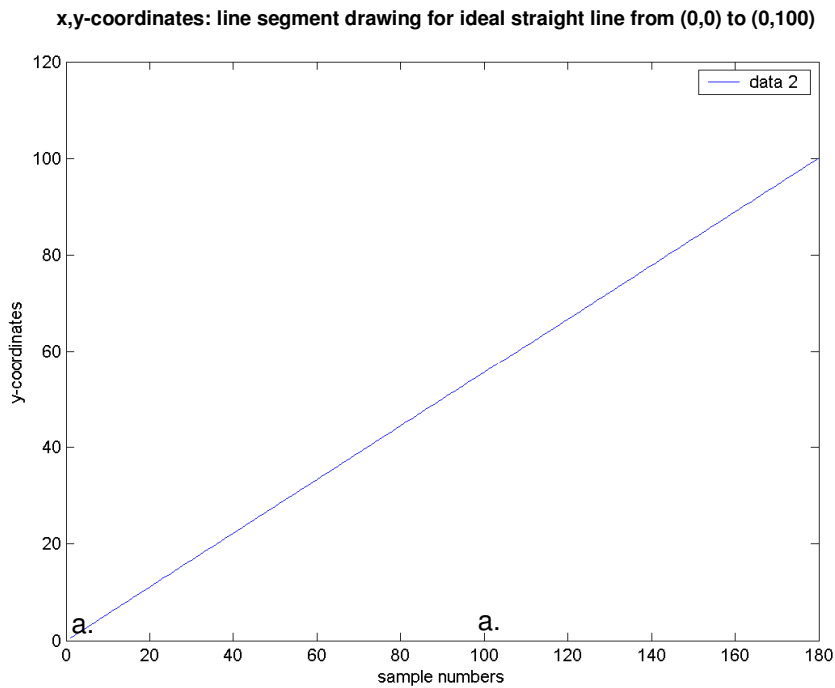


Fig. 4.17: Drawing of a straight line from coordinates (0,0) to (0,100)

- a: Resulting line
- b: R-Squares ( $R^2$ ) and Adjusted R-square, Sum of Squares Due to Error (SSE) and Root Mean Squared Error (RMSE).

#### 4.4.4.2 Linear regression and normalisation for assessing straightness of lines

The deviation from the ideal straight line is assessed for the line drawing experiment (chapter 5) by two different methods: measurement of the latitude of the line segment and a linear regression of each line segment. Both measures are explained here. The latitude is a peak measure of deviation in the direction perpendicular to the ideal line direction (Fig.4.18). The linear regression allows measures of the total deviation from the ideal straight line (over its total length and not just peak value as measured by latitude) to be reported as the variation of the coordinate values (deviation) around the mean (ideal straight line). The linear regression assesses the deviation from the ideal straight line by means of expressing measurement of the residuals as the Sum of Squares Due to Error (SSE) and Root Mean Squared Error (RMSE). The SSE measures the total deviation of the response values from the fit to the response values. A value closer to 0 indicates a better fit. The RMSE is also known as the fit standard error or the standard error of the regression and is derived from the SSE, taking into account the residual degrees of freedom (explained in section 4.4.4). A value closer to 0 indicates a better fit.

R-square value of a linear regression is the square of the correlation between the response values and the predicted response values and therefore represents how well the linear model explains the variation of the data. The R-square statistics can take values between 0 and 1 with 1 indicating a closer fit. Adjusted R-square uses the R-square value and adjusts it based on the residuals degree of freedom (explained in section 4.4.4).

Linear regression is illustrated for a line drawn from coordinates (0,0) to (0,100) in Fig. 4.19, Fig.4.20 and Fig.4.21. Fig. 4.19 and Fig.4.20 show the y-coordinates and the x,y-coordinates. Fig. 4.20 shows the linear regression fit to the drawn line with residuals (deviation from the vertical (y-direction) line).

Fitting a linear model to the line drawing coordinates in the x,y-plane does not in itself enable the straightness of the drawn line to be assessed. Instead, perpendicular measures of deviation from the line need to be assessed in respect to the residuals of the regression based on a time normalised representation of the data (Fig.4.21 and Fig.4.22). Without applying normalisation, the number of response values (samples) will vary as will the number of fitted values (for fitting the linear model) and the number of residuals (distance between fitted values and response

values). While sampling line drawing that is performed slowly, a larger number of samples will be recorded compared to fast line drawing. An increased sample number will give increased number of fitted values and residuals when applying linear regression and consequently higher SSE-values (sum of residuals. Linear regression is required to compare the straightness of lines that were not drawn at the same speed. It was decided to downsample all trials to 66 samplenumbers, which was the lowest number seen in all trials for the subjects in chapter 5. Fig. 4.22 shows the linear regression for the 12 o'clock target by subject 1 after normalisation (compare Fig. 4.21)

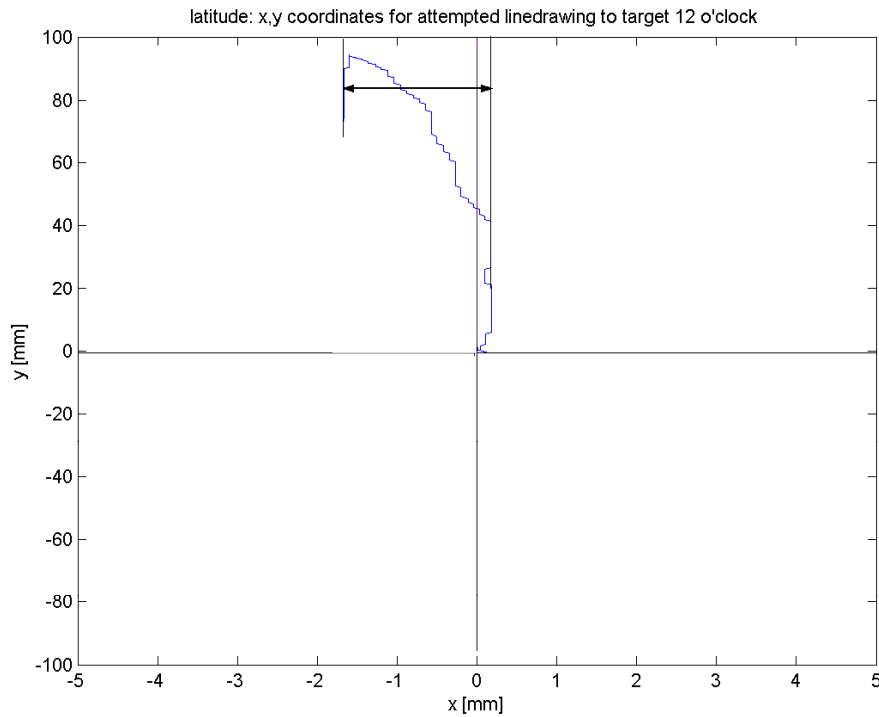


*Fig.4.18: Defining the latitude: the maximum deviation from the line towards the target direction and is therefore the difference between the minimum and maximum deviation perpendicular to the drawing direction.*

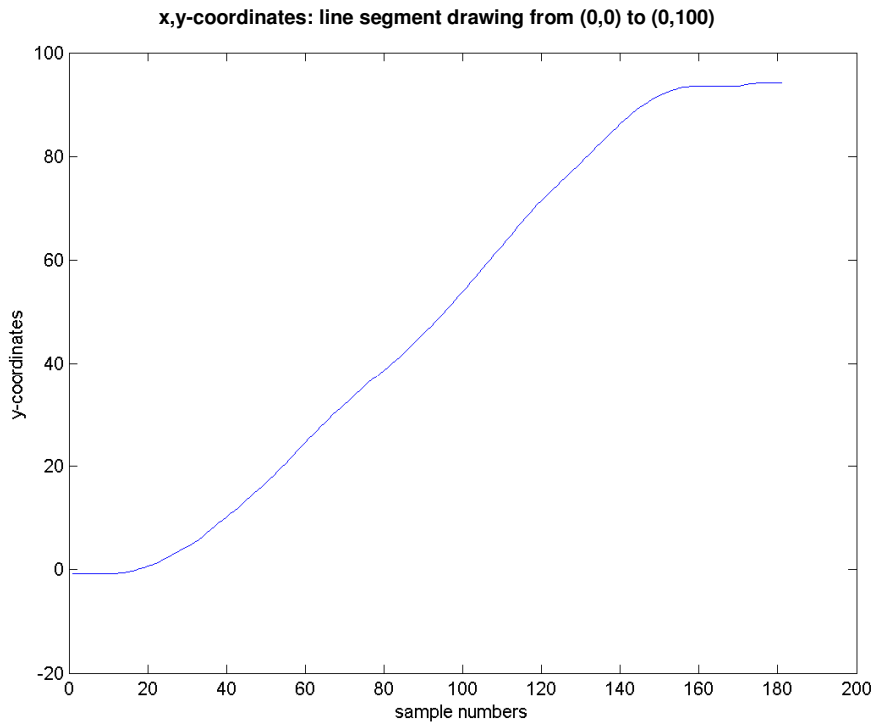


Fig. 4.19: Line drawing for target 12 o'clock by subject 1: y-coordinates.

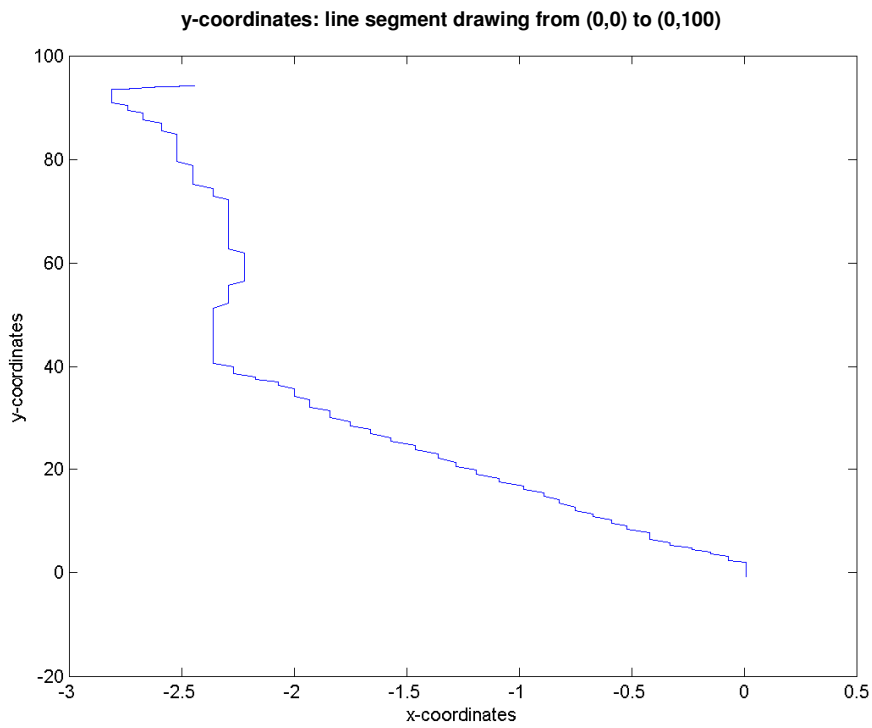


Fig. 4.20: Line drawing for target 12 o'clock by subject 1: x,y-coordinates.

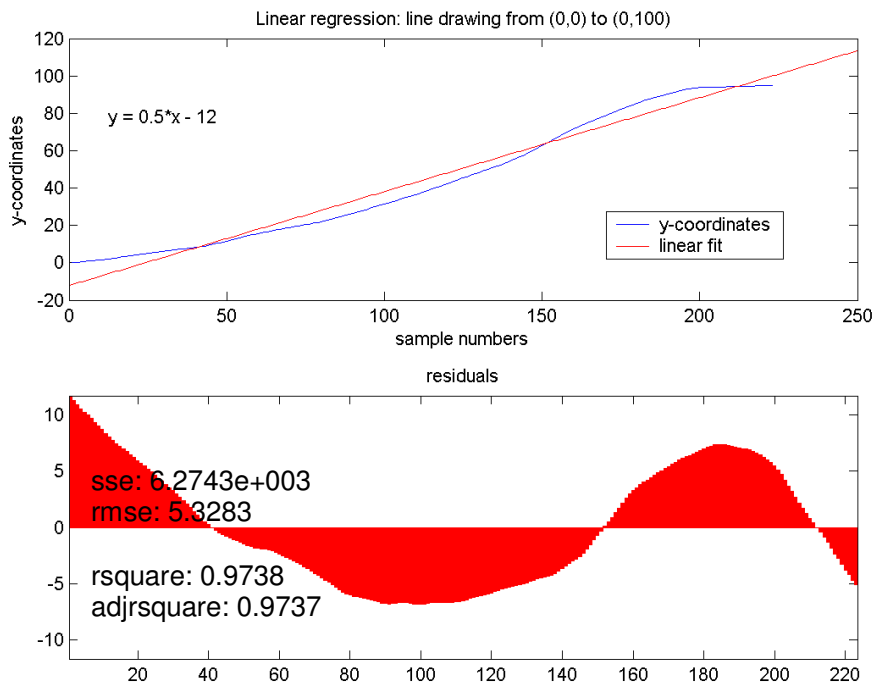


Fig. 4.21: linear regression of line drawing for target 12 o'clock by subject 1.

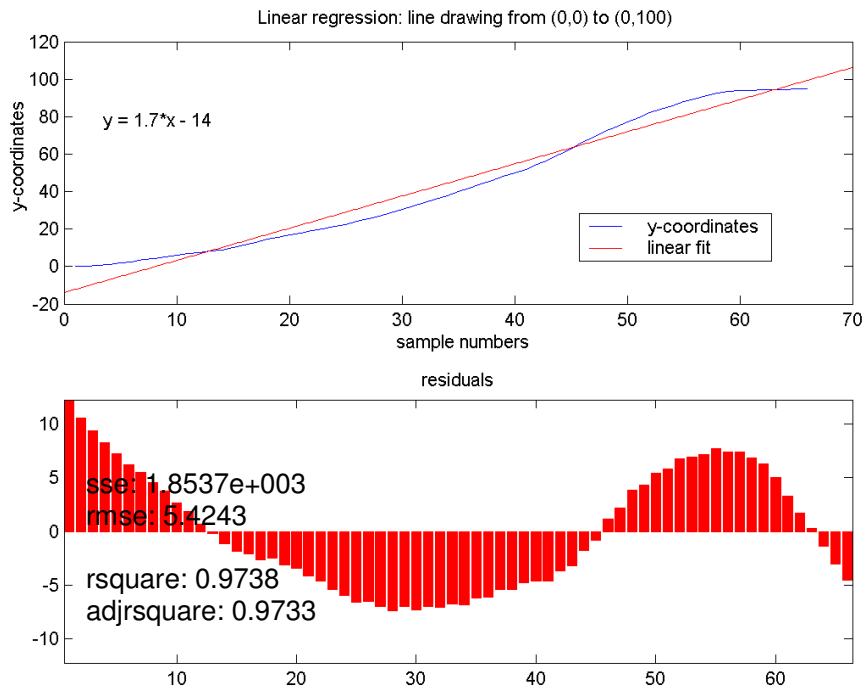


Fig. 4.22: linear regression of line drawing for target 12 o'clock by subject 1 after normalisation.

## 5 Subject testing: Line drawing

The aim of the line drawing experiments is to show that a comprehensive set of data associated with the use of the pen can be collected and that it forms a suitable platform for future studies on the neuromuscular control involved with drawing and handwriting. In these experiments, subjects draw lines in different directions to examine grip force modulation in a simple and reproduceable experiment.

Section 5.1 and 5.2 respectively describe the healthy test subjects and line drawing activities performed in detail. Section 5.3 describes the data collection process. The results are presented in 5.4.

### 5.1 Subjects

Four healthy volunteers with good writing ability were tested. All subjects were right hand dominant. Details of the the four subjects are given in Table 5.1. Data from subjects 1 and 2 will be presented in this chapter.

	Subject 1	Subject 2	Subject 3	Subject 4
<b>Gender</b>	male	male	male	female
<b>Age</b>	23	26	27	25

*Table 5.1: Details of subjects, included in the line drawing experiment.*

All procedures were approved by the departmental safety committee and all subjects provided informed consent to participate in the experiments, which were considered to be covered by a generic ethics approval for motion analysis and neurophysiological investigation in the Conway laboratory.

## 5.2 Activities

The subjects were instructed to perform a series of 12 line drawing tasks with every task starting from a common origin. Lines are required to be drawn from this starting position outward to one of 12 endpoints and back to the start point as shown in Fig.5.1. The endpoints of each of the 12 lines are 30° apart, so that the 12 lines resemble the hourly marks of a clock face. Target 1 is equivalent to the 12 o'clock position on a clock face with each other target following the other standard hour position (Fig.5.1). This cycle of line drawing from start point to endpoint is performed 5 times without interruption for each of the 12 trials as can be seen in Fig 5.2 (shown for positions 12, 3, 6 and 9 only). Each target is 10 cm from the origin. The drawing directions of the 12 trials were shown by lines to the target on paper that was placed below the transparent writing surface of the tablet and the subjects were tracing these 12 lines. There was no time restriction to the task.

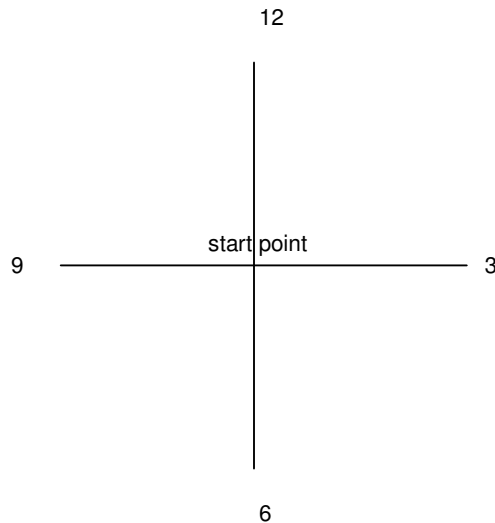


*Fig 5.1: Line drawing activity: start and end targets are shown in layout for each set of lines to be drawn. Each line is 10 cm long.*

### **5.3 Data collection and processing**

The comprehensive set of data simultaneously sampled in this experiment includes:

- script kinematics (x- and y-coordinates);
- pen tip pressure;
- pen grip pressure, applied by thumb, index and middle finger;
- upper limb and upper body kinematics.

The test equipment, data analysis and synchronisation techniques are described under methods in 4.2.

The test procedure was as follows. The volunteer is seated behind a table, whilst holding the grip measuring pen in tripod grip. On command of the investigator, the volunteer performs one trial (5 uninterrupted line drawing cycles from the start point to the selected endpoint target and back to start point). A pause of 30-60 seconds was given between line drawing to each of the 12 different targets.

Data collection was successful for all 4 subjects. For each subject line drawing recordings were collected to all 12 targets, which resulted in good quality data of script, limb motion and pen grip forces.

It was decided to only process and analyse data from horizontally and vertically directed lines drawing. Comparing the drawing processes for horizontal and vertical lines would enable to investigate the contributions of proximal (arm) and distal (finger) joints.

### **5.4 Results**

All subjects easily completed the experiment. For illustration purposes simple statistics on the measured line drawing features for targets 12, 3, 6 and 9 o'clock will be shown for subjects 1, 2, 3 and 4 (section 5.4.1). In addition, a more comprehensive description of the measured features will be presented and described for subjects 1 and 2 (section 5.4.2).

### 5.4.1 Line curvature and time duration.

The time taken for each subject to complete the drawing tasks are shown in Fig.5.2 and table 5.2 for four targets illustrated in Fig.5.3. As can be seen there is considerable variability in the time taken to complete each task. There is a variable level of performance for each subject and for each task performed by individuals as the variation in line curvature reveals. Subject 3 shows the greatest variability in time and was slowest for all lines when compared with the other subjects (Fig.5.2). The differences in time may reflect differences in strategy adopted by each subject and this can be further examined by studying the movement trajectories made by the pen a tip for each subject as shown in Fig.5.3. For example, subject 3 took the longest time to draw each set of lines and the trajectories produced deviate the least from the ideal straight line (Fig.5.3c). In contrast, subject 2 who is consistently the fastest produced the least accurate repetition of the line drawing task (Fig.5.3b).

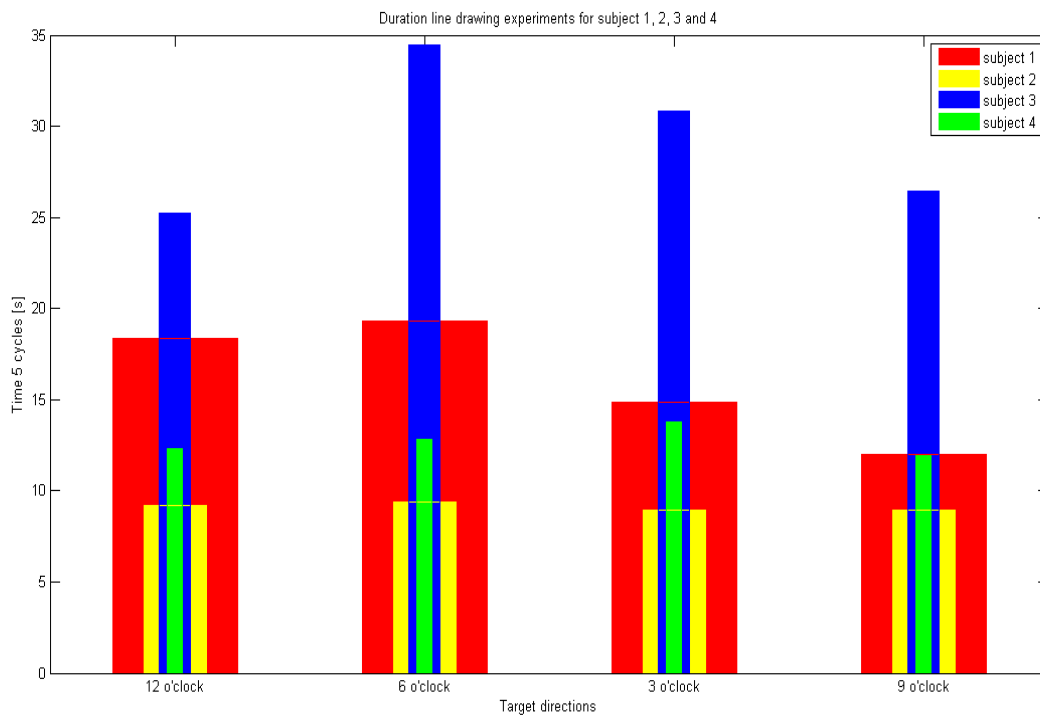


Fig 5.2: Duration of line drawing tasks (5 cycles) for different target directions for all four subjects 1 to 4.

	Vertical lines		Horizontal lines	
	12 o'clock	6 o'clock	3 o'clock	9 o'clock
Subject 1	18.38	19.34	14.85	12.00
Subject 2	9.22	9.41	8.96	8.94
Subject 3	25.24	34.47	30.82	26.45
Subject 4	12.30	12.81	13.80	11.96

Table 5.2: Total time for completing line drawing tasks (5 cycles) for 4 target directions for all four subjects.

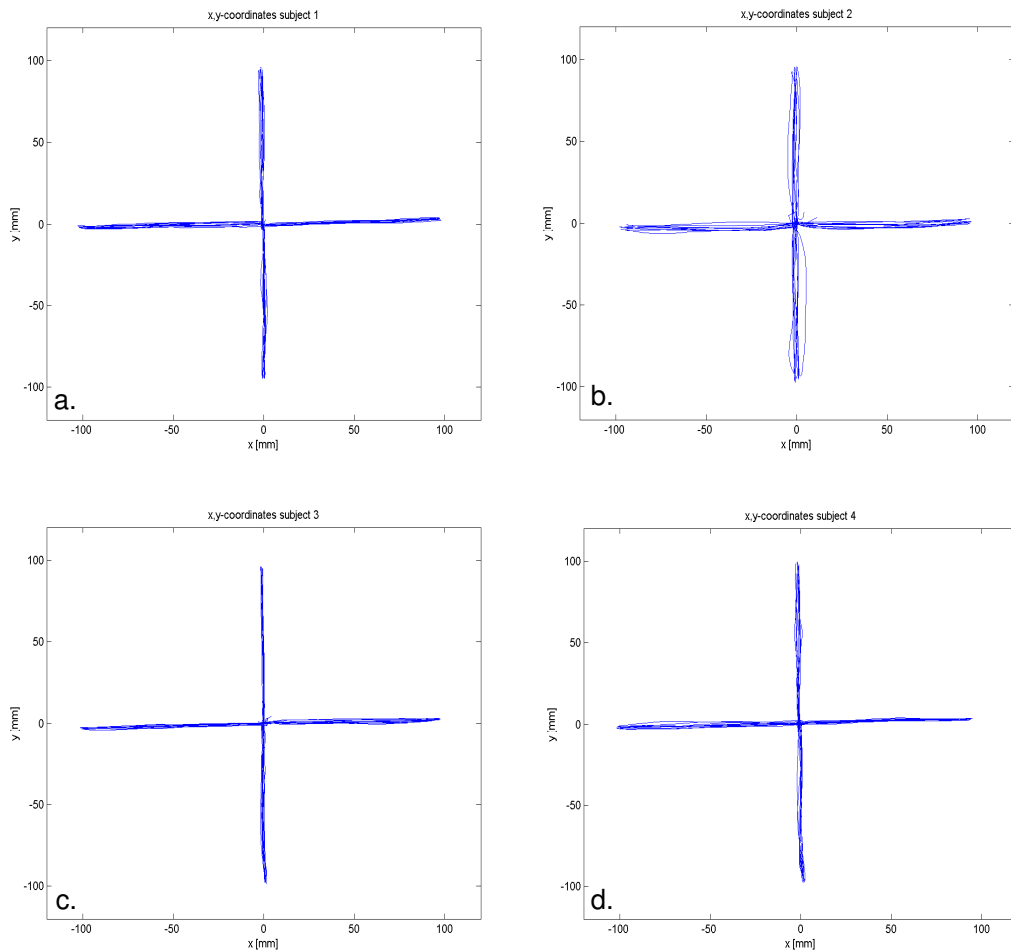


Fig 5.3: Sampled  $x,y$ -coordinates in [mm] for each of the four subjects: 5 cycles are performed for each set of lines drawn (shown for 12, 3, 6 and 9 o'clock targets only).

a:  $x,y$ -coordinates subject 1

b:  $x,y$ -coordinates subject 2.

c:  $x,y$ -coordinates subject 3.

d:  $x,y$ -coordinates subject 4.

The above results, which take very simple measures of time and a qualitative perspective on accuracy, highlight the potential to begin to explore the complexities and properties of the motor strategies associated with drawing and handwriting tasks. The following sections of this chapter explore in greater detail some of the measurable parameters that the data capture system allows us to investigate.

#### 5.4.2 Comprehensive description of line drawing features for subjects 1 and 2

The results from subjects 1 and 2 will be shown and compared for lines drawn to targets 12, 3, 6 and 9 o'clock. Subject 1 is chosen as the data is representative of that also found for subjects 3 and 4, while subject 2 is chosen as the task was performed in a way that focussed on speed, which affected accuracy.

The following results are presented for both subjects:

- Task accuracy. A number of performance parameters can be extracted from the data to be used as markers of accuracy. In the data to be presented the following parameters were chosen in relation to the 50% cycle length data point in a trial (target), which corresponds to the coordinate judged to be where the movement to a target ends and the return to origin commences:
  - Line segment length;
  - Deviation from the ideal straight line;
  - z-coordinates (tip pressure).

Statistics will be applied to the 50% cycle length (out of 5 the cycles for the complete task targeted to one direction) and is defined as a line segment from the start point (origin with coordinates (0,0)) to the target position or from target position to origin (0,0). The 50% cycle length refers to the travelled distance to the target rather than the time taken.

Both the length and the deviation of the 50% cycle line segment from the ideal straight line will be assessed. The deviation will be expressed by means of two measures: the linear regression and the measure latitude. The latitude is defined as the range or difference between the minimum and maximum deviation that was observed (Fig.5.4). This will be explained further in the discussion of the deviation.

The second outcome measure used to assess the task performance is to assess straightness of drawn lines by means of linear regression. For

statistical evaluation of goodness of fit, the following statistics are calculated: Sum of Squares Due to Error (SSE) and Root Mean Squared Error (RMSE) as explained in 4.4.4.

- x,y-coordinates over time;
- z-coordinates (pen tip pressure) during task performance;
- trajectories of shoulder, elbow, wrist and pen tip in x,y-coordinate frame.
- Grip force applied to the pen by Thumb, Index and Middle finger during performance of the task are shown together with the resultant grip force.

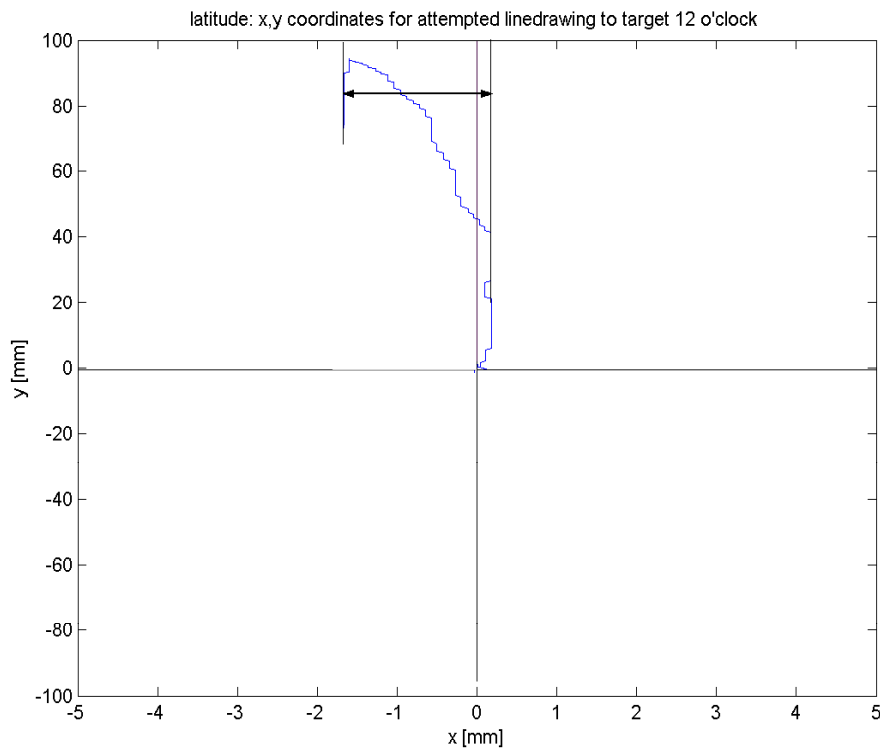


*Fig.5.4: Defining the latitude: the maximum deviation from the line towards the target direction and is therefore the difference between the minimum and maximum deviation perpendicular to the drawing direction.*

#### 5.4.2.1 Pen Tip X,Y- and Z-coordinates at 50% cycle length subject 1 and 2

The line drawing results for targets 12, 3, 6 and 9 o'clock for both subject 1 and subject 2 are shown in Fig.5.3a and 5.3b. The 10 line segments that make up the 5 cycles for each target were analysed separately for length and latitude perpendicular to the ideal straight line from origin to target. The ideal accurately drawn line should be length=100mm and latitude=0mm. Table 5.3 gives for each set of lines the mean line length with standard deviation (n=10) and the mean latitude and standard deviation (n=10). Fig 5.5 and 5.6 show the line length and latitude for subject 1 with Fig.5.7 and 5.8 providing data from subject 2. For each of the 10 lines drawn to targets 12, 3, 6 and 9 o'clock, (i.e. 5 lines to target, plus 5 lines to origin), Table 5.4 gives the start point and end point achieved by subject 1 and 2. For each line drawn and presented in Table 5.4, the corresponding linear regression analysis is given in Table 5.5 (SSE, RMSE and  $R^2$  and adjusted  $R^2$ ).

		Subject 1				Subject 2			
		vertical lines		horizontal lines		vertical lines		horizontal lines	
		12 o'clock	6 o'clock	3 o'clock	9 o'clock	12 o'clock	6 o'clock	3 o'clock	9 o'clock
50% cycle line length [mm]	mean	95.4	94.7	96.2	100.6	95.9	95.7	93.1	95.6
	STD	1.2	1.5	0.5	1.3	1.9	2.6	2.9	2.1
50% cycle line latitude [mm]	mean	1.7	1.4	4.2	2.9	2.4	2.9	3.3	3.3
	STD	0.6	0.5	0.9	0.7	1.1	1.5	1.2	1.4
deviation from ideal straight line	mean	-0.9	0.3	1.3	0	-0.6	-0.7	-1.1	-1.6
z-coordinates: 1024 tip pressure levels	mean	807	856	903	361	902	974	974	981
	max	963	916	985	692	1010	1002	1009	1002

Table 5.3: Statistics of line drawing results for subject 1 and subject 2: line length, latitude and z-coordinates (pen Tip pressure).

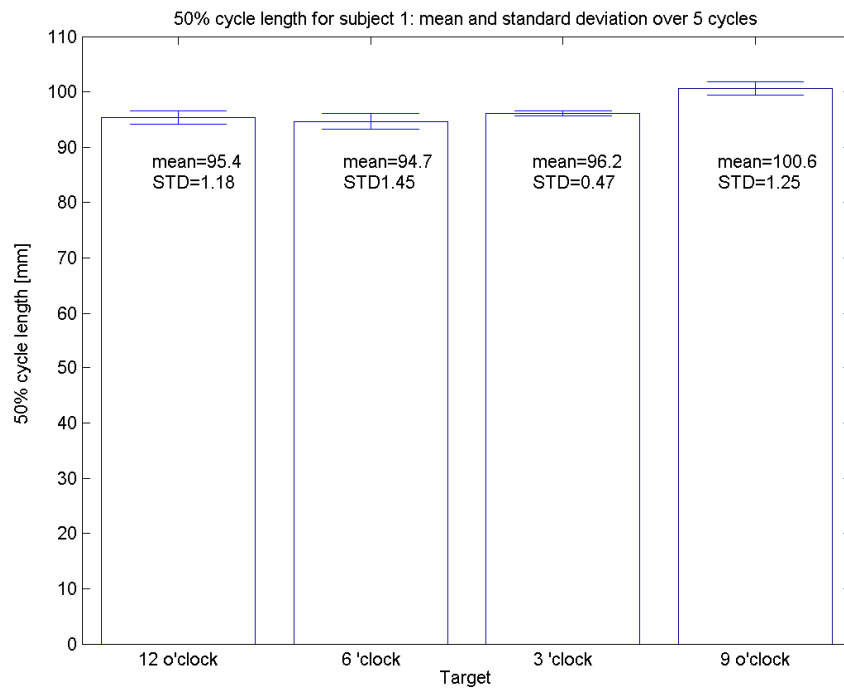


Fig.5.5: Line length of 50% cycle (out of 5 cycles) for subject 1: mean and standard deviation.

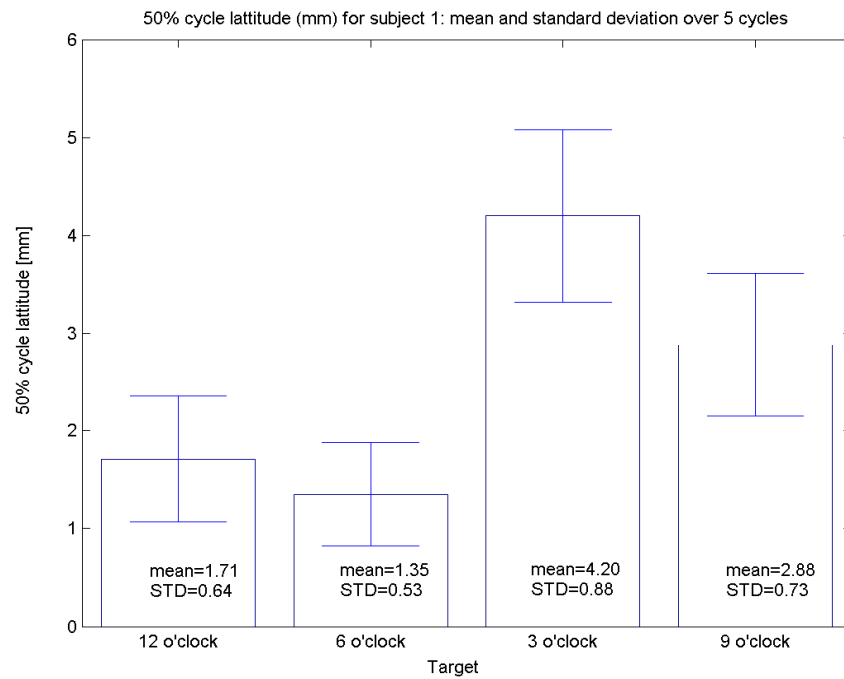


Fig.5.6: Latitude perpendicular to the ideal straight line length (50% cycle out of 5 cycles) for subject 1: mean and standard deviation.

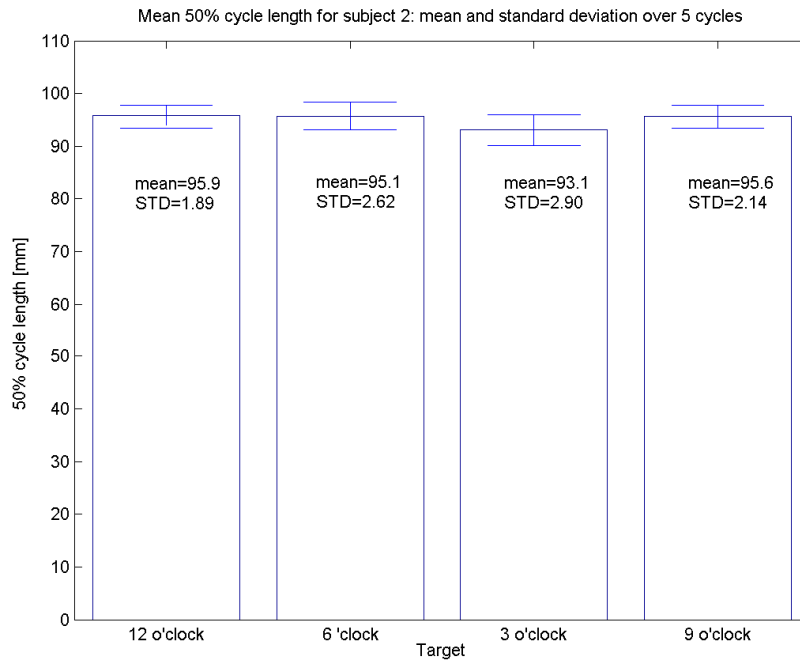


Fig.5.7: Line length of 50% cycle (out of 5 cycles) for subject 2: mean and standard deviation.

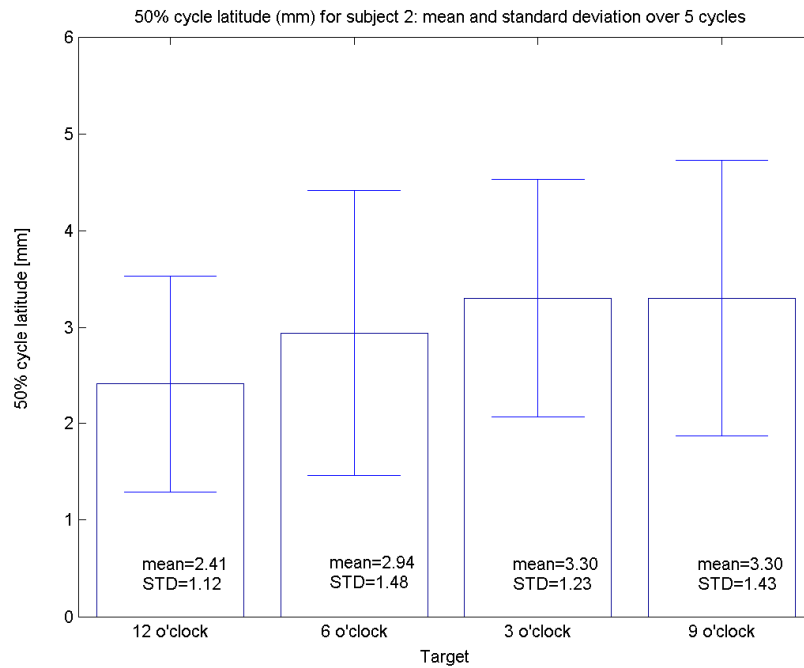


Fig.5.8: Latitude perpendicular to the ideal straight line length (50% cycle out of 5 cycles) for subject 2: mean and standard deviation.

Closeness to targets: coordinates of start and end points of drawn lines										
		Subject 1				Subject 2				
		vertical lines		horizontal lines		vertical lines		horizontal lines		
		12 o'clock	6 o'clock	3 o'clock	9 o'clock	12 o'clock	6 o'clock	3 o'clock	9 o'clock	
Coordinates of the start and end point of the 10 line segment as a measure of how close the target was reached.	1	start	0.1	0	0.4	0	0	0	0	
		end	94.8	-92.8	96.7	-101.9	93.2	-94.3	90.7	-94.3
		length	94.8	92.8	96.4	101.9	93.2	94.3	90.7	94.3
		deviation	5.2	7.2	3.3	1.9	6.8	5.7	9.3	5.7
	2	start	94.8	92.8	96.7	-101.9	93.2	-94.3	90.7	-94.3
		end	-0.7	-1.1	0.3	0.8	-1.7	-0.6	2.9	-0.8
		length	95.5	93.9	96.4	102.7	94.9	93.7	87.8	93.3
		deviation	0.7	1.1	0.3	0.8	1.7	0.6	2.9	0.8
	3	start	-0.7	-1.1	0.3	0.8	-1.7	-0.6	2.9	-0.8
		end	94.3	-94.3	96.6	-100.5	94.2	-93.1	93.6	-93.5
		length	95.0	93.3	96.3	101.3	95.9	92.4	90.7	92.7
		deviation	5.8	5.7	3.4	0.5	5.8	6.9	6.4	6.5
	4	start	94.3	-94.3	96.6	-100.5	94.2	-93.1	1.9	-93.5
		end	-2.2	0.0	0.3	0.2	-2.7	-0.5	93.6	0.4
		length	96.5	94.3	96.3	100.7	96.9	92.5	87.7	93.9
		deviation	2.2	0.01	0.3	0.2	2.7	0.5	1.9	0.4
	5	start	-2.2	0.0	0.3	0.2	-2.7	-0.5	1.9	0.4
		end	94.23	-94.5	96.0	-99.4	96.9	-94.7	95.1	-96.5
		length	96.5	94.5	95.7	99.5	98.6	94.2	85.2	97.0
		deviation	5.7	5.5	4.0	0.7	3.1	5.3	4.9	3.5
	6	start	94.3	-94.5	96.0	-99.4	95.9	-94.7	95.1	-96.5
		end	-0.9	1.5	0.9	-1.0	-1.3	1.6	1.7	1.9
		length	95.1	96.9	95.2	98.3	97.2	96.3	93.3	98.5
		deviation	0.9	1.5	0.9	1.0	1.3	1.6	1.7	1.9
	7	start	-0.9	1.5	0.9	-1.0	-1.3	1.6	1.7	1.9
		end	92.8	-94.0	96.8	-101.2	92.4	-95.6	95.8	-94.4
		length	93.7	95.5	95.9	100.2	93.7	97.1	94.2	96.3
		deviation	7.2	6.0	3.2	1.2	7.6	4.4	4.2	5.6
	8	start	92.8	-94.0	96.8	-101.2	92.4	-95.6	95.8	-94.4
		end	-0.3	2.1	0.6	-0.4	-1.1	2.0	-1.4	-0.1
		length	93.1	96.1	96.1	100.7	93.5	97.6	97.2	94.3
		deviation	0.3	2.1	0.6	0.4	1.1	2.0	1.4	0.1
	9	start	-0.3	2.1	0.6	-0.4	-1.1	2.0	-1.4	-0.1
		end	96.1	-94.4	97.5	-99.8	96.2	-96.7	94.8	-97.4
		length	96.4	96.4	96.7	99.7	97.3	98.7	96.4	97.3
		deviation	3.9	5.6	2.5	0.3	3.8	3.3	5.2	2.6
	10	start	96.1	-94.4	97.5	/	96.2	-96.7	95.0	-97.4
		end	0.7	1.3	1.0	/	-1.2	3.2	-0.3	1.1
		length	96.7	95.6	96.5	/	97.5	99.9	95.3	98.5
		deviation	0.7	1.3	1.0	/	1.2	3.2	4.7	1.1

Table 5.4: Statistics of line drawing results for subject 1 and subject 2: assessment of closeness to ideal line length and closeness to target. The assessment of straightness of the same lines is presented in Table 5.5.

Deviation from ideal straight line: measures from linear regression										
		Subject 1				Subject 2				
		vertical lines		horizontal lines		vertical lines		horizontal lines		
		12 o'clock	6 o'clock	3 o'clock	9 o'clock	12 o'clock	6 o'clock	3 o'clock	9 o'clock	
deviation from ideal straight line: statistics from linear regression for all 10 line segments within 5 cycles	1	SSE	2013	2109	4355	1425	493	271	1473	665
		RMSE	5.6	5.93	8.5	5.0	2.8	2.1	3.4	3.3
		R <sup>2</sup>	0.97	0.97	0.94	0.98	0.99	1.00	0.99	0.99
		R <sup>2</sup> adj	0.97	0.97	0.94	0.98	0.99	1.00	0.99	0.99
	2	SSE	76	1985	780	5622	722	1069	3277	2699
		RMSE	1.1	5.9	3.9	9.6	3.4	4.1	6.7	6.7
		R <sup>2</sup>	1.00	0.97	0.99	0.94	0.99	0.98	0.96	0.96
		R <sup>2</sup> adj	1.00	0.97	0.99	0.94	0.99	0.98	0.96	0.96
	3	SSE	948	2110	3018	1800	1297	776	2729	2324
		RMSE	4.0	5.8	7.5	5.7	4.3	3.6	5.5	6.0
		R <sup>2</sup>	0.99	0.97	0.96	0.98	0.98	0.99	0.97	0.97
		R <sup>2</sup> adj	0.99	0.97	0.96	0.98	0.98	0.99	0.97	0.97
	4	SSE	853	258	1906	6568	933.98	2295	1918	1753
		RMSE	3.7	2.0	5.8	10.8	3.9	6.2	5.2	5.2
		R <sup>2</sup>	1.00	1.00	0.98	0.92	0.99	0.97	0.98	0.98
		R <sup>2</sup> adj	0.99	1.00	0.97	0.92	0.99	0.97	0.98	0.98
	5	SSE	941	2507	5241	867	1031	952	1765	1264
		RMSE	3.8	6.4	10.0	4.1	4.1	3.9	4.5	4.5
		R <sup>2</sup>	0.99	0.97	0.92	0.99	0.99	0.99	0.98	0.99
		R <sup>2</sup> adj	0.99	0.97	0.92	0.99	0.99	0.99	0.98	0.98
	6	SSE	1756	268	3340	18621	1521	1133	1628	1380
		RMSE	3.5	2.1	7.6	17.2	4.9	4.3	4.5	4.8
		R <sup>2</sup>	0.99	1.0	0.95	0.77	0.98	0.98	0.98	0.98
		R <sup>2</sup> adj	0.99	1.0	0.95	0.77	0.98	0.98	0.98	0.98
	7	SSE	1024	1852	3576	2404	843	1522	2442	2066
		RMSE	4.2	5.4	7.9	6.5	3.7	5.00	5.6	5.7
		R <sup>2</sup>	0.99	0.98	0.95	0.97	0.99	0.98	0.97	0.97
		R <sup>2</sup> adj	0.99	0.98	0.95	0.97	0.99	0.98	0.97	0.97
	8	SSE	2037	212	2191	11052	1173	1361	1988	1899
		RMSE	5.6	1.9	6.6	13.7	4.3	4.2	5.5	5.5
		R <sup>2</sup>	0.98	1.0	0.97	0.86	0.98	0.99	0.98	0.98
		R <sup>2</sup> adj	0.98	1.0	0.97	0.86	0.98	0.99	0.98	0.98
	9	SSE	370	260	4521	1016	1288	1026	1985	1619
		RMSE	2.5	2.1	9.2	4.2	4.5	4.0	5.1	5.2
		R <sup>2</sup>	0.99	1.0	0.94	0.99	0.98	0.99	0.98	0.98
		R <sup>2</sup> adj	0.99	1.0	0.94	0.99	0.98	0.99	0.98	0.98
	10	SSE	827.4	635	2233	/	1070	1022	2119	1827
		RMSE	3.7	3.3	6.5	/	4.3	4.3	5.4	5.4
		R <sup>2</sup>	0.99	0.99	0.97	/	0.98	0.99	0.98	0.98
		R <sup>2</sup> adj	0.99	0.99	0.97	/	0.98	0.99	0.98	0.98

Table 5.5: Statistics of line drawing results for subject 1 and subject 2: assessment of closeness to ideal straight line for each line segment by means of linear regression. The assessment of closeness of targets of the same lines is presented in Table 5.4.

### ***Line length***

The following observation can be made from figures Fig.5.5, Fig.5.7 and Table 5.3. For subject 2 the mean line length is shorter (between 3 and 6 millimeters) than the ideal line (traced line length is 100 mm) for all targets, while for subject 1 the mean line length is shorter (between 3 and 6 millimeters) for three out of four targets (12, 3 and 6). Only the ideal line length for the 9 o'clock target is on average slightly longer (0.6 mm) than the ideal line in subject 1. Lines drawn to this target (9) can be seen from Table 5.4 to be less than 100mm for trials 5, 6 and 9. All other line segments are longer than 100mm. In general subject 2 shows more variation between the line lengths than subject 1.

### ***Deviation from ideal straight line: line latitude and linear regression***

The deviation from the ideal straight line is assessed by two different methods: measurement of the latitude of the line segment and a linear regression of each line segment. The latitude is a peak measure of deviation in the direction perpendicular to the ideal line direction (Fig.5.9). The linear regression allows measures of the total deviation from the ideal straight line (over its total length and not just peak value as measured by latitude) to be reported as the variation of the coordinate values (deviation) around the mean (ideal straight line). Measures of deviation from the line need to be assessed in respect to the residuals of the regression based on a time normalised representation of the data (section 4.4.4.2). It was decided to downsample all trials to 66 samplenumbers, which was the lowest number seen in all trials for both subjects.

The linear regression assesses the deviation from the ideal straight line by means of expressing measurement of the residuals as the Sum of Squares Due to Error (SSE) and Root Mean Squared Error (RMSE). The SSE measures the total deviation of the response values from the fit to the response values. A value closer to 0 indicates a better fit. The RMSE is also known as the fit standard error or the standard error of the regression and is derived from the SSE, taking into account the residual degrees of freedom. A value closer to 0 indicates a better fit.

R-square value of a linear regression is the square of the correlation between the response values and the predicted response values and therefore represents how

well the linear model explains the variation of the data. The R-square statistics can take values between 0 and 1 with 1 indicating a closer fit. Adjusted R-square uses the R-square value and adjusts it based on the residuals degree of freedom. This is further explained in section 4.4.4.1.

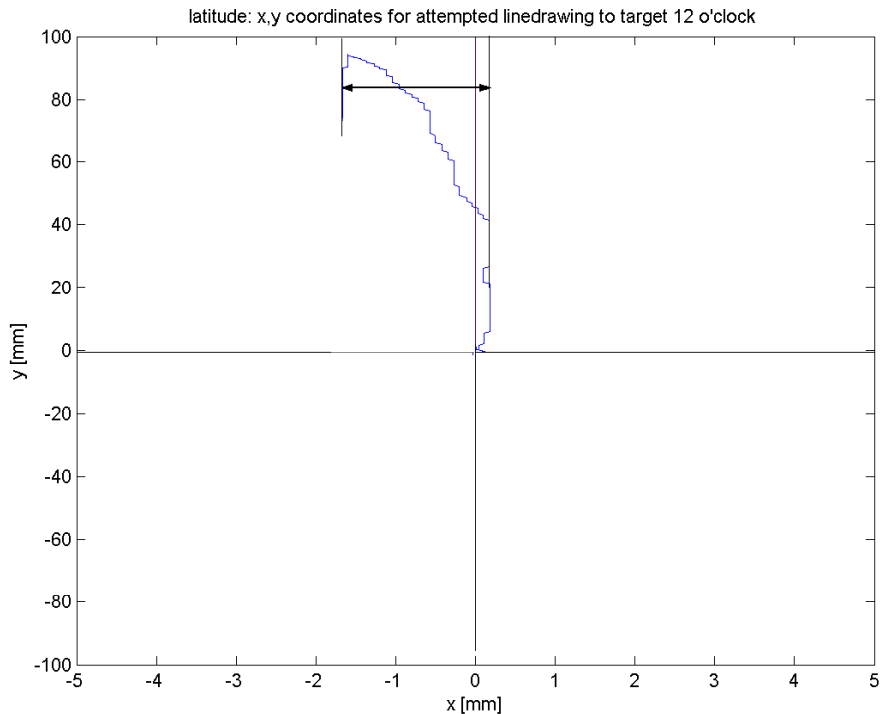


*Fig.5.9: The latitude is defined as the maximum deviation from the line towards the target direction and is therefore the difference between the minimum and maximum deviation perpendicular to the drawing direction.*

From Fig.5.6 and 5.8 it can be concluded that both subjects show less deviation in drawing vertical lines than when drawing horizontal lines. In addition, the results of linear regression on each of the 10 individual line segments in Table 5.5 also show less deviation for vertical line drawing than when drawing horizontal lines as can be seen from the SSE and RMSE values. Lower SSE and RMSE values for vertical line drawing, indicate residuals of the linear regression lying closer to the linear fit. In Table 5.6 the SSE-values from Table 5.5 are arranged with the SSE-values for horizontal sets of lines (3 o'clock and 9 o'clock) grouped in one column and vertical sets of lines (12 o'clock and 6 o'clock) in the next column for both subjects. The significance was evaluated statistically with a t-test with 99% confidence interval.

Two-sided t-test were performed for each subject to determine whether the two samples (2 sets of 10 horizontal lines for 3 and 9 o'clock and 2 sets of 10 vertical lines for 12 and 6 o'clock) from one subject could have the same mean when the standard deviations are unknown but assumed equal. For both subjects it was concluded that null hypothesis can be rejected with significance level of 99%. It was concluded that the mean of the SSE sample-values of vertical trials differ significantly from the mean of the SSE sample-values of the horizontal trials. The R-square values are equal or mostly higher than 0.9, indicating that the linear model fits the lines well.

Sum of Squares due to error			Subject 1		Subject 2	
			horizontal	vertical	horizontal	vertical
lines 1 to 10	1	SSE	2013	4355	493	1473
	2	SSE	76	780	722	3277
	3	SSE	948	3018	1297	2729
	4	SSE	853	1906	933.98	1918
	5	SSE	941	5241	1031	1765
	6	SSE	1756	3340	1521	1628
	7	SSE	1024	3576	843	2442
	8	SSE	2037	2191	1173	1988
	9	SSE	370	4521	1288	1985
	10	SSE	827	2233	1070	2119
lines 1 to 10	1	SSE	2109	1425	271	665
	2	SSE	1985	5622	1069	2699
	3	SSE	2110	1800	776	2324
	4	SSE	258	6568	2295	1753
	5	SSE	2507	867	952	1264
	6	SSE	268	18621	1133	1380
	7	SSE	1852	2404	1522	2066
	8	SSE	212	11052	1361	1899
	9	SSE	260	1016	1026	1619
	10	SSE	635	/	1022	1827
Mean SSE			1152	4239	1090	1941
Difference SSE vertical - horizontal			3087		851	

Table 5.6: Sum of Squares due to Error (SSE) values from linear regression for horizontal and vertical targets for both subjects.

The reduced deviation for vertical targets is most obvious for subject 1 and most likely relates to the lower drawing velocity of pen motion in vertical direction. The low velocity appears with decreased curvature (Fig.5.3 and Table 5.3). For subject 1, the duration of the up and down line drawings (12 and 6 o'clock targets) are respectively 18.4 and 19.3 seconds, whereas the duration of the horizontal trials (3 and 9 o'clock targets) are respectively 14.9 and 12 seconds.

In addition, for subject 2, the line latitude varies more between the 50% cycle line segments for each target (along with more variation in line length) than for subject 1 as revealed by the larger standard deviations of the latitude for subject 2 (Fig.5.6, Fig.5.8 and Table 5.3).

For subject 1, interestingly, only for 9 o'clock does the mean for the set of lines approach zero (Table 5.4). For subject 2 the mean values are below zero for all target directions: -0.62 mm for 12 o'clock; -0.68mm for 6 o'clock; -1.1mm for 3 o'clock and -1.6mm for 9 o'clock. It can be concluded that both subjects do not achieve a constant accuracy of higher than +/-1mm, but this can still be considered as quite skilful.

In Fig.5.10 it can be seen that for the horizontal line drawing towards the 9 o'clock target (Fig.5.10a), the deviation from the horizontal line (Fig.5.10b, directed vertically and perpendicular to the horizontal line direction) is related to the drawing direction: with positive horizontal movement there is upward vertical movement and with negative horizontal movement there is downward vertical movement.

### ***Z-Coordinates***

From Table 5.3 it may be observed that for subject 1 the mean and maximum tip pressure (z-coordinates) are much lower for target 9 o'clock than for other targets (Table 5.3). This can be explained from the way the pen and tablet operate. In the beginning of the trial (for +/- 2.5 seconds), the pen was just lifted up from the tablet and was dragged just over the surface of the tablet. Although, the pen tip was close enough to the tablet to still sample x- and y- coordinates without any significant contact as may be seen in Fig.5.9c. In addition, during the rest of the trial the tip pressure remains lower than in other trials for subject 1 (Table 5.3) and all trials for subject 2 (Table 5.3).

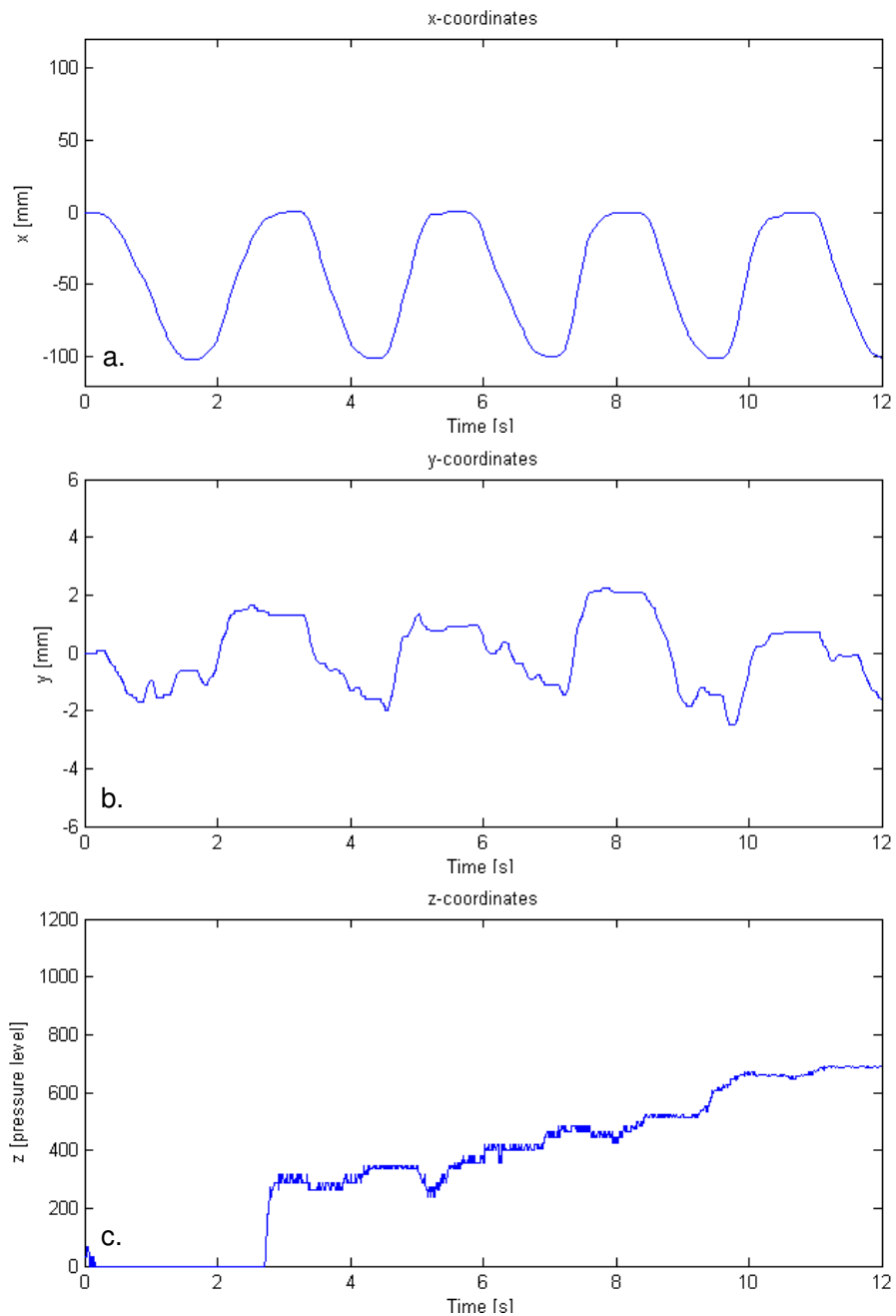


Fig.5.10: x,y- and z-coordinates for target direction 9 o'clock by subject 1:

a: x-coordinates;

b: y-coordinates;

c: z-coordinates: during first part of the line drawing activity the pen is lifted from the tablet, but remains close enough to the tablet to sample x- and y-coordinates. For the rest of the trial the pen-tablet pressure is low. This explains the low mean and maximum tip pressure in Table 5.3 compared to other trials.

#### 5.4.2.2 Subject 1: description of line drawing mechanics

This section gives a detailed description of the biomechanical aspects associated with line drawing that were recorded with the developed system in addition to the assessment of writing coordinates in 5.4.2.1. The inter-related biomechanical measures that are going to be discussed are:

- script x,y-coordinates over time;
- z-coordinates (pen tip pressure) during task performance;
- trajectories of shoulder, elbow, wrist and pen tip in x,y-coordinate frame;
- changes in pen grip force application by the Thumb, Index and Middle finger.

The changes in pen grip force associated with movement patterns observed in drawing lines to target directions 12, 3, 6 and 9 o'clock (experiments 1, 4, 7 and 10) by subject 1 are described below, followed by a brief discussion. The minimum, maximum and average values of Thumb, Index and Middle finger forces are shown in Table 5.7. In addition, minimum and maximum values of Shoulder, Elbow and Wrist joint trajectory coordinates (in mm) obtained with a Vicon motion analysis system are also presented in Table 5.7.

		Subject 1				Subject 2			
		vertical lines		horizontal lines		vertical lines		horizontal lines	
		trial 1	trial 7	trial 4	trial10	trial 1	trial 7	trial 4	trial10
thumb force [N]	min	065	1.38	2.20	4.81	1.01	1.43	0.65	1.15
	max	7.80	6.36	6.06	6.19	2.94	3.34	2.64	2.64
	average	6.39	6.0	5.18	5.74	2.21	2.73	1.99	2.09
middle force [N]	min	0.75	1.43	1.52	2.28	0.48	0.51	0.34	0.37
	max	5.08	4.38	3.78	3.78	1.29	1.06	1.02	1.02
	average	3.64	3.17	2.74	2.92	0.86	0.84	0.80	0.68
index force [N]	min	0.36	1.14	2.44	3.22	0.90	1.25	0.54	0.92
	max	7.26	5.74	6.45	5.65	2.26	2.58	1.80	1.91
	average	5.87	4.59	4.04	4.10	1.81	2.12	1.35	1.45
x-coordinates shoulder trajectory [mm]	min	117.5	73.42	36.5	-0.15	189.34	175.05	175.86	138.51
	max	138.4	83.0	90.8	17.1	204.81	189.45	193.38	174.67
y-coordinates shoulder trajectory [mm]	min	-385.8	-387	-330.5	-328.5	-349.98	-374.97	-380.53	-366.88
	max	-323	-323.1	-272.2	-308.7	-327.14	-356.97	-359.36	-341.29
z-coordinates shoulder trajectory [mm]	min	221.0	259.6	251.3	248.1	226.12	225.26	230.13	235.70
	max	245.82	274.2	274.8	288.4	239.33	243.40	243.43	262.80
x-coordinates elbow trajectory [mm]	min	246.3	241.9	137.5	62.4	324.44	343.33	337.93	271.69
	max	300.5	275.2	155.8	82.9	358.68	376.47	385.46	336.27
y-coordinates elbow trajectory [mm]	min	-276.5	-370.5	-376.0	-380.5	-228.74	-257.50	-298.73	-247.34
	max	-186.6	276.0	-346.2	350.7	-169.47	-216.73	-232.02	-181.88
z-coordinates elbow trajectory [mm]	min	-12.0	33.1	-8.5	2.00	-14.51	-7.46	-6.18	-3.06
	max	25.89	61.9	7.3	9.14	8.75	30.07	14.09	35.99
x-coordinates wrist trajectory [mm]	min	73.85	67.9	22.2	-76.1	125.64	122.87	125.09	29.90
	max	104.8	83.2	86.0	14.4	141.46	130.59	208.28	130.75
y-coordinates wrist trajectory [mm]	min	-65.7	-165.9	-113.6	-114.4	-37.76	-88.69	-70.23	-46.45
	max	25.9	-77.9	-105.0	-107.3	43.13	-36.76	-44.73	-20.94
z-coordinates wrist trajectory [mm]	min	20.3	26.3	16.9	24.1	19.33	0	0	17.55
	max	30.2	62.9	30.3	29.8	31.97	16.12	34.98	29.17
Time [s]		18.38	19.34	14.85	12.00	9.22	9.41	8.96	8.94

Table 5.7: Line drawing results for subjects 1 and 2: trajectories and force values..

### Line drawing mechanics for target 12 o'clock

The grip force variation is shown in Fig. 5.11a. Overall, the force measurement can be seen to change in a cyclic manner in synchrony with the line drawing task (Fig.5.11b). At the start of the trial there is a sudden increase of the index finger force (from 5N to 7.15N, with peak value of 7.1N) before actual vertical pen tip movement (compare y-coordinates in Fig.5.11b). Simultaneously, with the increase of index finger force, a slight increase of the middle finger force (+0.3N) and thumb

force (+/-0.2N) can also be seen prior to pen tip motion. The peaks of the three finger forces lead to a peak resultant grip force that has a negative value before the vertical pen tip movement starts (Fig.5.11c). It can be hypothesised that these pre-motion changes in grip force are associated with the subject preparing to move and the requirement to stabilise pen position in the hand.

The resultant grip force magnitude and direction as shown in Fig.5.11 and Fig.5.12 were calculated as follows with a Matlab script. Firstly, the force components in forward (x-) direction and up- and downward (y-) direction for each of the three fingers (thumb, index and middle finger) were calculated for every force sample, using trigonometry. Then the sum in the x-direction and the sum in the y-direction of the three forces applied (by thumb, index, and middle finger) are calculated for each sample. The resultant force is then calculated from the force in x- and y-direction, using Pythagoras' theorem.

The finger force magnitude and the pen orientation angle in the plane through the longitudinal pen axis determine the components in x- and y-direction. This can be seen in the drawings of the pen orientation in the top right corners of the resultant force graphs in Fig.5.11 and Fig.5.12.

After the pre-motion finger pen grip activity, the finger forces involved with the line drawing is as follows. Inspection of Fig.5.11a and Fig.5.11b reveals that the index finger is mainly associated with downward pen tip movement as its relative contribution increases during downward drawing phase, which results in tip movement in negative y-direction (seen from y-coordinates in Fig. 5.11b). While index force increases, the middle finger force compensates to preserve balance and slight adaptations of thumb force can be seen. The resultant force vector consequently points downwards (negative y-direction). This can be seen for all 5 line drawing cycles.

The upward pen tip movement is established by decreasing the index finger pressure, leading to an upward resultant force vector (See Fig. 5.11a and Fig.5.11b).

The index finger's role in establishing up- and downward pen movement can be seen more clearly from Fig.5.12 which shows in an expanded scale the recordings of finger forces, resultant force vector and y-coordinates for the 4th cycle of the 12 o'clock target trial. It can be seen from Fig.5.12a that the changes of index finger

force precede the changes of the other two finger forces and the Index finger may therefore have an important role for this subject in controlling the gripping activities during line drawing.

Along with script ( $x,y,z$  measures) and finger force recordings, the joint trajectories of shoulder, elbow and wrist were recorded using a Vicon motion analysis system. The joint trajectories for the drawing of 5 lines to the 12 o'clock target are shown in Fig.5.13, Fig.5.14, Fig.5.15, Fig 5.16, Fig 5.17 and Fig 5.18 from different viewing angles. Fig. 5.14, Fig 5.15 and Fig.5.16 zoom in to the motion of pen tip and wrist, elbow and shoulder, respectively. The up- and downward pen tip motion in the writing plane is established by synergy activities of the shoulder, elbow and wrist joints and finger motion as follows. The shoulder instigates a rotational movement of the limb around the z-axis, which leads to a linear elbow joint path with diagonal orientation in the horizontal writing plane. At the same time, rotation of the forearm around the elbow joint enables the linear wrist joint motion to be directed more in the y-direction of the writing plane than the linear elbow motion that was orientated diagonally. The pen tip motion with up- and downward orientation is enabled by wrist joint motion and finger movement. It may be concluded that although the Index finger establishes resultant pen grip force that is positive with upward pen tip motion and negative with downward pen tip motion (as described, see Fig. 5.11a, b and c), the actual line drawing motion is established by the limb effectors. The finger pen grip plays a role in converting the wrist joint motion that is orientated diagonally in the  $x,y$ -plane into an up- and downward pen tip motion. Although one may assume that wrist rotation also plays a role in converting diagonal wrist motion into vertical pen tip motion by positioning the hand, for this example of line drawing in the y-direction, the wrist mainly provides a linear motion for positioning of the hand (Fig.5.14).

There may be minor wrist rotation around the three main axes (See Fig.5.16), but it does not seem to make a substantial contribution to establishing the pen tip motion relative to the wrist. This minor rotation is firstly around an axis perpendicular to the longitudinal axis and pointing upwards when the hand and arm are placed flat on the writing surface ( $X_f$  in Fig.5.19). In addition, there is rotation around an axis perpendicular to the longitudinal axis, pointing to the right from the writer's point of view when the hand and arm are placed flat on the writing surface ( $Z_f$  in Fig. 5.19). From Fig. 5.18 it can be clearly seen that with every line drawn, the shoulder, elbow

and wrist position move forward (towards the drawn line), which requires the wrist joint to flex around the Zf-axis (see Zf-axis in Fig. 5.19).

There may also be minor rotation around the longitudinal axis of the forearm (Yf in Fig.5.19). There is no up and down going rotational motion of the wrist in the vertical plane perpendicular to the writing surface. The exact change of angles around the Xf axis and Zf axis were not analysed yet, but could be exported from the Vicon motion analysis data.

The shoulder joint trajectories in Fig.5.18 reveal that the shoulder does not just instigate a rotation motion for the limb around the vertical (z) axis, but there is an up and down going rotational motion of the shoulder as well in the vertical plane perpendicular to the writing surface. Fig.5.16 shows a close up of the shoulder rotational movement.

Overall, it can be concluded that despite shoulder, elbow and wrist trajectories being different in every cycle, the pen tip trajectories as expected and demonstrated in 5.13 are very similar for each cycle. This emphasizes the flexibility in coordinating the biomechanical plant formed by the hand, arm and upperbody for producing drawing and that a particular action can be generated by a variety of movement patterns when there are many degrees of freedom in the actuators.

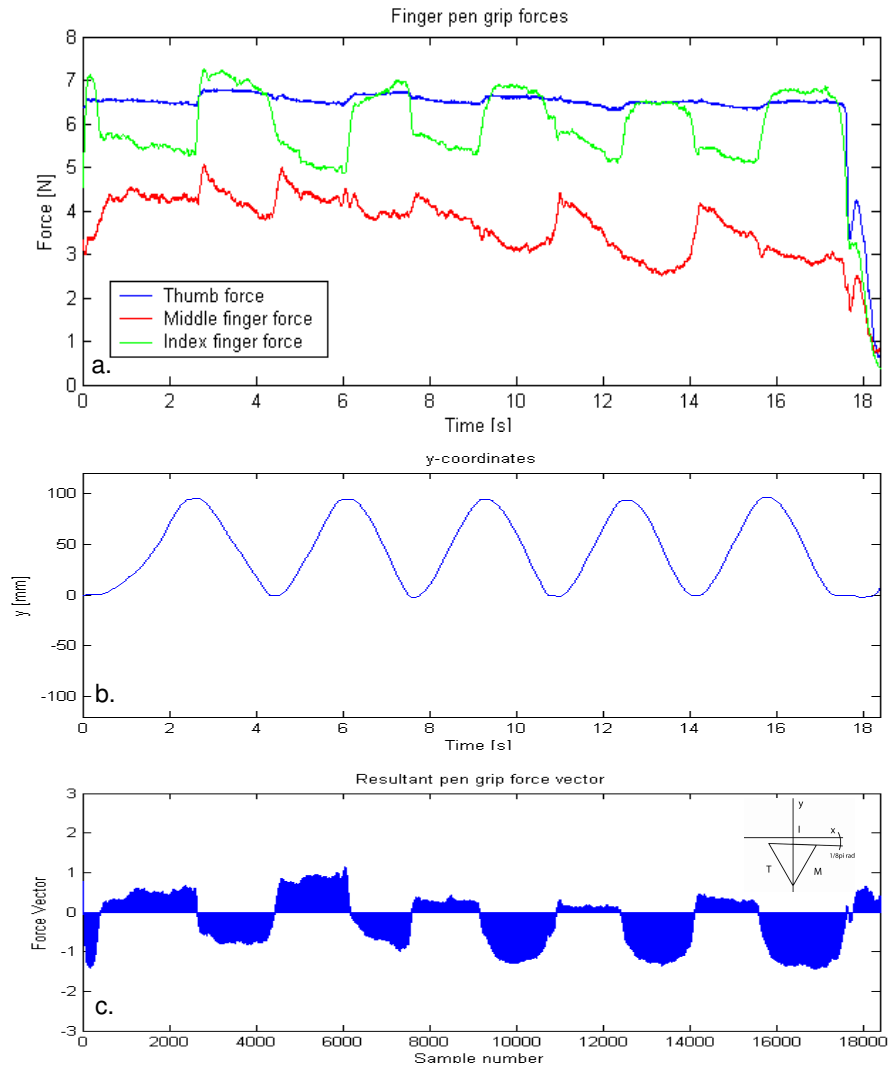


Fig.5.11: Recording for 12 o'clock target by subject 1.

a: Finger forces for target direction 12 o'clock for subject 1.

b: y-coordinates for target direction 12 o'clock for subject 1.

c: Resultant grip force vector for target direction 12 o'clock for subject 1.

The first index finger peak force does not lead to any pen tip movement (Fig.5.11a) and may be exerted to ensure a stable grip prior to vertical pen tip motion. The changes in vertical pen tip movement precede changes in the other two finger forces. For downward tip movement, the index finger's relative contribution increases, which results in tip movement in negative y-direction, while a slight adaptation in middle finger force can be seen to preserve balance. The consequent resultant pressure vector points downwards (negative y-direction). For upward pen tip movement, the index finger pressure is decreased along with slight peak increase of middle finger force, leading to an upward resultant pressure vector.

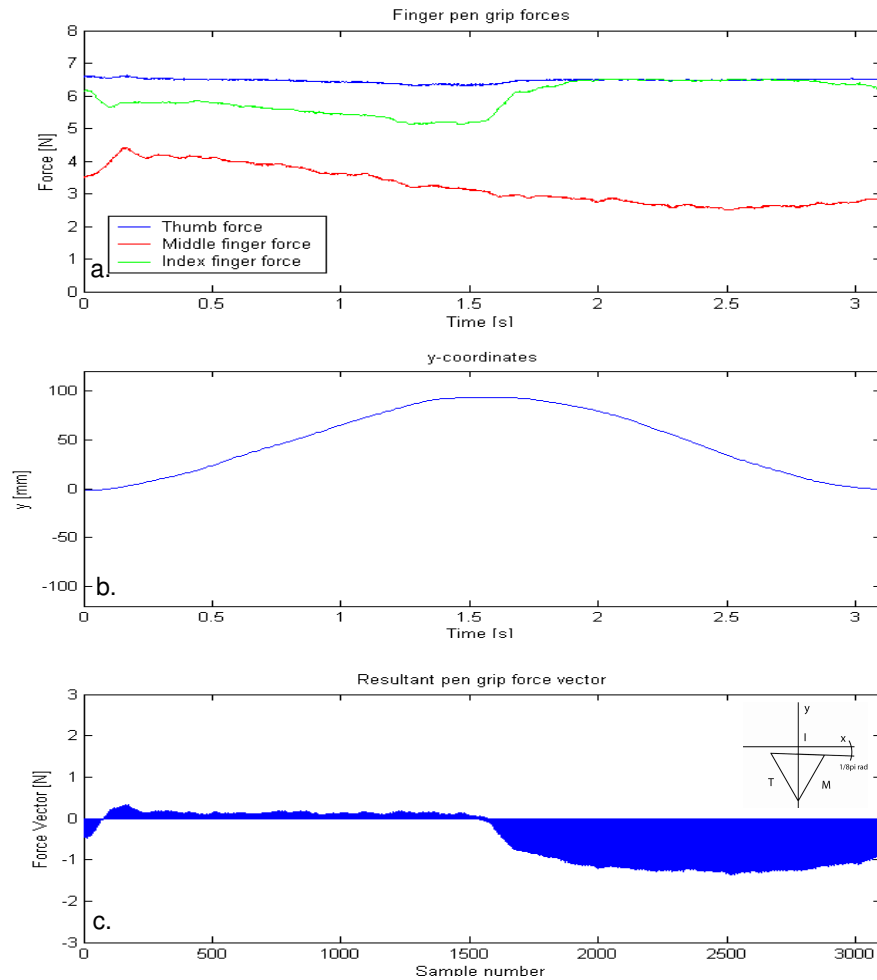


Fig.5.12: Recording for the 4th cycle of the 12 o'clock target by subject 1.

- a: Finger forces for target direction 12 o'clock for subject 1.
- b: y-coordinates for target direction 12 o'clock for subject 1.
- c: Resultant grip force vector for target direction 12 o'clock for subject 1.

The index finger is mainly responsible for downward tip movement: its relative contribution increases during downward phase, resulting in tip movement in negative y-direction (Fig. 5.12b). The middle finger force is adapted according to changes in index finger force to preserve the balance while allowing the vertical movement. The subsequent resultant pressure vector points downward (negative y-direction) (Fig.5.12c). The upward pen tip movement is established by decreasing the index finger force and slightly increasing middle finger force, leading to an upward resultant pressure vector (See Fig. 5.12a and Fig.5.12b).

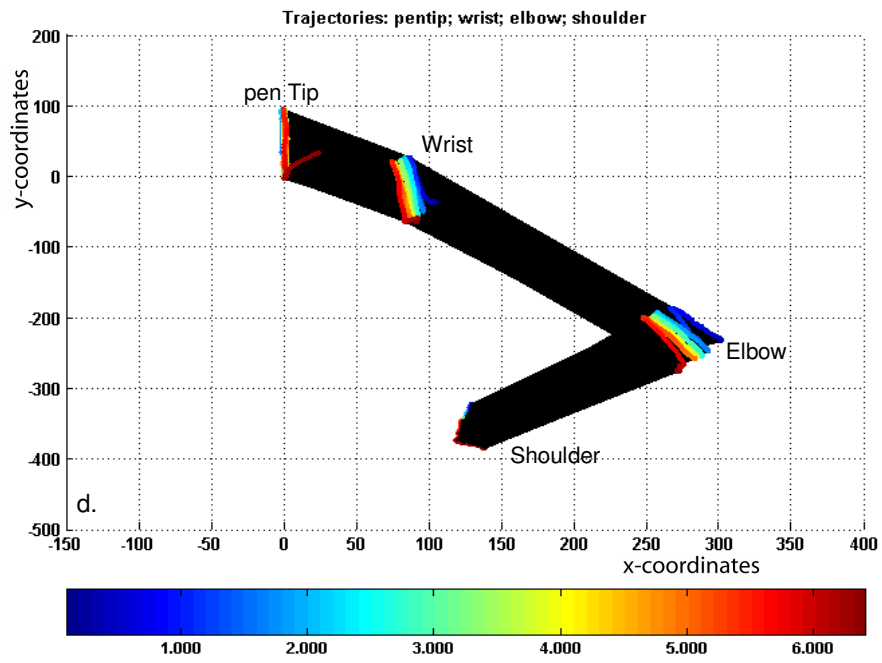


Fig.5.13: Recorded trajectories (pen tip and joints: shoulder, elbow and wrist) for 12 o'clock target by subject 1.

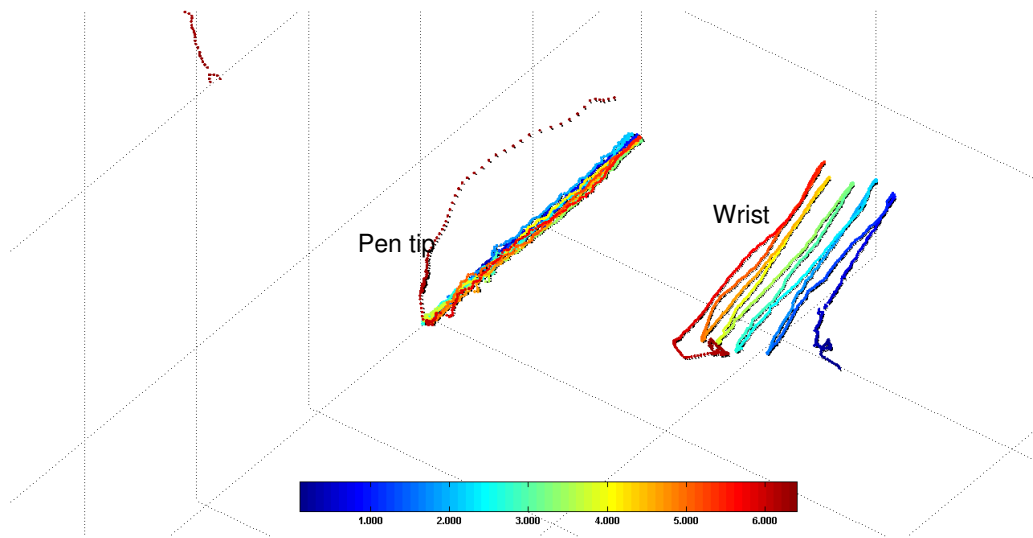


Fig.5.14: Recorded pen tip and wrist joint trajectories in 3 dimensions: linear motion.

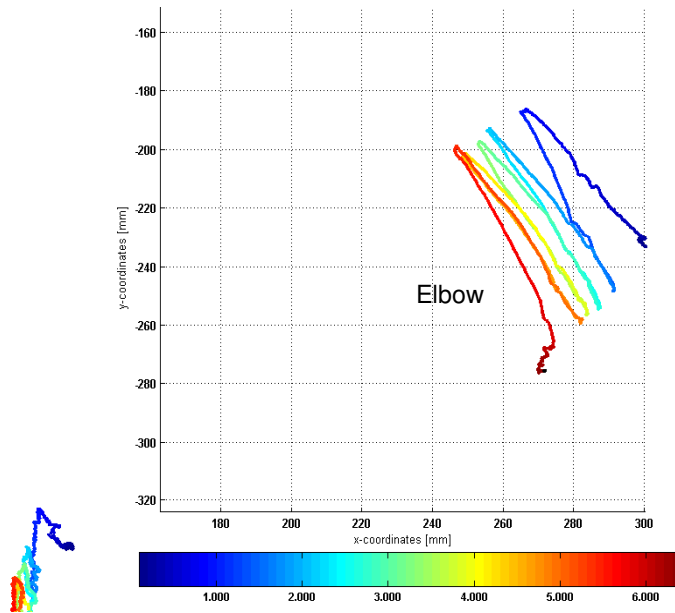


Fig.5.15 Recorded elbow joint trajectories in 3 dimensions: linear motion.

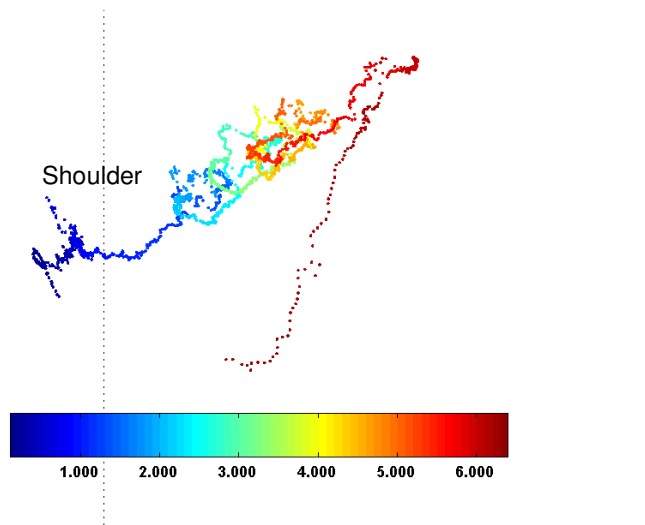


Fig.5.16: Recorded shoulder joint trajectories in 3 dimensions. Rotational motion is seen.

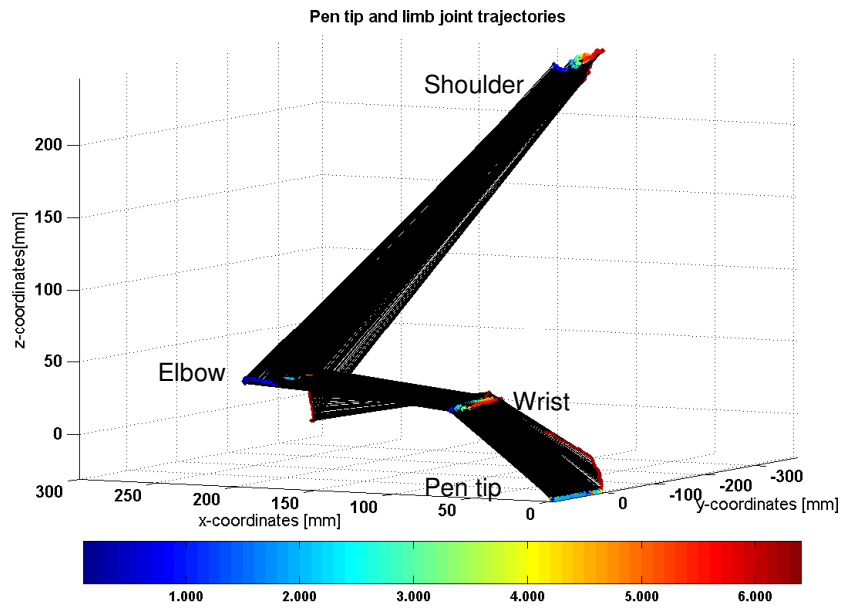


Fig.5.17: Recorded trajectories in 3 dimensions (pen tip and joints: shoulder, elbow and wrist) for 12 o'clock target by subject 1.

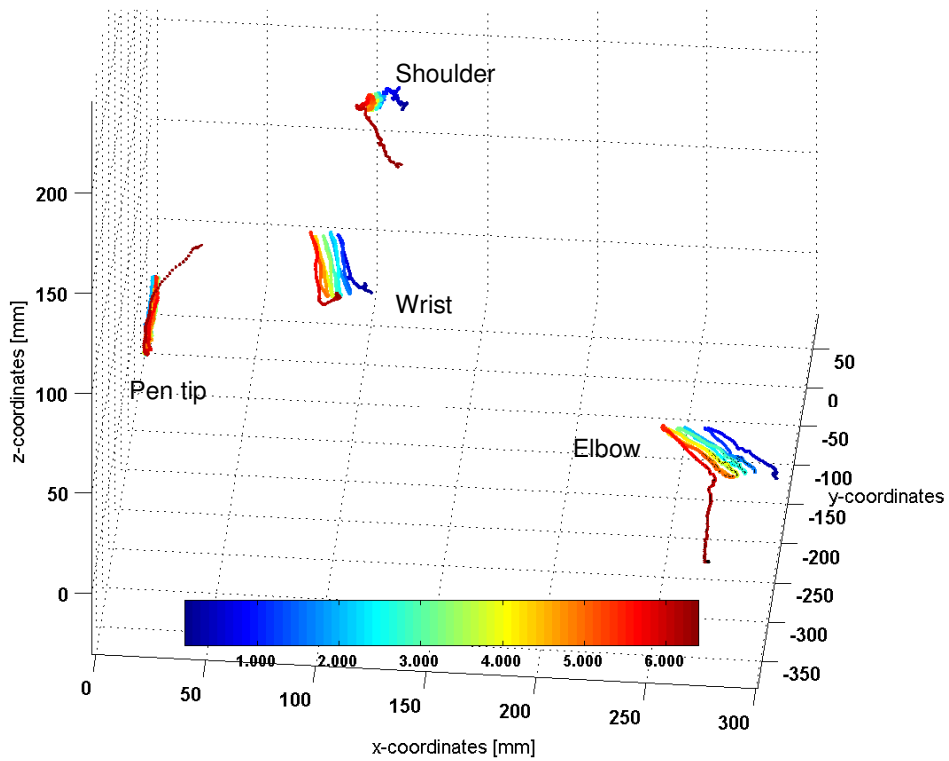
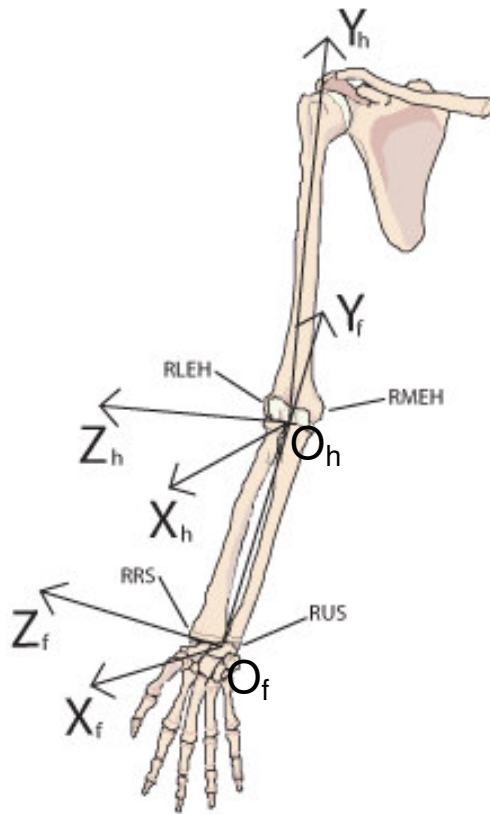


Fig.5.18: Recorded trajectories in 3 dimensions without connection lines between joints (pen tip and joints: shoulder, elbow and wrist) for 12 o'clock target by subject 1.



**Fig.5.19: Right arm anatomical axis frame in anterior view (copy Fig.4.6):**

**Humerus:**

$O_h$ : origin coincident with elbow joint centre (E) between RMEH and RLEH;

$Y_h$ -axis: The line connecting the right shoulder joint centre (RSJC) to the midpoint between RMEH and RLEH, pointing upward;

$X_h$ -axis: The line perpendicular to the plane formed by RMEH, RLEH and RSJC, pointing forward.

$Z_h$ -axis: The common line perpendicular to the  $X_h$ - and  $Y_h$ -axes, pointing to the left.

**Forearm:**

$O_f$ : origin coincident with wrist joint centre (W) between RUS and RRS;

$Y_f$ -axis: The line connecting midpoint between RUS and RRS and the midpoint between RMEH and RLEH, pointing upward;

$X_f$ -axis: The line perpendicular to the plane formed by RUS, RRS and the midpoint between RMEH and RLEH, pointing forward.

$Z_f$ -axis: The common line perpendicular to the  $X_f$ - and  $Y_f$ -axes, pointing to the left.

### **Line drawing mechanics for target 3 o'clock**

The grip force modulation during pen drawing towards the 3 o'clock target and back to the origin is shown in Fig. 5.20a. As for the 12 o'clock target, a peak in the index finger force can be seen (from 4.3N to 6.4N) at the beginning of the trial prior to the actual horizontal pen tip movement begins (compare x-coordinates in Fig.5.20b). Next, a very small peak in thumb and index finger occurs simultaneously, while the middle finger forces reaches its lowest value, followed by decreasing thumb and index finger forces and increasing middle finger force. These grip force changes occur without any horizontal movement towards the 3 o'clock target and the grip control actions seem to only associate with establishing a stable pen grip before starting the actual horizontal pen tip motion towards the 3 o'clock target.

In general, there appears to be more thumb pen grip force involvement with less index finger force than seen for moves to target direction 12 o'clock. Unlike the 12 o'clock target direction, the modulation of the index finger force does not clearly precede variations of thumb and middle finger force.

The applied thumb force contributes to the forward tip movement as its relative contribution increases during the forward phase (movement in positive x-direction, seen from x-coordinates in Fig. 5.20b). However, the pen tip movement in horizontal direction is not only established by increasing thumb pressure as the resultant grip force vector (Fig.5.20 c and d) and wrist rotation (Fig. 5.21) reveal. The resultant force vector does not only point forwards, but also upwards (positive x- and y-direction) during forward movement (Fig 5.20c). This is shown more clearly in the expanded graph of 5.20d for intervals [10697,10720]. From this it can be assumed that wrist movement plays an important role in forward pen tip movement during horizontal line drawing and this is confirmed by the arm joint trajectories data shown in the figures (Fig.5.21 and Fig.5.22). The figures show that main forward movement is established by forward Wrist movement. In addition, Fig.5.21 and Fig.5.22 show that the actual drawn horizontal line is longer than the horizontal wrist trajectory, while the elbow does not provide any significant horizontal displacement. It can be concluded that Wrist rotation plays an important role in addition to Wrist translation. The wrist rotation is assumed to be concurrently around the three main axes (See Fig.5.23). There is rotation around the longitudinal axis of the forearm ( $Y_f$  in Fig.5.23). There is also rotation around an axis perpendicular to the longitudinal axis and pointing upwards when the hand and arm are placed flat on the writing surface ( $X_f$  in

Fig.5.23). There is a third axis perpendicular to the longitudinal axis, pointing to the right from the writer's point of view when the hand and arm are placed flat on the writing surface ( $Z_f$  in Fig. 5.23). The exact change of angles around the three axis were not analysed yet, but could be exported from the Vicon data.

The short elbow trajectories also reveal that there is little shoulder joint rotation and Fig.5.22 shows that the shoulder motion is linear over a part of the trajectory, although not synchronised with the wrist and pen tip movement.

Overall, there is very little variation of pen tip trajectories in every drawn line. The main movement that enables the horizontal pen tip motion comes from the wrist. The shoulder and elbow positions and trajectories show relatively small changes with little variation between cycles, while the wrist and tip show distinct time dependent behaviour as the pen is moved. This contradicts markedly with how vertical pen motion is produced.

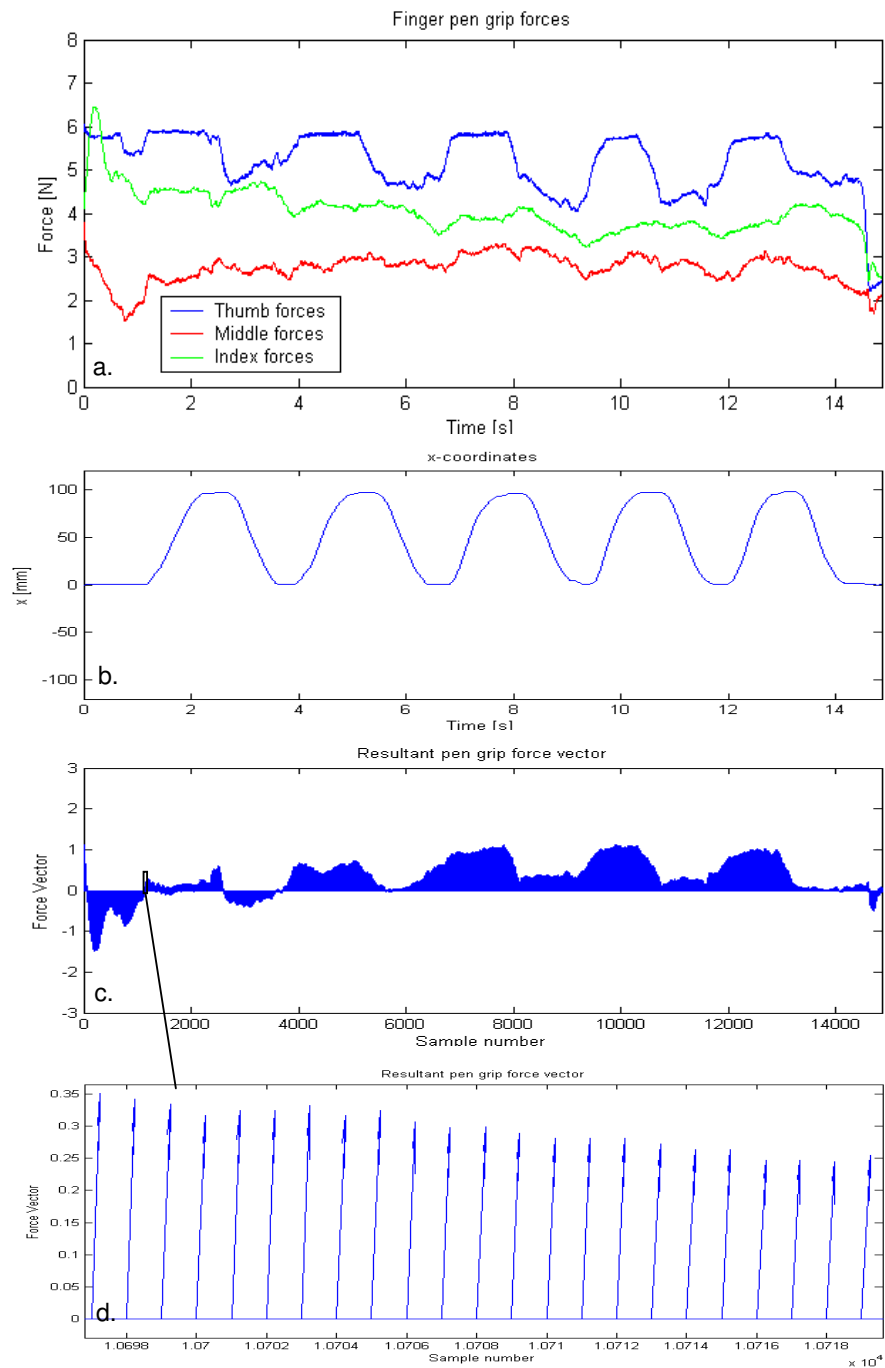


*Fig.5.20: Recording for 3 o'clock target by subject 1.*

- a: Finger forces for target direction 3 o'clock for subject 1.*
- b: y-coordinates for target direction 3 o'clock for subject 1.*
- c: Resultant grip force vector for target direction 3 o'clock for subject 1.*
- d: Resultant grip force vector for target direction 3 o'clock for subject 1: zooming in between sample numbers 10696 to 10720 to illustrate the forward and upward direction.*

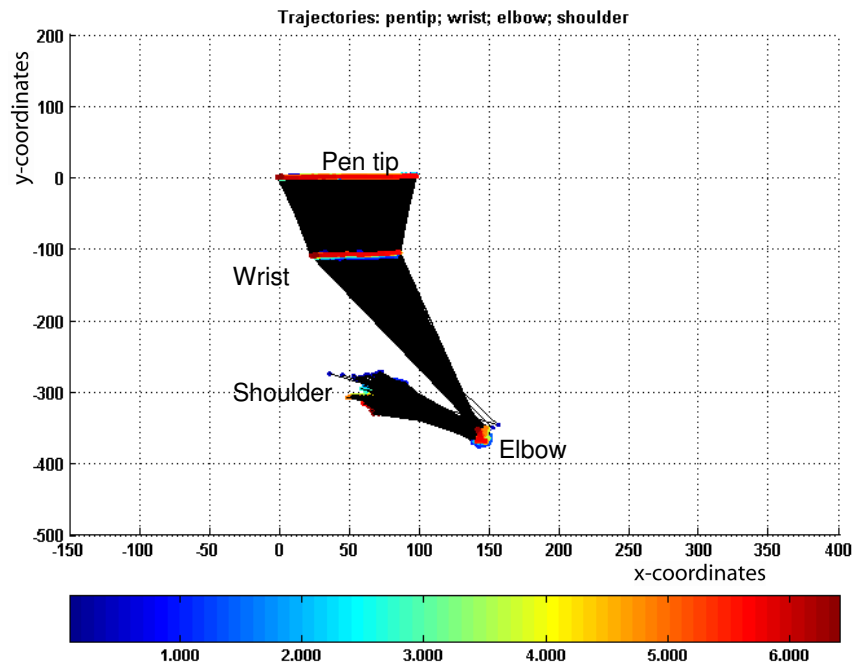


Fig.5.21: Recording for 3 o'clock target by subject 1:Trajectories (pen tip and joints: shoulder, elbow and wrist) for target direction 3.

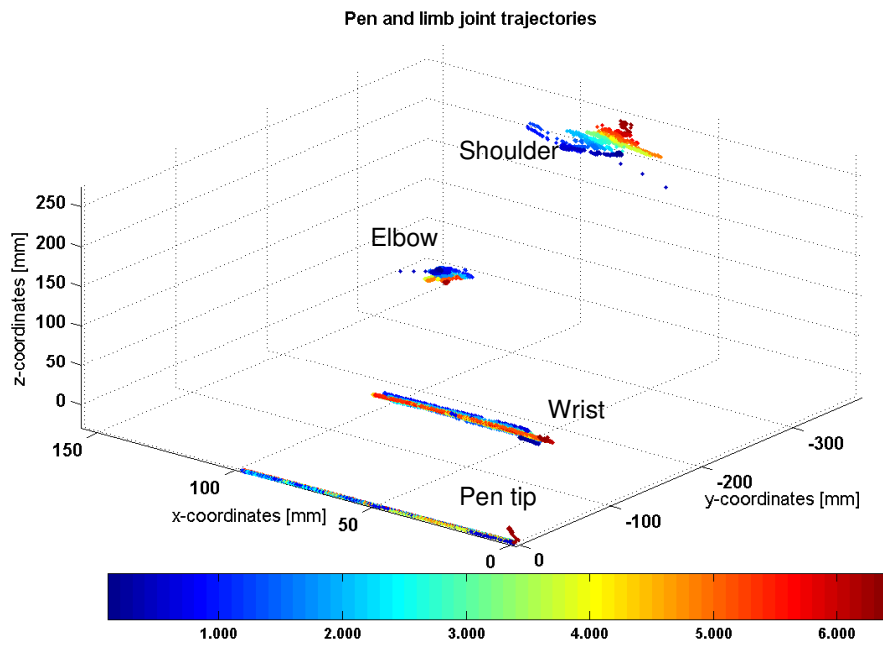
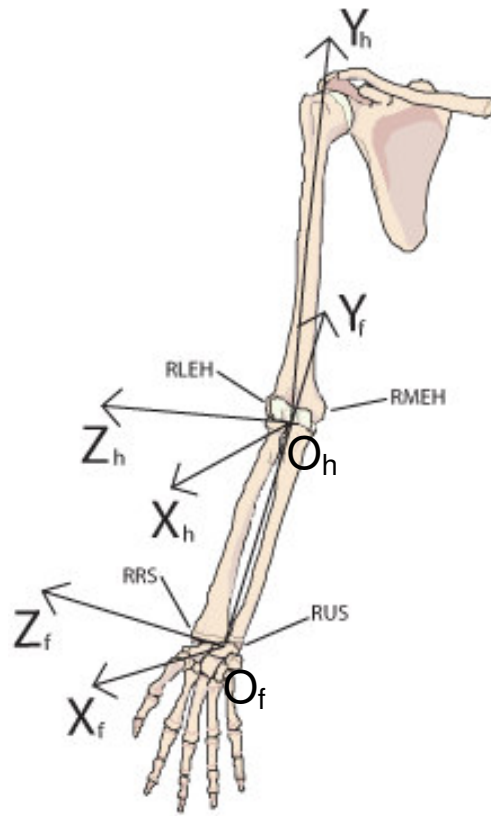


Fig.5.22: Recording for 3 o'clock target by subject 1:Trajectories (pen tip and joints: shoulder, elbow and wrist) for target direction 3 (segments not shown).



**Fig.5.23: Right arm anatomical axis frame in anterior view (copy Fig.4.6):**

**Forearm:**

$O_f$ : origin coincident with wrist joint centre ( $W$ ) between  $RUS$  and  $RRS$ ;

$Y_f$ -axis: The line connecting midpoint between  $RUS$  and  $RRS$  and the midpoint between  $RMEH$  and  $RLEH$ , pointing upward;

$X_f$ -axis: The line perpendicular to the plane formed by  $RUS$ ,  $RRS$  and the midpoint between  $RMEH$  and  $RLEH$ , pointing forward.

$Z_f$ -axis: The common line perpendicular to the  $X_f$ - and  $Y_f$ -axes, pointing to the left.

## Line drawing mechanics for target 6 o'clock

Unlike the lines drawn to the 12 and 3 o'clock targets, no clear force peaks for the three fingers can be identified before the actual pen tip movement for line drawing to target 6 commences. It can only be assumed that pen stabilisation had occurred in the subject's hand prior to data collection beginning. An increase in index finger force initiates the downward pen tip movement, which is accompanied with slight increases of thumb and middle finger force to maintain a stable grip.

As for the 12 o'clock target, the index finger (green line in Fig.5.24) is mainly responsible for the downward pen tip movement. The same force pattern can be observed as for 12 o'clock target direction. The index finger's relative contribution increases during downward phase, which results in tip movement in the negative y-direction (seen from y-coordinates in Fig. 5.24b). The resultant force vector consequently points downwards (negative y-direction) during this phase of line drawing.

While index force increases, the middle finger force adapts according to the change in index finger pressure to preserve the balance. Although there is not much variation in the thumb force, it adjusts in concordance with the middle finger force. Fig. 5.24a shows that for every peak of middle finger force, a small peak in thumb force occurs, which enables the subject to maintain a stable grip.

The upward pen tip movement (6 o'clock to neutral) is established by decreasing the index finger force, leading to an upward resultant pressure vector (See Fig. 5.24a and Fig.5.24c).

As for the 12 o'clock target, it can be seen from Fig.5.24a that the changes of index finger force precede the changes of the other two finger forces and the index finger therefore seems to have an important role in guiding the drawing task.

The difference with 12 o'clock target direction is that the index pressure values are lower than in 12 o'clock target direction, leading to a stronger resultant upward vector (positive y-direction) and weaker resultant downward vector (negative y-direction) for respectively up- and downward phase.

The up- and downward pen tip motion in the writing plane is established by synergy activities of the shoulder, elbow and wrist joints and finger motion in an analogue fashion to what was observed for target 12 o'clock. The shoulder provides a rotational movement of the limb around the z-axis, which leads to a linear elbow joint

path with diagonal orientation in the horizontal writing plane. At the same time, rotation of the forearm around the elbow joint enables the linear wrist joint motion to be directed more up- and downward in the writing plane than the linear elbow motion that was orientated diagonally. The pen tip motion with up- and downward orientation is enabled by wrist joint rotation and finger movement.

The difference with line drawing to target 12 is that for target 6 that there is a consistent linear shoulder motion along with shoulder rotation and that the angle of the line of motion of the pen tip with both the wrist and elbow are smaller.

The wrist rotation is assumed to be concurrently around the three main axes (See Fig.5.23). It can be seen clearly that with every line drawn, the shoulder, elbow and wrist position move forward (towards the drawn line), which requires the wrist joint to flex around the Zf-axis (see Zf-axis in Fig. 5.23). This is the axis perpendicular to the longitudinal axis, pointing to the right from the writer's point of view when the hand and arm are placed flat on the writing surface (Zf in Fig. 5.23).

It may be concluded that although the Index finger establishes resultant pen grip force that is positive with upward pen tip motion and negative with downward pen tip motion (as described, see Fig. 5.24a, b and c), the actual line drawing motion is established by the limb effectors. The finger pen grip plays a role in converting the wrist joint motion that is orientated diagonally in the x,y-plane into a up- and downward pen tip motion in the x,y-plane together with the wrist that enables rotation for positioning of the hand.

From the limb trajectory in Fig.5.25 and Fig.5.26 for the 6 o'clock target, it can be seen that despite of elbow and wrist trajectories being different in every cycle, the pen Tip trajectories are very consistent. The shoulder joint path is more consistent than for the 12 o'clock target trial. The trajectories again illustrate the flexibility and redundancy in the musculoskeletal system by providing pen motion with quite well controlled accuracy but significant cycle to cycle variation in arm joint kinematics.

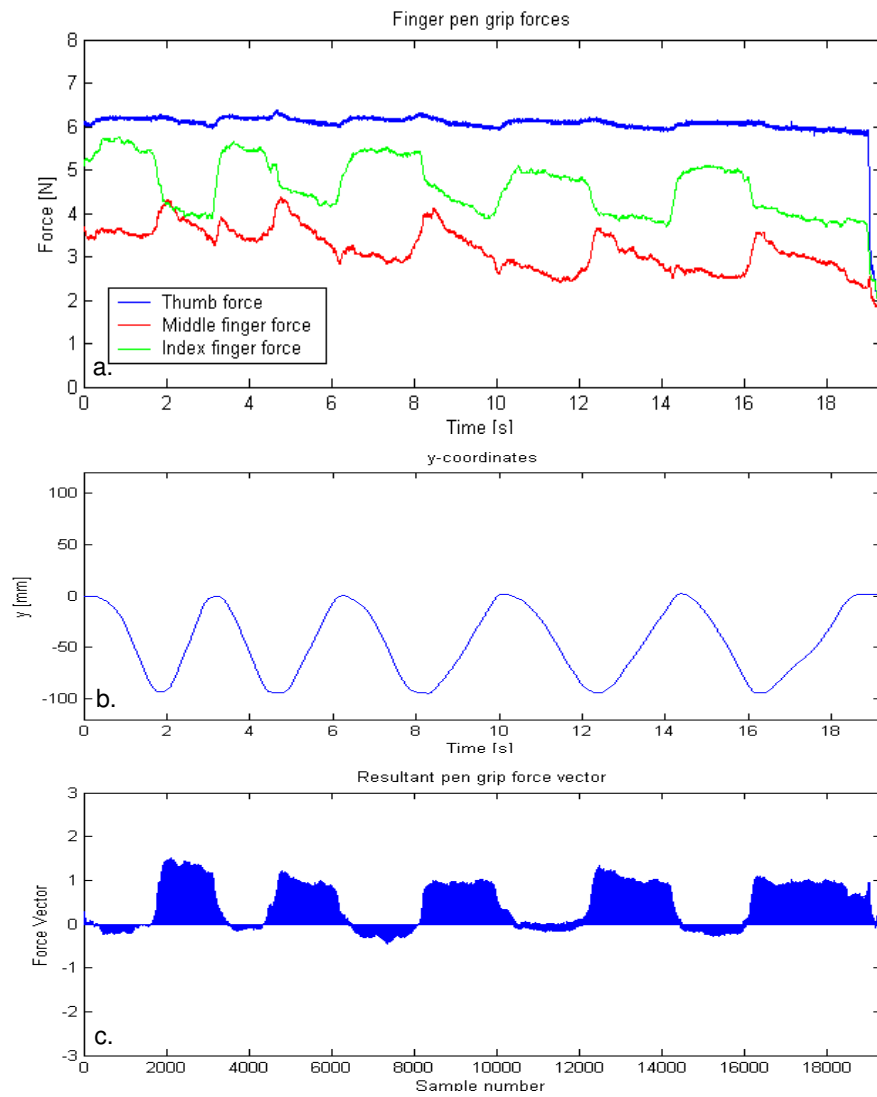


*Fig.5.24: Recording for 6 o'clock target by subject 1.*

*a: Finger forces for target direction 6 o'clock for subject 1.*

*b: y-coordinates for target direction 6 o'clock for subject 1.*

*c: Resultant grip force vector for target direction 6 o'clock for subject 1.*

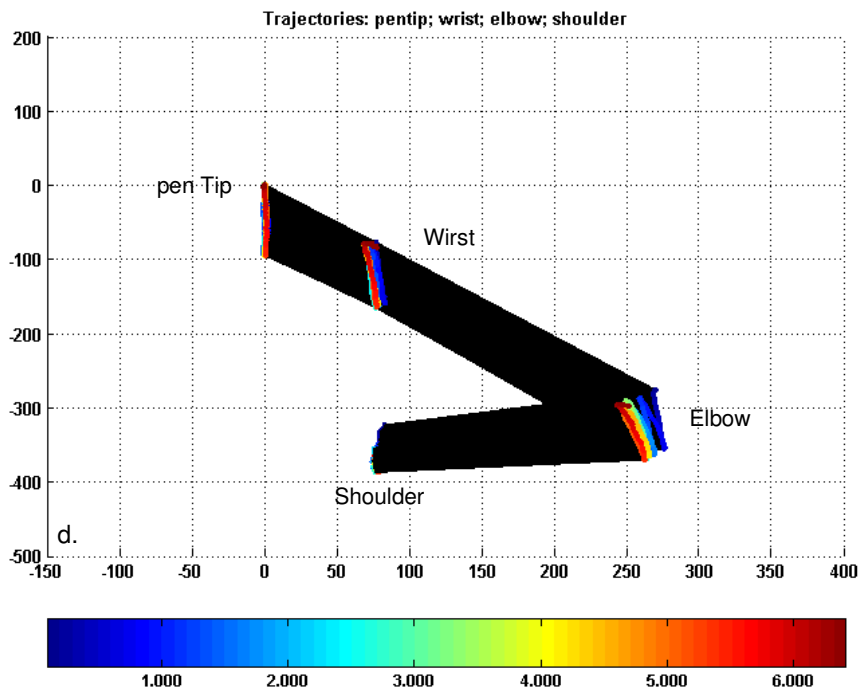


Fig.5.25: Recording of pen tip limb and joint trajectories for 6 o'clock target by subject 1.

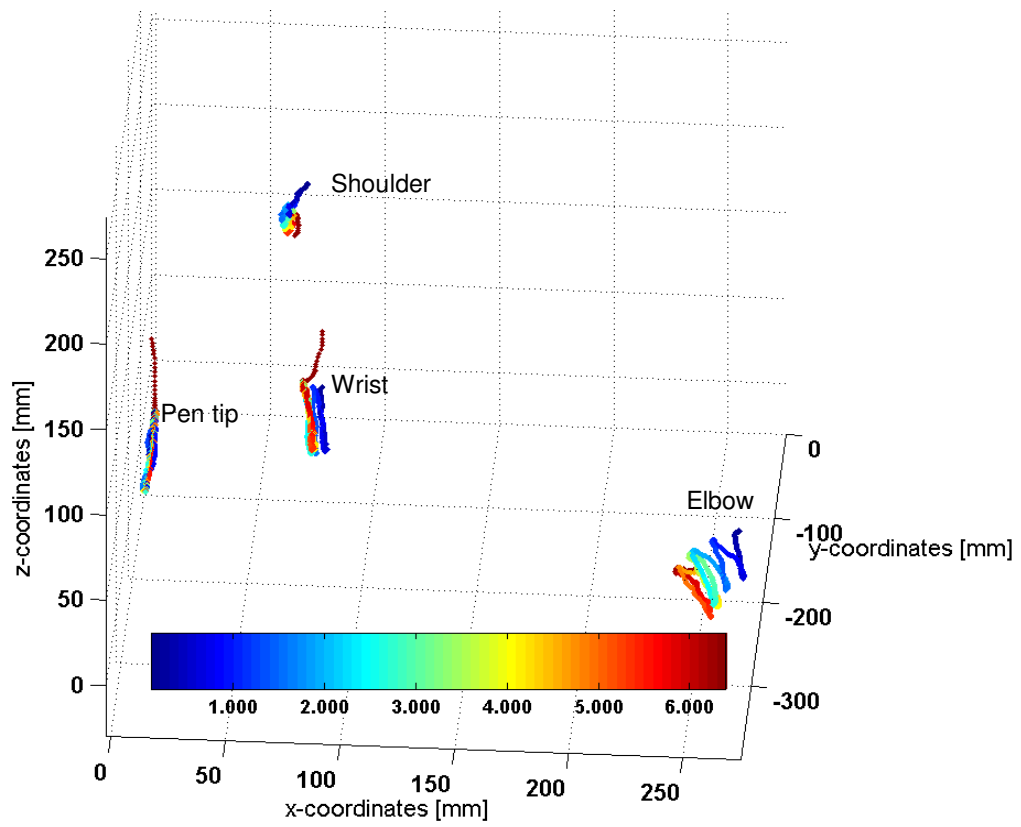


Fig.5.26: Recording of pen tip and limb and joint trajectories for 6 o'clock target by subject 1 (limb segments not shown).

## Line drawing mechanics for target 9 o'clock

As in the previous data set, the period preceding pen motion does not show any large force peaks, but this period is relatively short and it is assumed that the pen grip is already stable no force peaks for stabilising pen grip are identified (Fig.5.27a). The start of the movement to target 9 coincides with an increase in index finger force (green line). The thumb is less involved with horizontal pen tip movement than for the 3 o'clock target. The index and middle finger pressure may contribute to movement in negative x-direction (seen from x-coordinates in Fig.5.27a and Fig.5.27b) as their relative contribution increase during this phase. The changes in applied force may therefore be a strategy for stabilising the pen grip as no clear relationship can be found between the direction of the resultant grip force vector (Fig. 5.27c) and the pen tip movement (Fig.5.27b). Tip movement seems to originate from the wrist movement (Fig.5.28 and Fig.5.29). Some wrist rotation is involved as is revealed by the longer movement vector of the pen tip compared to the movement vector of the wrist. The pen tip and wrist both have very similar trajectories in every cycle. Only slight movements of the shoulder and wrist can be seen with some linear elbow motion (Fig.5.29), but these do not clearly influence the pen tip movement. In addition, for the 9 o'clock target, modulation of the index finger force does not clearly precede variations of thumb and middle finger force (as was seen for the 3 o'clock target direction and unlike the vertical target directions). If the force control strategy is not aimed at steering the pen in a particular direction, but rather at ensuring a stable grip (as assumed from the individual finger forces in Fig.5.27a), then this may explain why adaptations of the Index finger force do not precede variations of thumb and middle finger force.

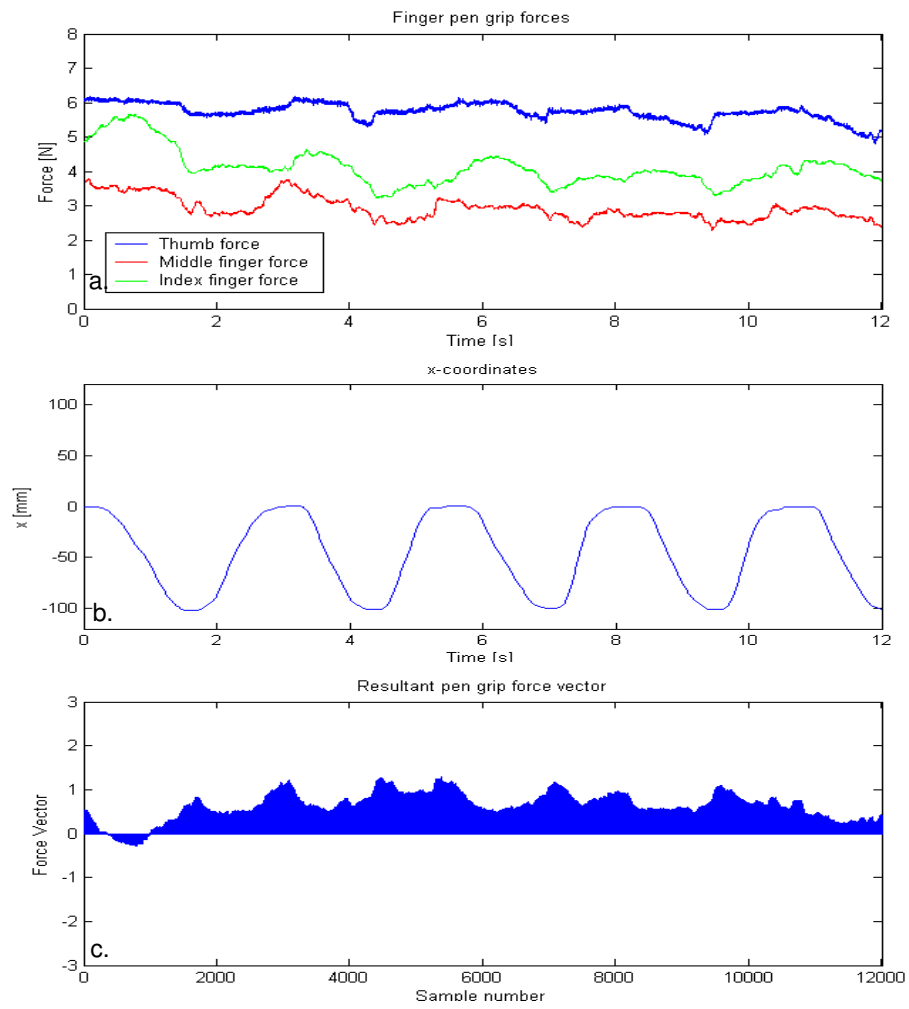


Fig.5.27: Recording for 9 o'clock target by subject 1.

- a: Finger forces for target direction 9 o'clock for subject 1.
- b: y-coordinates for target direction 9 o'clock for subject 1.
- c: Resultant grip force vector for target direction 9 o'clock for subject 1.

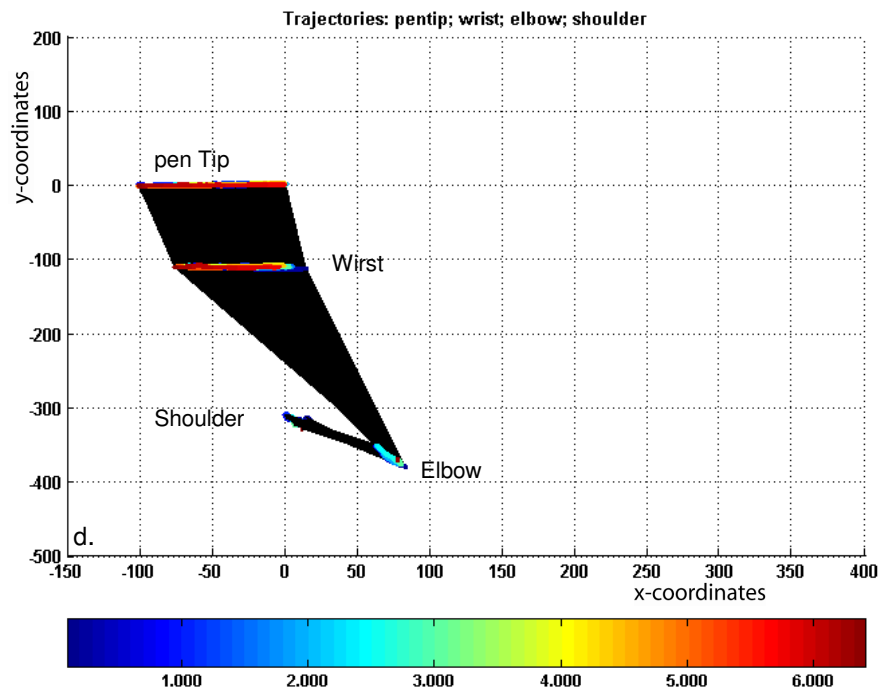


Fig.5.28: Recording for 9 o'clock target by subject 1.  
 Trajectories (pen tip and joints: shoulder, elbow and wrist) for target direction 9 o'clock for subject 1.

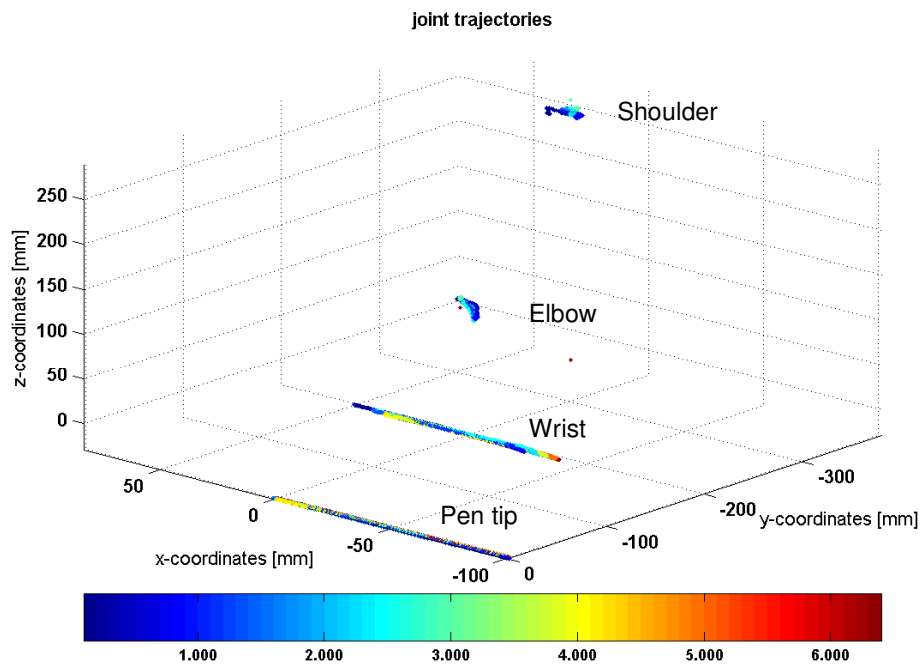


Fig.5.29: Recording of pen tip and limb joint trajectories for 9 o'clock target by subject 1.

### Discussion subject 1

For vertical targets (12 o'clock and 6 o'clock), it is observed that control of index finger force dominates and therefore plays a greater role in the overall process that enables pen tip movement over the distances the lines are drawn. The index finger is mainly responsible for the up- and downward pen tip movement. The index finger's relative contribution increases during downward phase and the consequent Resultant force vector points downwards (negative y-direction), which results in tip movement in the negative y-direction. The upward pen tip movement is established by decreasing the index finger force, leading to an upward resultant pressure vector (Fig. 5.24a and Fig.5.24c) and pen tip movement in positive y-direction. The changes of index finger force (5.24a) precede the changes of the other two finger forces. For vertical pen tip movement, the middle finger and thumb forces adapt according to changes in index finger pressure to either preserve the balance or sometimes contribute to the overall pen movement.

The kinematics show large translation of wrist and elbow, suggesting that shoulder action is an important factor with up and down line drawing.

For horizontal target directions 3 o'clock and 9 o'clock, the pen tip movement mainly originates from wrist translation and wrist rotation. The individual finger forces do stabilise the grip and contribute to the horizontal pen tip movement, but their contribution is not as obvious as for the vertical trials. For target direction 3 o'clock, the applied thumb force contributes to the forward tip movement, but the pen tip movement is not just established by increasing thumb pressure. Wrist translation and rotation in the first place cause forward pen tip movement.

Although for target direction 9 o'clock increased index and middle finger forces are observed during horizontal movement towards the target, no clear relation between force and pen tip motion is observed and the wrist and to lesser extent also elbow and shoulder joints clearly provide the horizontal pen tip motion.

It can be concluded that even simple task, such as line drawing, involve coordination of distal and proximal muscle groups. The joint trajectories illustrate the redundancy and flexibility of the neuromuscular system. Variation in shoulder, wrist and elbow trajectories is observed within trials, while still producing a nearly equal line over five cycles. In section 1.4.2.1 it was shown that the deviation from the ideal straight line was stronger for the horizontal experiments with target positions 3 and 9 o'clock than for vertical experiments with target positions 12 and 6 o'clock and that the velocity was higher for horizontal than for the vertical trials. Fingertip path curvature increases with increasing speed, according to Klein Breteler et al (1998), which may partly explain the differences observed.

#### 5.4.2.3 Subject 2: description of line drawing mechanics

The changes in pen grip force associated with movement patterns observed in drawing lines to target directions 12, 3, 6 and 9 o'clock (experiments 1, 4, 7 and 10) by subject 2 are described below, followed by a brief discussion. The minimum, maximum and average values of thumb, index and middle finger forces are shown in Table 5.7. In addition, minimum and maximum values of shoulder, elbow and wrist joint trajectory coordinates (in mm) obtained with a Vicon motion analysis system are also presented in Table 5.7.

## Line drawing mechanics for target 12 o'clock

From the Fig.5.30a, b and c, it can be seen that finger synergies (organised co-variation) of index finger and thumb are responsible for either up- or downward motion in the following fashion.

For movement towards the 12 o'clock target, the thumb pressure increases while index pressure decreases (Fig.5.30a), leading to resultant pressure vector (Fig.5.30c) pointing upwards (positive y-direction) and resulting in upward movement (movement in positive y-direction, seen in Fig.5.30b).

For downward movement, thumb pressure decreases while index pressure increases (Fig.5.30a), leading to resultant pressure vector (Fig.5.30c) pointing downwards (negative y-direction) and resulting in downward movement (movement in negative y-direction, seen in Fig.5.30b).

The first cycle has slightly longer duration than the other cycles as revealed by the y-coordinates over time (Fig.30b) and the timing of the upward force vector in Fig.30b that is in time with increased thumb force in this phase.

Interestingly, for every cycle a dip in thumb force can be seen before reaching the maximum y-value. This may be an anticipatory grip action (Fig.5.30a).

The mean and maximum grip force values are relatively low for subject 2: around half or less of the mean and maximum value of Subject 1 (Table 5.7).

Trajectories for shoulder, elbow, wrist and tip are very constant in every cycle (Fig.5.31 and Fig.5.32). While moving the pen tip towards the 12 o'clock target direction, the wrist and elbow motion is directed diagonally: there is motion in the positive y-direction and negative x-direction at the same time. This motion results from shoulder rotation around the z-axis, which is directed perpendicular to the writing plane. The diagonal wrist motion requires the wrist to flex and finger forces to adapt (in particular the thumb and index finger as described above) in order to move the pen tip in the positive x-direction relative to the wrist in order to produce a vertical line without lateral (x) movement of the pen tip. The motion is reversed while moving from the 12 o'clock target back towards the start point (centre) and shoulder, elbow and wrist joint motion follows the same trajectory back to their starting position. These lines of motion seem preferred.

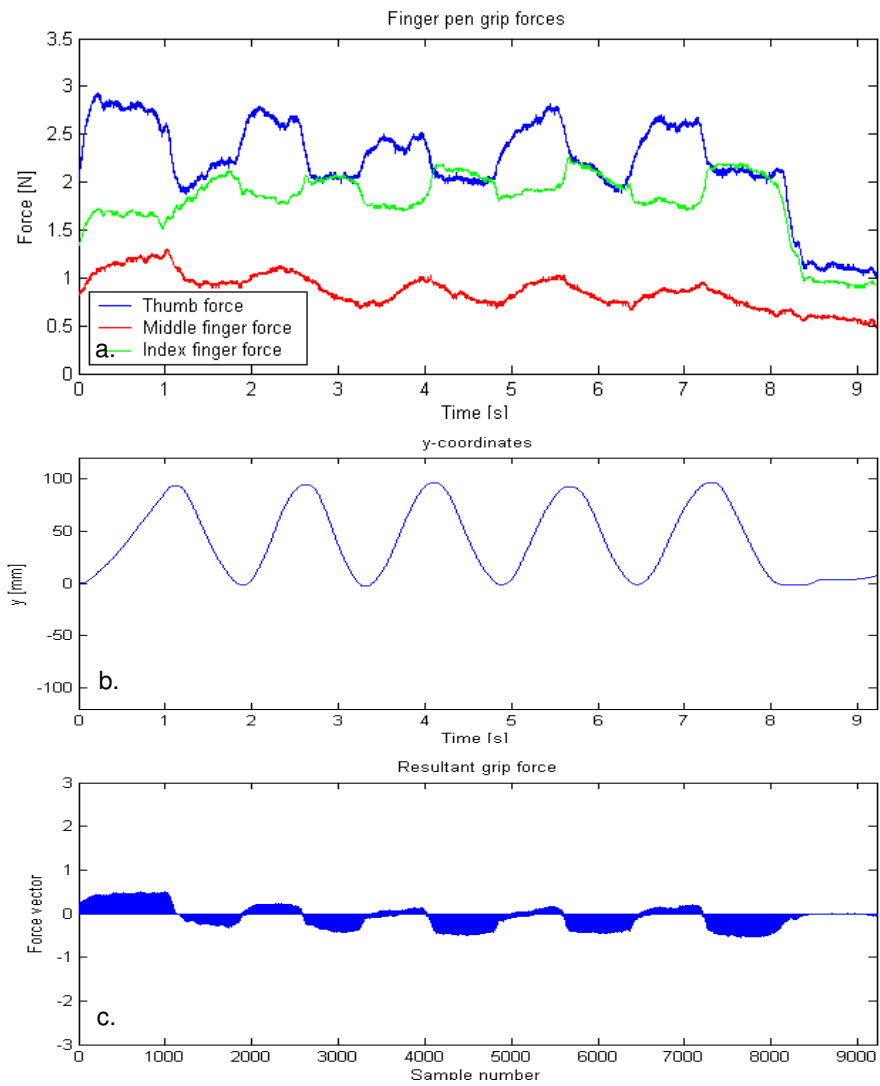


Fig.5.30: Recording for 12 o'clock target by subject 2.

a: Finger forces for target direction 12 o'clock for subject 2.

b: y-coordinates for target direction 12 o'clock for subject 2.

c: Resultant grip force vector for target direction 12 o'clock for subject 2.

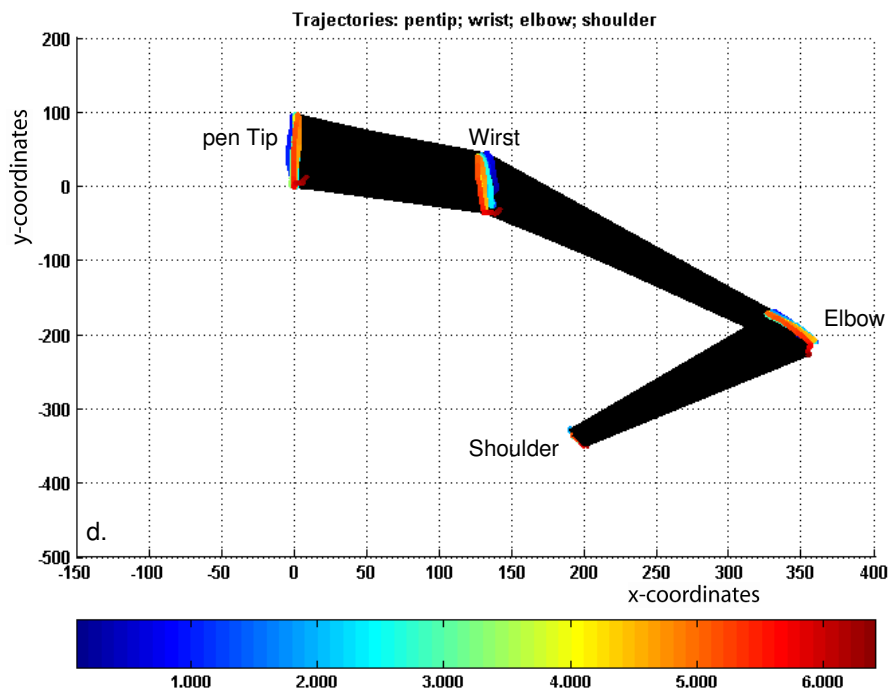


Fig.5.31: Recording for 12 o'clock target by subject 2: Trajectories (pen tip and joints: shoulder, elbow and wrist) for target direction 12 o'clock for subject 2.

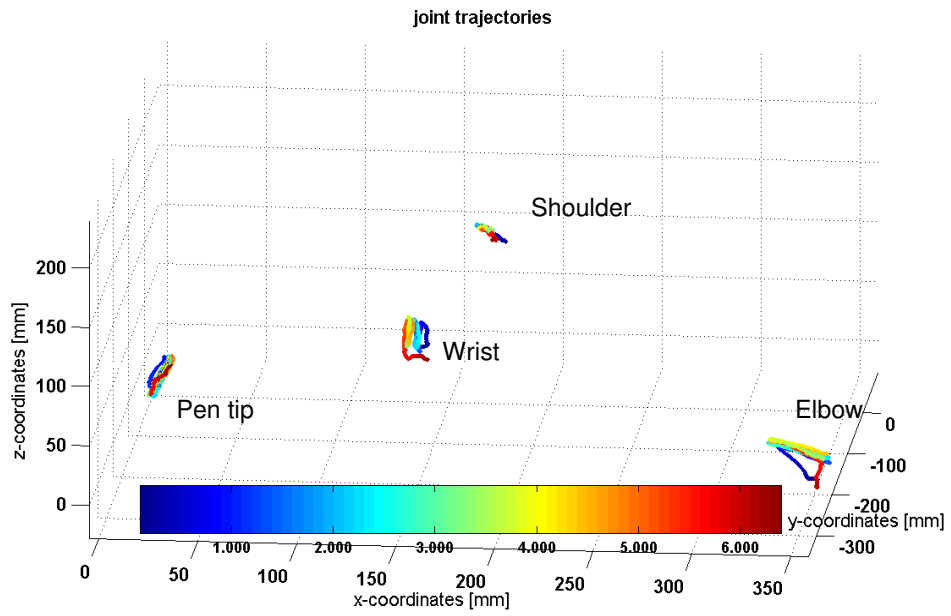


Fig.5.32: Recording for 12 o'clock target by subject 2: Trajectories (pen tip and joints: shoulder, elbow and wrist). The limb segments are not shown.

## Line drawing mechanics for target 3 o'clock

For line drawing towards the target 3 o'clock, the applied thumb force may contribute to the forward tip movement (Fig.5.33a) as its relative contribution increases during the forward phase (movement in positive x-direction, seen from x-coordinates in Fig. 5.33b). However, the resultant force vector points upwards and not forwards during the 5 cycles (Fig.5.33d) and therefore, the main pen tip movement must originate from the wrist translation as is seen in Fig. 5.33. The index finger force is adjusted in a synchronised fashion with thumb force, which is assumed to stabilise the grip. Ensuring a stable grip seems the most important criteria for grip modulation and the grip does not steer the pen the horizontal movement.

For movement in negative x-direction (Fig. 5.33), the middle finger force increases, while the thumb and index finger force decrease. On arrival at the origin, the middle force (red line) is minimal.

Variation in thumb force precedes the variation in index and middle finger force and it is expected that the thumb has crucial role in the grip modulation.

Double differentiation of the x-coordinates of the pen tip (Fig.5.33b), gives the pen tip acceleration signal (Fig.5.33c). As the pen tip x-coordinates almost resemble a perfect sinoid, the tip acceleration signal is expected to resemble an inverse sinoid. In Fig.5.33c the Tip acceleration signal [ $\text{mm/s}^2$ ] is shown after filtering (using Robust loess method in Matlab with a span of 20% of the total time span, which is the time of one cycle). The filtered tip acceleration signal is indeed an almost perfect inverse sinoid.

When the maximum tip acceleration occurs - around  $x=0$  mm (start point) in every cycle, the resultant pressure vector reaches its lowest values (Fig.5.33c).

The phase in which the highest resultant pressure vector is reached (Fig.5.33c) is between three quarters of the cycle and the end of a complete cycle - between  $x=50$  mm en  $x=0$ mm (Fig.: 5.33b and c) - just before the resultant pressure vector (Fig.5.33d) goes down to its lowest value. This yields for all cycles except the 4th cycle. The pen tip acceleration signal and related pressure patterns are similar within this phase among different cycles.

Trajectories for shoulder, elbow, wrist and tip are very similar in every cycle (Fig.5.34 and Fig.5.35). As for line drawing to target 12, the wrist, elbow and shoulder motion is directed diagonally: there is motion in the positive x-direction and negative y-direction at the same time, which originates from shoulder rotation (around z-axis, perpendicular to the writing surface). This requires wrist rotation and and finger adaptation in order to move the pen tip in the positive y-direction relative to the wrist in order to produce a horizontal line towards target position 3 o'clock without vertical (y) movement of the pen tip.

The wrist rotation is assumed to be concurrently around the three main axes (See Fig.5.23). It is expected that the flexion of the wrist joint is strongest around the Zf-axis (see Zf-axis in Fig. 5.23). This is the axis perpendicular to the longitudinal axis, pointing to the right from the writer's point of view when the hand and arm are placed flat on the writing surface (Zf in Fig. 5.23)

The fingers also play an important role here in directing the pen tip in a straight horizontal line, despite of the finger forces not directly and independently causing the horizontal movement as described above. The pen tip motion is reversed in the second half of each cycle (Fig.5.34 and 5.35), but the limb joints are still moving along the same line in order to produce a straight line of the pen tip back to its origin.

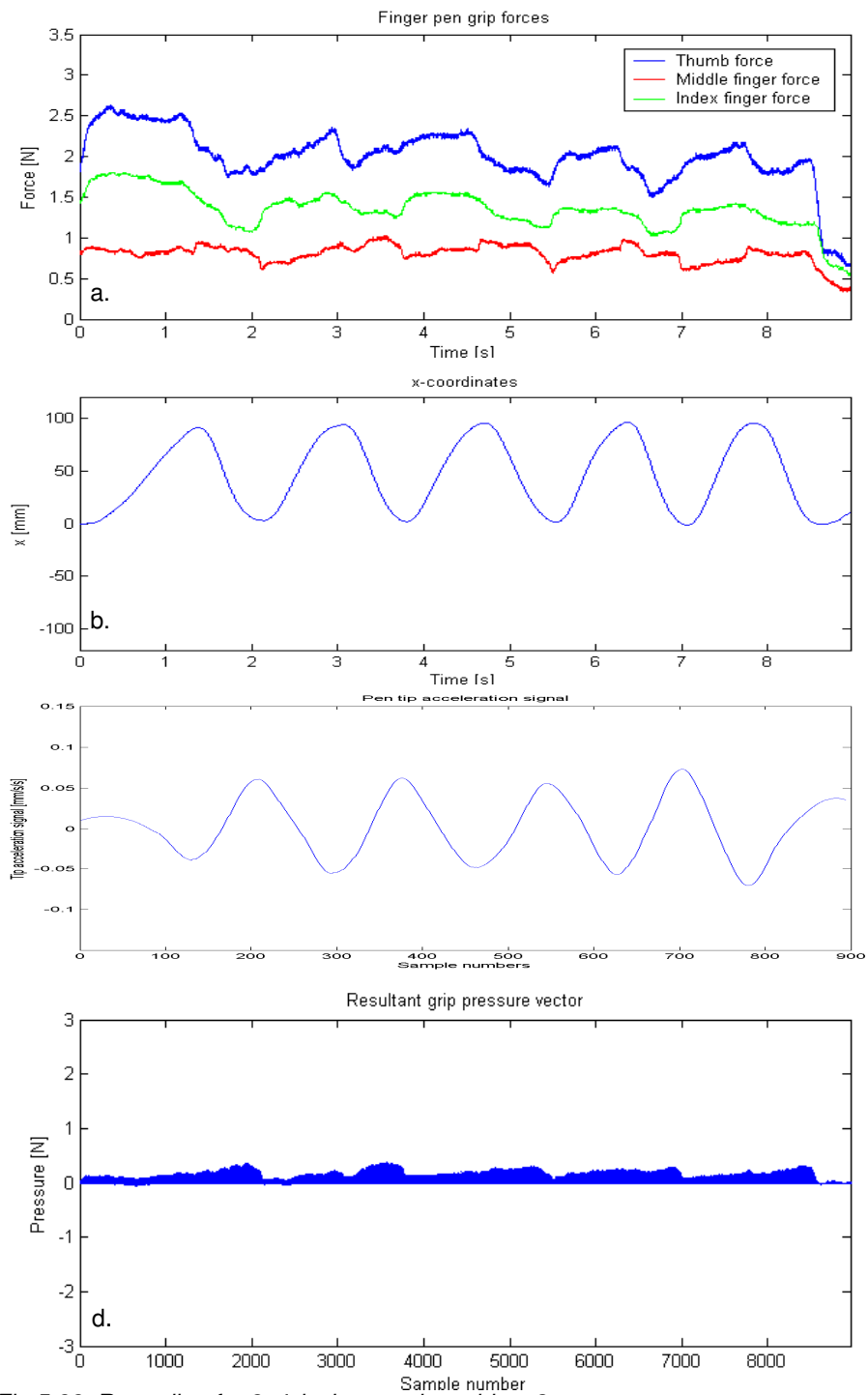


Fig.5.33: Recording for 3 o'clock target by subject 2.

- a: Finger forces for target direction 3 o'clock for subject 2.
- b: x-coordinates for target direction 3 o'clock for subject 2.
- c: Pen tip acceleration signal for target 3 o'clock for subject 2
- d: Resultant grip force vector for target direction 3 o'clock for subject 2.

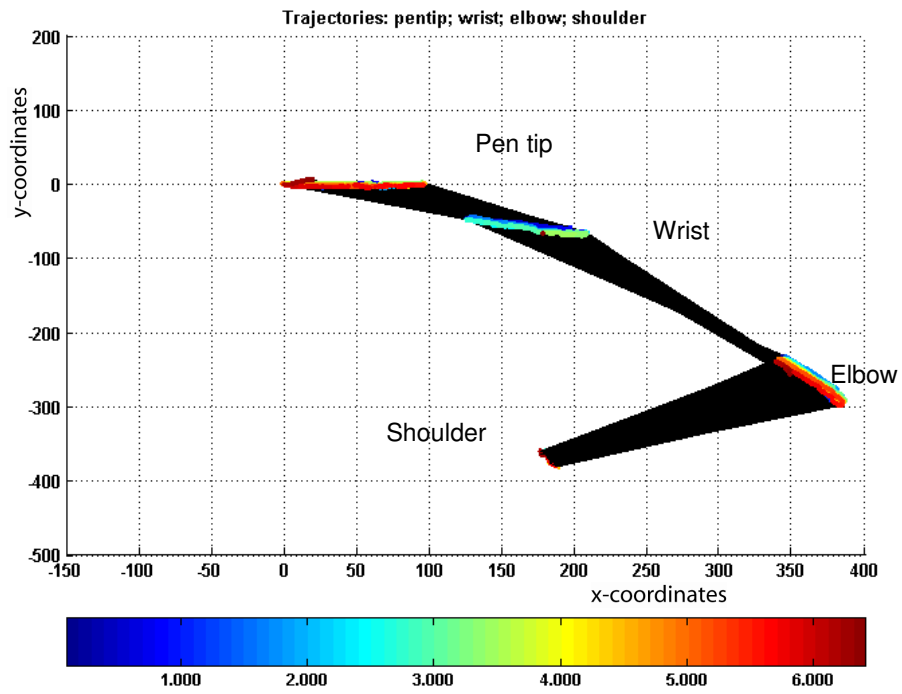
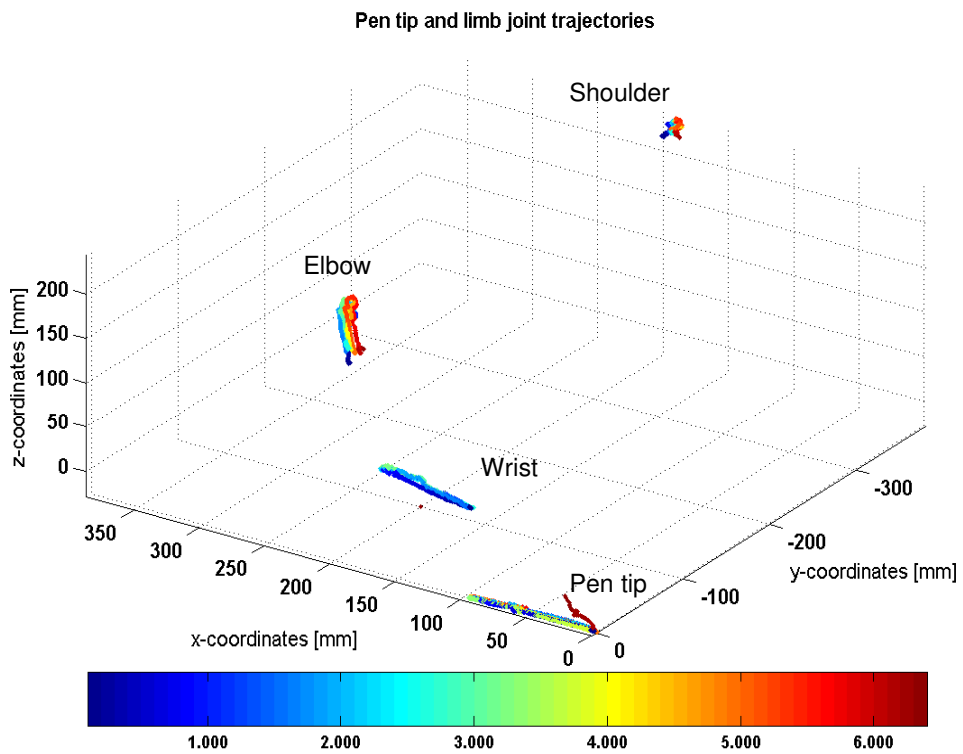


Fig.5.34: Recording for 3 o'clock target by subject 2: Trajectories (pen tip and joints: shoulder, elbow and wrist) for target direction 3 o'clock for subject 2.



*Fig.5.35: Recording for 3 o'clock target by subject 2: Trajectories (pen tip and joints: shoulder, elbow and wrist) for target direction 3 o'clock for subject 2. The limb segments are not shown.*

### **Line drawing mechanics for target 6 o'clock**

Fig.5.36a presents the pen grip forces while drawing lines towards the 6 o'clock target. The force pattern is similar to the pattern for target direction 12 o'clock (Fig.5.30a), but the force variations are smaller. From the Fig.5.36a, b and c, it can be seen that the Index finger and Thumb are responsible for either up-or downward motion in the following fashion. For movement towards the 6 o'clock target, the Index finger force increases while Thumb finger force decreases (Fig.5.36a), leading to a resultant pressure vector (Fig.5.36c) pointing downwards (negative y-direction) and resulting in downward movement (movement in negative y-direction, seen in Fig.5.36b).

For upward movement, index finger force decreases while the thumb force increases (Fig.5.36a), leading to resultant pressure vector (Fig.5.36c) pointing upwards (positive y-direction) and resulting in upward movement (movement in negative y-direction, seen in Fig.5.36b).

The force values are higher for this target direction than for other target directions for subject 2, although the force values for this target direction are relatively low and close to half the force value compared to subject 1.

The expected anticipatory grip action - a dip in Thumb pressure before reaching the maximum y-value - seen for target position 12 o'clock, is seen less clearly during this vertical movement.

Trajectories for shoulder, elbow, wrist and tip are very similar in every cycle and similar to what was observed for target direction 12 o'clock, although with reversed target direction (Fig.5.37 and Fig.5.38). Elbow and shoulder motion and to some extent wrist motion is directed diagonally: there is motion in the negative y-direction and positive x-direction at the same time, which originates from shoulder rotation. This requires wrist rotation and adaptation of the fingers to control the pen tip movement in the negative x-direction relative to the wrist in order to produce a vertical line without lateral (x) movement of the pen tip. The fingers clearly contribute to the vertical motion as described above.

The motion is reversed while moving from the 6 o'clock target back towards the start point (centre) and shoulder, elbow and wrist joint motion follows the same trajectory back to their starting position (Fig.5.37 and Fig.5.38). This trajectory line seems preferred and has the same orientation as was seen for target direction 12 o'clock, although the exact trajectory differs as can be seen from Table 5.8.

In addition, there is slightly more wrist rotation involved than was observed for the 12 o'clock target direction.

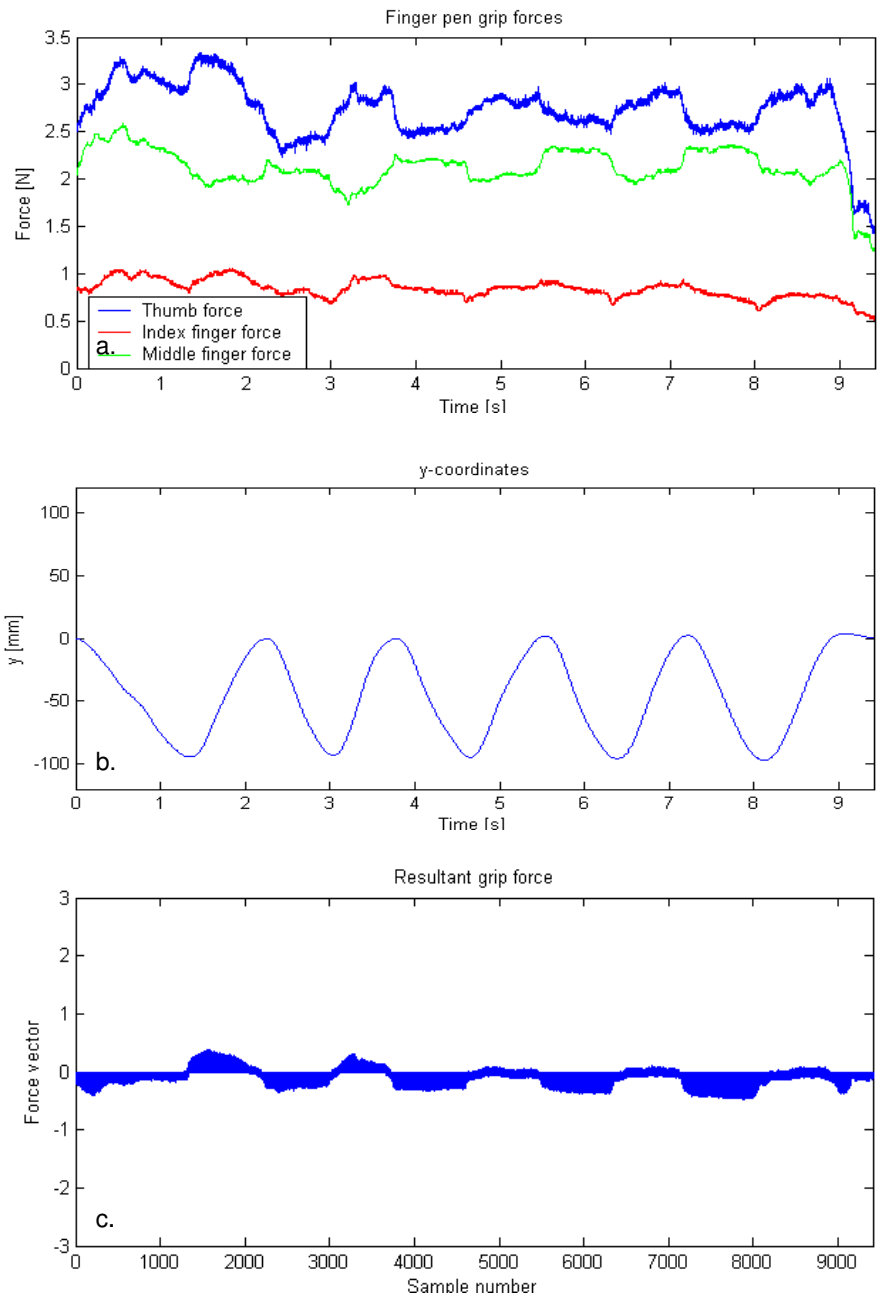


Fig.5.36: Recording for 6 o'clock target by subject 2.

- a: Finger forces for target direction 6 o'clock for subject 2.
- b: y-coordinates for target direction 6 o'clock for subject 2.
- c: Resultant grip force vector for target direction 6 o'clock for subject 2.

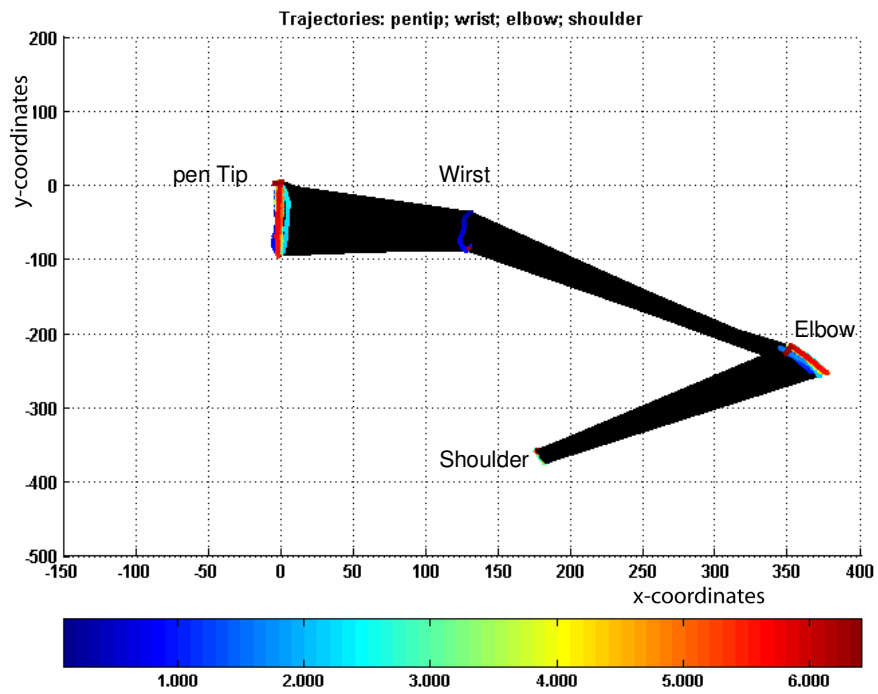


Fig.5.37: Recording for 6 o'clock target by subject 2: Trajectories (pen tip and joints: shoulder, elbow and wrist) for target direction 6 o'clock for subject 2.

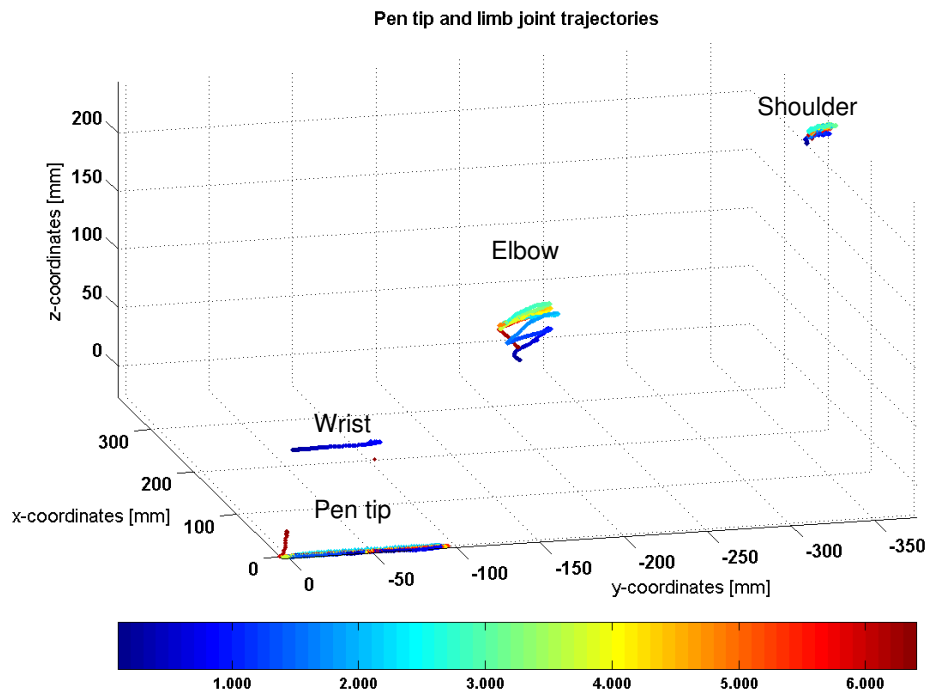


Fig.5.38: Recording for 6 o'clock target by subject 2: Trajectories (pen tip and joints: shoulder, elbow and wrist) for target direction 6 o'clock for subject 2. The limb segments are not shown.

## Line drawing mechanics for target 9 o'clock

The biomechanical features for drawing horizontal lines between the origin and the 9 o'clock target are shown in Fig. 5.39. Fig. 5.39a shows that during the phase towards the 9 o'clock target (movement in negative x-direction, seen from x-coordinates in Fig. 5.39b), the middle finger force's relative contribution increases, while the thumb and index finger force decrease. This is assumed to stabilise the grip while the main pen tip movement originates from the wrist translation as is seen in Fig. 5.40. In addition, the applied thumb and index finger force increase in a synchronised fashion during the forward phase (movement in positive x-direction, seen from x-coordinates in Fig. 5.39b). Variation in thumb force precedes the variation in index and middle finger force and the thumb may therefore have crucial role in the grip modulation, just as was seen for the 3 o'clock target.

It is striking how the Resultant pressure vector varies (Fig.5.39d): it is negative in the forward phase (in positive x-direction as seen from x-coordinates (Fig.5.39a) of the cycle - from  $x = -100$  until  $x = 0$ mm and it is positive in the backward phase (in negative x-direction as seen from x-coordinates) of the cycle - from  $x = 0$  until  $x = -100$ mm. This distinct modulation was not seen in the experiment for target direction 3 o'clock.

The force modulation observed here does not seem to have a direct relation with the pen tip movement. While the pen tip motion is in the horizontal direction, the resultant grip force points upwards rather than forwards.

Double differentiation of the pen tip x-coordinates (Fig.5.39a), gives the pen tip acceleration signal (Fig.5.39c). As the pen tip x-coordinates almost resemble a perfect sinoid, the tip acceleration signal is expected to resemble an inverse sinoid. The tip acceleration signal is shown in red in Fig.5.39c (after filtering, using Robust loess method in Matlab with a span of 20 samples). The red graph of the pen tip acceleration signal resembles the inverse sinoid, although the acceleration is not smooth, which may be due to tremor. The same signal is repeated in blue after applying the same filtering technique, but with a span of 20% of the total time span (the time span of one cycle). The blue acceleration signal closely resembles an inverse sinoid.

The pen tip acceleration signal and related pressure patterns are similar for all 5 cycles. As for the 3 o'clock target direction, when the maximum tip acceleration (Fig.5.39c) occurs - around  $x = -100$  mm in every cycle, the resultant pressure vector (Fig.5.39d) reaches its lowest values. As for the 3 o'clock target direction, this point marks the minimum x-value.

Looking at the red acceleration curve, it can be concluded that the peak Tip acceleration coincides exactly with the 9 o'clock target, although this becomes less obvious when the Tip acceleration signal is filtered stronger to make it resemble an nearly perfect inverse sinoid (blue graph in Fig.5.39d).

It was initially not intended to report on pen tip accelerations, but the observations of pen tip acceleration that were made for the 9 o'clock trace for subject 2 seemed worthwhile to report here. For other traces and subjects pen tip acceleration was not described.

The trajectories of shoulder, elbow, wrist and tip (Fig.5.40 and Fig.5.41) are very similar in every cycle. The shoulder, elbow and wrist trajectories are slightly larger than seen for target direction 3 o'clock, but the same line of motion is observed. Shoulder rotation facilitates wrist and elbow diagonal motion in the negative x-direction and positive y-direction at the same time. This requires wrist rotation and finger pen grip control to direct the pen tip in the negative y-direction relative to the wrist in order to produce a horizontal line towards target position 9 o'clock without vertical (y-directed) movement of the pen tip. The motion is reversed in the second half of each cycle, but the joints are still moving along the same line.

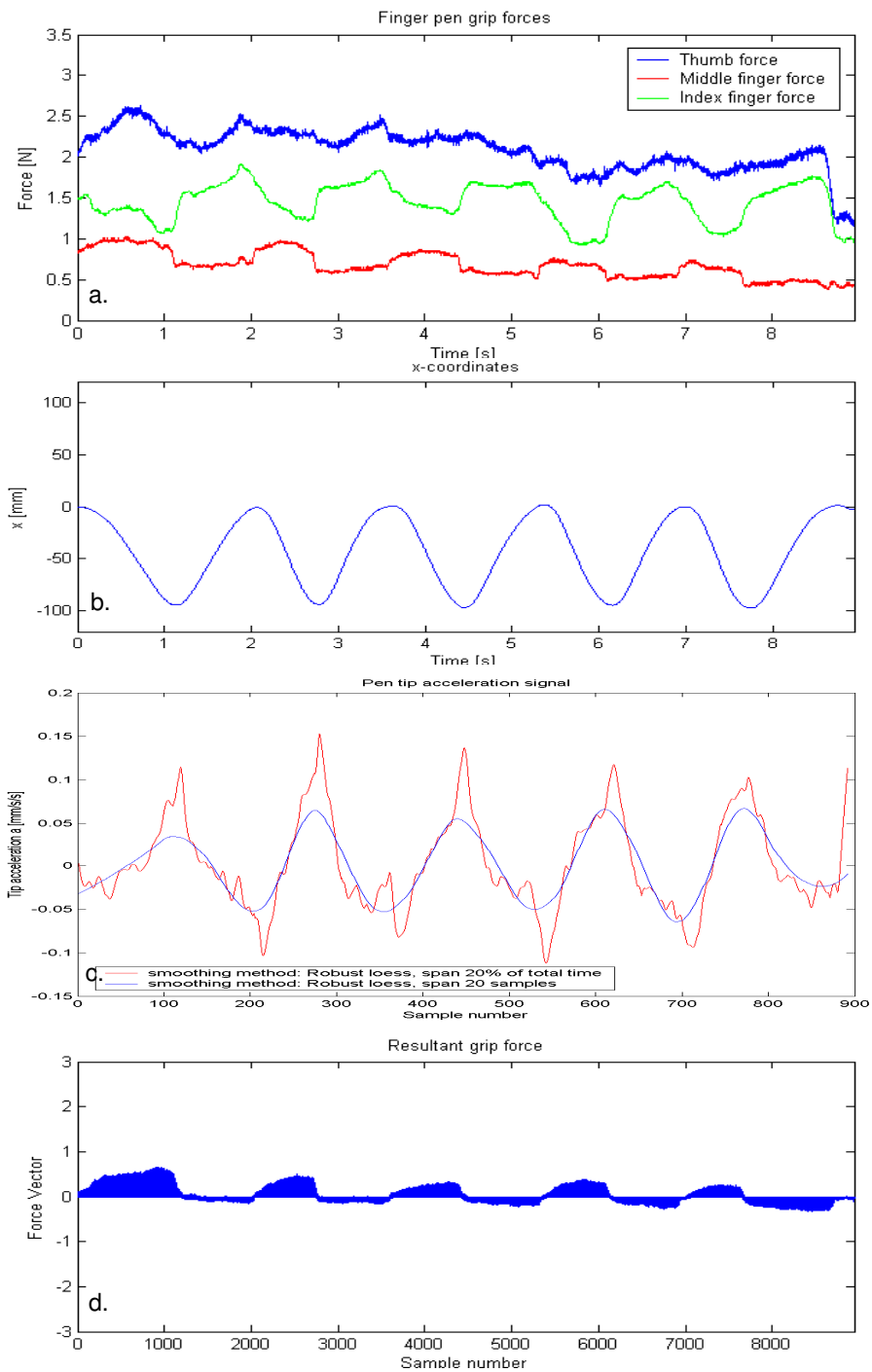


Fig.5.39: Recording for 9 o'clock target by subject 2.

- a: *Finger forces for target direction 9 o'clock for subject 2.*
- b: *y-coordinates for target direction 9 o'clock for subject 2.*
- c: *Pen tip acceleration signal for target 9 o'clock for subject 2*
- d: *Resultant grip force vector for target direction 9 o'clock for subject 2.*

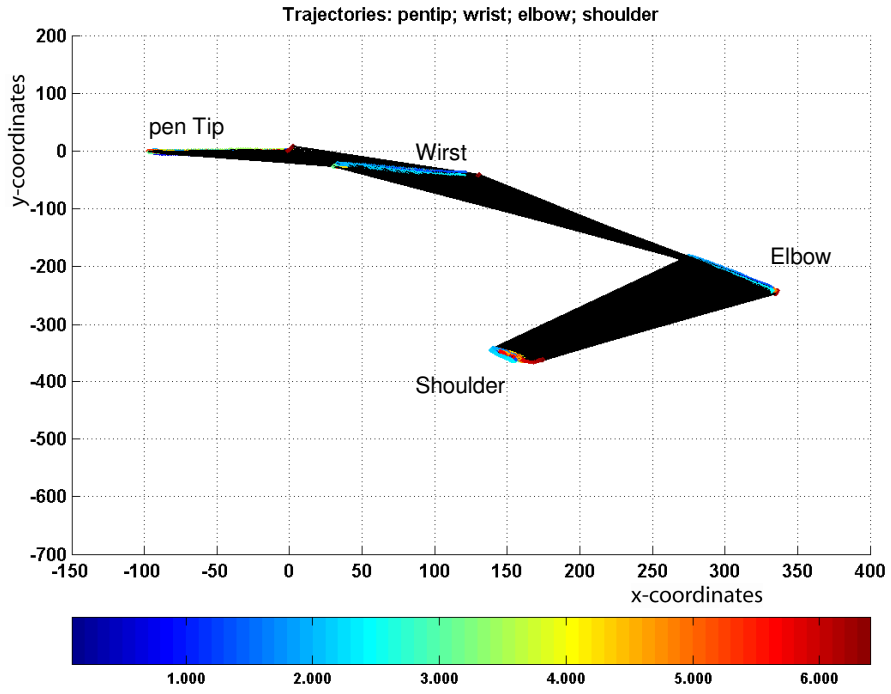


Fig.5.40: Recording for 9 o'clock target by subject 2: Trajectories (pen tip and joints: shoulder, elbow and wrist) for target direction 9 o'clock for subject 2.

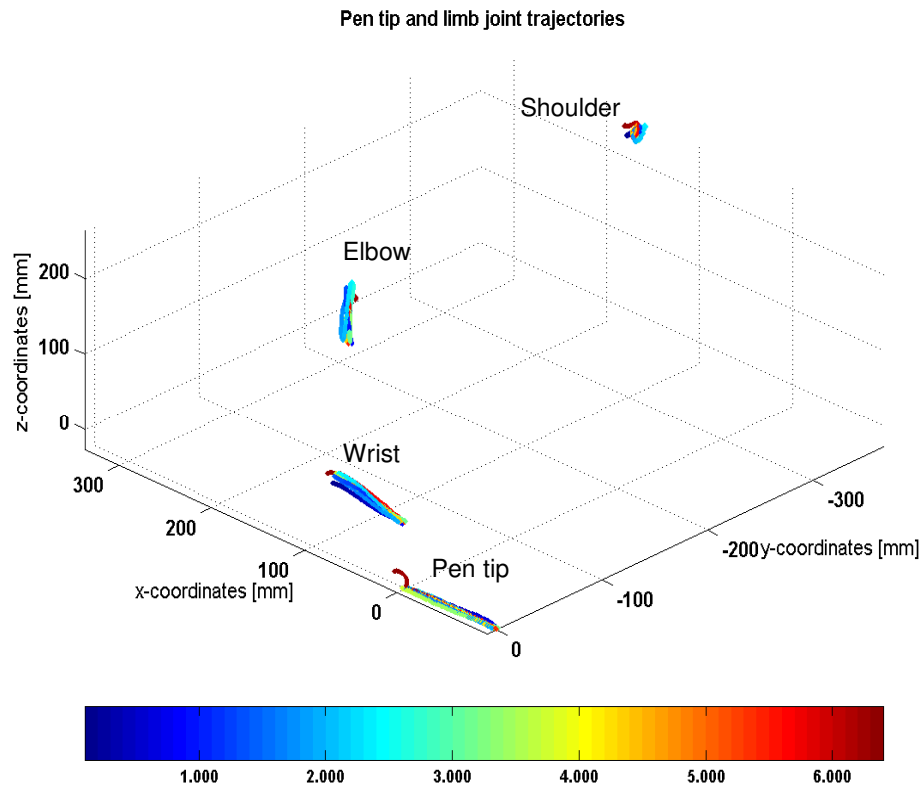


Fig.5.41: Recording for 9 o'clock target by subject 2: Trajectories (pen tip and joints: shoulder, elbow and wrist) for target direction 9 o'clock for subject 2. The limb segments are not shown.

### Discussion subject 2

For vertical motion to targets 12 o'clock and 6 o'clock, it is observed that control of thumb and index finger force plays an important role in the overall process that enables pen tip movement. The thumb makes a stronger contribution to the pen tip motion than observed for subject 1.

For upwards pen tip motion, the thumb pressure increases while index pressure decreases (Fig.5.30a and Fig.5.65a), leading to resultant pressure vector (Fig.5.30c and fig.5.36c) pointing upwards (positive y-direction) and resulting in upward movement (movement in positive y-direction, seen in Fig.5.30b and fig.5.36b).

For downward movement, Thumb pressure decreases while index pressure increases (Fig.5.30a), leading to resultant pressure vector (Fig.5.30c) pointing

downwards (negative y-direction) and contributing to downward movement (movement in negative y-direction, seen in Fig.5.30b).

Only for vertical motion to target directions 12 o'clock and 6 o'clock, finger force modulation results in a resultant grip force vector that steers the pen either up- or downwards. During horizontal line drawing the finger force modulation may contribute to pen tip motion in horizontal direction on some occasions, but it is the limb motion in the first place that enables the horizontal pen tip motion to be executed. Despite of observed relations between resultant pen grip forces and pen tip movement in horizontal direction that seem to facilitate horizontal movement (target 3 o'clock: Fig.5.33b and d; target 9 o'clock: Fig5.39b and d), the anatomy of the hand and fingers do not allow the fingers to move in lateral direction relative to the hand. Limb joint movement needs to be involved to enable horizontal pen tip movement. When the limb joints and in particular the wrist joint do not move in a straight horizontal line, but along a diagonal line, wrist rotation is required to produce a straight horizontal line along with flexion/extension of the fingers to ensure a stable grip.

For both up and down line drawing the kinematics show large transitions of wrist and elbow, suggesting that shoulder rotation is an important factor with both up and down line drawing (12 and 6 o'clock targets) and for- and backward line drawing (3 and 9 o'clock targets). For subject 1 this was only seen for line drawing to targets 12 and 6 o'clock.

Interestingly, if a closer look is taken at the process involved with the production of very similar horizontal lines for targets 3 and 9, it becomes clear that the processes are very different. Particularly, the pressure modulation in both trials is very different. The experiment to target direction 9 o'clock shows a very similar pressure modulation pattern in every cycle, that has a direct relation to the line drawing result: during horizontal movement in negative x-direction (towards the 9 o'clock target), the Middle finger force increases, while the thumb and index finger force decrease. However, for target direction 3 o'clock the pressure modulation varies between every cycle. For both target directions 3 and 9 o'clock, it is likely that grip modulation ensures a stable pen grip rather than pen tip movement in the desired movement direction. The direction of the resultant force (Fig.5.33d and Fig.5.39d) vector does

not directly relate to the actual motion direction of the pen tip, which originates from controlling the wrist, elbow and shoulder joint torques in the first place.

In addition, the shoulder and elbow are more involved for target direction 9 o'clock as the shoulder and elbow trajectories are larger than for target direction 3 o'clock.

The joint trajectories again illustrate the flexibility of the neuromuscular system. Variation in shoulder, wrist and elbow trajectories is observed within trials, while still producing a nearly equal line over five cycles. In section 1.4.2.1 it was shown that the deviation from the ideal straight line was stronger for experiments with target positions 3 and 9 o'clock than for experiments with target positions 12 and 6 o'clock. Moreover, the velocity was higher for trials with target positions 3 and 9 o'clock than for the trials with target positions 12 and 6 o'clock. Fingertip path curvature increases with increasing speed, according to Klein Breteler et al (1998), which may partly explain the differences observed.

#### 5.4.3 Comparing line drawing features for subjects 1 and 2

Below differences between specific features for line drawing by subjects 1 and 2 are discussed.

##### **Writing velocity and deviation from the line straight line**

Subject 2 tends to complete the task the lines faster than subject 1, but with this speed is more variability in straightness of the lines (curvature), which may be a consequence of the higher velocity, as was reported by Klein Breteler et al in 1998. An exception is the experiment with target direction 9 o'clock by subject 1. Although the line is not produced very fast, there is clear path curvature - the path deviates strongly from the ideal straight horizontal line. Velocity is not the only feature determining line quality and cannot be observed on its own. The overall process determining the coordination of effectors needs to be taken into account, which is far more complicated. It may be that the excessive line curvature to the 9 o'clock target is due to the limited wrist rotation. It may be hypothesised from other horizontal trials of both subjects that wrist rotation is required with the production of horizontal lines

without excessive deviation. The theoretical section 5.4.4 on literature on the coordination of effectors in handwriting will expound on this.

For subject 1 the duration of the vertical trials (12 and 6 o'clock targets) are respectively 18.4 and 19.3 seconds, whereas the duration of the horizontal trials (3 and 9 o'clock targets) respectively are only 14.9 and 12 seconds. The deviation from the ideal straight line is less for the vertical targets (12 and 6 o'clock) than for the horizontal targets (3 and 9 o'clock) (SSE and RMSE values in Table 5.3, Table 5.5 and Table 5.6). It is assumed that the lower deviations in the vertical direction are related to the writing velocity.

For subject 2 the duration of the vertical trials (12 and 6 o'clock targets) are respectively 9.22 and 9.41 seconds, whereas the duration of the horizontal trials (3 and 9 o'clock targets) are respectively 8.96 and 8.94 seconds. Although the horizontal lines were drawn faster, the difference is small. Nevertheless, the deviation from the ideal straight line is less for vertical direction than for horizontal targets (SSE and RMSE values in Table 5.4, Table 5.5 and Table 5.6), as was seen for subject 1.

In Fig.5.14 it was illustrated for the 9 o'clock target that for the horizontal targets (3 and 9 o'clock) for subject 1, the deviation from the horizontal line (in vertical direction) is related to the drawing direction: with positive horizontal movement there is upward vertical movement and with negative horizontal movement there is downward vertical movement.

### **Finger pressure**

For both subject 1 and subject 2, finger force directly relates to vertical pen movement for experiments with target directions 12 and 6 o'clock, while that relation seems less obvious for horizontal line drawings (target directions 3 and 9 o'clock) . The following figures illustrate this. Fig. 5.11, Fig.5.12 and Fig.5.24 show for subject 1 that mainly the index finger is responsible for up- and downward pen tip movement to the 12 and 6 o'clock targets. Fig.5.30 and Fig.5.36 illustrate that the thumb and index finger are responsible for controlling up- and downward tip motion to the 12 and 6 o'clock targets.

Both subject 1 and subject 2 seem to modulate finger grip force while drawing a vertical line in a more repeatable and predictable fashion than while drawing a horizontal line. Looking at the vertical line production for target positions 12 (Fig.5.11, 5.12 and 5.30) and 6 o'clock (Fig.5.24 and Fig. 5.36) for both subjects, a very similar force pattern can be seen for the two trials of each subject; only the force value differs, dependent on the movement direction. It is plausible that the same finger synergies are active in both vertical trials for one subject. This corresponds to what is reported for normal handwriting. The vertical pen tip movements are caused by up and down going finger movements relative to the hand, whereas horizontal progression of the hand, relative to an external reference frame, originates from wrist, elbow and shoulder movements (Van der Gon, 1965; Edelman S, 1987; Hollerbach, 1981). The relative contributions of these two motions to kinematics of pen tip can vary and it is assumed that during normal handwriting both components contribute to the trajectory of the pen on the paper by coordination of muscular activity on fingers, wrist and arm (Lacquaniti, Ferrigno, Pedotti, Soechting, Terzuolo, 1987; Meulenbroek, Thomassen, van Lieshout, Swinnen, 1998; Dounskaia, van Gemmert, Stelmach, 2000). These observations reflect earlier assumptions on pen-hand coordination and the contributions of finger and arm joints in relation to pen tip movement direction. These views had not been evaluated and no empirical evidence existed (Meulenbroek, 1998).

The exact finger force coordination does differ between subjects. The force values for all three fingers are lower for subject 2 than for subject 1. Subject 1 steers the pen in vertical direction by in the first place controlling the Index finger force level, whereas subject 2 steers in vertical direction by controlling force levels of both index finger and thumb to the same extent.

### **Joint trajectories**

Subject 2's strategy is very constant for attempting to produce similar straight lines of the pen tip: the trajectories of shoulder, elbow, and wrist are very similar among cycles. Subject 1, however, uses more variable trajectories of shoulder, elbow, and wrist among cycles in one trial, but nevertheless produces similar approximately straight lines for every cycle.

Subject 1 uses wrist rotation to drag the pen tip in horizontal (for-/backward) direction in trials for target directions 3 and 9 o'clock. Subject 2, however, uses wrist rotation in vertical (up-/downward direction) in trials for target directions 12 and 6 o'clock as well. The large transitions of wrist and elbow observed for subject 2 for both up and down line drawing, suggest that shoulder rotation is an important factor with both up and down line drawing (12 and 6 o'clock targets) and for- and backward line drawing (3 and 9 o'clock targets). For subject 1 this was only seen for up and down line drawing to targets 12 and 6 o'clock.

For subject 1, elbow motion mainly contributes to vertical movement in trials for target directions 12 and 6 o'clock, whereas elbow is not much involved in horizontal trials for target directions 3 and 9 o'clock.

For subject 2, the elbow is involved with both horizontal and vertical trials and its contribution is even stronger for drawing horizontal lines (trial 4 and 10).

This highlights the redundancy in pen tip coordinations tasks as drawing and writing. In other words the neuromuscular system's flexibility enables to produce the same motion end points, using different kinematics.

#### 5.4.4 Further discussion on coordination of line drawing

Some issues from literature on motor processing of handwriting that may help to understand how the work of different effectors can jointly result in the required line drawing movement, are summarised below. The results seen above cannot be explained at current research stage yet and further testing and analysis is required to explain the observed behaviour. The expound may be a framework for further discussion of the results and extended research. It also illustrates the complexity of the motorprocessing involved.

Literature explains the following. Motor activity is the contractile state of agonist-antagonist muscle groups over time, changed by neural control signals. The simplest motor command changes the angle of a joint from one value to another and for a rotary joint the Cartesian space motion of the distal end of the segment is curved.

Based on the finding that the spatial trajectory is more variant than the joint rotations or than force-time patterns (Teulings et al., 1986; Morasso, 1981, 1986; Abend et al, 1982), models for script generation have been proposed (Edelman and Flash, 1987;

Schomaker et al, 1989; Plamondon, 1989, 1992; Dooijes, 1983) that assume planning in two-dimensional or three-dimensional space, with continuous mapping from this space into the joint space that controls motor execution (Bullock et al, 1993). A neural controller specifies desired trajectories in a 3-D spatial coordinate system (e.g. polar or cartesian) and then maps the resulting trajectory into joint angles changes (Greve et al, 1992; Bullock, 1993). Later, the idea was adopted that pointing and grasping movements in joints with three degrees of freedom, such as the shoulder, are subject to a reduction of degrees of freedom and movements are produced in 2D rather than 3D (Gielen et al, 1997; Klein Breteler et al, 1998). It was found that spatial characteristics were even found to be quite similar across different effector systems, e.g. across handwriting and arm writing with hand joints fixed (Greve et al, 1992; Bullock, 1993). Finally, the first computational model for handwriting that enables to produce essentially the same written output with different effectors, in different planes and in different amplitude scales, was developed by Meulenbroek et al (1995), based on the reaching model by Rosenbaum et al (1993, 1995) and incorporating the above suggestion on how such a model might work and other optimisation concepts (Meulenbroek et al, 1995).

In investigations of planar arm movements, initially only straight paths were reported (Morasso, 1981; Soechting and Lacquaniti, 1981; Abend et al, 1981; Flash, 1987). Atkeson and Hollerbach (1985) reported curved paths in the vertical plane only and speculated that path curvature may be caused by the action of gravity. However, Cruse and Brüwer (1987) and Klein Breteler et al (1998) found that curved paths also appear in planar movements. The results of this chapter support the idea that curved paths occur in planar movements.

More specifically, Morasso (1981) and Cruse and Brüwer (1987) observed that curved paths seem to appear for those movements in which the trajectories in joint space would have to be strongly linear. Curved paths are adopted to simplify the tasks of the control system to draw a straight line. This implies that reaching movements reflect a compromise between the tendency of subjects to try to simultaneously produce a straight line in workspace and a straight line in joint space. This is in agreement with Hollerbach et al (1986) and was later confirmed by Klein Breteler et al (1998).

The movement of individual joints is not independent, but there is a superimposed control centre that (globally) controls the timing of the individual muscles during the

movement. The calculations of actual path and of incremental angle changes is done on the local level (distal effectors), according to Cruse and Brüwer (1987). The hypothesis by Hollerbach et al (1986), on the other hand, suggested that the form of the path and muscle activation is also done on the global level. However, one may conclude that controlling both on global level implies that the problem of redundancy of the effector system is not addressed.

The path is determined by both start and stop point ( that indicate movement direction and distance) and starting and ending postures (Cruse and Brüwer, 1987; Rosenbaum et al, 1995). The control system of the movement of the redundant human arm can be interpreted as compromise between four requirements: Firstly, an equal contribution of all joints is desired. Secondly, the total cost value as small as possible, which means means that joint angles are to be chosen near the middle of the range (e.g. shoulder: 0 degrees; elbow: 80 degrees; wrist: 10 degrees), which is the most comfortable position (Cruse, 1986). Thirdly, inertial force is minimised by following a straight workspace path. Fourthly, the pattern of muscle activity is simplified (e.g. avoiding non-monotonic joint movement), which may lead to a linear path in joint space and consequent non-linear path in work space (Cruse and Brüwer, 1987).

A start towards further explaining the observed behaviour would be assessing the movements in joint space by calculating the angles between the limb segments and plot them combined in one graph showing angles rather than coordinates. These angles are: the elbow angle (between upper arm and forearm), elevation (between saggital projection of the upper arm and a vector pointing forward through the trunk) and azimuth (between projection of the upperarm in the horizontal plane and the forward writing direction), according to Klein Breteler et al (1998).

## 6 Subject testing: Writing activity

The aim of this experiment is firstly to show that a comprehensive set of quantifiable data, associated with the use of the developed pen, can be collected that allows future study of the neuromuscular control involved with writing tasks. Secondly, the experiment aims to illustrate the flexibility of the processes involved with script production by comparing these processes for different writing positions.

Paragraph 6.1 and 6.2 respectively describe the healthy test subjects and writing activities that were performed in detail. Section 6.3 describes the data collection process. The comprehensive measurements of kinetics and pen grip are discussed in 6.4 for three subjects, followed by a brief discussion. In 6.5 the results are discussed further, using methods for quantifying the data for five subjects.

### 6.1 Subjects

Five healthy volunteers with good writing ability were tested. All subjects were right hand dominant and of varied ethnic origin. Details of the subjects, whose data will be described in this chapter, are given in Table 6.1.

	1	2	3	4	5
<b>Ethnic origin</b>	white	white	white	Indian	Indian
<b>Gender</b>	female	female	male	male	male
<b>Age</b>	26	25	26	27	23

*Table 6.1: Subjects whose writing activity data is discussed.*

### 6.2 Activities

The subjects were asked to write the same sentence four times, but each time in a different quadrant of the tablet. An example of the task is shown in Fig. 6.1. The sentence written was: "She sells great sea shells by the great sea shore." This sentence was chosen as it contains many repetitions of both words and sequences

of letters. Performing the same writing in four different page positions (i.e. locations) enables comparison of both script and the writing processes. For each writing position the upper body and limb position may differ and the experiment allows investigating whether different muscle groups may be recruited or used in a variety of ways for the different writing positions. N.B.: The four writing locations do not correspond to the four quadrants of a Cartesian coordinate system. Instead, the first position in this experiment is the top left corner of the tablet with the second, third and fourth position following in a clockwise fashion. The reason for following this sequence is that it came more natural to subjects as was seen during the preliminary tests prior to data collection.

There was no defined starting point for the writing to enable subjects to maintain their writing as natural as possible. There was no time restriction to the task.

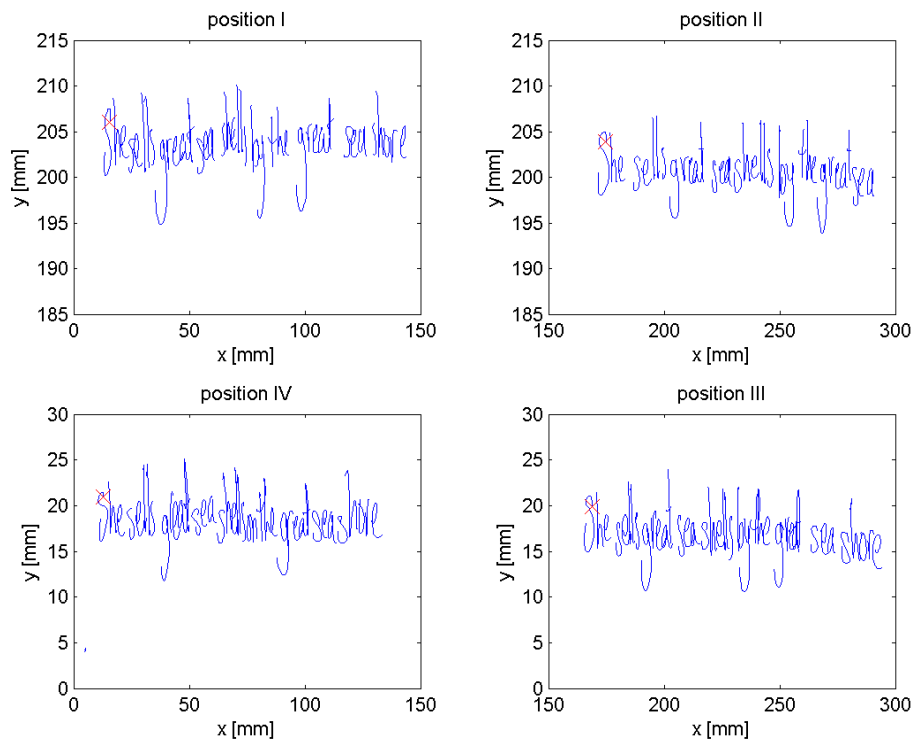


*Fig 6.1: Writing task in four quadrants of the tablet: "She sells great sea shells by the great sea shore." The starting points are marked with a red cross. The four different starting positions (x- and y-coordinates) reveal the distance between the four trials on the writing tablet. The exact starting points were not defined, but it was left up to the subjects to freely choose where within the four quadrants to exactly start the writing.*

### 6.3 Data collection and processing

The comprehensive set of data sampled in this experiment includes:

- script kinematics (x- and y-coordinates);
- pen tip pressure;
- pen grip pressure, applied by thumb, index and middle finger;
- limb and trunk kinematics.

Quantifying data was possible by using the following techniques:

- basic statistics of pen grip measurement for each finger, including mean, maximum, standard deviation and sum of forces;
- Root Mean Square (RMS) values of pen grip measurements for each finger. The Root mean square (RMS), also known as the quadratic mean, is a statistical measure of the magnitude of a varying quantity. The name comes from the fact that it is the square root of the mean of the squares of the values. This is further explained in 4.4.3.
- Power Spectral Density (PSD) of pen grip signal for each finger.

The power spectral density analysis allows the frequency components of the waveform contained in a physiological signal and the relative power at each frequency to be viewed. Visually this can be easier to follow than structures in the time domain. This process can be automated by Matlab functions. This is further explained in 4.4.2.

Most grip modulation occurs in the 0 -10 Hz band (Van Galen, 1990; Raethjen et al, 2000; Santello, 2000; Rearick, 2002) and therefore grip modulation will be studied in this experiment by means of PSD within this band only. It was required to remove the DC-term in order to make the frequencies of force application visible and this was achieved by eliminating the lowest frequencies. The DC-term was removed from the grip applications signals before obtaining spectrograms. The DC removal process has one argument,  $p$ , which refers to a time period in seconds. A time period of  $p=100$  ms was chosen. The output at time  $t$  is defined as the input value at time  $t$  minus the average value of the input data points from time  $t-p$  to  $t+p$ . The channel scale is not affected, but the channel offset is set to zero. The actual frequencies that are eliminated by DC-term removal differ from trial to trial, but frequencies of 1Hz and over (up to 10Hz) are included in the signal.

The test equipment, data analysis and synchronisation techniques are described under methods in 4.2.

The test procedure was as follows. The volunteer is seated behind a table, while holding the grip measuring pen in tripod grip. On command of the investigator, the volunteer performed one writing task at one position at a time. Between the 4 positions there was 30-60 seconds pause. The trials that consisted of writing at all 4 positions was repeated four times for each of the five subjects.

Subjects were not allowed to move the table, tablet or chair during the experiment to minimise variability in writing production. Only their body positioning relative to the experiment setup could vary.

Data collection was successful for 4 out of 5 subjects, resulting in good quality data of script, limb motion and pen grip forces. Data collection for subject 5 failed, which was not due to technical errors, but due to the subject having an emergency that required the subject to leave the testing session.

## **6.4 Results: Comparison pen grip for writing the whole sentence**

### **6.4.1 Introduction**

The writing process grip features are compared for subjects 1, 2, 3 and 4 in this paragraph by means of the following methods that allow quantification of the pen grip finger forces:

- Root Mean Square (RMS) values (RMS measures are explained in section 6.3);
- Total and maximum band power in the range from 1-10Hz, using Power Spectral Density (PSD) analysis (PSD measures are explained in section 6.3).
- Basic statistics, including: mean, maximum, standard deviation and sum of Thumb, Index and Middle finger pressure. These measures are further explained in section 4.4.4.

The techniques used to obtain the features mentioned above are described in detail in 4.4 on data analysis techniques. For each subject four repetitions of the trial are reported and each trial includes writing tasks at four tablet positions.

The graphs and tables with grip features for Subject 1 shows interesting features, which are presented in section 6.4.2 for illustrative purposes. The comparison of pen grip features of all four subjects will then be presented in 6.4.3.

#### 6.4.2 Description of pen grip features for subject 1

The pen grip features for writing by subject 1 are shown as graphs and tables in this section. This includes:

- basic statistics (mean, standard deviation, maximum and sum) in Table 6.2;
- Sum of forces (sum of force values over duration of one trial) in Fig.6.2.;
- Root Mean Square (RMS) in Table 6.3 and Fig.6.3;
- Total and maximum Power Spectral Density (PSD) in Fig.6.4.

Observations that may be made from the grip measurements of subject 1 are:

- The thumb force values are higher than middle and index finger force values for writing in nearly every position in each of the 4 trials as can be seen from the sum of forces (Fig. 6.2), RMS-value (Fig.6.3 and Table 6.3) and Maximum and Total Power values (Fig.6.4).
- There is more thumb, index and middle finger pen grip modulation in trial 1 (for nearly all 4 positions) than in the other 3 trials as can be seen from the Sum of forces (Fig. 6.2), RMS-value (Fig.6.3 and Table 6.3) and Maximum and Total Power values (Fig.6.4).
- In addition, from the Sum of forces (Fig. 6.2), RMS-value (Fig.6.3 and Table 6.3) and Maximum and Total Power values (Fig.6.4) it can be observed that, no consistent relationship can be found between trials numbered 1 to 4 and the force values. The force values tend to be highest in trial 1, whilst the values in trial 2 are slightly lower than in trial 1. The values in trials 3 and 4 are quite similar and slightly lower than in trial 2.
- In addition, the variation in thumb, middle and index finger force values between writing positions I to IV is higher in trial 1 than in trials 2, 3 and 4 as

can be seen from the Sum of forces (Fig. 6.2), RMS-value (Fig.6.3 and Table 6.3) and Maximum and Total Power values (Fig.6.4).

- No consistent relation can be found between tablet positions I to IV and grip force values (Mean and Sum of forces (Fig. 6.2), RMS-value (Fig.6.3 and Table 6.3) and Maximum and Total Power values (Fig.6.4)).

### Basic statistics of finger forces for subject 1

Trial number	Thumb Force [N]									
	pos	mean	std	max	sum	pos	mean	std	max	sum
1	I	0.99	0.29	1.75	19285	II	1.62	0.47	3.18	36887
	IV	1.17	0.55	3.01	28438	III	1.62	0.59	3.02	46378
2	I	0.99	0.37	1.94	23759	II	0.94	0.30	2.20	19158
	IV	0.56	0.26	1.73	11095	III	0.75	0.27	1.42	13721
3	I	0.66	0.27	1.54	15181	II	0.48	0.22	1.17	9419
	IV	0.46	0.19	1.08	9681	III	0.61	0.22	1.29	11484
4	I	0.64	0.21	1.50	12216	II	0.83	0.25	1.47	13675
	IV	0.59	0.22	1.21	13163	III	0.55	0.16	1.15	10682

Trial number	Middle Force [N]									
	pos	mean	std	max	sum	pos	mean	std	max	sum
1	I	0.87	0.27	1.58	17005	II	1.26	0.30	2.22	28635
	IV	0.83	0.42	1.98	20284	III	1.20	0.32	2.32	34331
2	I	0.74	0.33	1.58	17759	II	0.88	0.30	1.91	18046
	IV	0.65	0.25	1.47	12734	III	0.81	0.28	1.48	14794
3	I	0.56	0.22	1.16	12892	II	0.53	0.24	1.21	10373
	IV	0.46	0.21	0.99	9702	III	0.61	0.22	1.26	11334
4	I	0.63	0.22	1.23	11953	II	0.72	0.23	1.28	11846
	IV	0.71	0.32	1.47	15745	III	0.70	0.20	1.29	13638

Trial number	Index Force [N]									
	pos	mean	std	max	sum	pos	mean	std	max	sum
1	I	0.79	0.31	1.61	15472	II	0.94	0.41	2.20	21287
	IV	0.67	0.40	1.84	16265	III	0.67	0.46	2.06	19196
2	I	0.56	0.32	1.44	13480	II	0.70	0.33	1.88	14266
	IV	0.54	0.26	1.52	10694	III	0.46	0.25	1.17	8406
3	I	0.51	0.28	1.23	11656	II	0.42	0.23	1.23	8256
	IV	0.39	0.24	1.19	8176	III	0.44	0.23	1.14	8194
4	I	0.50	0.27	1.30	9403	II	0.60	0.27	1.37	9977
	IV	0.43	0.26	1.12	9554	III	0.38	0.21	0.96	7344

Table 6.2: Basic statistics of Thumb, Index and Middle finger forces (4 writing positions for each of 4 trials): mean, standard deviation, maximum and sum of forces for subject 1.

### Sum of force values for subject 1

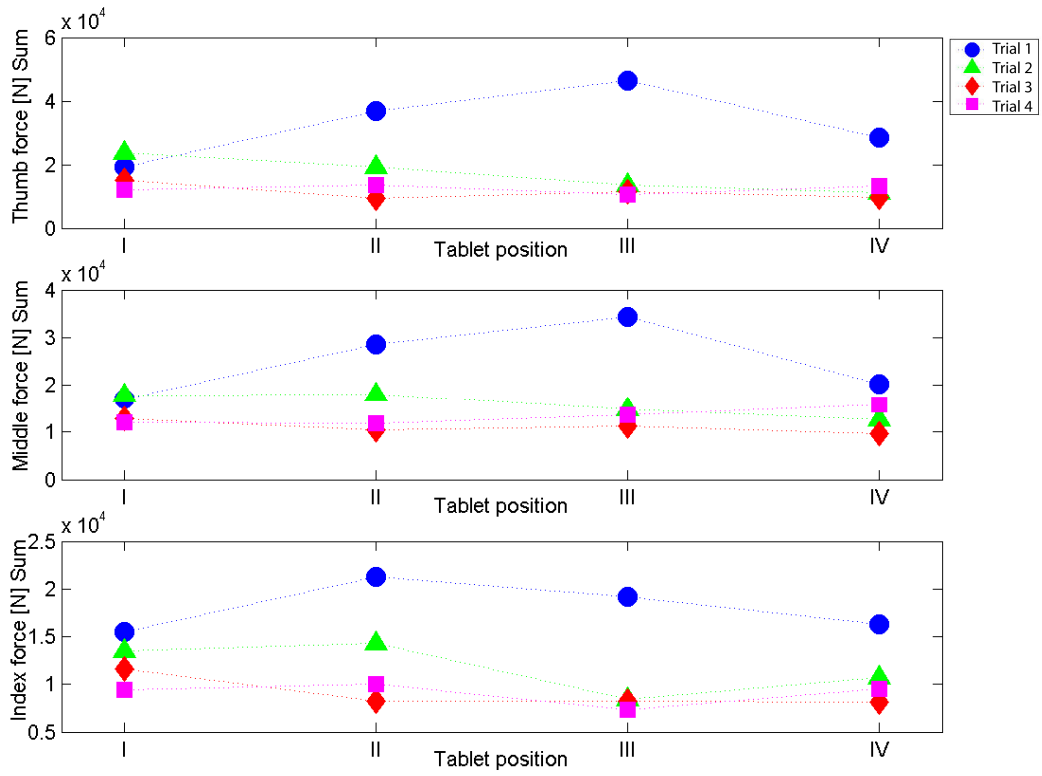


Fig.6.2: Sum of force values during the whole trial for Thumb, Index and Middle finger forces (4 writing positions for each of 4 trials) for subject 1.

### RMS force values for subject 1

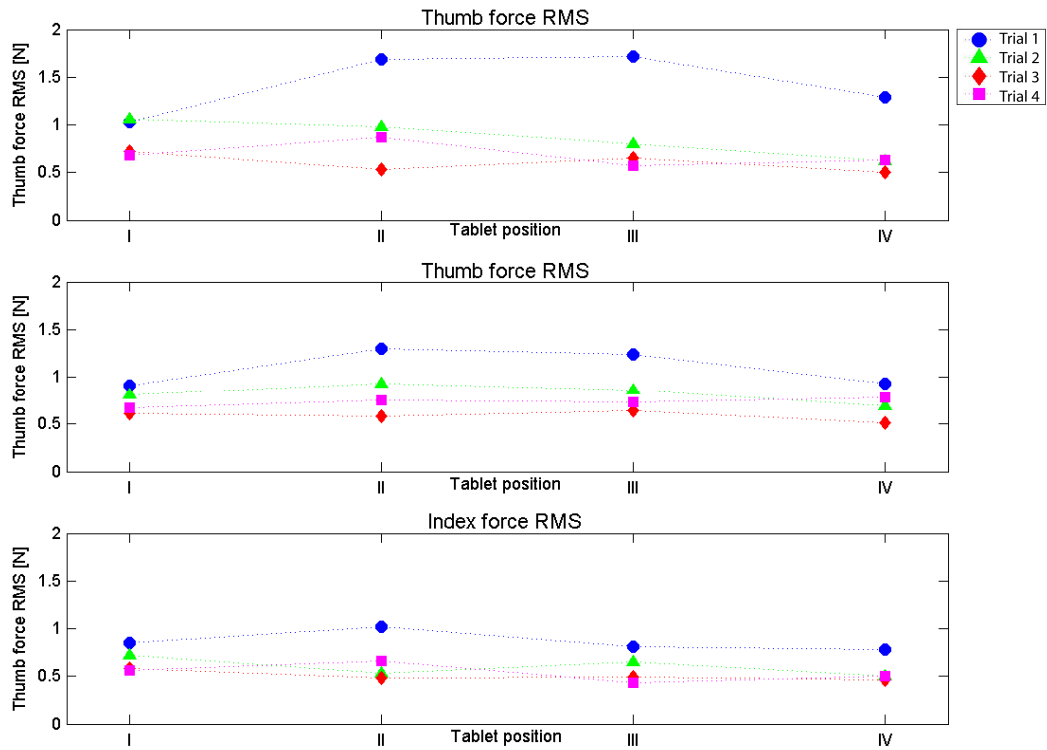


Fig. 6.3: Root Mean Square (RMS) values for Thumb, Index and Middle finger forces (4 writing positions for each of 4 trials).

RMS Force [N]	Position	Trial number			
		1	2	3	4
Thumb	I	1.0318	1.0549	0.71748	0.67839
	II	1.6898	0.98312	0.53075	0.86599
	III	1.7181	0.79677	0.65198	0.5742
	IV	1.2872	0.61923	0.50018	0.63096
Middle	I	0.91375	0.81033	0.60713	0.66817
	II	1.2969	0.93305	0.58108	0.75273
	III	1.2375	0.85613	0.64449	0.73051
	IV	0.93355	0.69232	0.50986	0.77685
Index	I	0.8534	0.71748	0.58155	0.56434
	II	1.0214	0.53075	0.4814	0.66318
	III	0.81233	0.65198	0.49646	0.43229
	IV	0.77843	0.50018	0.4609	0.50145

Table 6.3: Root Mean Square (RMS) values for Thumb, Index and Middle finger forces (4 writing positions for each of 4 trials for subject 1).

## Power Spectral Density analysis for subject 1

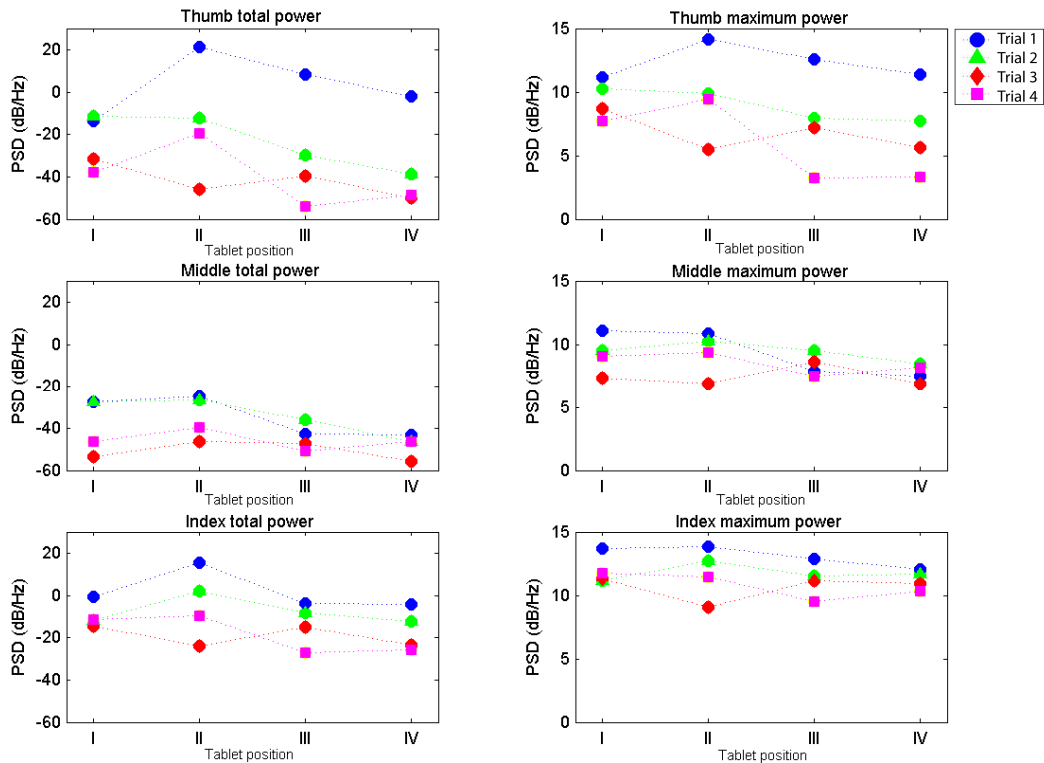


Fig.6.4: Total and maximum band power within the 0-10Hz band (4 writing positions for each of 4 trials).

### 6.4.3 Comparison of pen grip for all 4 subjects

The following pen grip features for subjects 2, 3 and 4 are shown in the graph and tables below:

- RMS:
  - 3 graphs (thumb, middle and index finger), showing RMS-value for trials 1 to 4 (Fig. 6.6; 6.9; 6.12);
  - Table with exact RMS values (Table 6.5; 6.7; 6.9)
- PSD:
  - 3 graphs (thumb, middle and index finger), showing value of total (0-10Hz) band power for trials 1 to 4 (Fig.6.7; 6.10; 6.13).
  - 3 graphs (thumb, middle and index finger), showing value of maximum power in 0-10Hz band and frequency at which the

maximum power that occurs for trials 1 to 4 (Fig.6.7; 6.10; 6.13).

- Pen grip force:
- Table with mean, maximum, standard deviation and sum of thumb, index and middle finger pressure (Table 6.4; 6.6; 6
  - 3 graphs (thumb, middle and index finger), showing Sum of force value for trials 1 to 4 (Fig. 6.5; 6.8; 6.11).

### ***Force levels observed for 4 subjects***

There is a large variation in force level that is applied by the four different subjects as can be seen from the basic statistics on forces (Table 6.2, Table 6.4, Table 6.6, Table 6.8), the RMS-values (Fig.6.3, Fig.6.5, Fig.6.7, Fig.6.9 and Table 6.3, Table 6.5, Table 6.7, Table 6.9) and average force values (Fig.6.10). The average force values for each finger in Fig. 6.10 reveals that forces applied to the pen by Subject 2 and subject 3 are relatively high, whereas the forces applied by subjects 4 and 1 (in decreasing order) have values that are only half or less the values applied by subjects 2 and 3. With increased mean force values the standard deviation tends to be higher.

### ***Force level differences between fingers observed for each subject***

For each subject a different force level applied by each finger can be observed that is consistent for each subject. For subject 1 the thumb force values are higher than middle and index finger force values for writing in nearly every position in each of the 4 experiments as can be seen from the basic statistics on forces (Fig. 6.2), the RMS-values (Fig.6.3 and Table 6.3) and average force values (Table 6.10).

For subject 2 the middle finger force values are higher than thumb and index finger force values for writing in nearly every position in each of the 4 experiments as can be seen from the basic statistics on forces (Table. 6.4), the RMS-values (Fig.6.6 and Table 6.5) and average force values (Table 6.10). However, there is not a large difference between the force values for each of the three fingers.

For subject 3 (as for subject 1) the thumb force values are higher than middle and index finger force values for writing in nearly every position in each of the 4 experiments as can be seen from the basic statistics on forces (Fig. 6.6), the RMS-values (Fig.6.9 and Table 6.7) and average force values (Table 6.10). In addition, there is a large difference between values of thumb force compared to middle and index finger force.

For subject 4 the Index finger force values are higher than thumb and middle finger force values for writing in nearly every position in each of the 4 experiments as can be seen from the basic statistics on forces (Table. 6.8), the RMS-values (Fig.6.12 and Table 6.9) and average force values (Table 6.10).

### ***Power Spectral Density and force values***

In Fig.6.4, Fig.6.7, Fig.6.10 and Fig.6.13 the power spectral density (PSD) analysis of the thumb, index and middle finger force signals are presented for the subjects 1 to 4 respectively, showing both the band power (0-10Hz band) and the maximum PSD value within the band. The power spectral density analyses show that the total and maximum power levels relate to force values. High average force values observed (Table 6.10) for one experiment (4 positions) are generally accompanied by high total and maximum power spectral density values within the 0-10 Hz frequency band (Fig.6.4, Fig.6.7, Fig.6.10 and Fig.6.13). The power spectral density within the 0-10Hz frequency band therefore gives an indication of how much gripping activity is going on. However, the exact difference in force values between different positions within one experiment or the exact difference in force values between different experiments is not reflected by the power spectral density. Nevertheless, in general the power spectral density (total and maximum) values for each finger for Subject 2 and subject 3 are relatively high, whereas the power (total and maximum) values for subjects 4 and 1 (in decreasing order) have values that are only half or less the values applied by subjects 2 and 3. This order is identical to the order of force values of force values observed: the basic statistics on forces (Table 6.2, Table 6.4, Table 6.6, and Table 6.8), the RMS-values (Fig.6.3, Fig.6.5, Fig.6.6, Fig.6.9 and Table 6.3, Table 6.5, Table 6.7, Table 6.9) and average force values (Fig.6.10).

### Basic statistics of finger forces for subject 2

Trial number	Thumb Force [N]									
	pos	mean	std	max	sum	pos	mean	std	max	sum
1	I	4.03	1.19	6.62	72947.59	II	3.79	1.26	6.73	62655
	IV	5.09	1.45	7.15	105141.83	III	4.08	1.18	6.80	72160
2	I	5.13	1.27	7.04	81493.81	II	3.89	1.29	6.96	61431
	IV	4.03	1.16	6.68	63097.02	III	4.18	1.16	6.82	67429
3	I	4.70	1.11	6.94	70615.59	II	3.36	1.07	6.27	51912
	IV	3.73	1.26	6.83	59689.77	III	3.83	1.10	6.80	61516
4	I	2.81	1.06	6.36	41776.03	II	4.32	1.43	7.15	64560
	IV	2.80	1.47	6.76	56534.90	III	5.05	1.37	7.34	78853

Trial number	Middle Force [N]									
	pos	mean	std	max	sum	pos	mean	std	max	sum
1	I	4.58	1.12	7.63	82836.35	II	4.45	1.20	8.71	73583
	IV	5.51	1.51	10.68	113838.77	III	4.74	1.25	9.29	83897
2	I	5.54	1.33	9.46	88052.37	II	4.66	1.35	10.10	73523
	IV	4.72	1.07	8.43	73895.12	III	4.59	1.04	8.76	73987
3	I	4.82	1.24	8.88	72473.80	II	4.10	0.98	7.00	63355
	IV	4.96	1.38	9.49	79304.32	III	4.04	0.95	8.43	64866
4	I	3.45	1.00	7.36	51357.98	II	4.32	1.43	10.29	64557
	IV	3.30	1.54	8.79	66627.04	III	5.20	1.46	11.02	81175

Trial number	Index Force [N]									
	pos	mean	std	max	sum	pos	mean	std	max	sum
1	I	3.66	1.31	7.66	66314.09	II	3.62	1.26	7.93	59785
	IV	4.67	1.81	8.22	96574.37	III	3.48	1.23	7.89	61587
2	I	4.01	1.28	7.86	63735.34	II	3.84	1.39	7.93	60577
	IV	3.15	1.06	6.90	49357.43	III	3.30	1.12	7.71	53217
3	I	4.31	1.35	8.18	64841.70	II	3.52	1.02	7.28	54479
	IV	3.74	1.38	7.75	59786.14	III	3.27	1.20	7.80	52460
4	I	2.63	0.97	6.21	39057.67	II	3.95	1.49	8.20	59061
	IV	2.69	1.47	7.42	54330.40	III	3.56	1.25	7.68	55570

Table 6.4: Basic statistics of Thumb, Index and Middle finger forces (4 writing positions for each of 4 trials): mean, standard deviation,

maximum and sum of forces for subject 2.

### Sum of force values for subject 2

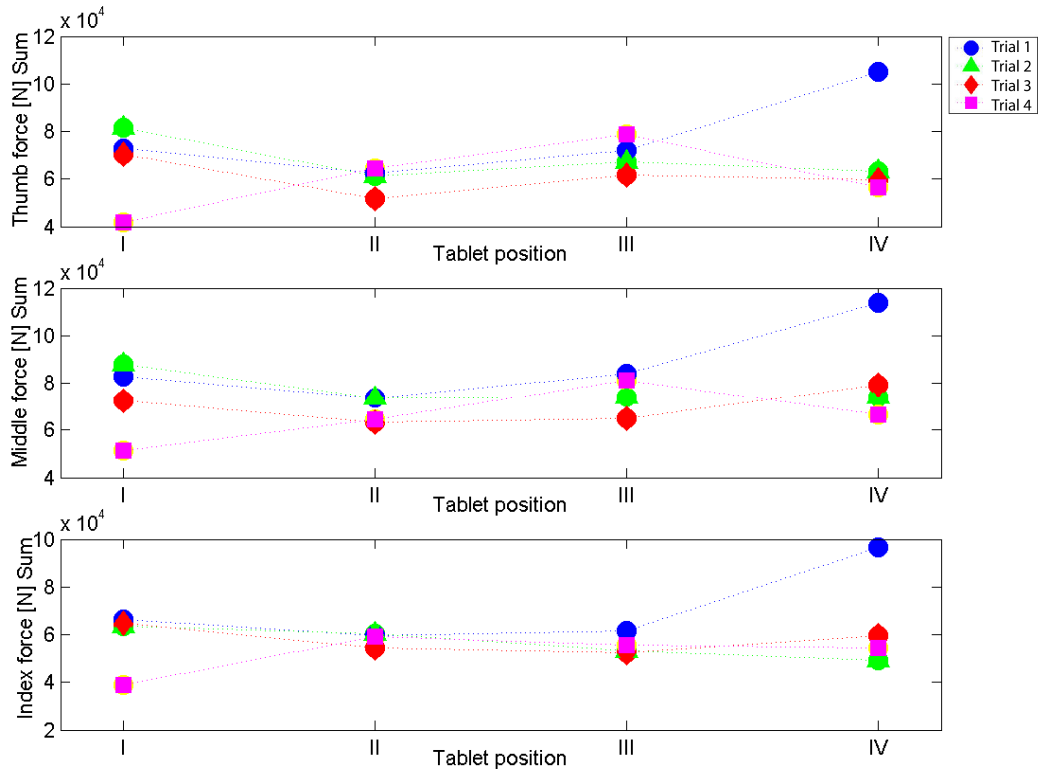


Fig.6.5: Sum of force values during the whole trial for Thumb, Index and Middle finger forces (4 writing positions for each of 4 trials) for subject 1.

RMS Force [N]	Position	Trial number			
		1	2	3	4
Thumb	I	4.2023	5.2829	4.8277	3.0019
	II	3.9954	4.0976	3.5236	4.5501
	III	4.2441	4.3406	3.9887	5.2359
	IV	5.288	4.1949	3.9397	3.1642
Middle	I	4.7117	5.6984	4.9794	3.5967
	II	4.6114	4.8487	4.2143	4.548
	III	4.9006	4.7053	4.1511	5.403
	IV	5.7117	4.8409	5.149	3.647
Index	I	3.8905	4.2087	4.5211	2.8012
	II	3.8284	4.0817	3.6678	4.2227
	III	3.6919	3.4856	3.4808	3.7759
	IV	5.0105	3.3278	3.9867	3.0695

Table 6.5: Root Mean Square (RMS) values for Thumb, Index and Middle finger forces

(4 writing positions for each of 4 trials) for subject 2.

### RMS force values for subject 2

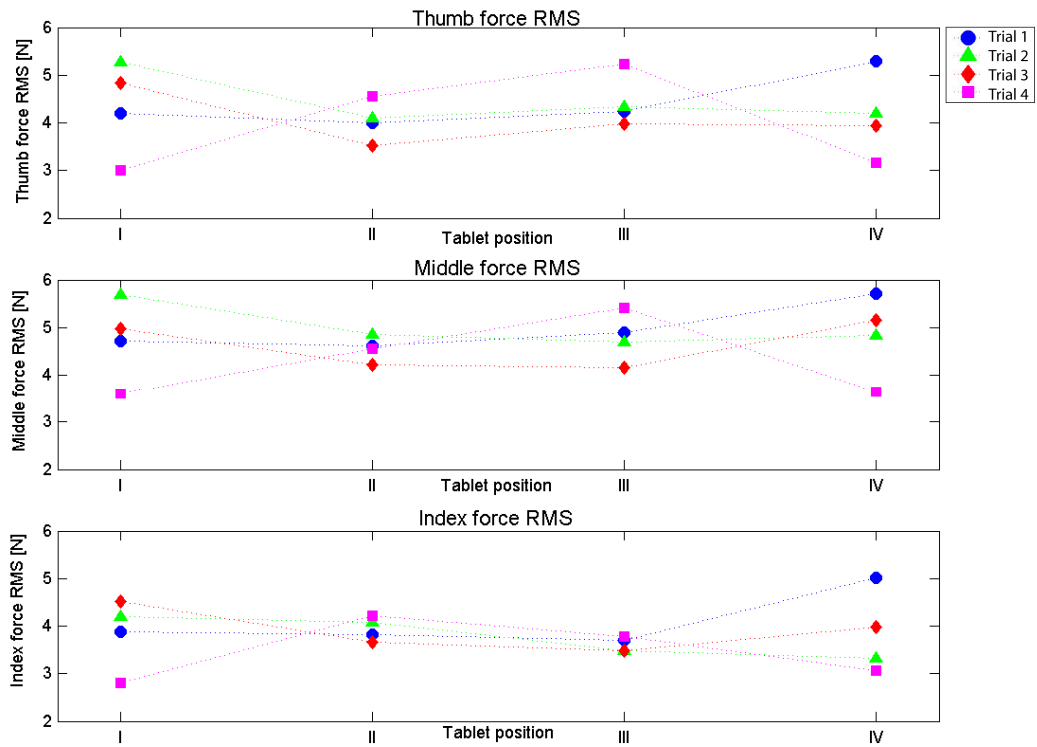


Fig. 6.6: Root Mean Square (RMS) values for Thumb, Index and Middle finger forces (4 writing positions for each of 4 trials) for subject 2.

## Power Spectral Density analysis for subject 2

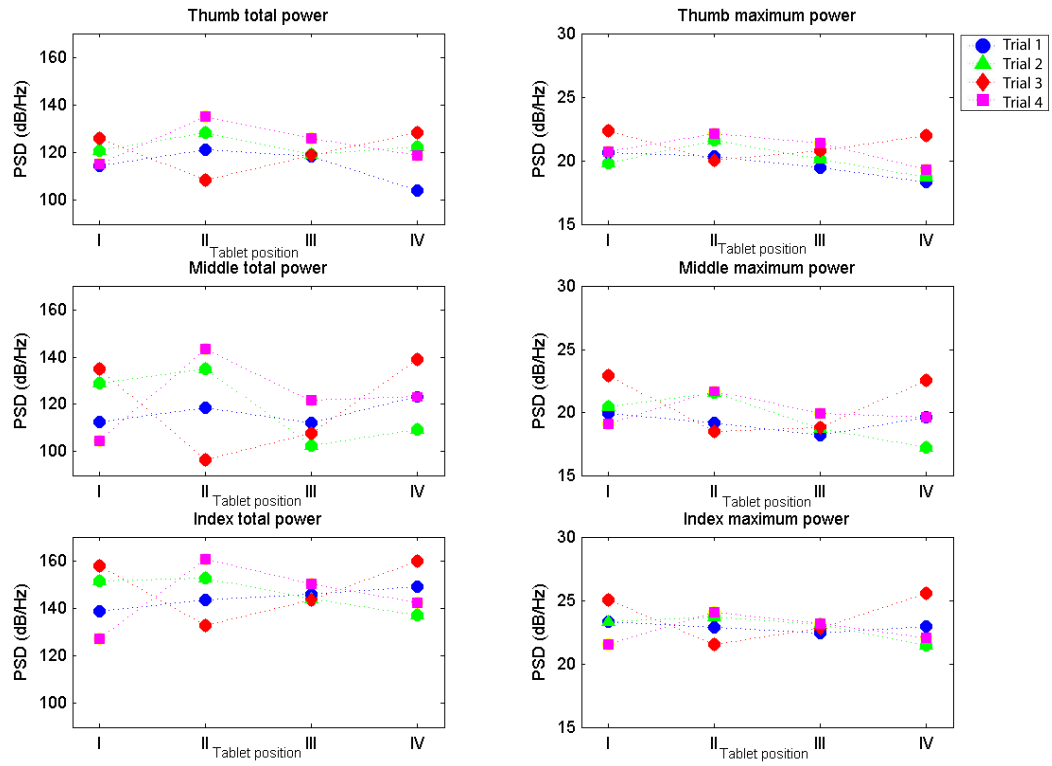


Fig. 6.7: Total and maximum power spectral density (PSD) values for Thumb, Index and Middle finger forces (4 writing positions for each of 4 trials) for subject 2.

### Basic statistics of finger forces for subject 3

Trial number	Thumb Force [N]									
	pos	mean	std	max	sum	pos	mean	std	max	sum
1	I	4.81	1.51	6.94	126473	II	4.89	1.51	6.85	111711
	IV	4.83	1.49	7.06	128475	III	4.65	1.56	6.87	99800
2	I	4.68	1.43	6.90	116486	II	5.09	1.48	6.87	119323
	IV	4.81	1.41	6.96	125076	III	4.73	1.42	6.82	110590
3	I	5.19	1.31	7.03	126484	II	5.35	1.39	7.01	132411
	IV	4.72	1.54	7.25	132882	III	4.73	1.35	6.75	113390
4	I	4.57	1.45	6.80	107049	II	4.62	1.39	6.73	109065
	IV	4.31	1.29	6.76	112844	III	3.75	1.30	6.62	93576

Trial number	Middle Force [N]									
	pos	mean	std	max	sum	pos	mean	std	max	sum
1	I	2.54	0.84	5.49	66867	II	2.50	0.80	4.72	57163
	IV	2.41	0.87	5.62	64155	III	2.35	1.00	5.26	50441
2	I	2.51	0.76	5.11	62510	II	3.18	1.00	6.07	74473
	IV	2.75	0.87	5.74	71331	III	2.58	0.88	5.54	60175
3	I	2.71	0.80	5.66	65990	II	2.71	0.91	5.32	67068
	IV	2.53	0.90	7.21	71292	III	2.53	0.77	5.06	60479
4	I	2.22	0.75	4.67	52090	II	2.46	0.77	4.79	58099
	IV	2.27	0.68	5.13	59570	III	1.93	0.68	4.52	48123

Trial number	Index Force [N]									
	pos	mean	std	max	sum	pos	mean	std	max	sum
1	I	2.20	0.76	4.44	57885	II	2.21	0.75	4.28	50542
	IV	2.50	0.91	5.31	66403	III	2.15	0.66	4.05	46085
2	I	2.33	0.66	4.57	57899	II	2.12	0.67	3.96	49712
	IV	2.25	0.65	4.33	58401	III	1.94	0.54	3.68	45357
3	I	2.10	0.60	3.83	51331	II	2.45	0.63	4.19	60689
	IV	2.15	0.66	3.90	60549	III	2.05	0.48	3.52	49067
4	I	2.00	0.60	3.65	46824	II	1.87	0.53	3.45	44236
	IV	1.86	0.51	3.38	48629	III	1.63	0.41	3.11	40565

Table 6.6: Basic statistics of Thumb, Index and Middle finger forces (4 writing positions for each of 4 trials): mean, standard deviation, maximum and sum of forces for subject 2.

### Sum of force values for subject 3

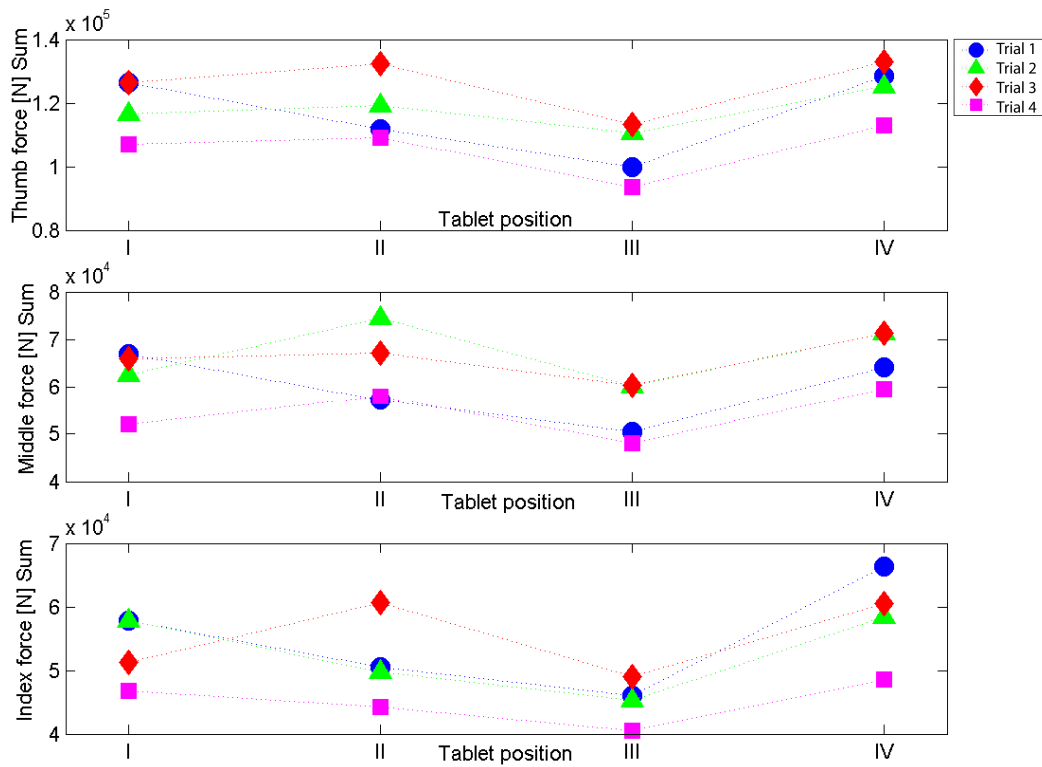


Fig.6.8: Sum of force values during the whole trial for Thumb, Index and Middle finger forces (4 writing positions for each of 4 repetitions of the trial) for subject 3.

RMS Force [N]	Position	Trial number			
		1	2	3	4
Thumb	I	5.0427	5.0174	4.9413	5.5231
	II	5.1167	4.8945	4.9643	4.923
	III	4.9059	5.3021	5.3489	4.497
	IV	5.0555	4.9059	5.3021	5.3489
Middle	I	2.6793	2.6799	2.7219	2.8551
	II	2.6269	2.6247	2.686	2.6398
	III	2.5547	3.331	2.8227	2.3752
	IV	2.5631	2.5547	3.331	2.8227
Index	I	2.3307	2.341	2.0157	2.529
	II	2.3352	2.4185	2.2493	2.1036
	III	2.2457	2.2241	2.1874	1.9265
	IV	2.6569	2.2457	2.2241	2.1874

Table 6.7: Root Mean Square (RMS) values for Thumb, Index and Middle finger forces (4 writing positions for each of 4 trials) for subject 3.

### RMS force values for subject 3

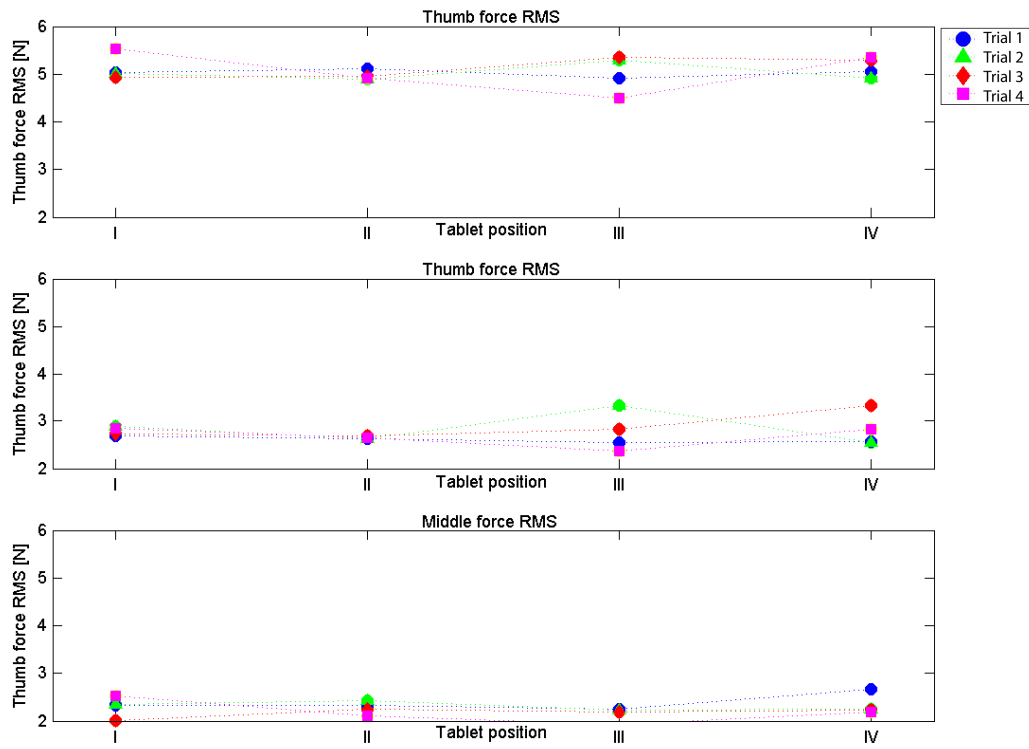


Fig. 6.9: Root Mean Square (RMS) values for Thumb, Index and Middle finger forces (4 writing positions for each of 4 trials) for subject 3.

### Power Spectral Density analysis for subject 3

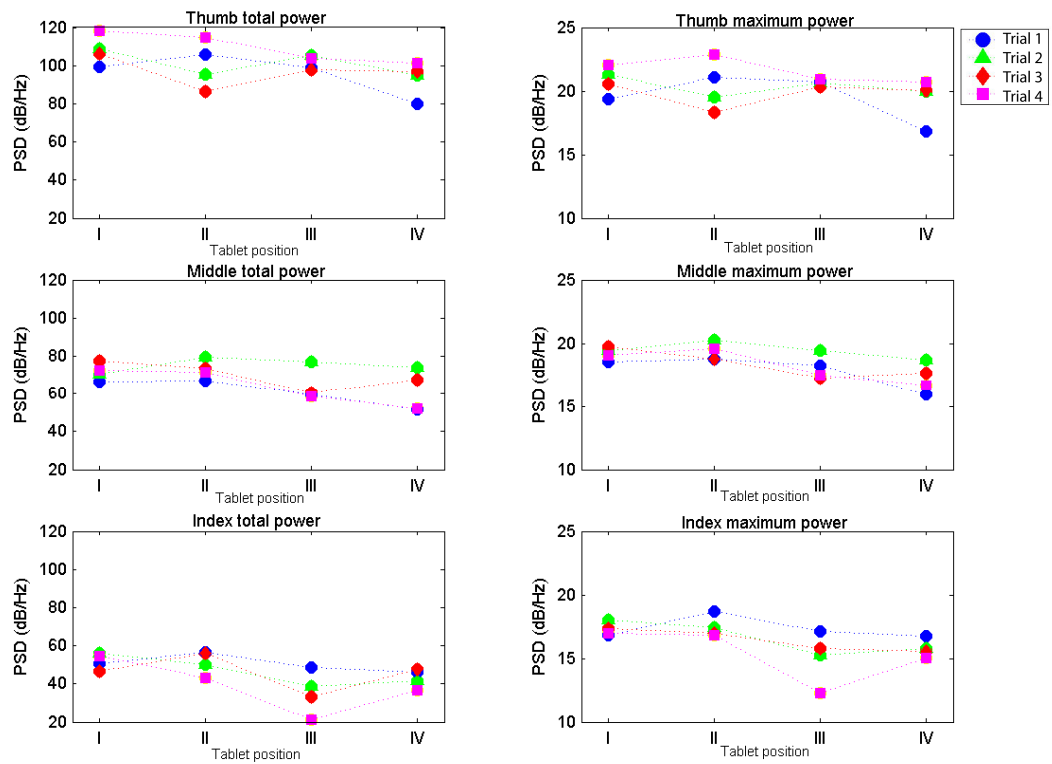


Fig. 6.10: Total and maximum power spectral density (PSD) values for Thumb, Index and Middle finger forces (4 writing positions for each of 4 trials) for subject 3.

### Basic statistics of finger forces for subject 4

Trial number	Thumb Force [N]									
	pos	mean	std	max	sum	pos	mean	std	max	sum
1	I	4.81	1.51	6.94	126473	II	4.89	1.51	6.85	111711
	IV	4.83	1.49	7.06	128475	III	4.65	1.56	6.87	99800
2	I	4.68	1.43	6.90	116486	II	5.09	1.48	6.87	119323
	IV	4.81	1.41	6.96	125076	III	4.73	1.42	6.82	110590
3	I	5.19	1.31	7.03	126484	II	5.35	1.39	7.01	132411
	IV	4.72	1.54	7.25	132882	III	4.73	1.35	6.75	113390
4	I	4.57	1.45	6.80	107049	II	4.62	1.39	6.73	109065
	IV	4.31	1.29	6.76	112844	III	3.75	1.30	6.62	93576

Trial number	Middle Force [N]									
	pos	mean	std	max	sum	pos	mean	std	max	sum
1	I	2.54	0.84	5.49	66867	II	2.50	0.80	4.72	57163
	IV	2.41	0.87	5.62	64155	III	2.35	1.00	5.26	50441
2	I	2.51	0.76	5.11	62510	II	3.18	1.00	6.07	74473
	IV	2.75	0.87	5.74	71331	III	2.58	0.88	5.54	60175
3	I	2.71	0.80	5.66	65990	II	2.71	0.91	5.32	67068
	IV	2.53	0.90	7.21	71292	III	2.53	0.77	5.06	60479
4	I	2.22	0.75	4.67	52090	II	2.46	0.77	4.79	58099
	IV	2.27	0.68	5.13	59570	III	1.93	0.68	4.52	48123

Trial number	Index Force [N]									
	pos	mean	std	max	sum		mean	std	max	sum
1	I	2.20	0.76	4.44	57885	II	2.21	0.75	4.28	50542
	IV	2.50	0.91	5.31	66403	III	2.15	0.66	4.05	46085
2	I	2.33	0.66	4.57	57899	II	2.12	0.67	3.96	49712
	IV	2.25	0.65	4.33	58401	III	1.94	0.54	3.68	45357
3	I	2.10	0.60	3.83	51331	II	2.45	0.63	4.19	60689
	IV	2.15	0.66	3.90	60549	III	2.05	0.48	3.52	49067
4	I	2.00	0.60	3.65	46824	II	1.87	0.53	3.45	44236
	IV	1.86	0.51	3.38	48629	III	1.63	0.41	3.11	40565

Table 6.8: Basic statistics of Thumb, Index and Middle finger forces (4 writing positions for each of 4 trials): mean, standard deviation, maximum and sum of forces for subject 4.

### Sum of force values for subject 4

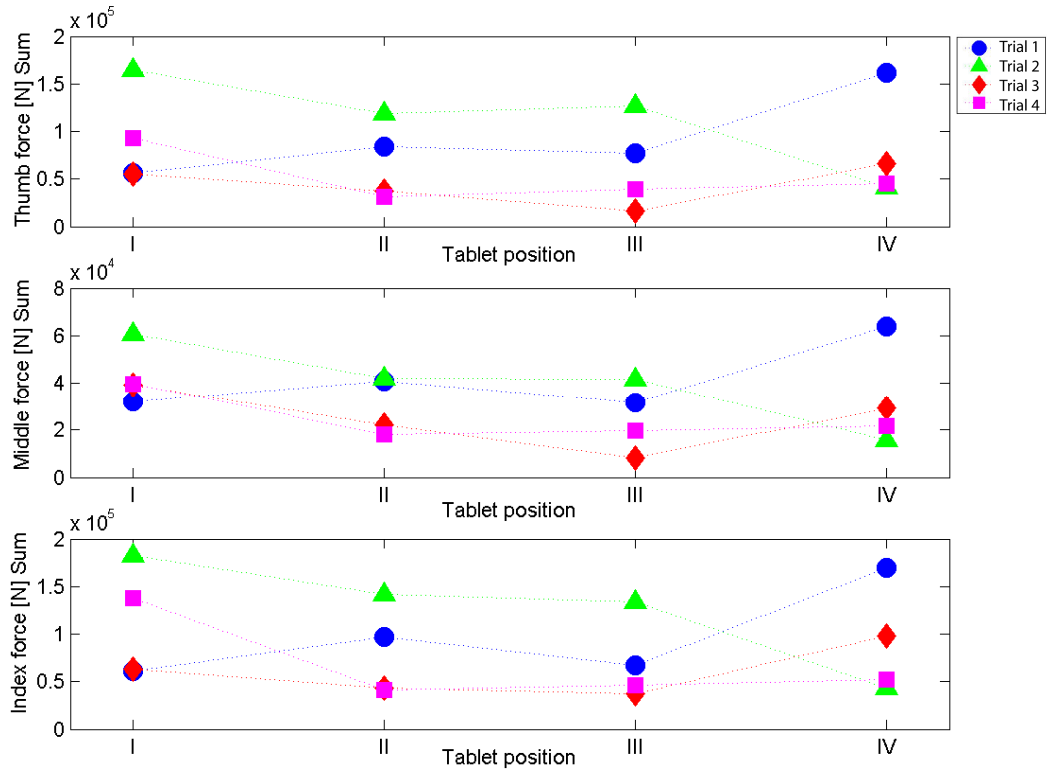


Fig.6.11: Sum of force values during the whole trial for Thumb, Index and Middle finger forces (4 writing positions for each of 4 repetitions of the trial) for subject 4.

RMS Force [N]	Position	Trial number			
		1	2	3	4
Thumb	I	1.7775	2.222	1.8848	1.2254
	II	1.4352	1.8087	1.9689	1.9332
	III	1.4014	2.0199	0.86817	2.0574
	IV	2.1842	2.2528	1.1241	2.0757
Middle	I	1.0106	1.0402	1.3677	0.6037
	II	0.77221	0.84786	1.1034	1.0717
	III	0.6264	0.76918	0.43339	0.97053
	IV	1.0665	0.87884	0.56206	0.90954
Index	I	1.8395	2.4283	1.9656	1.7145
	II	1.509	2.007	2.1924	2.4047
	III	1.2521	2.0034	1.798	2.3184
	IV	2.2469	2.3335	1.4139	2.4055

Table 6.9: Root Mean Square (RMS) values for Thumb, Index and Middle finger forces (4 writing positions for each of 4 trials) for subject 4.

### RMS force values for subject 4

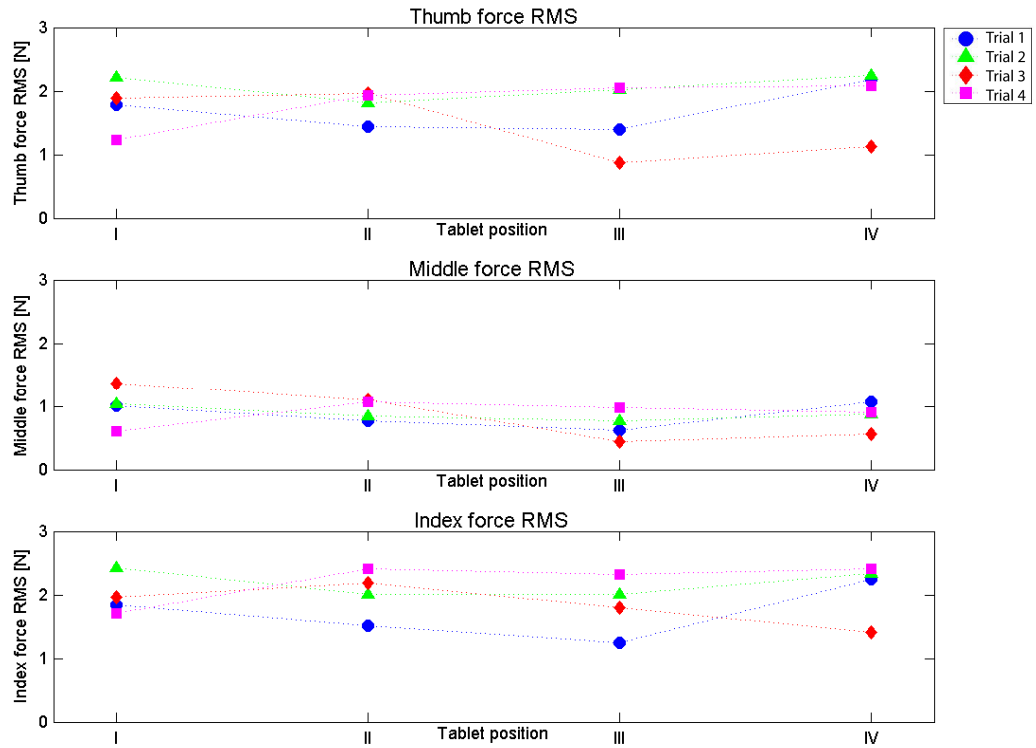


Fig. 6.12: Root Mean Square (RMS) values for Thumb, Index and Middle finger forces (4 writing positions for each of 4 trials) for subject 4.

### Power Spectral Density analysis for subject 4

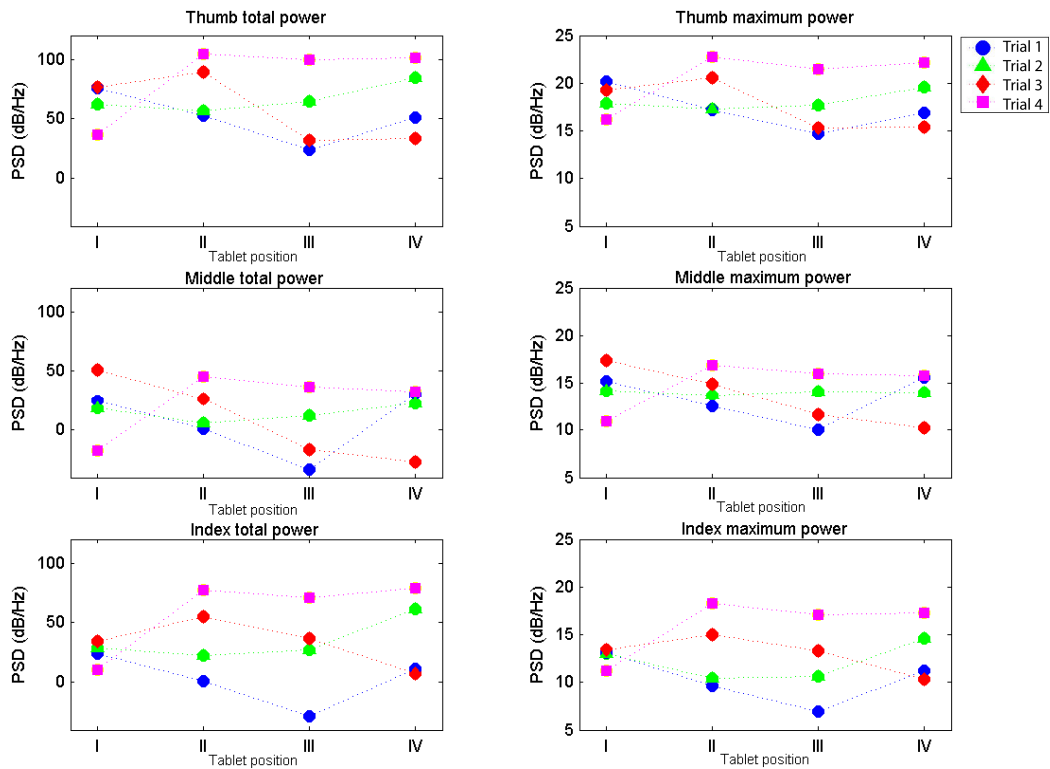


Fig. 6.13: Total and maximum power spectral density (PSD) values for Thumb, Index and Middle finger forces (4 writing positions for each of 4 trials) for subject 4.

Subjects	Finger forces [N]		
	Thumb	Middle finger	Index finger
Subject 1	0.84	0.76	0.56
Subject 2	4.04	4.56	3.59
Subject 3	4.73	2.51	2.11
Subject 4	1.44	0.67	1.70

Table 6.10: Average finger force over 4 trials and 4 tablet positions.

## 6.5 Results: Variations in measures of repeated word writing

### 6.5.1 Introduction

The features of script and script production process for the first and second writing of the word 'great' in one sentence are described for three subjects: Subject 1, 2 and 5 in respectively 6.5.2, 6.5.3 and 6.5.4. Data for one trial (out of four repetitions of the trial) is presented only. Each single experiment already shows all features in four tablet positions for each of the three subjects. For each subject individually a comparison will be made between the features of the writing processes of the first 'great' at the four different tablet positions. Then, a comparison will be made between the first and second writing of 'great' in the same sentence, looking both at the script (x-,y-coordinates) and the writing process. In 6.5.5 a comparison is made between writing performance of the three subjects 1, 2 and 5.

The following features are graphically shown for the first writing of 'great' and the second writing of 'great' in the trial, respectively:

- *x,y-coordinates;*
- *x-coordinates;*
- *y-coordinates;*
- *pressure applied to the pen by individual fingers: thumb, index and middle finger;*
- *resultant grip force;*
- *z-coordinates (pen tip pressure);*
- *trajectories of shoulder, elbow, wrist and pen tip in x,y-coordinate frame.*

Time [s]		Subject 1	Subject 2	Subject 5
position I	1st	2.3	1.9	2.6
	2nd	2.3	1.9	2.3
position II	1st	2.2	1.9	2.3
	2nd	2.2	1.8	2.0
position III	1st	2.4	1.8	2.3
	2nd	2.1	1.8	3.8
position IV	1st	3.1	2.0	2.2
	2nd	3.3	1.9	2.1

Table 6.11: Duration of writing first and second 'great' in four positions for subjects 1, 2 and 5.

## 6.5.2 Subject 1: Writing 'great' twice in 4 tablet positions

### 6.5.2.1 Subject 1: Comparing writing features of '1st great' in 4 positions.

#### ***Timing for subject 1***

The duration of writing the first 'great' differs in all four writing positions as can be seen from table 6.11. The second trial (position II, duration 2.2s) is written slightly faster than the first trial (position I, duration 2.3s). The third and fourth trial (position III and IV, duration 2.4 and 3.1) have longest duration.

#### ***Script for subject 1***

The writing of the first 'great' in the four positions are shown in Fig. 6.14. The shape of all letters is variable for the four positions. Overall, the script is not very constant and shows quite a bit of variability of all letters within one position and between positions. It is doubtful if the four trials could actually be recognised as one person's handwriting.

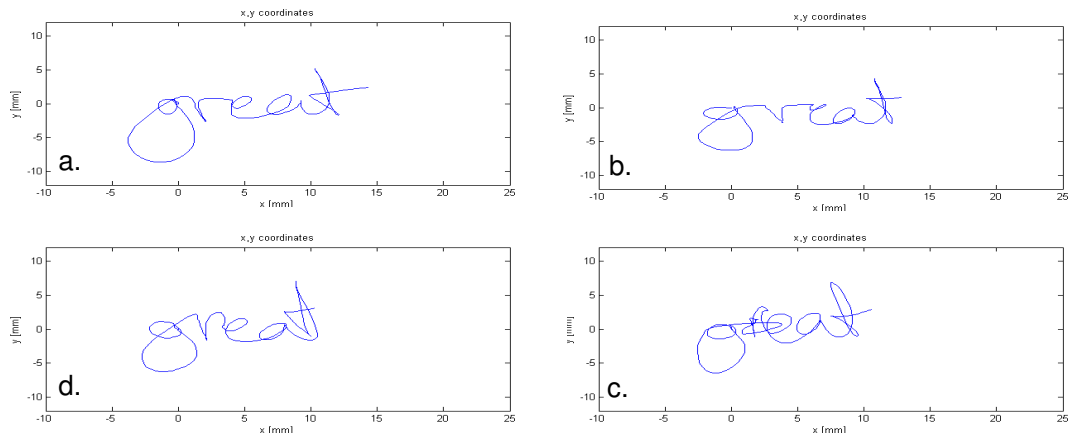


*Fig.6.14: Script of writing the 1st 'great' in the four tablet positions:*

*a: position I;*

*b: position II;*

*c: position III;*

*d: position IV.*

*Little consistency between letters and script in four different tablet positions is seen.*

## Trajectories for subject 1

The trajectories vary between trials (Fig.6.15). For position II, III and IV, horizontal wrist movement and wrist rotation play a crucial role and there is very little involvement of shoulder and elbow. The shoulder and elbow just seem to position the lower arm for excursion. For trial I, there is more horizontal wrist movement and there is also shoulder movement involved.

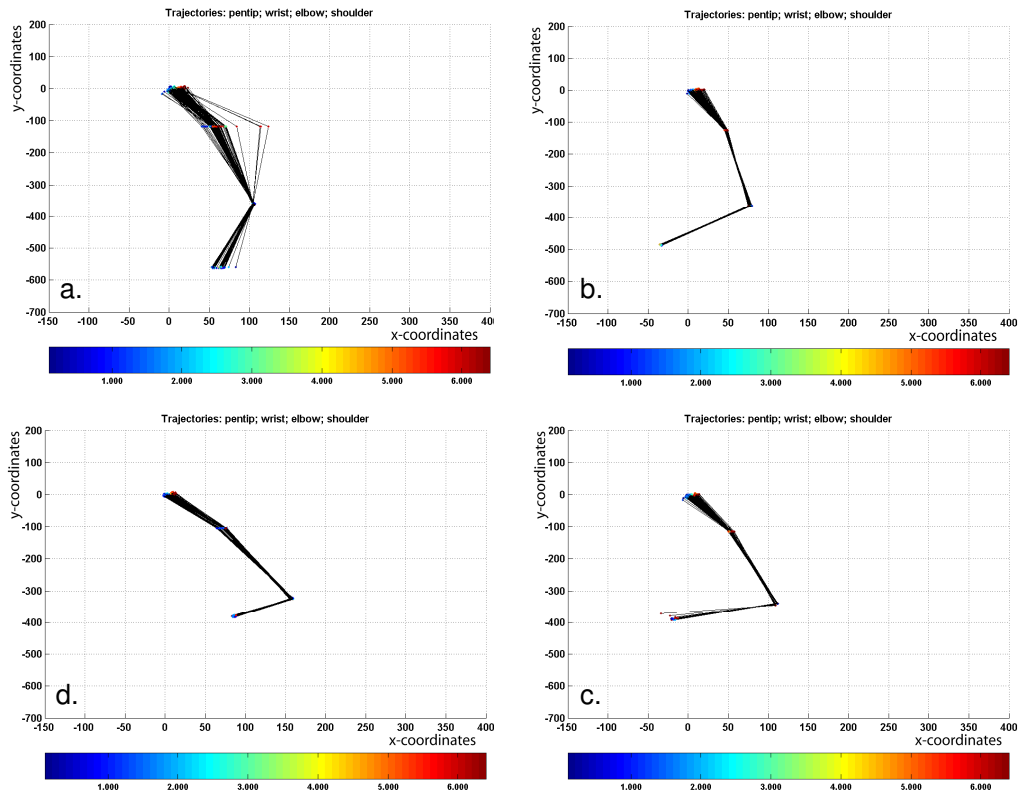


Fig.6.15: Trajectories of Shoulder, Elbow, Wrist and pen Tip while writing the 1st 'great' in the four tablet positions:

- a: position I;
- b: position II;
- c: position III;
- d: position IV.

Wrist translation and rotation plays an important role. For positions II, III and IV the shoulder and elbow mainly performs a function for positioning of the forearm.

### **Pen grip force for subject 1**

The grip force levels stay below 4N for subject 1 (Fig.6.16). The modulation patterns appear similar in time, particularly for position II and III, but the amplitude varies between trials.

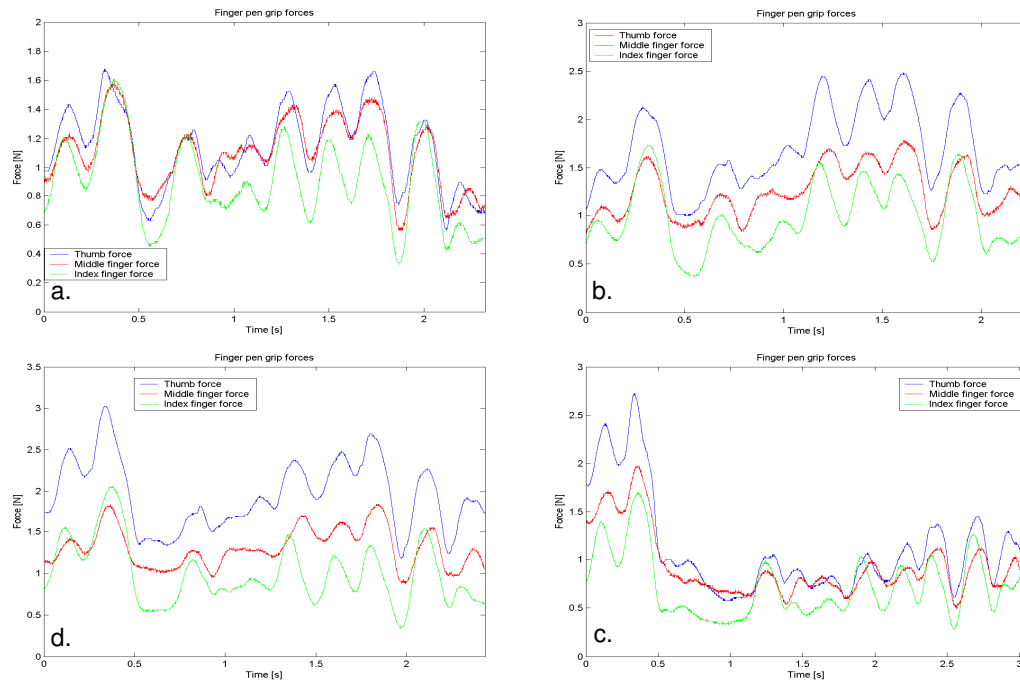


*Fig. 6.16: Thumb, Middle and Index finger forces while writing the 1st 'great' in the four tablet positions:*

*a: position I;*

*b: position II;*

*c: position III;*

*d: position IV.*

*The grip force patterns resemble strongly, but the amplitude varies between trials.*

### **Script and x- and y-coordinates for subject 1**

The resultant grip force patterns for the four trials differ (Fig.6.17). Most resemblance can be seen between the resultant pen grip force patterns in positions II and III. The resultant pen grip forces vary around zero for all four positions, which illustrates the up- and downward movement by the fingers.

The rotational orientation of the pen in the horizontal plane relative to the base line of writing (that is determined by finger positioning during tripod pen grip) differs for

position I relative to the other three positions. This is shown as a projection of the triangular pen shaft onto the resultant grip force drawing in the upper right corner of the figures.

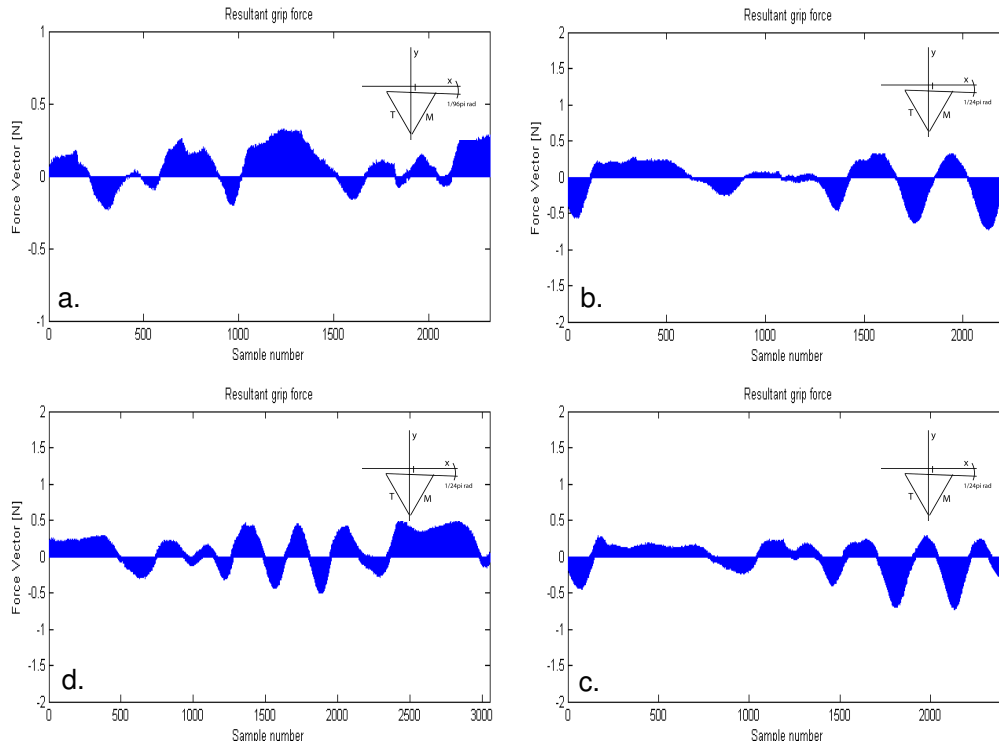


Fig. 6.17: Resultant pen grip forces while writing the 1st 'great' in the four tablet positions:

a: position I;

b: position II;

c: position III;

d: position IV.

The resultant grip forces strongly vary between trials. The resultant pen grip force in positions II and III resemble to some extent. The resultant grip forces show varying up- and downward finger force in all positions. The orientation of the pen shaft (see project in upper right corners of the graphs) is different for position I than for the other three positions.

### Discussion for subject 1

Both the script and the writing process differ. The script shows variability of letters within one tablet position and between positions. There is much variation between the writing processes, described by finger pen grip forces and shoulder, elbow, wrist and pen tip coordinates. Characteristic of this subject is the low force level, relative

to other subjects, which does not seem to positively or negatively affect the person's ability to balance and steer the pen. The force patterns reflect the fingers' contribution to script production by moving the pen tip in (positive/negative) vertical direction, while maintaining a stable grip.

#### 6.5.2.2 Comparing writing features for 1st and 2nd 'great' for subject 1

##### ***Script and x- and y-coordinates for subject 1***

The only obvious and constant difference between the script of first and second 'great' is that the first 'great' is written with a slight incline compared to the writing line: the vertical slants in the letter 'r' and the letter 't' are not placed under a right (90°) angle with the writing line. The second 'great' is placed in a more upright position as can be seen from the letters 'r' and 't'. This can be seen for writing in all four positions, but is most obvious in positions I, II and III.

No other clear and constant difference in script quality and writing technique can be seen between the first and second 'great' in one sentence.

##### ***Writing production for subject 1***

For trial III, the writing velocity is higher for writing the second than for writing the first 'great' with durations of respectively 2.1 and 2.4 seconds. For position IV, the writing velocity is higher for writing the first than for writing the second 'great' (Table 6.11) with durations of respectively 3.1 and 3.3 seconds. For positions I and II, the writing velocity is equal while writing the first and second 'great' (Table 6.11). It is concluded that the writing velocity does not reflect the position in the sentence (whether first or second 'great' is created).

The strategy used to create both first and second 'great' varies and the strategy does not reflect the position in the sentence as can be seen from the joint trajectories in Fig.6.20 and 6.21. For example, there is more horizontal (positive x-direction) wrist movement involved for the second 'great' in position II and III, but this does not yield for position I and IV. For position I, there is wrist movement involved for both writings of 'great'. For position IV, there actually is more wrist movement

involved for writing the first 'great', whereas for the second 'great', there is only wrist rotation involved. The tablet position does not have a direct effect on the script production process and the consequent joint trajectories.

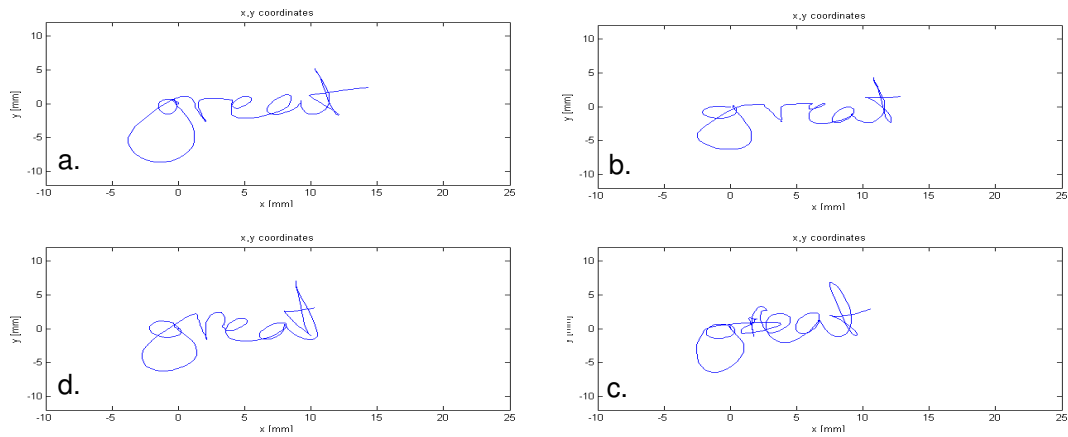


*Fig.6.18: Script of writing the 1st 'great' in the four tablet positions:*

- a: position I;*
- b: position II;*
- c: position III;*
- d: position IV.*

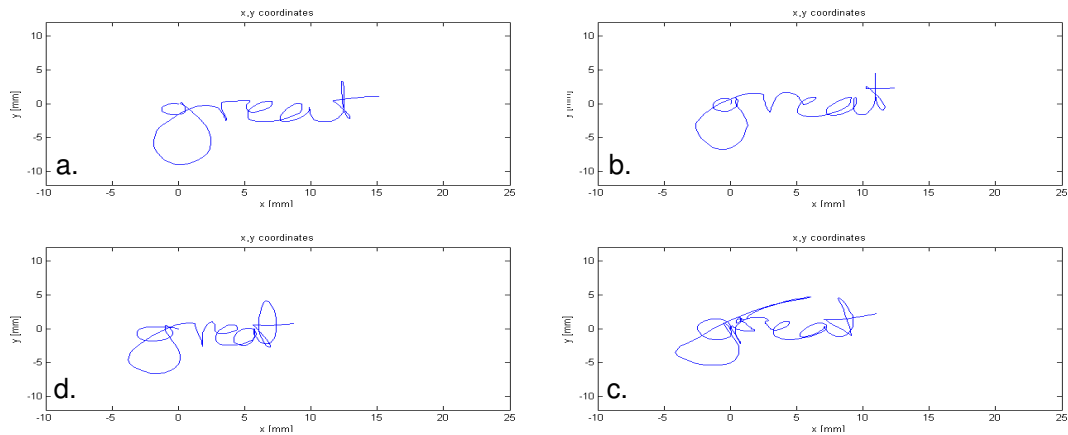


*Fig.6.19: Script of writing the 2nd 'great' in the four tablet positions:*

- a: position I;*
- b: position II;*
- c: position III;*
- d: position IV.*

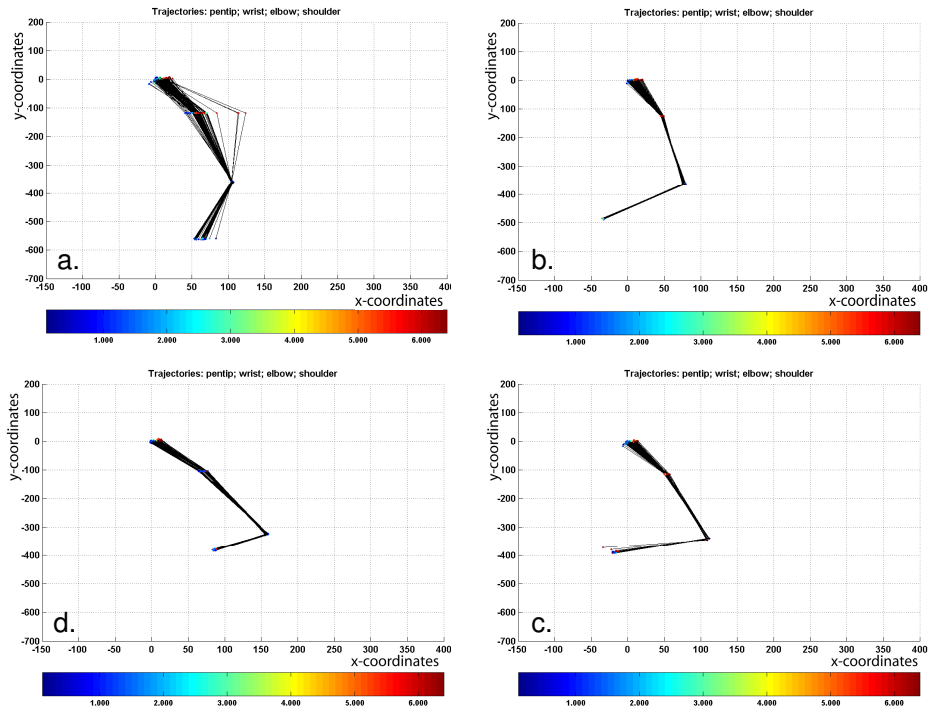


Fig.6.20: Trajectories of Shoulder, Elbow, Wrist and pen Tip while writing the 1st 'great' in the four tablet positions: a: position I; b: position II; c: position III; d: position IV.

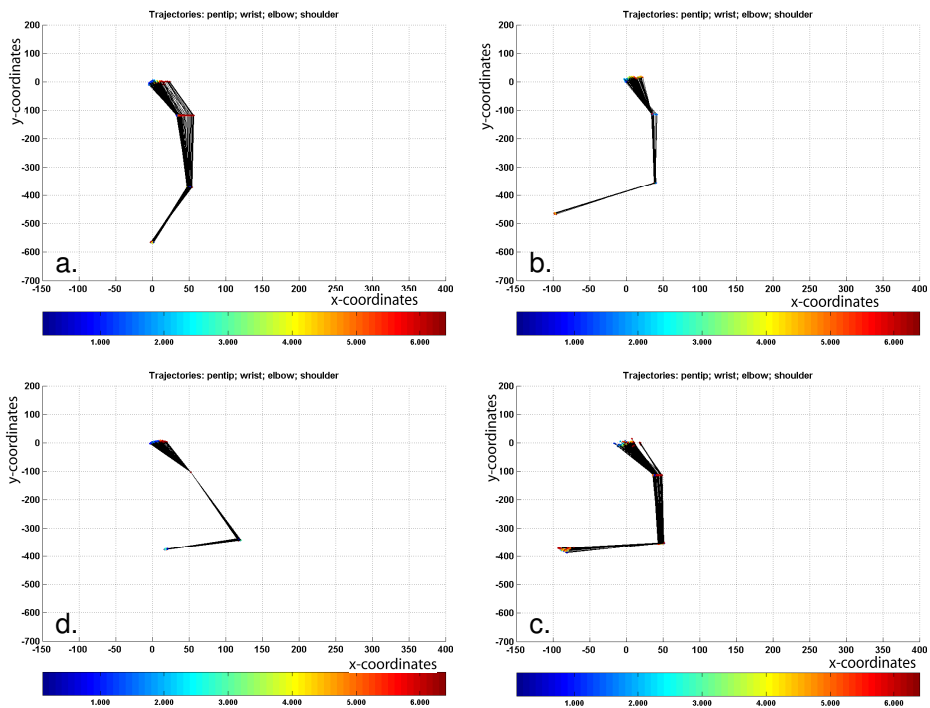


Fig.6.21: Trajectories of Shoulder, Elbow, Wrist and pen Tip while writing the 2nd 'great' in the four tablet positions: a: position I; b: position II; c: position III; d: position IV.

### 6.5.3 Subject 2: Writing 'great' twice in 4 tablet positions

#### 6.5.3.1 Comparing writing features of 1st 'great' in 4 positions

##### **Timing for subject 2**

There is not much variation in the duration of writing all four trials. Table 6.11 shows the following durations for positions I, II, III and IV, respectively: 1.9s, 1.9s, 1.8s, 2.0s. In addition, writing of the first and second 'great' in three positions have equal duration, but in position IV there is a difference of 0.10 seconds between writing of first and second great. Taking into account the timing inaccuracies while sampling script due to ScriptAlyzer as explained in 4.3.5, it can be concluded the differences in timing are not significant.

##### **Script for subject 2**

The script produced by subject 2 contains many characteristics that are constant for each of the four positions as can be seen from script and x-,y-coordinates in Fig.6.22. Only the letter 't' exhibits a lot of variation.

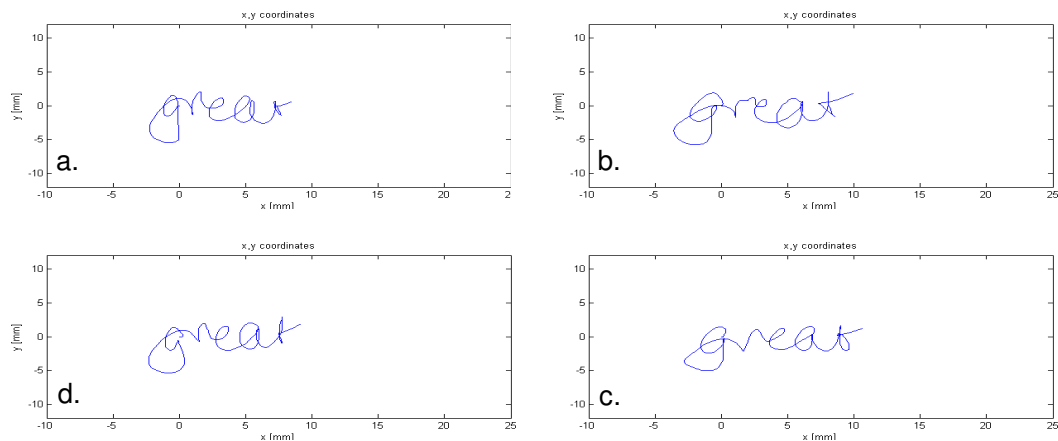


*Fig.6.22: Script of writing the 1st 'great' in the four tablet positions:*

*a: position I;*

*b: position II;*

*c: position III;*

*d: position IV.*

*The script in four different tablet positions is very consistent and can be recognised as one's characteristic script.*

## Trajectories for subject 2

In these trials wrist rotation plays a crucial role in the writing process (Fig. 6.23). In addition, for positions II and IV some horizontal wrist translation can be observed. There is very little involvement of shoulder and elbow. Shoulder and elbow appear to position the wrist and hand to enable wrist and finger excursion.

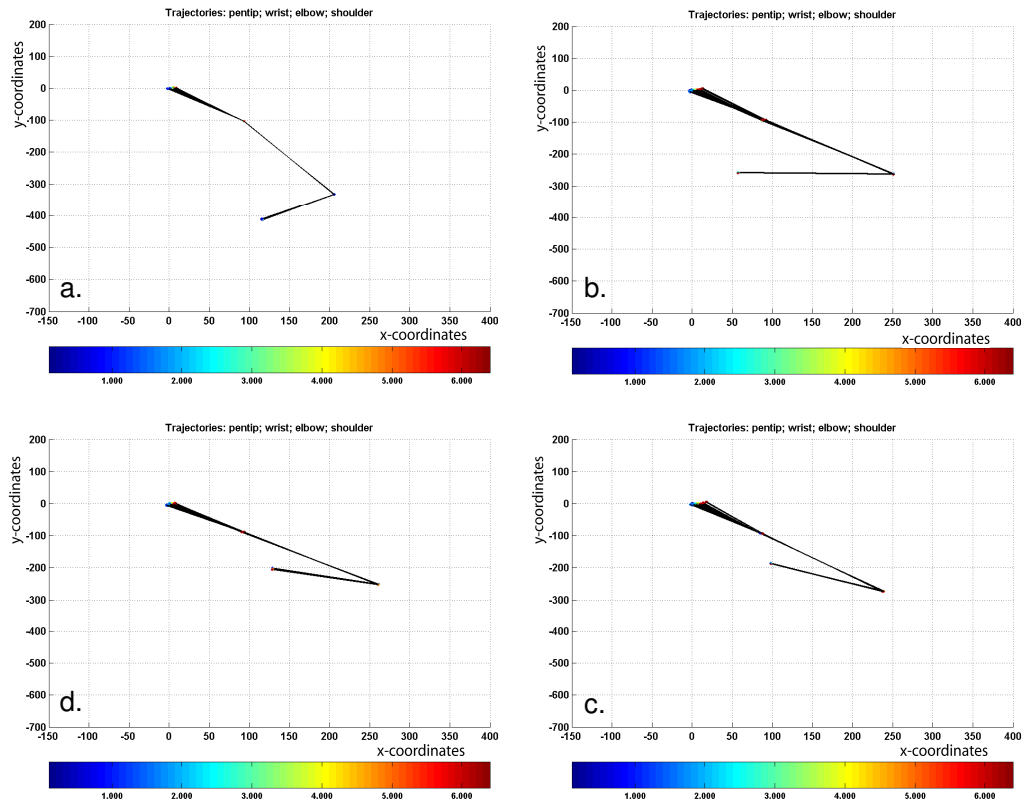


Fig.6.23: Trajectories of Shoulder, Elbow, Wrist and pen Tip while writing the 1st 'great' in the four tablet positions:

- a: position I;
- b: position II;
- c: position III;
- d: position IV.

Wrist rotation plays an important role in the writing process. The shoulder and elbow mainly performs a function for positioning of the forearm.

## Pen grip force for subject 2

Pen grip finger force patterns appear consistent. The amplitude is also very similar among the trials as can be seen in Fig.6.24. In Fig.6.25 it can be seen that resultant grip force patterns, particular between position I, III and IV in the second half of the writing are also reasonably stable.

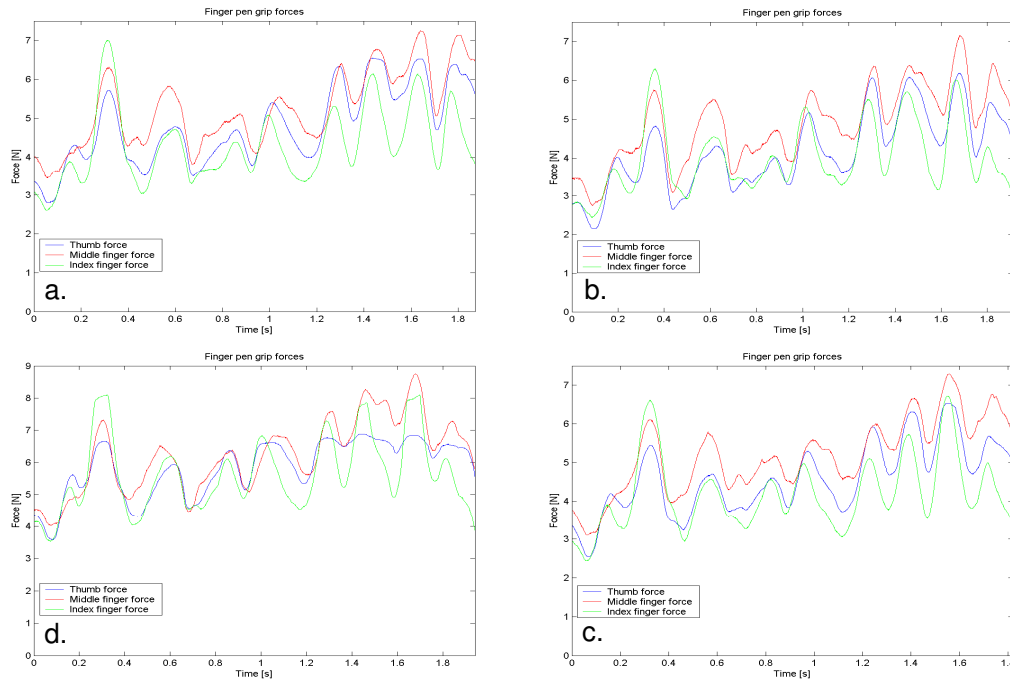


Fig. 6.24: Thumb, Middle and Index finger forces while writing the 1st 'great' in the four tablet positions:

a: position I;

b: position II;

c: position III;

d: position IV.

The grip force patterns resemble strongly, but the amplitude varies between trials.

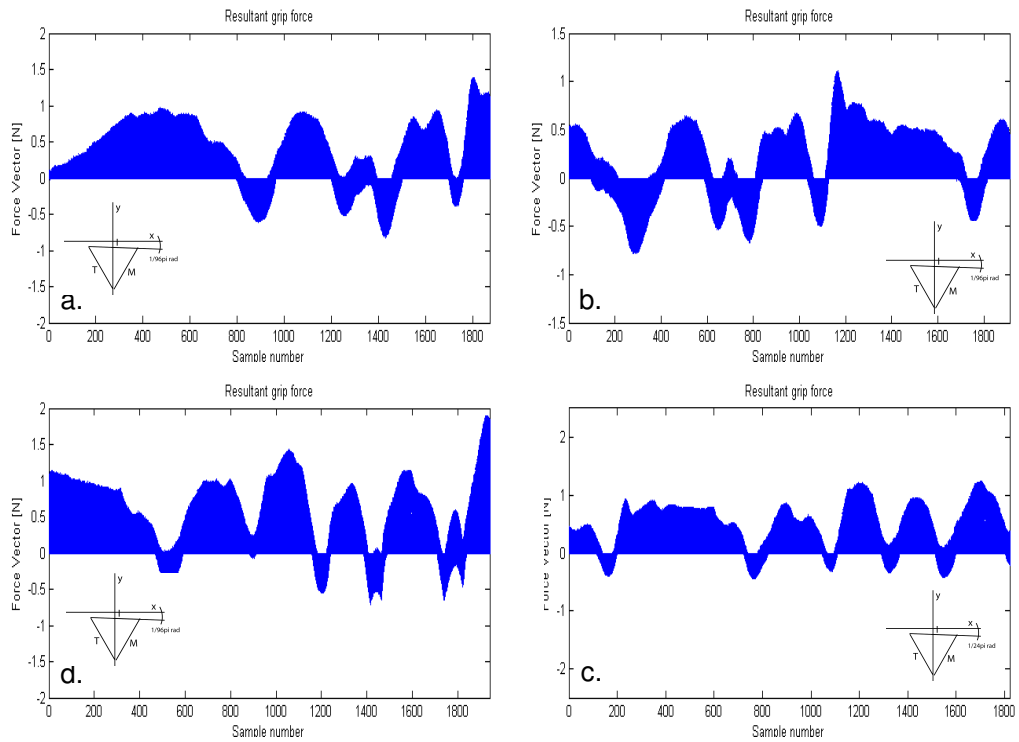


*Fig. 6.25: Resultant pen grip forces while writing the 1st 'great' in the four tablet positions:*

*a: position I, angle of triangular pen cross section with horizontal (writing direction)*

*$1/96\pi$  rad;*

*b: position II, angle of triangular pen cross section with horizontal (writing direction)*

*$1/96\pi$  rad;*

*c: position III, angle of triangular pen cross section with horizontal (writing direction)*

*$1/24\pi$  rad;*

*d: position IV, angle of triangular pen cross section with horizontal (writing direction)*

*$1/96\pi$  rad.*

### **Discussion for subject 2**

It can be said that handwriting production by subject 2 is very constant for each of the four positions as can be seen from script and x-,y-coordinates, timing, finger pressure and trajectories.

### 6.5.3.2 Comparing writing features for 1st and 2nd 'great' for subject 2

#### ***Script and x- and y-coordinates for subject 2***

There are no clear distinctions between coordinates and script quality for the first and second 'great' in the sentence, as can be concluded from a comparison between Fig.6.26 and Fig.6.27. The variation between the first and second script for 'great' in one sentence do not relate to the position in the sentence.

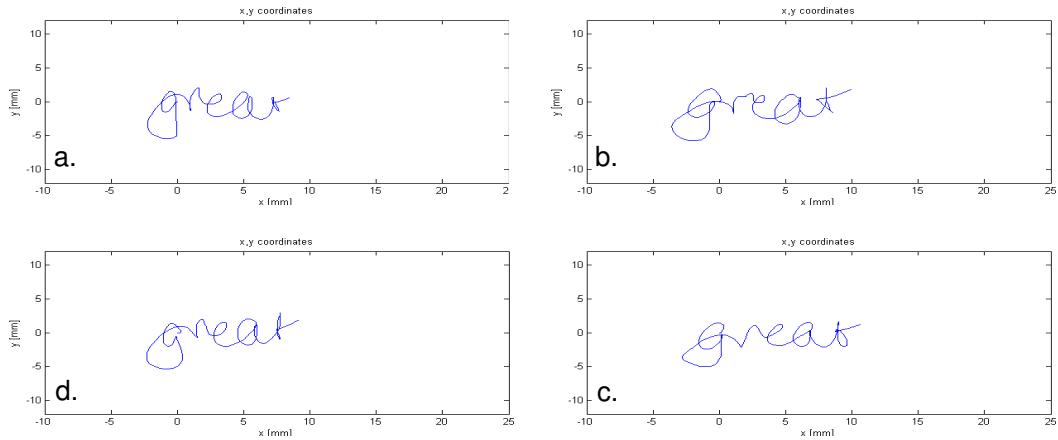


*Fig.6.26: Script of writing the 1st 'great' in the four tablet positions:*

*a: position I; b: position II; c: position III; d: position IV.*

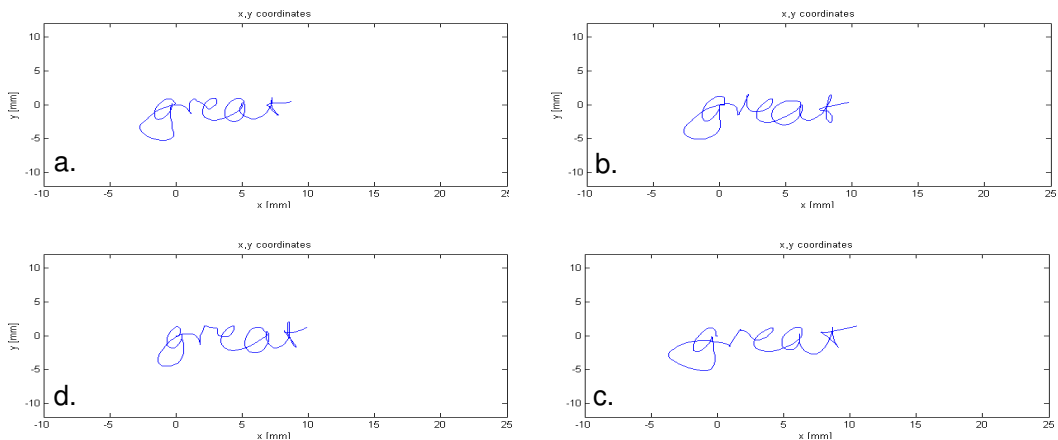


*Fig.6.27: Script of writing the 2nd 'great' in the four tablet positions:*

*a: position I; b: position II; c: position III; d: position IV.*

## ***Writing production for subject 2***

For position I, the writing velocity is higher for writing the first than for writing the second 'great' (Fig.6.11). For the other three trials, the writing velocity is higher for writing the second than for writing the first 'great'. There is no obvious relation between writing velocity and writing position.

The resultant pen grip forces in the four tablet positions for writing the first and second 'great' are shown in Fig. 6.28 and 6.29. In addition, for writing the 2nd 'great' in tablet positions II, III and IV, the angle between the horizontal of the pen cross sectional area and the writing direction is  $1/24\pi$  rad, whereas for position I, the angle between the horizontal of the pen cross sectional area and the writing direction is  $1/96\pi$  rad. From the joint trajectories in Fig.6.30 and Fig.6.31 it can be seen that while writing the second 'great' for position II, III and IV, there is more wrist rotation and less wrist translation involved than for position I. It may be concluded that the wrist rotation has an effect on the pen orientation as seen from the angle between the horizontal of the pen cross sectional area and the writing direction. For writing the first 'great' in position III, the pen orientation is different from the other positions. The pen rotational orientation in the horizontal plane for positions I, II and IV is  $1/96\pi$  rad (angle between the horizontal of the pen cross sectional area and the writing direction), while the pen orientation in position III is  $1/24\pi$  rad. The larger angle for position III is expected to be an effect of a larger wrist rotation angle than in the other three positions.

The fact that the angle between the horizontal of the pen cross sectional area and the writing direction is  $1/24\pi$  rad for three out of two tablet positions for writing the *second* 'great', while the angle is  $1/96\pi$  for for two out of three tablet positions for writing the *first* 'great' cannot be explained by increased wrist rotation towards the end of the sentence (Compare Fig. 6.30 and 6.31). It is more likely that in addition to wrist rotation the fingers also enable to rotate the pen relative the wrist. It is possible to rotate the pen around its centre by changing the finger forces while maintaining a stable wrist position. Perhaps this mechanism might explain why the resultant grip force patterns look so different.

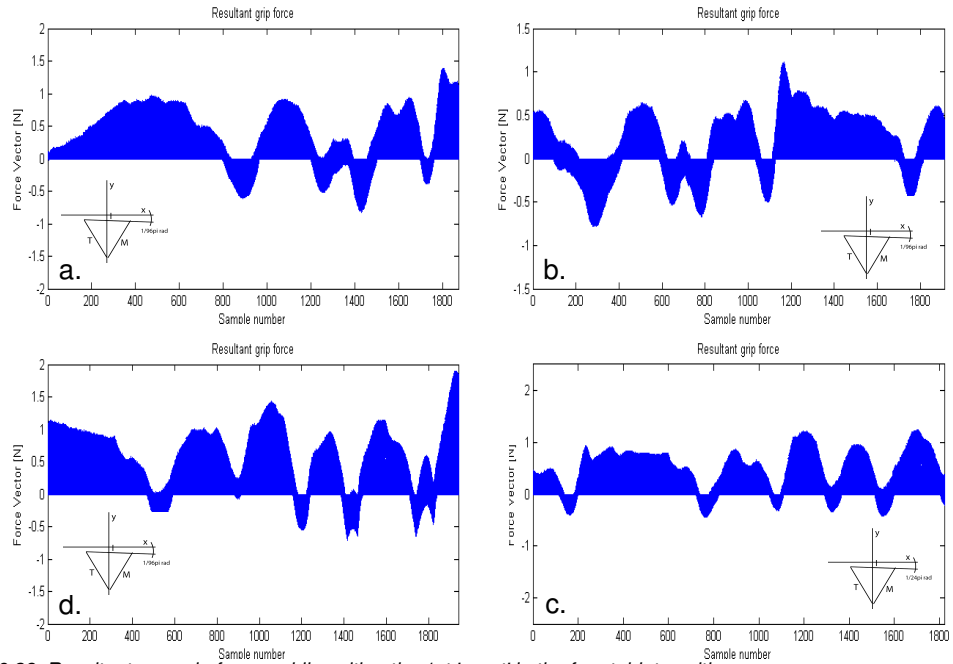


Fig. 6.28: Resultant pen grip forces while writing the 1st 'great' in the four tablet positions:

- a: position I, angle of triangular pen cross section with horizontal (writing direction)  $1/96\pi$  rad;
- b: position II, angle of triangular pen cross section with horizontal (writing direction)  $1/96\pi$  rad;
- c: position III, angle of triangular pen cross section with horizontal (writing direction)  $1/24\pi$  rad;
- d: position IV, angle of triangular pen cross section with horizontal (writing direction)  $1/96\pi$  rad.

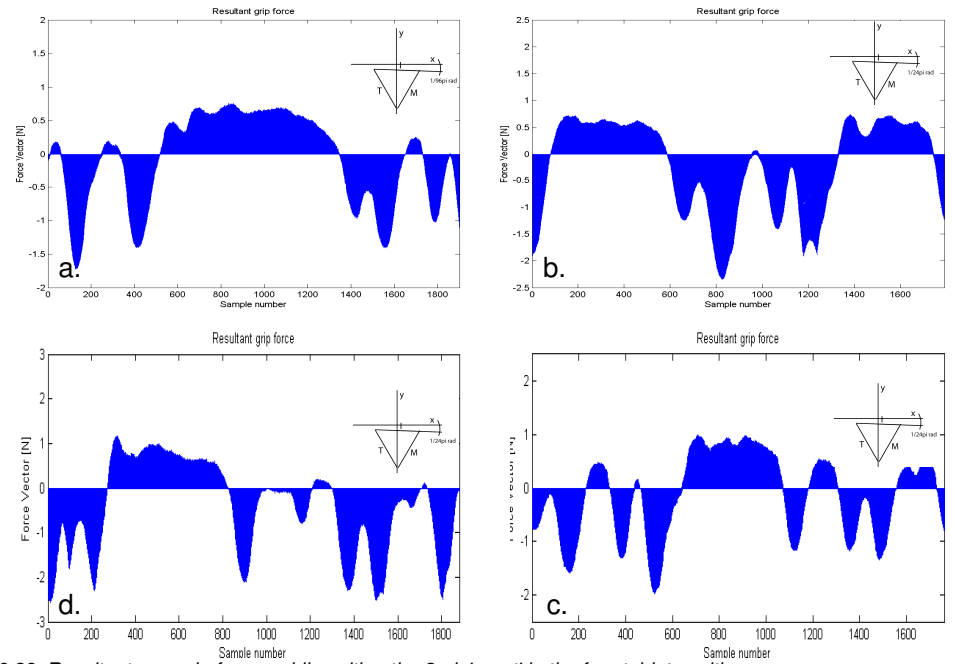


Fig. 6.29: Resultant pen grip forces while writing the 2nd 'great' in the four tablet positions:

- a: position I, angle of triangular pen cross section with horizontal (writing direction)  $1/96\pi$  rad;
- b: position II, angle of triangular pen cross section with horizontal (writing direction)  $1/24\pi$  rad;
- c: position III, angle of triangular pen cross section with horizontal (writing direction)  $1/24\pi$  rad;
- d: position IV, angle of triangular pen cross section with horizontal (writing direction)  $1/24\pi$  rad.

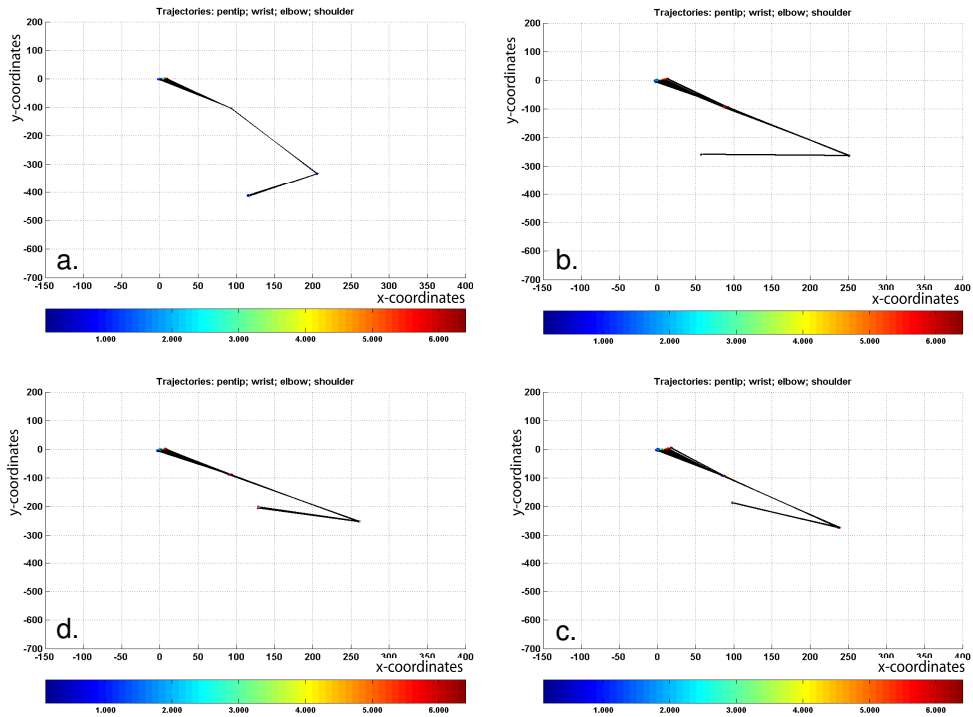


Fig.6.30: Trajectories of Shoulder, Elbow, Wrist and pen tip while writing the 1st 'great' in the four tablet positions: a: position I; b: position II; c: position III; d: position IV.

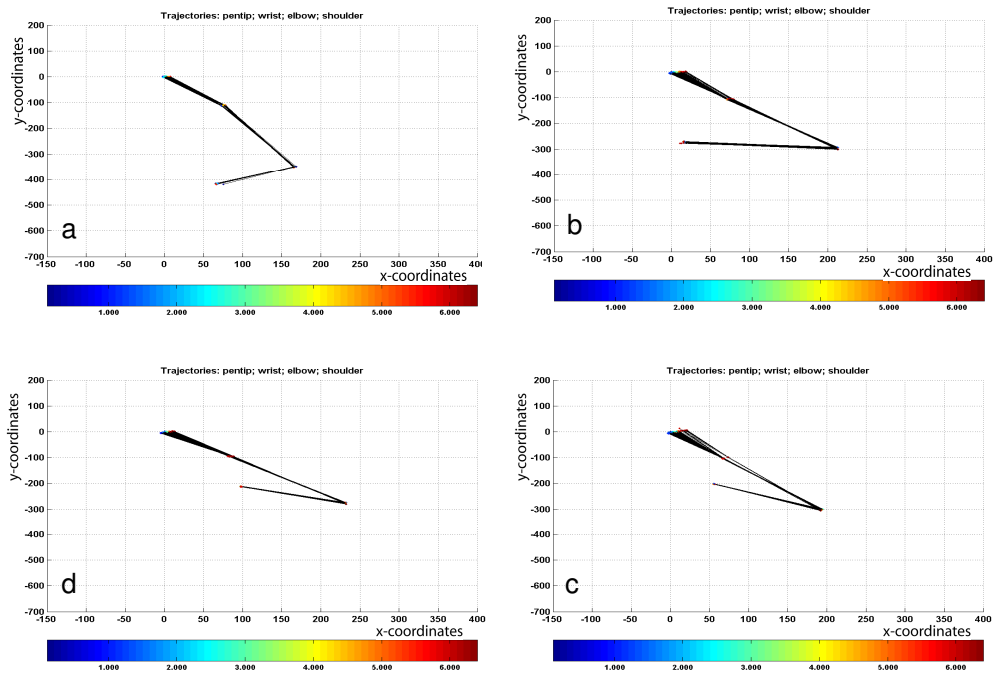


Fig.6.31: Trajectories of Shoulder, Elbow, Wrist and pen tip while writing the 1st 'great' in the four tablet positions: a: position I; b: position II; c: position III; d: position IV.

## 6.5.4 Subject 5: Writing 'great' twice in 4 tablet positions

### 6.5.4.1 Comparing writing features of 4 positions for subject 5

#### **Timing for subject 5**

There is variation in the duration of writing the first 'great' in the four tablet positions (Table 6.11). The writing velocity increases slightly from tablet position I to tablet position IV as follows: position I, duration: 2.6s; position II, duration: 2.3s; position III, duration: 2.3s and position IV, duration: 2.2s.

#### **Script for subject 5**

The script produced by subject 5 contains many characteristics that are repeated in each of the four positions as can be seen from the script x-,y-coordinates in Fig.6.32. The incline of the letters varies and the loops of the letters 'g', 'e' and 'a' vary in size, although the shapes of the letters are often close to identical.

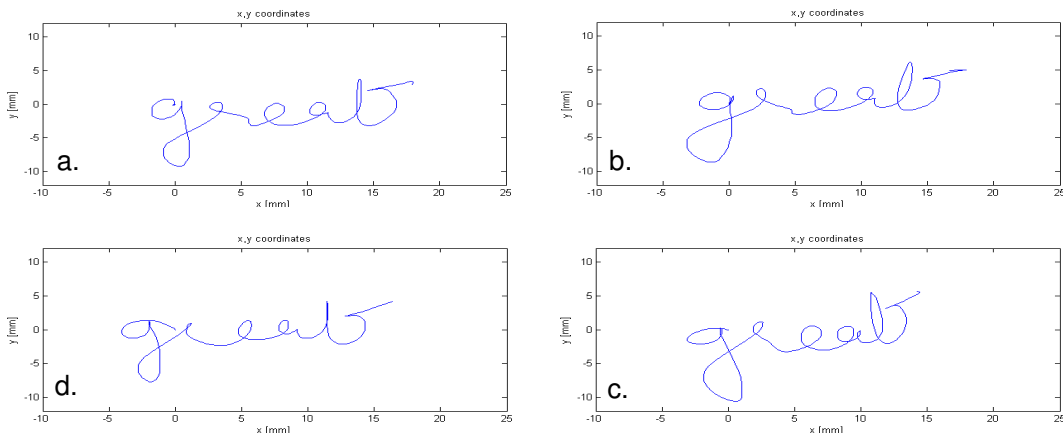


*Fig.6.32: Script of writing the 1st 'great' in the four tablet positions:*

*a: position I;*

*b: position II;*

*c: position III;*

*d: position IV.*

*The shapes of the letters in four different tablet positions is very consistent, but the size varies strongly.*

## Trajectories for subject 5

Particular wrist translation in the horizontal plane plays a crucial role in the writing process (Fig. 6.33). In addition, some wrist rotation can be observed from the fact that the pen tip trajectories are larger than the wrist trajectories for at least part of the task. In Fig. 6.33b for the tablet position II, the connection lines between wrist and pen tip that make up the stick figure of the arm, reveal that the horizontal line drawn by the pen tip can be produced by both linear wrist movement (seen from single connection lines between wrist and pen tip) and wrist rotation (seen from the triangular shaped area of overlapping lines that originate from the same point on the wrist trajectory).

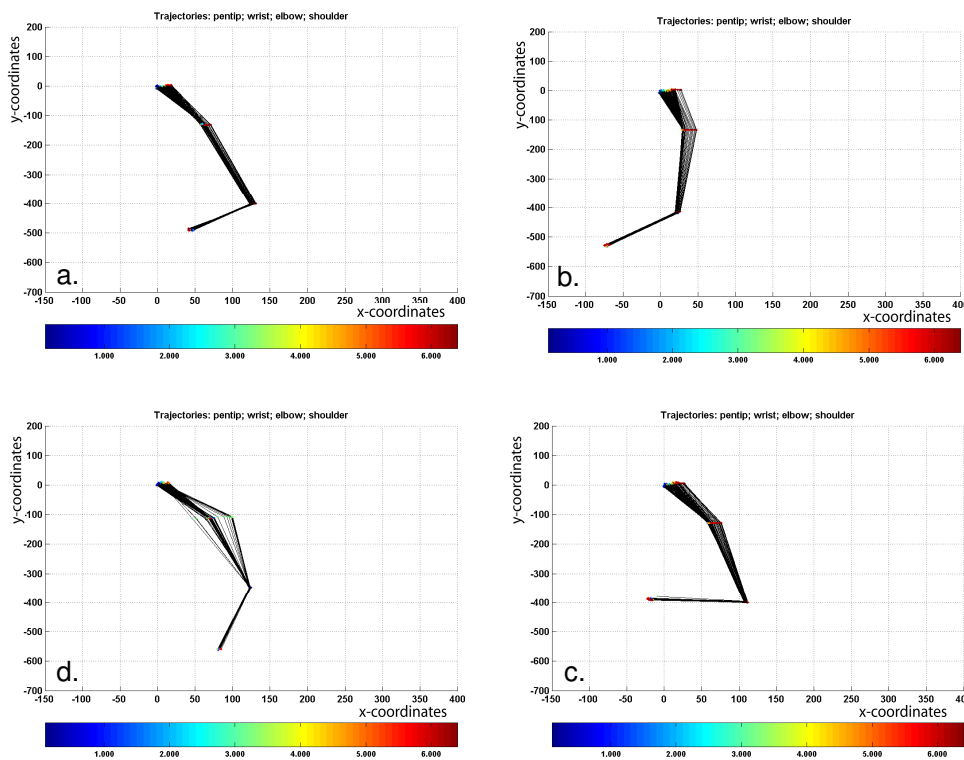


Fig.6.33: Trajectories of Shoulder, Elbow, Wrist and pen Tip while writing the 1st 'great' in the four tablet positions:

a: position I;

b: position II;

c: position III;

d: position IV. Wrist rotation plays an important role in the writing process. The Elbow contributes to a lesser extent. The shoulder mainly performs a function for positioning of the forearm.

There is involvement of the elbow in writing positions I, II and III, while the shoulder just seems to position the arm to enable the execution of elbow, wrist and hand joint movements.

### ***Pen grip force for subject 5***

Pen grip finger force patterns for subject 5 can be seen in Fig.6.34. The force patterns and amplitude are very similar for tablet positions I, II and III. However, for tablet position IV the amplitude of the thumb force (blue line) and middle finger force (red line in Fig.6.34d), is quite different from what was observed for other tablet positions. For tablet position IV, the middle finger force values are much higher than the thumb finger force values, whereas for other tablet positions it is the other way around. For position IV, the similarity of the thumb force to the pattern of the middle finger force seems more obvious than for the other three positions. Fig.6.32 shows that the script for tablet position IV also differs from the other positions. Most obvious is that the loops of the letters 'e' and 'a' are smaller for position IV. In addition, Fig.6.33 shows different involvement of the wrist for position IV. There is more lateral movement, which seems slightly erratic with jumps from one position to the next. In Fig.6.25 it can be seen that resultant pressure patterns are very different for all four positions.

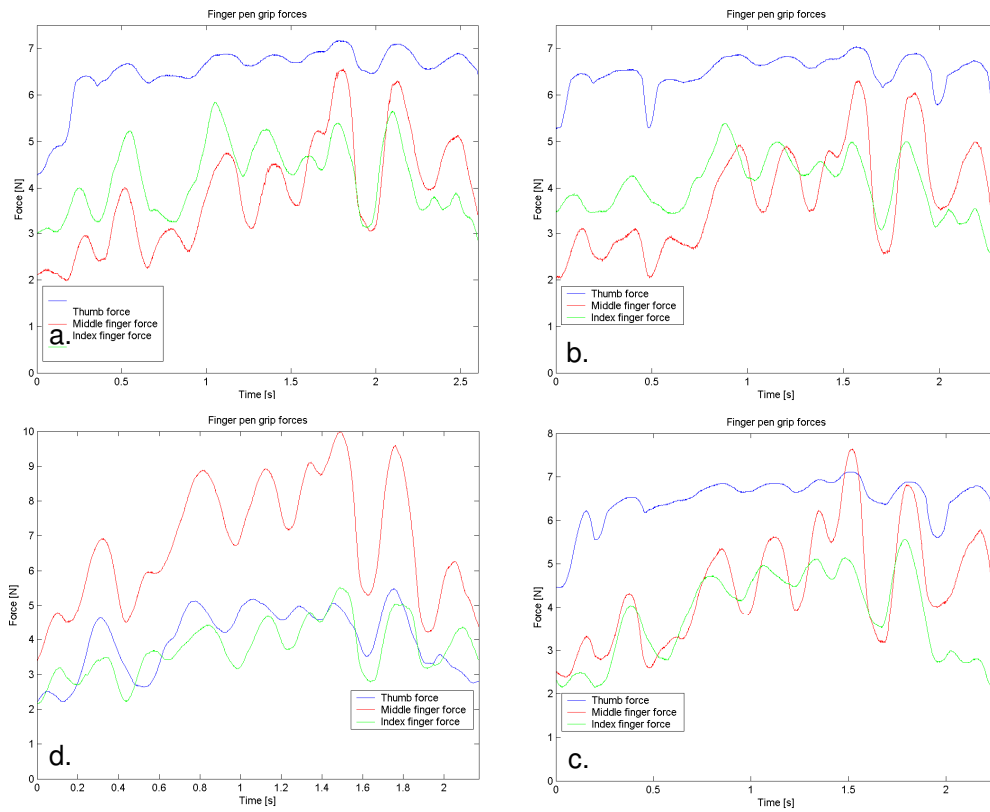


*Fig. 6.34: Thumb, Middle and Index finger forces while writing the 1st 'great' in the four tablet positions:*

*a: position I;*

*b: position II;*

*c: position III;*

*d: position IV. The grip force patterns resemble strongly, but the amplitude varies between trials.*

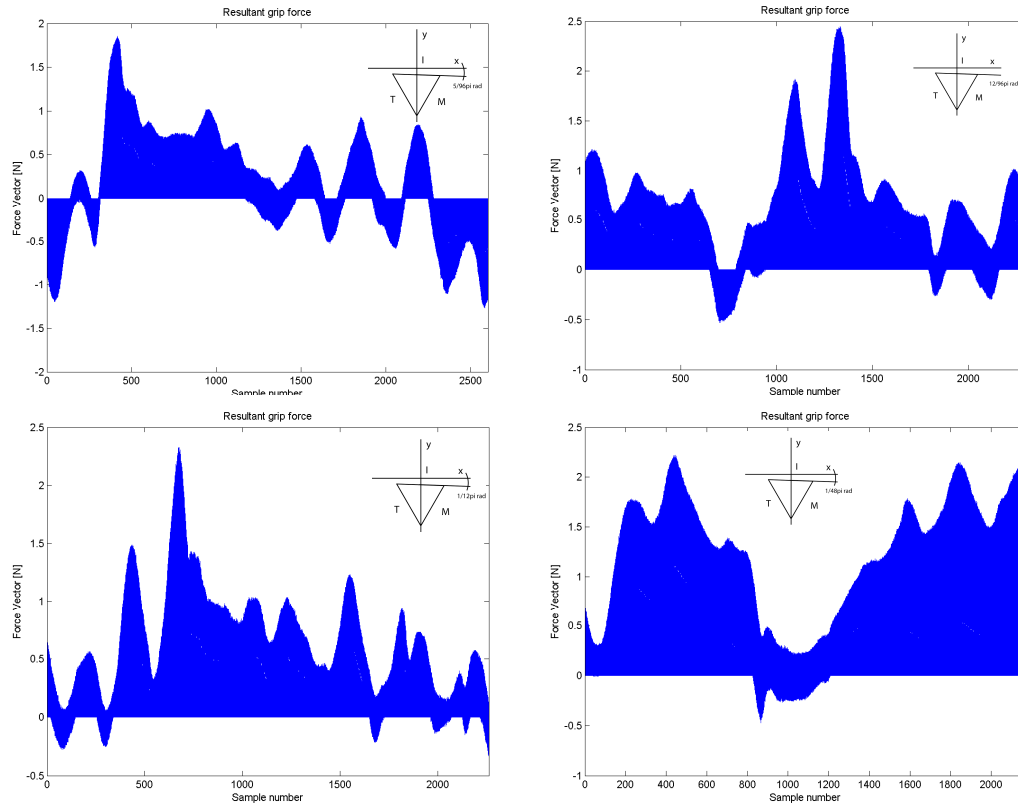


*Fig. 6.35: Resultant pen grip forces while writing the 1st 'great' in the four tablet positions:  
a: position I, angle of triangular pen cross section with horizontal (writing direction)  $5/96\pi$  rad;  
b: position II, angle of triangular pen cross section with horizontal (writing direction)  $12/96\pi$  rad;  
c: position III, angle of triangular pen cross section with horizontal (writing direction)  $1/48\pi$  rad;  
d: position IV, angle of triangular pen cross section with horizontal (writing direction)  $1/12\pi$  rad.*

### Discussion for subject 5

The script produced in the four tablet positions by subject 5 are very similar with only slight differences between positions (Fig.6.31). The biggest difference is observed for position IV compared to the other three positions. However, looking at the mechanical features of script production, it becomes clear that the mechanics actually are very different and far more different than one might anticipate based on the resulting script. The middle finger force values (blue line) are much higher than the thumb force values (red line) in Fig.6.34, whereas for other tablet positions it is the other way around. The thumb force pattern also resembles the pattern of the middle finger force more clearly than for the other three positions. In addition, the wrist seems more involved for position IV (Fig.6.33).

One might suggest that the slight differences between the produced scripts directly relate to the differences in force patterns. However, the production of script is more complicated.

As an example, it can be seen in trial for position II that at time  $t=0.5s$  there is an obvious trough in thumb force when the pen tip  $y$ -coordinates reach the lowest value (Fig.6.37). In the experiment for position I, however, this trough in thumb force cannot be found at lowest value for tip  $y$ -coordinates (Fig.6.36), despite of the pen tip describing a similar curve at bottom of the 'g' and the middle and index finger forces being very similar in the two trials (Fig.32, 36 and 37).

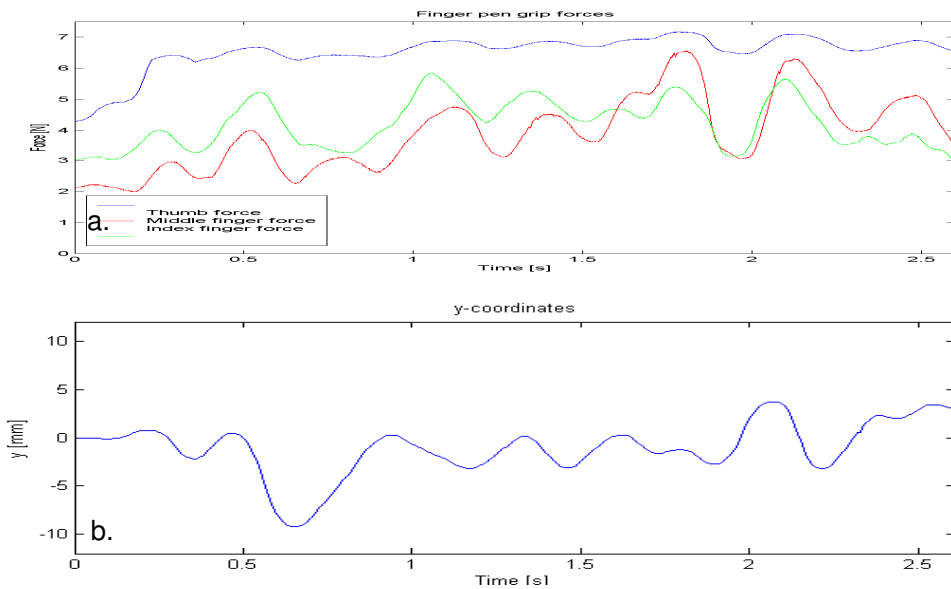


Fig.6.36: Tablet position I: a.: Finger forces and b.:  $y$ -coordinates.

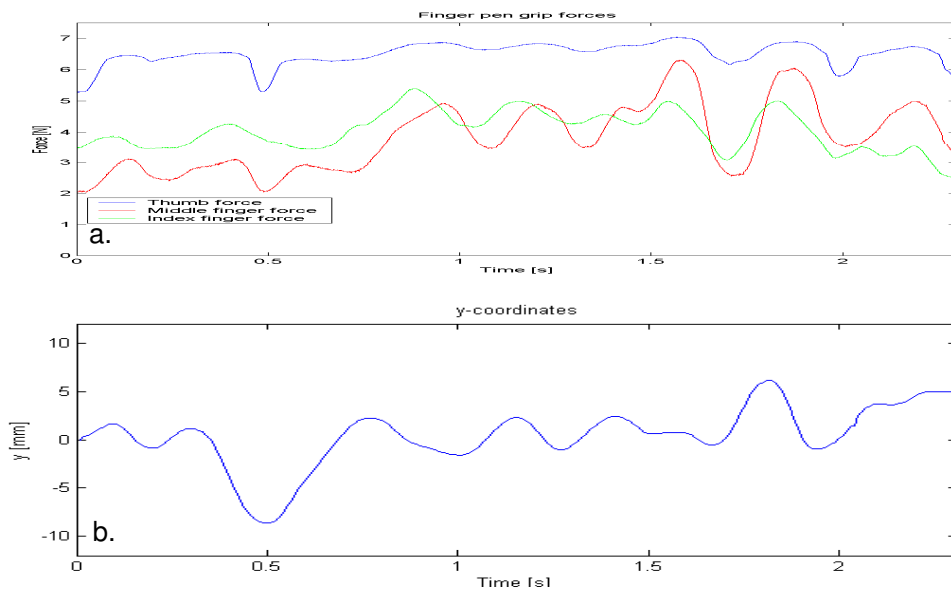


Fig.6.37: Tablet position II: a.: Finger forces and b.: y-coordinates.

The difference might be explained from constraints, imposed by the overall hand-arm mechanism that moves the pen and determines orientation and incline of the pen. Further analysis of the pen orientation is required to fully understand the process.

The following speculation may explain the observed mechanics. At times it might be the fingers only that move the pen in vertical (y-) direction, whereas at the next instant, it might be the limb only while the fingers just ensure a stable grip. As the pen incline changes, gravity will have more or less effect on the pen and in order to maintain the balance of the pen, finger forces need to be adapted. This may be a reason for the observed dip in thumb force. In addition, there are four contact points with the pen and only the three points where major pressure modulation takes place are measured. The fourth point will have an effect that is unknown at present, but which is likely to give support to the pen over a large part the writing trajectory and therefore affect the resultant grip force.

Also, changing orientation of the pen will also require a different strategy to steer the pen in a certain direction. For example, rotating the pen around its vertical (z) axis while dragging the pen in an upward direction, will require adapting finger forces to keep steering the pen in upward direction.

These measures underline the flexibility and redundancy in the coordination of the pen tip. Very different biomechanical processes enable to produce a script that is very similar. In both trials all building blocks of the neuromuscular system involved

with the production of writing work in a coordinated fashion, but in a completely different way to nevertheless produce an almost equal end result.

#### 6.5.4.2 Comparing writing features for 1st and 2nd 'great' for subject 5.

##### **Script and x- and y-coordinates**

The script coordinates are shown in Fig. 6.38. The only obvious and constant difference between the script of first and second 'great' is that the loop in the letter 't' is larger for the second 'great' in all four writing positions. No other clear and constant difference in script quality and writing technique can be seen between the first and second 'great' in one sentence.

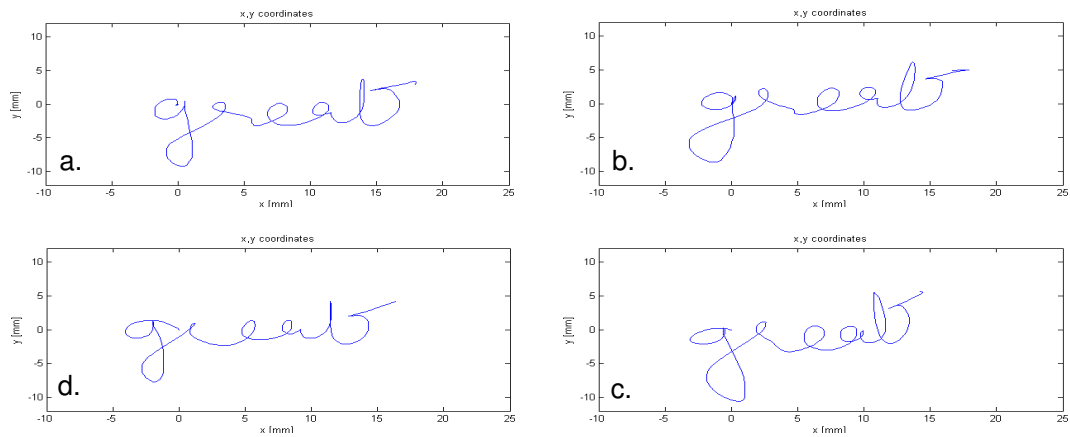


*Fig.6.38: Script of writing the 1st 'great' in the four tablet positions by subject 5:*

*a: position I; b: position II; c: position III; d: position IV.*

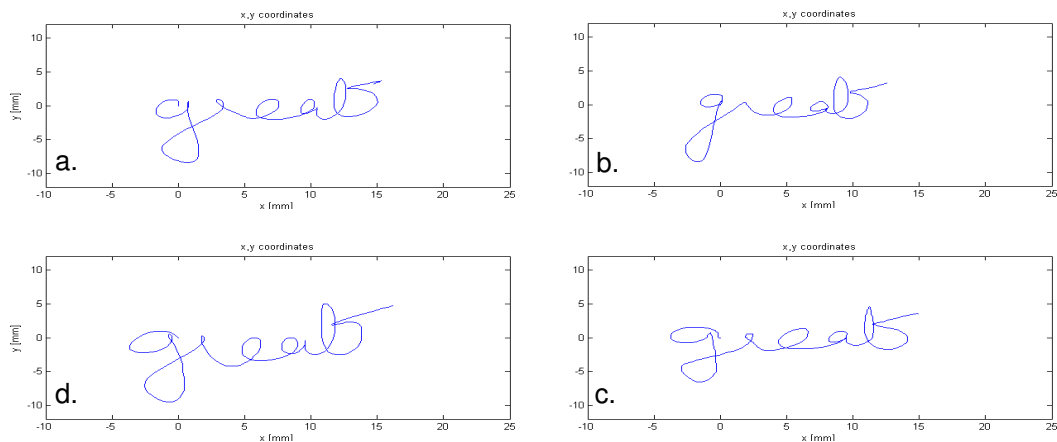


*Fig.6.39: Script of writing the 2nd 'great' in the four tablet positions by subject 5:*

*a: position I; b: position II; c: position III; d: position IV.*

### ***Writing production***

There is variation in the duration of writing 'great' twice in the four trials (Table 6.11). More specifically, for writing in tablet positions I, II and IV, writing the first 'great' is performed slightly faster than writing the second 'great'. The differences between the first and second 'great' for tablet positions I, II and IV respectively are: 0.3s; 0.3s and 0.1s. However, for tablet position III, writing the second 'great' is performed much slower and takes 3.8 s compared to 2.3 seconds for the first 'great'. The duration of writing the second 'great' in the positions I, II and IV are 2.3, 2.0 and 2.1 respectively. No relation between tablet position or order in the sentence and the writing velocity is seen here.

The resultant pen grip forces in the four tablet positions for writing the first and second 'great' are shown in Fig. 6.40 and 6.41. It may be concluded from the resultant grip patterns that the way the pen and hand interact even differs between the same words that are written within one sentence. Interestingly, the pen rotational orientation angle (between the pen cross section and the writing line) increases with lateral progression in every experiment. The angles shown in Fig.6.41 are larger than the angles shown in Fig.6.42. This is what one might expect, given that lateral pen tip motion is established by controlling the joint torques that enable rotational motions around the joints. Most of the lateral progression seems to originate from elbow rotation and combined rotation and translation of the wrist (Fig.6.42 and 6.43). Therefore, it is not surprising that with progressed lateral pen tip movement (from first to second writing of 'great'), there is increased rotation around the wrist joint and increased angle between the pen cross sectional area and the writing line (Fig.6.41). Interestingly, the resultant pen grip force for positions III and IV on the lower end of the tablet (Fig. 6.41c and d) only have positive values. This was not observed yet. A plausible explanation is that while the pen is held by the thumb, index and middle finger, the pressure exerted by both thumb against the index finger and the fourth contact point (at the upper half of the pen) may provide a stable grip that is laterally orientated relative to the wrist. The resultant force at the gripping area of the pen then does not directly relate to the up- and downward pen motion over the paper (perpendicular to the writing direction). The up- and downward pen motion could be established by more wrist rotation around the axis through the wrist, directed in the writing direction.

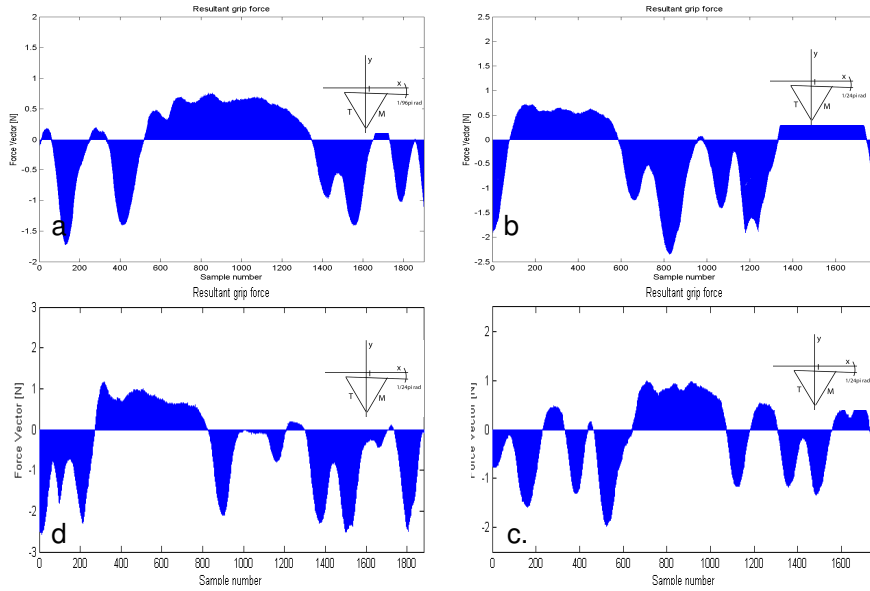


Fig. 6.40: Resultant pen grip forces while writing the 1st 'great' in the four tablet positions by subject 5:

- a: position I, angle of triangular pen cross section with horizontal (writing direction)  $1/96\pi$  rad;
- b: position II, angle of triangular pen cross section with horizontal (writing direction)  $1/24\pi$  rad;
- c: position III, angle of triangular pen cross section with horizontal (writing direction)  $1/24\pi$  rad;
- d: position IV, angle of triangular pen cross section with horizontal (writing direction)  $1/24\pi$  rad.

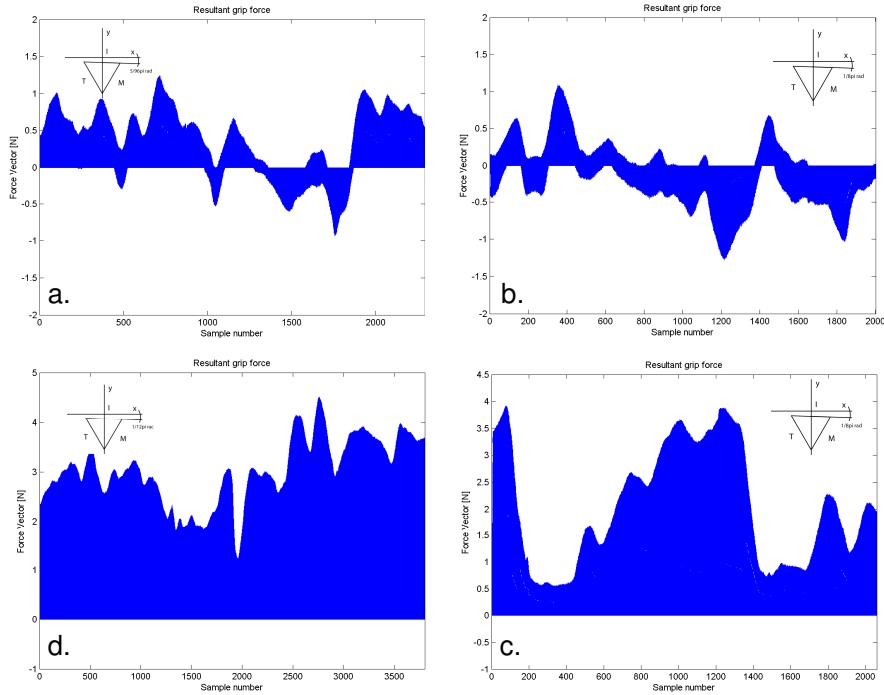


Fig. 6.41: Resultant pen grip forces while writing the 2nd 'great' in the four tablet positions by subject 5:

- a: position I, angle of triangular pen cross section with horizontal (writing direction)  $5/96\pi$  rad;
- b: position II, angle of triangular pen cross section with horizontal (writing direction)  $1/8\pi$  rad;
- c: position III, angle of triangular pen cross section with horizontal (writing direction)  $1/8\pi$  rad;
- d: position IV, angle of triangular pen cross section with horizontal (writing direction)  $1/12\pi$  rad.

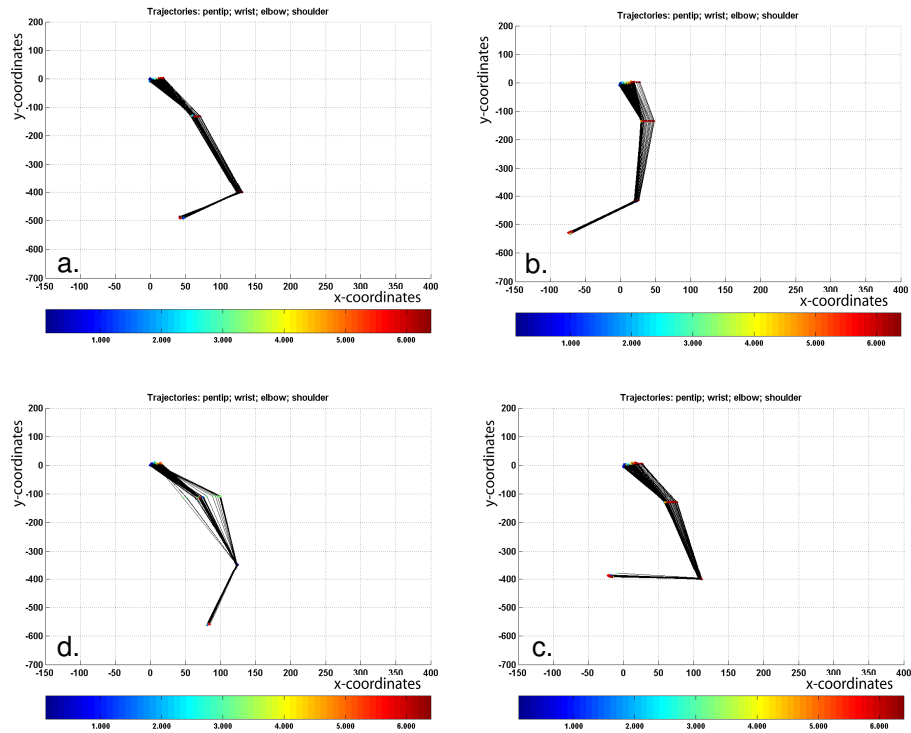


Fig.6.42: Trajectories of shoulder, elbow, wrist and pen tip while writing the 1st 'great' in the four tablet positions by subject 5: a: position I; b: position II; c: position III; d: position IV.

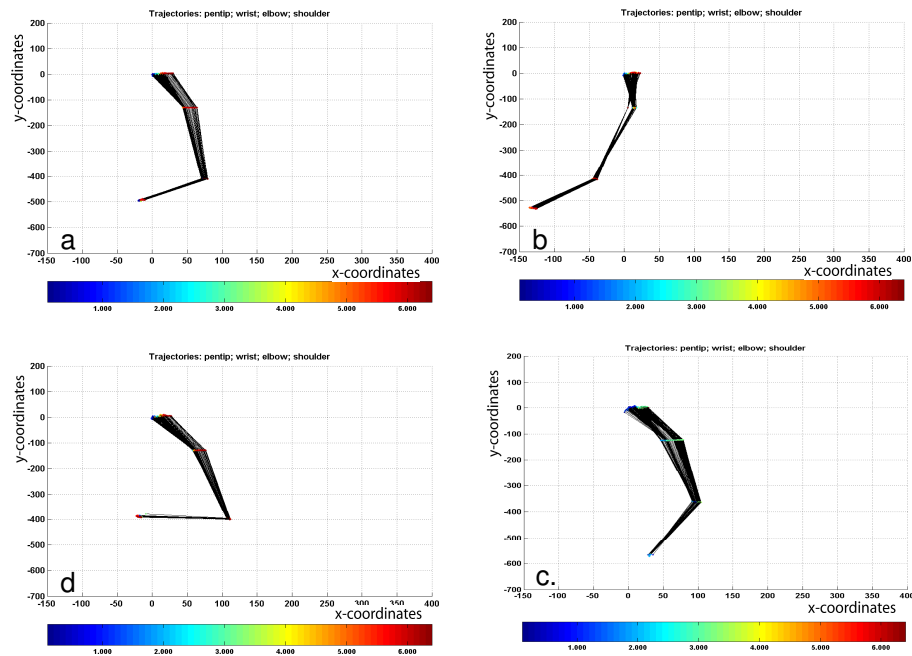


Fig.6.43: Trajectories of shoulder, elbow, wrist and pen tip while writing the 2nd 'great' in the four tablet positions by subject 5: a: position I; b: position II; c: position III; d: position IV.

### 6.5.5 Comparison subjects 1, 2 and 5 and conclusion.

The first obvious conclusion from comparing the x,y-coordinates of the three subjects (Fig.6.14; 2.33 and 6.32) is that Subject 2 and 5 show a more 'characteristic' handwriting than subject 1, which is more variable and therefore seems to have less repetitive characteristics.

Subject 2 shows very repetitive biomechanical processes. The duration of the script, the limb joint movement, the pattern and amplitude of finger forces are all very similar in each tablet position and each trial (including four positions). On the other hand, subjects 1 and 5 show more variation.

For subject 2 a stronger similarity is seen than for subjects 1 and 5 in limb activities to establish lateral progression in every trial. Therefore, one might suggest that for subject 2 the differences between force patterns relate more directly to the differences in produced script. Perhaps, as a result of the more constant lateral movement (compared to subject 1), less adaption of pen grip by the fingers is required. Pen incline, orientation and differences in produced script should then relate more directly to the small differences in force pattern in each trial. However, at current stage these thoughts remain speculations.

No direct relation was found between the tablet position and the writing process or duration of the writing for any of the three subjects. The writing location does not seem to have a specific effect on the resulting script.

It was concluded that for all three subjects, based on the resultant grip patterns that the way the pen and hand interact differs when the same word is produced within a sentence.

In addition, the rotational pen orientation angle (between the pen cross section and the writing line) was found to increase with lateral progression in every experiment. (e.g. Fig.6.41 and Fig.6.42). The most plausible explanation is that lateral pen tip motion is established by rotational motions around the limb joints (Some shoulder rotation, particular elbow rotation and combined rotation and translation of the wrist, e.g. Fig.6.42 and 6.43).

The discussion on biomechanical aspects of handwriting production for the three subjects, including joint trajectories, pen finger grip and script, illustrates that no two

trials performed by one subject share an identical writing process, not even when the writing results are (nearly) identical. The neuromuscular control apparatus is highly flexible and works in a coordinated fashion that allows the production of a nearly equal end result, but by means of different mechanical and therefore neuromuscular processes.

## **7 Spiral Drawing**

This chapter reports a preliminary study that was performed to investigate the potential for using the grip force measuring pen for investigating neurological deterioration associated with aging or disease. The study focused on tremor severity measurement by means of combining spiral drawing with grip force measurement. The background of tremor measurement is first of all described in 7.1. The background leads to the description of experimental methods for assessing spiral drawing activities: the experiment activity in 7.2; data collection and processing in 7.3 and subjects in 7.4. The results are presented in 7.5.

### **7.1 Background**

Tremor severity measurement and recording takes an important place in the process of movement disorder diagnosing, treatment management and planning of surgical intervention for impairments such as Parkinson's disease, multiple sclerosis and essential tremor. Moreover, assessing tremor is essential for elucidating the underlying disorders.

There are a number of ways of visualising tremor severity that reflect the effect of tremor on patient's everyday lives. In clinical methods, such as scaling rate, as described by Bain and Findley (1993) and the Unified Parkinson Disease Rating Scale (Fahn et al, 1987), a score is given by a rater, who decides for each of the tremor forms (rest, postural and intentions) at specific anatomical sites. Tremor is scaled as mild, moderate or severe and can also be numerically rated. The advantage of such tests is that they are relatively simple and available to everyone. However, they require experience and are not quantitative and repeatable as instrumental methods (Rudzínska et al, 2007).

Spiral drawing is particularly interesting because tremor is more obvious in drawing spirals than in handwriting assessments and spiral drawing involves both proximal and distal joints.

It used to be common practice to rate tremor severity while drawing an Archimedes spiral on a scale from one to ten. In performing the task, the pen should be held in a normal way and the hand should not be stabilised by the other arm, but the forearm may rest on the table. At least four turns of a spiral should be made. The two critical

factors in determining the grade of a particular spiral are the degree of perpendicular displacement of the track from the spiral, intended to be drawn and the extent to which tremor persists during each turn. In general tremor becomes more prominent as the number of turns increase and the distance from the centre grows.

Handwriting is included for measuring tremor severity since it can be linked to the patient's history through old samples of written text. In the method used by Bain and Findley the scores obtained from handwriting correspond to those obtained by assessment of spiral drawing (Bain and Findley, 1993).

Quantitative methods for assessing both magnitude and frequency of complex arm tremor with differentiation of components originating from proximal and distal joints (Liu et al, 1999) is useful for planning stereotactic surgery (Liu et al, 2000): thalamic surgery is effective in alleviating distal tremor, but when the tremor also originates from the shoulder, the subthalamic region should be targeted as well in order to completely suppress complex arm tremor. As with increasing size of the cycles of a drawn spiral, the magnitude of contribution of the proximal joints increase, the tremor seen in particular cycles of the spiral can be differentiated as originating proximally or distally. Wang et al (2005) reported a 'main diagonal' axis of orientation of the tremor along the orientation of the forearm, indicating a predominantly proximal tremor driven by the shoulder and a 'cross diagonal' axis of orientation of tremor (perpendicular to the forearm), indicating that the tremor is predominantly distal and driven by the elbow or the wrist.

Tremor was first quantified with a digitiser tablet in 1990 (Elble et al). The system was validated with an accelerometer and EMG (Elbe et al, 1996) and although the system was found to be objective and sufficiently sensitive, there has only been moderate interest from clinicians since (Rudzińska et al, 2007).

Rudzińska et al (2007) suggested the Automated Computer Tremor Score (ACTS), using a digitizing tablet and artificial neural networks to assess motor function. The study showed that neural networks may be taught to rate tremor severity analogically to human rating and automated scoring may be a useful method in clinical practice (Rudzińska et al, 2007). Saunders-Pullman et al (2008) validated the usefulness of analysing spiral drawing recordings. Selected indices derived from the analysis of spiral recordings were compared to the Unified Parkinson's Disease Rating Scale Part III (Fahn, 1987) in patients with early PD. The results show that automated spiral drawing analysis may supplement motor assessment in PD,

although further analysis of spiral metrics and a larger data sample should be evaluated.

Although only rest tremor is described in PD, today it is generally accepted that PD can be accompanied with kinetic tremor (Kraus et al, 2006). In the past spiral drawing for diagnostics in PD was common practice (Bain and Findley, 1993). There currently is a renewed interest in opportunities for spiral drawing and computerized assessment of kinetic and force tremor (Aly et al, 2007; Rudzinska et al, 2007; Saunders-Pullman et al, 2008). Nevertheless, at present the kinetic tremor in patients is hardly examined during clinical practice and no attention is paid to it in clinical rating scales.

Patients with PD may have a postural tremor with increased amplitude between 5 and 12 Hz (Brown et al., 1997; Lance et al., 1963). Forssberg et al (2000) reported an action (force) tremor between 5 and 12 Hz in PD. Different studies do not agree on the effect of PD on grip force amplitude. Ingvarsson et al. (1997), Vaillancourt et al (2001) and Rearick et al (2002) reported PD patients producing the same grip force amplitudes. On the contrary, Muller et al (1990) and Fellows (1998) et al reported different force amplitudes in PD.

Assessing modal frequencies and force amplitude might not be revealing in itself (Rearick et al, 2002; Vaillancourt et al, 2001). Modal frequency can remain unaffected, while there is an alteration in the time-dependent structure of the signal and this is referred to as a change in the regularity of physiological output (Lipsitz and Goldberger, 1992; Pincus and Goldberger, 1994). Regularity can be quantified by approximate entropy (ApEn) in the time domain (Pincus, 1991). Vaillancourt et al (2000b, 2001) reported that the time-dependent structure of tremor (ApEn) provided valuable additional information beyond that of amplitude and modal frequency analyses and is useful in differentiating tremor in healthy people from those with PD.

A study by Rearick et al (2002) revealed potential importance of frequency domain analysis in diagnostics of PD. Although subjects coordinated five digit force comparable to age-matched controls and the same force amplitudes and force sharing patterns were seen in both groups across all grasping phases, in the frequency domain differences were observed in PD patients exhibiting obvious action tremor (AT) at a single modal frequency. There was a systematic disruption, i.e., a phase-shifting away from 0°, in-phase force synchronization patterns that are

normally observed between digits and this disruption typically occurred at and around the AT frequency, while at many other frequencies synchronization patterns were maintained.

The above described tremor assessments methods above have all proven to be valuable in different situations. The novel comprehensive script analysis systems described in this thesis allows simultaneous measurement of both action grip force modulation during spiral drawing and writing activities and the corresponding drawing/writing result, which can be combined with advanced analysis techniques that allow investigation on physiological processes as suggested by Lipsitz and Goldberger, 1992; Pincus and Goldberger, 1994; Vaillantcourt et al, 2001 and Rearick et al, 2002. Combining recording of script/drawing and investigation of action force modulation could potentially make an important contribution to the further development of tremor assessment methods in. A series of tests was performed to illustrate the usefulness of the novel system in sampling grip force along with sampling spiral drawing.

## **7.2 Activities**

### ***Spiral drawing***

The subjects, described in 7.4, were asked to trace a spiral clockwise from inside to outside. An example of the spiral is shown in fig 7.1. The maximal outside diameter of the spiral was 120mm and four cycles with incremental changes of 17mm between the cycles were drawn. The spiral outside diameter of 120 mm was chosen as this size requires the proximal joints to be recruited as well as the distal joints. Each subject performed a total of 10 spiral drawing trials. The spiral that was traced was printed on paper that was placed below the transparent surface of the writing tablet. There was no time restriction to the task.

### ***Circle drawing***

The subjects were also asked to clockwise trace a circle with a diameter of 120mm and a total of 10 cycles were completed in every trial. The circle drawing activity was

included in addition to spiral drawing as it was not clear if the power spectra of spiral drawing were representative. The trial lasted less than 30 seconds and peaks in the power spectra of the spirals may originate from noise or tremor rather than representing a normal frequency spectrum. Therefore, grip force spectra of 10 circle drawing cycles were analysed with the same outer diameter (120mm) as the outer circle of the spiral.

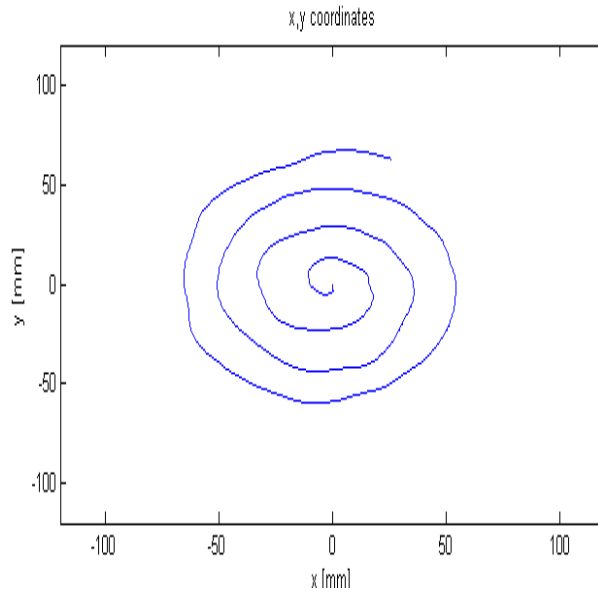


*Fig 7.1: spiral drawing activity: drawing clockwise from inside to outside with outer diameter  $d=120\text{mm}$ .*

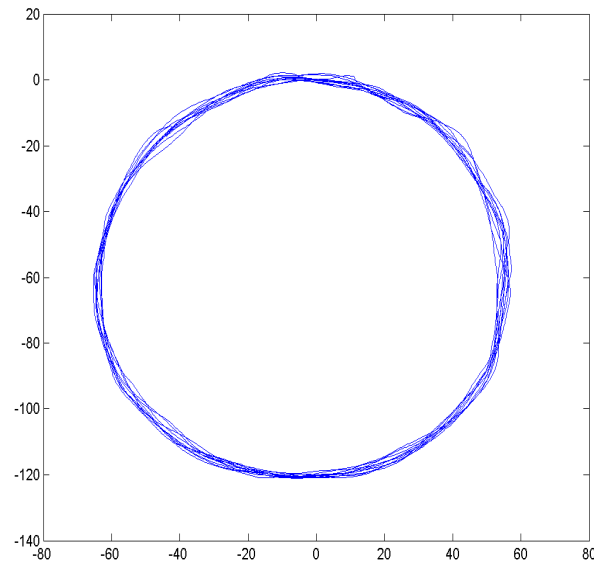


*Fig 7.2: circle drawing activity: drawing cycles clockwise with outer diameter  $d=120\text{mm}$ .*

### **7.3 Data collection and processing**

The comprehensive set of data sampled in this experiment includes:

- pen tip kinematics (x- and y-coordinates);
- pen tip pressure;
- pen grip pressure, applied by thumb, index and middle finger;
- limb and upper body kinematics.

The test equipment, data analysis and synchronisation techniques are described in detail under methods in 4.2.

Data on spiral drawing and circle drawing was recorded for a total of 7 subjects, which resulted in good quality data. However, it was chosen to only present data here for 2 subjects (Table 7.1) for illustrative purpose. Both subjects were considered representative of the normal healthy population. The aim was to show that the system enables to collect good quality data, which is useful for comparing drawing processes of different subjects and potentially for comparing healthy with impaired subjects.

#### ***Test procedure***

The test procedure was as follows. The volunteer is seated behind a table, while holding the grip measuring pen in tripod grip. On command of the investigator, the volunteer performs one spiral drawing trial. A pause of 30-60 seconds was given between each different trial.

#### ***Data processing***

The tremor during spiral drawing was investigated from the recordings of the pen grip forces. For the analysis of frequencies of finger force oscillations, the following background reading gave direction. Previous work indicates that those oscillations associated with sensorimotor processes are below 4 Hz and processes related to physiological and pathological tremor are expressed at frequencies above 4 Hz

(Freund and Hefter, 1993; McAuley et al., 1997; Slifkin et al., 2000; Vaillancourt and Newell, 2000a; Vaillancourt et al., 2001).

Subjects with PD exhibited force oscillations with a clearly definable frequency (approximately 7-11 Hz) for finger tip force action tremor. Some subjects also exhibited a second lower frequency peak (approximately 5 Hz) (Forsberg et al, 2000; Vaillancourt et al, 2001).

Finger tremor showed, subject to the arm position, maximally 3 and at least two distinct frequency bands (1-4, 6-11 and 15-30 Hz) reflecting the resonance frequencies of the whole arm, the hand and the finger, respectively during rest (Raethjen et al, 2000). Rearick et al (2002) suggested investigating tip force oscillations in the range of 0.5-17Hz for PD patients.

The exact frequency of the DC-term of the recordings in this experiment differs between trials, but was below 0.5 Hz. The DC-term was removed from the grip applications signals before obtaining spectrograms. The DC removal process has one argument,  $p$ , which refers to a time period in seconds. The output at time  $t$  is defined as the input value at time  $t$  minus the average value of the input data points from time  $t-p$  to  $t+p$ . The channel scale is not affected, but the channel offset is set to zero. A time period  $p=100$  ms was chosen.

The effect of DC-removal of the grip force signal during drawing of a spiral with four turns is shown in Fig.7.3. Based on the above, it was decided to investigate tremor between frequencies of 0.5 to 30Hz as these were likely to be most revealing.

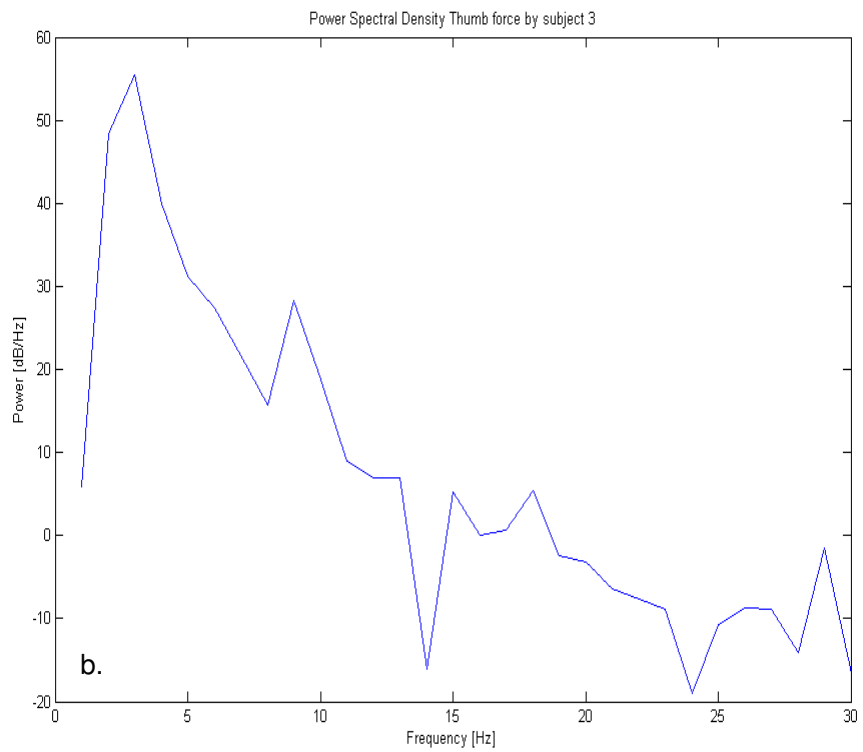
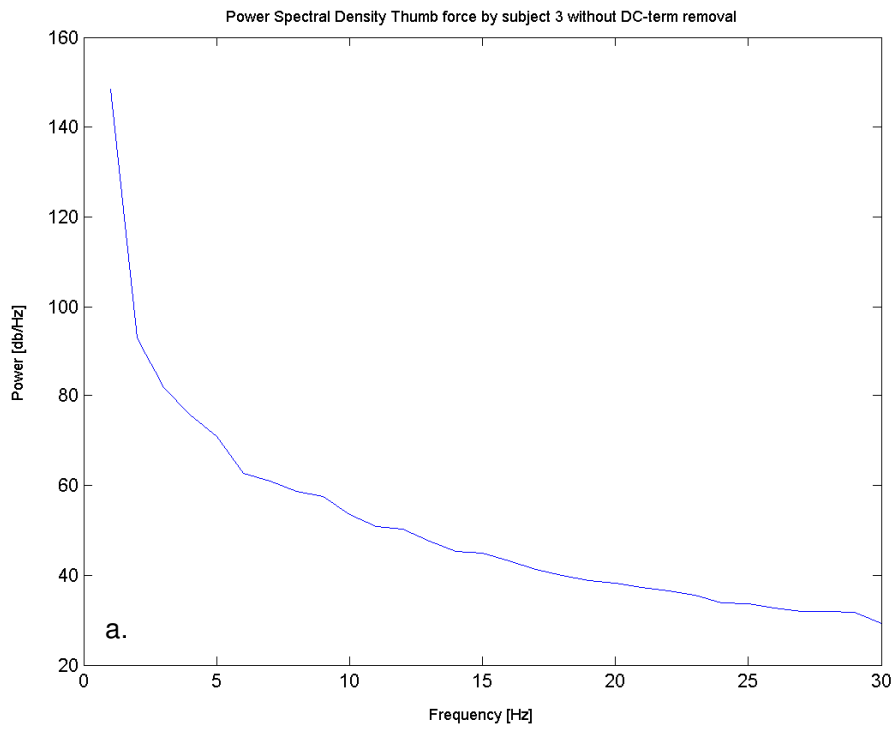


Fig 7.3.: Power Spectral Density without (a) and with DC-removal (b) for the grip force signal during drawing of a spiral with four turns.

## 7.4 Subjects

Four volunteers were tested. All subjects were right hand dominant and of varied ethnic origin. Details of the the five subjects are given in Table 7.1. Subject 1 showed enhanced physiological tremor in the left hand, whilst the functioning of the right hand was normal. All other subjects had normal motor functioning.

	<b>Subject 1</b>	<b>Subject 2</b>
<b>Ethnic origin</b>	white British	Indian
<b>Gender</b>	male	male
<b>Age</b>	27	27

*Table 7.1: Details of subjects, included in the spiral drawing experiment.*

## 7.5 Results

This section gives a detailed description of the biomechanical aspects associated with spiral drawing that were recorded with the developed system. The inter-related biomechanical measures that are going to be discussed are:

- pen tip kinematics (x,y-coordinates of the spiral);
- joint kinematics (x,y-coordinates of shoulder, elbow and wrist);
- pen grip pressure applied by thumb, index and middle finger;
- resultant grip force

The changes in pen grip force and joint kinematics associated with movement patterns observed in spiral drawing are described below for subjects 1 (section 7.5.1 ) and 2 (section 7.5.2), followed by a brief discussion.

### 7.5.1 Spiral drawing by subject 1

#### ***Kinematics***

Overall, subject 1 performed the spiral drawing activity without any difficulties. Fig. 7.4 shows the result of spiral drawing (x,y-coordinates) by subject 1. In addition, Fig. 7.5 and 7.6 show the x- and y-coordinates as function of time for the shoulder, elbow and wrist joint and the pen tip. The pen tip and joint paths follow a smooth pattern.

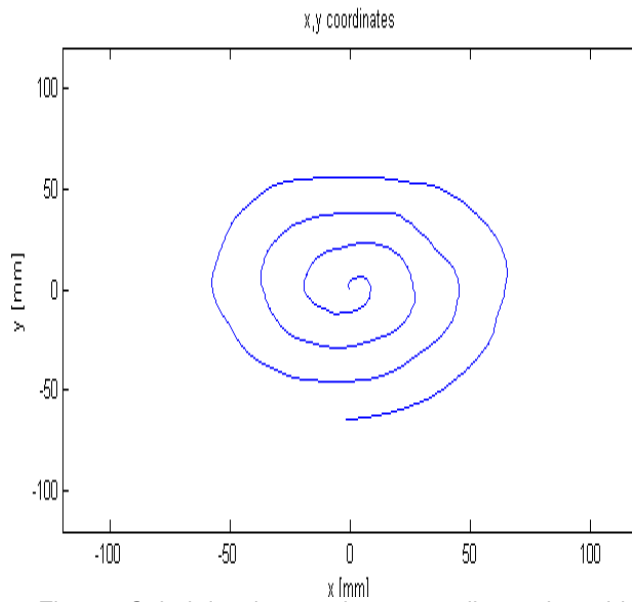
From the x- and y-coordinates in Fig. 7.5 and Fig. 7.6 it can be seen that spirals are produced by subject 1 by the superposition of oscillations in 2 orthogonal directions of the plane of motion, that are scaled in both orthogonal directions over time while the tip velocity remains constant. Both amplitude and oscillation period increase over the course of the trial.

Fig.7.7 and Fig.7.8 illustrate the oscillations of the pen tip and joint paths in two dimensions (x,y-frame) and three dimensions (x,y,z-frame). The harmonic oscillations are seen in all limb joints involved in spiral drawing. The shoulder, elbow and wrist joint trajectories (Fig.7.5 and 7.6) are all oscillatory and originate from sinusoidal changes in orientation angles of shoulder, elbow and wrist joints.

Interestingly, the sinusoidal changes in all three joints show fixed phase relations as may be seen from Fig.7.5, Fig.7.6, Fig.7.7 and Fig.7.8. A phase difference between the oscillation of the radius of the wrist joint and the elbow joint is seen. However, the phase differences are fixed and therefore remain constant throughout the trial. The radius of the angular motion at the pen tip, wrist, elbow and shoulder joint and pen tip over the course of the 4 cycles is presented in Fig.7.9 to 7.12. Interestingly, for spiral drawing the amplitude of the angular motion at the shoulder (Fig.7.12), elbow (Fig.7.11) and wrist (Fig.7.10) joints roughly scale with the size of the spiral in every cycle for subject 1. This is different from observation made by Lacquaniti et al (1987), who reported for the drawing of circles and elliptical figures that only the amplitude of the angular motion at the shoulder and elbow joints scale with the amplitude of the radius of the circle. The amplitude of the angular motion at the wrist was found not to scale with the amplitude of the radius of the circle, according to Lacquaniti (1987).

The variation of pen tip x-coordinates (blue line) and y-coordinates (red line) is presented in Fig.7.13. The changes in pen tip x-coordinates over time are found to

be delayed relative to changes in pen tip y-coordinates. This phase lag between x- and y-coordinates increases slightly during each spiral cycle. It may be hypothesised that the changes of pen tip in y-direction prior to changes in x-direction may be part of a strategy adopted by the neuromuscular system to control and regulate the fine finger and limb movements involved with spiral drawing. The upper and lower extremes of coordinate values are higher for the x-coordinates than the y-coordinates within one spiral turn. This in addition to the phase lag between x- and y-coordinates gives an elliptical shape to the resulting spiral (Fig.7.4).



*Fig.7.4: Spiral drawing result: x,y-coordinates by subject 1.*

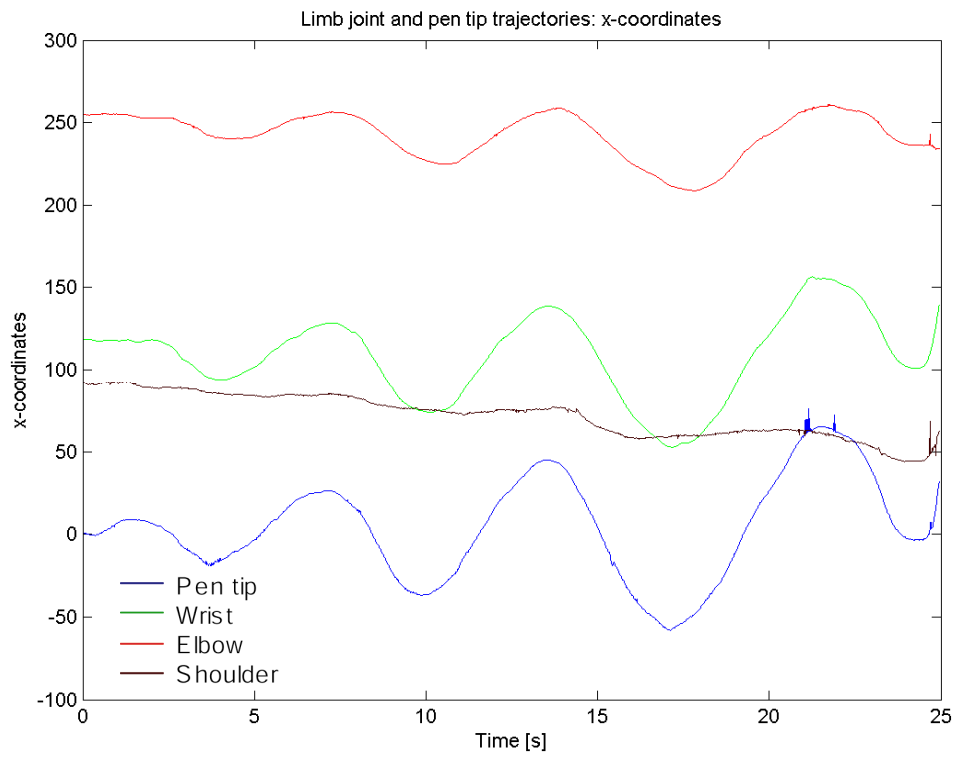


*Fig.7.5: Spiral drawing kinematics: x-coordinates of pen tip and wrist, elbow and shoulder joints by subject 1.*

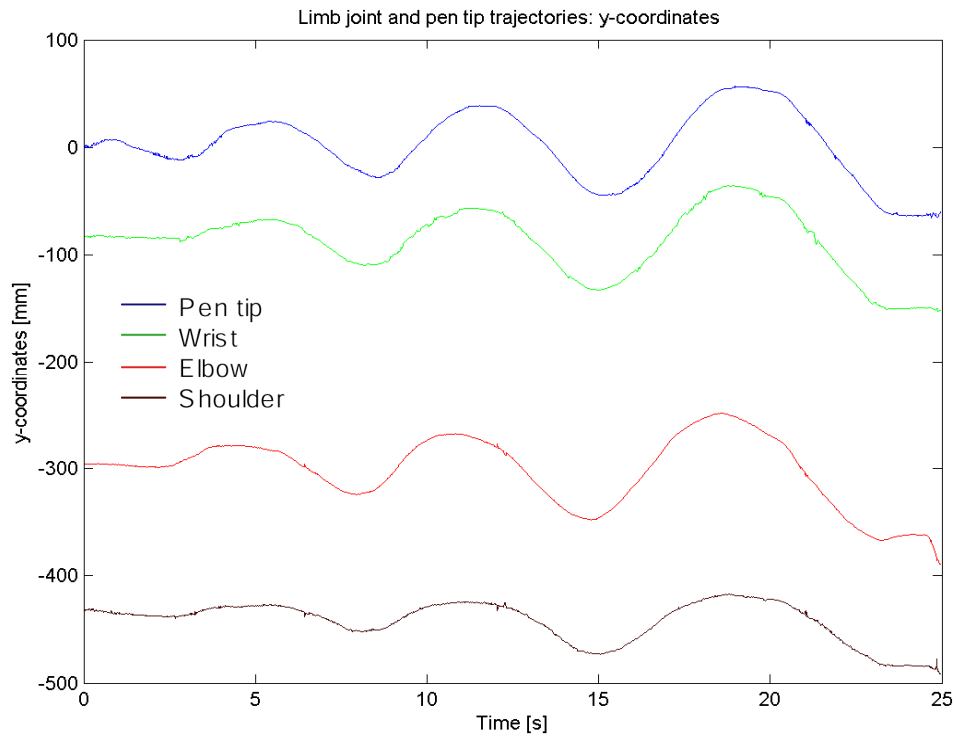


Fig.7.6: Spiral drawing kinematics: y-coordinates of pen tip and wrist, elbow and shoulder joints by subject 1.

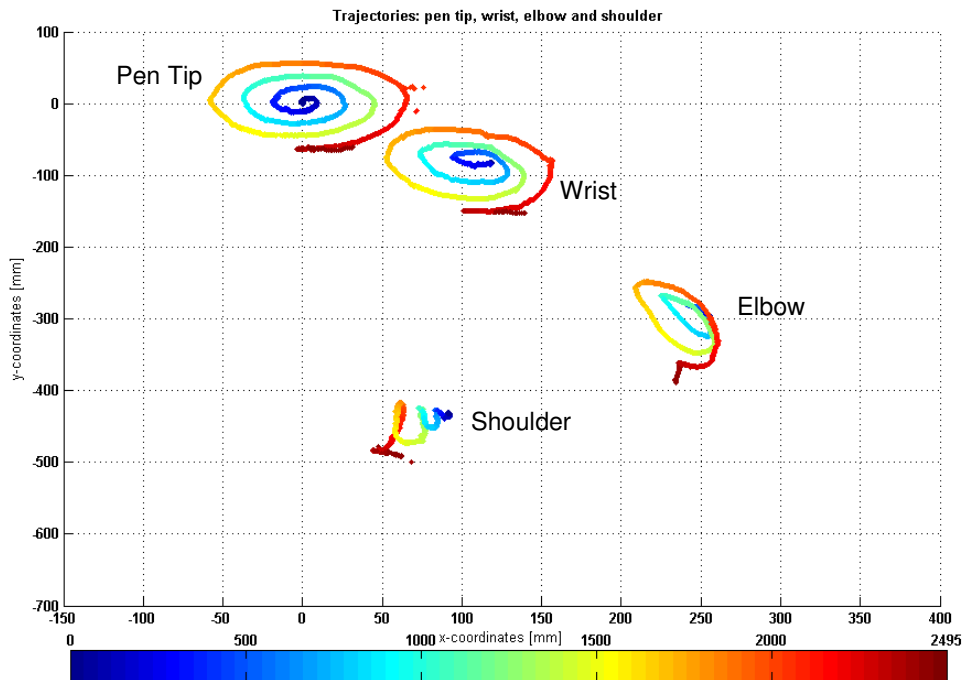


Fig.7.7: Pen tip and joint trajectories in the x- and y-frame for subject 1.

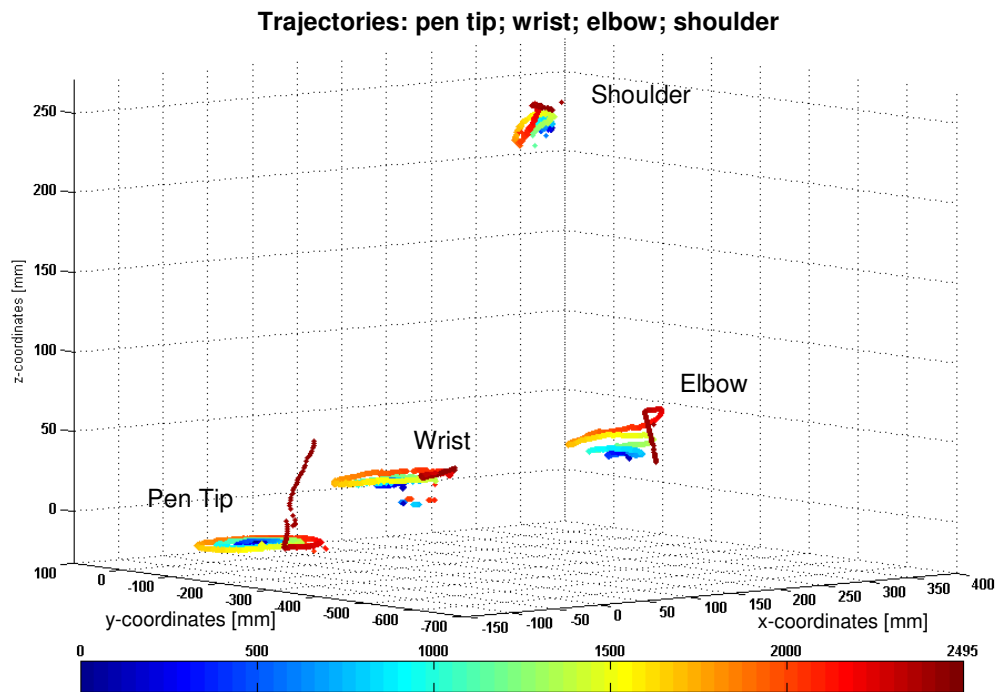


Fig.7.8: Pen tip and joint trajectories in three dimensions for subject 1.

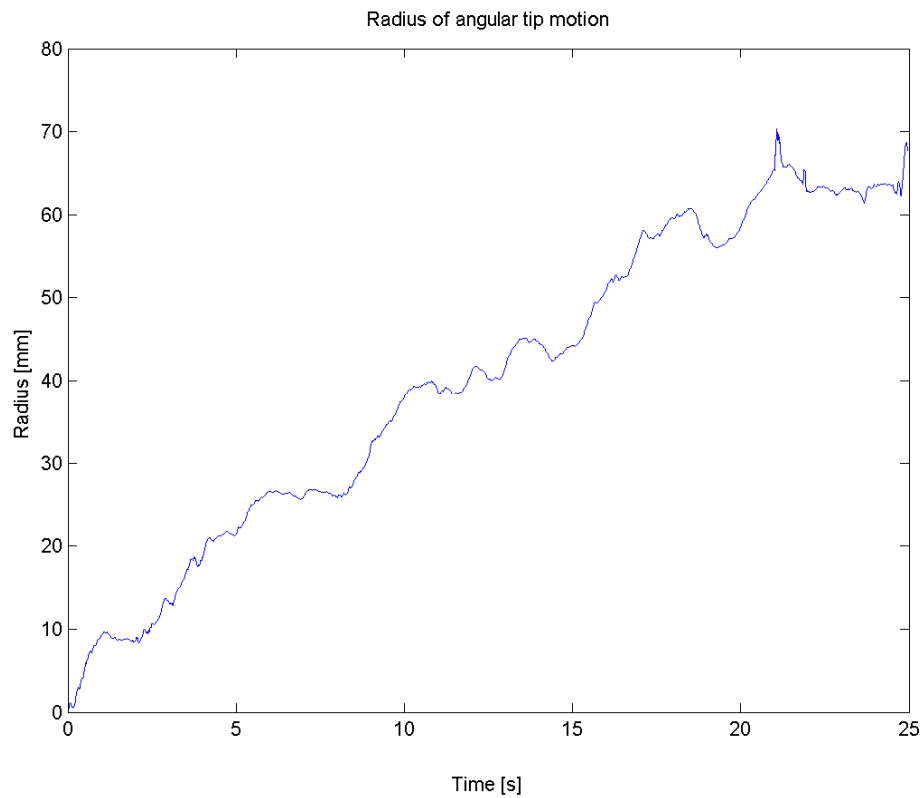


Fig.7.9: Radius of angular motion of the pen tip for subject 1.

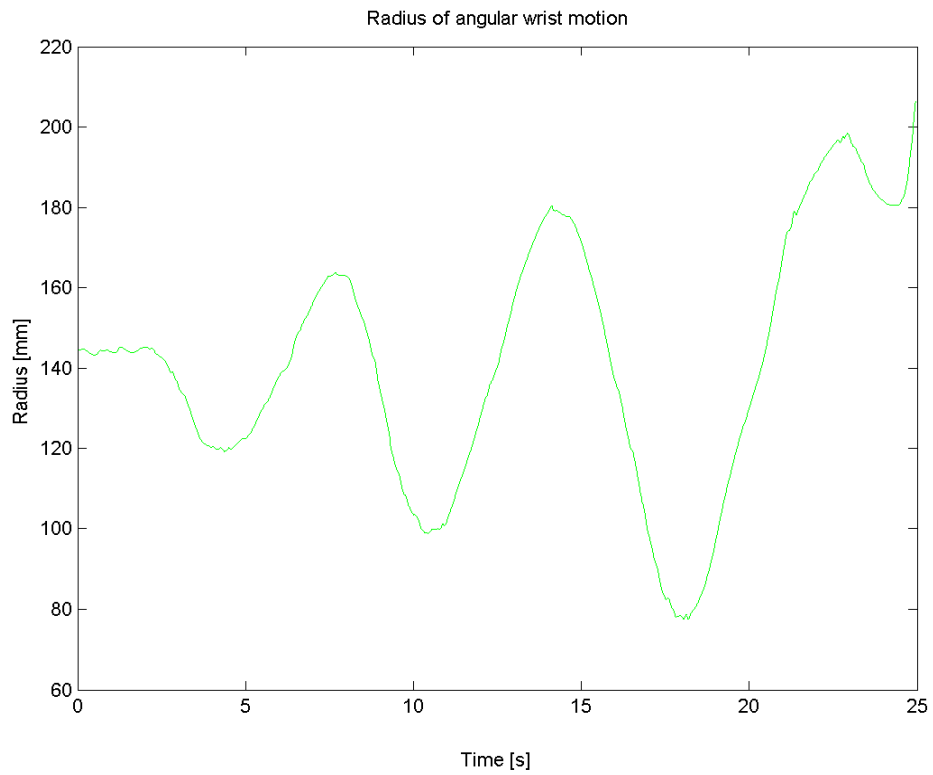


Fig.7.10: Radius of angular motion of the wrist joint for subject 1.

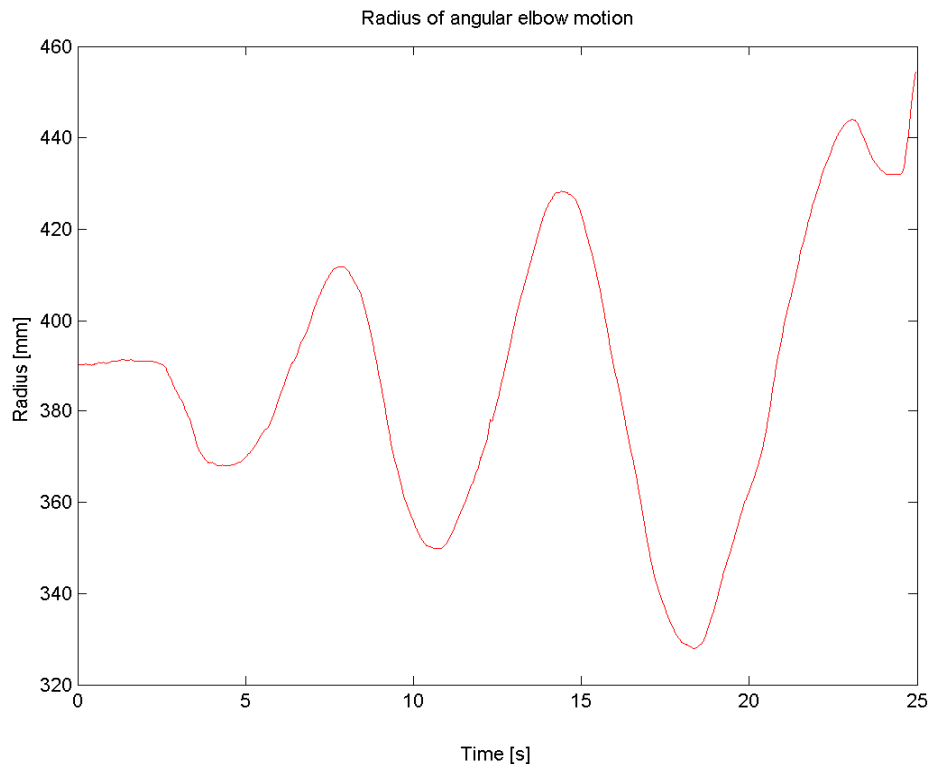


Fig.7.11: Radius of angular motion of the elbow joint for subject 1.

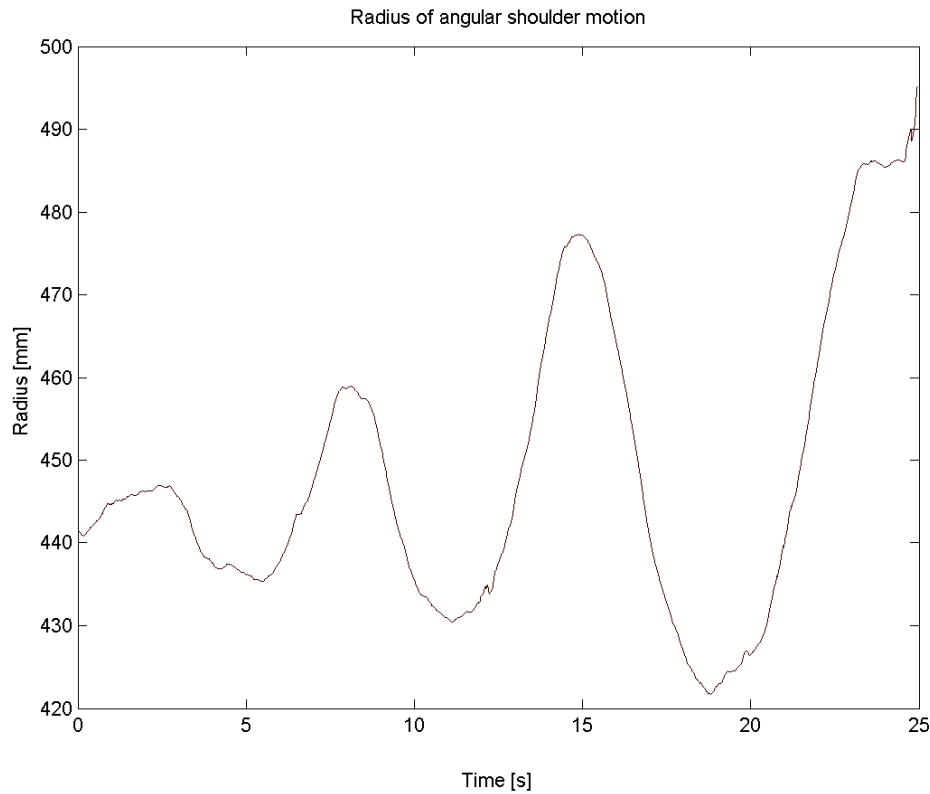


Fig.7.12: Radius of angular motion of the shoulder joint for subject 1.

### **Pen grip force**

The grip forces applied by the fingers to the pen during spiral drawing by subject 1 are shown in Fig.7.14. The resulting pen tip motion is presented as changes in x- and y-coordinates in Fig.7.13. The pattern of the middle finger force from t=5 seconds (red line in Fig.7.13) may remind one of a sinusoid with slightly increasing period and amplitude. The index finger force (green line in Fig.7.14) shows until t=5 seconds a similar pattern as the middle finger force (red line in Fig.7.14) and from t=5 seconds the opposite pattern from the middle finger force.

Interestingly, the changes in the middle finger force values precede the changes in the index finger force (Fig.7.14). The middle finger force may have a special role as part of a strategy adopted by the neuromuscular system involved with the control of the pen-hand interaction. The thumb force (blue line in Fig.7.14) shows significantly less variation than the index and middle finger forces and consistently had a high value of around 6.5N. Although the variation observed is small, peaks in thumb values can be recognised that coincide with peaks of middle and index finger force.

The timing of the pattern of finger forces is not directly related to pen tip movement and is not in phase with the variation of x- and y-coordinates (Fig.7.13). This is confirmed by the resultant pen grip force in Fig.7.15. The resultant grip force vector points upward over most of the course of spiral drawing for subject 1, whereas the pen tip varies between up- and downward motion. The upward directed (positive y-direction) resultant grip forces from t=4 seconds in Fig.7.15 reveal that the joints of the shoulder, elbow and wrist must provide most of the up and down going pen motion. This is confirmed by the joint movements in Fig.7.7 and 7.8. An exception to the upward direction (positive y-direction) of the resultant grip force are the first 4 seconds of the trial. The resultant grip force (Fig.7.15) shows values that vary between positive and negative close to zero.

During the second half of the spiral, the resultant pen grip force is seen to increase with increasing index finger force (green line in Fig.7.14). Surprisingly, the individual finger forces (Fig.7.14) do not seem to provide any obvious explanation that support the difference in resultant grip force values between the first 4 seconds (positive and negative values that vary around zero) and the rest of the trial (positive values that vary between 1.2 and 1.9N). For example in Fig.7.14 there is not much differences between the finger forces around t=3.1 s and t=7.4 seconds, although the resultant grip forces are very different in value. It is assumed that the difference cannot be explained at current stage due to the limitations of the analysis technique used here. Calculation of the resultant pen grip force was carried out in two dimensions and not in three dimensions, whereas the actual situation is a three-dimensional problem. Therefore changes in pen incline and non-perpendicular contact between finger tips and pen were not taken into account in the analysis. In addition, there are four and not three contact points between the pen and hand. Not measuring the fourth contact point may contribute to inaccuracies.

The pressure applied by the pen tip to the writing surface is shown in Fig.7.16. The pressure sensor's output is seen to remain constant throughout the trial, which points towards saturation of the pressure sensor at 1024 pressure levels. A pressure increase over the course of spiral drawing was anticipated based on observations by Van den Heuvel et al (1998). In those experiments the pen tip pressure was seen to increase with increasing size of each spiral turn. It is expected that the same pen tip force pattern was applied by subject 1, but that it was not measured due to sensor saturation.

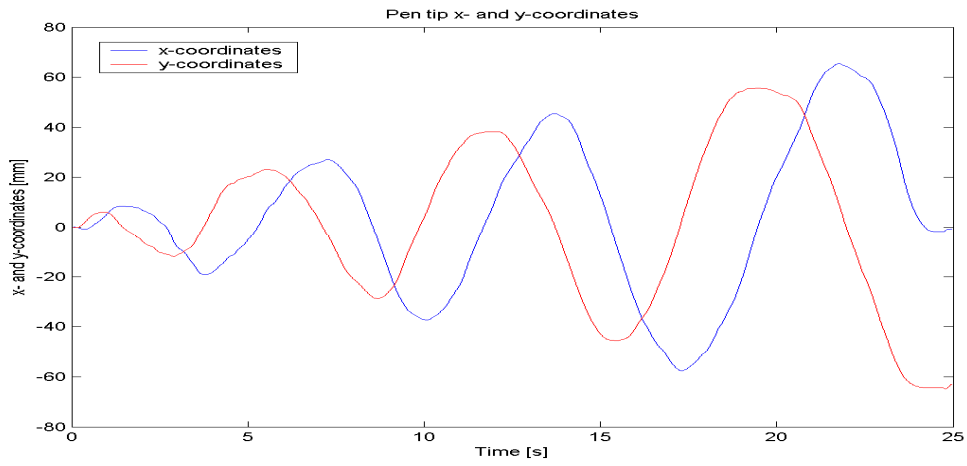


Fig.7.13: Pen tip x- and y-coordinates for subject 1.

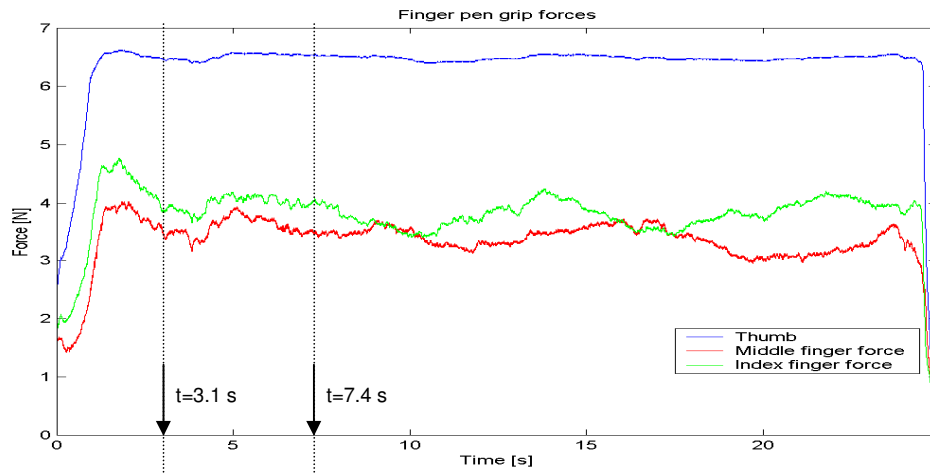


Fig.7.14: Thumb, Middle and Index finger pen grip force for subject 1.

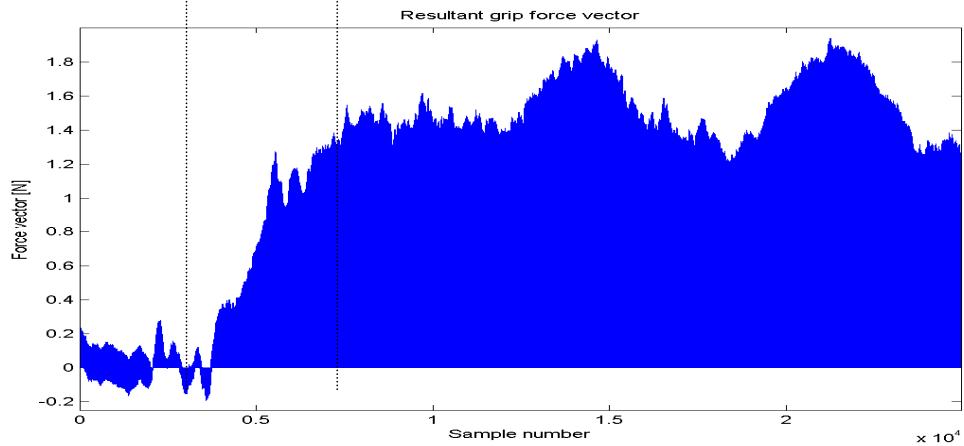


Fig.7.15: Pen grip force: Thumb, Middle and Index finger force for subject 1.

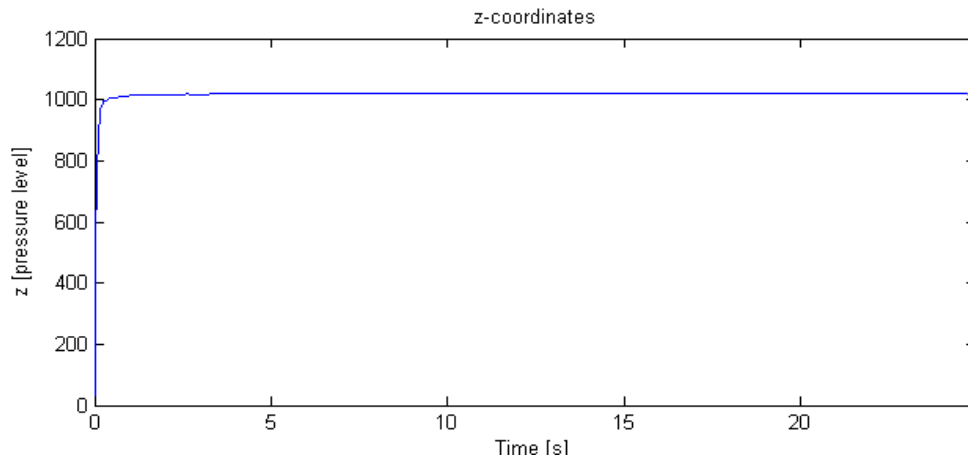


Fig.7.16: Pen tip force (in z-direction) for subject 1.

### **Frequency analysis**

Analysis of the limb kinematics during spiral drawing enables to visualise movement patterns in three dimensions. This has potential for locating tremor origin and the different muscle groups from which the tremor originates. Grip force measurement during spiral drawing enables an assessment of changes in grip force application, such as average and peak values applied by the thumb, index and middle finger and timing of the force application. In addition, there is a potential for assessment of motor function by further analysis of the frequency content of the forces applied by the thumb, index and middle finger. This may help to gain better insights in those specific changes that take place in the neuromuscular actions that are measured as pen grip force and which relate to neuromotor impairments. This knowledge may also be used in assessment of impairments, such as Parkinson's Disease.

The frequency content of the neuromuscular actions in both fingers and limb that enable the pen tip motion can be derived from Power spectral density analysis (PSD). PSD allows investigation of force modulations applied to the pen and its frequencies. The frequencies may not only relate to the fingers, but tremor frequencies measured at the contact sides with the pen may also originate from the hand or arm. The theory behind PSD is further explained in section 4.4.2.

For illustration purpose, the Power spectral density analysis for modulation of the thumb, index and middle finger force in the 0-30Hz frequency band by subject 1 are

shown in Fig. 7.17. The vertical axis shows the power (dB/Hz) at the specific frequency in the force signal. The peaks reveal which are the largest frequency components present in the signal.

Raethjen et al (2000) found that finger tremor shows, subject to the arm position, maximally 3 and at least two distinct frequency bands (1-4, 6-11 and 15-30 Hz) reflecting the resonance frequencies of the whole arm, the hand and the finger, respectively (Raethjen et al, 2000). In addition, hand tremor frequency (mean 7.7 Hz) was reduced significantly by added inertia (mean 5.2 Hz) and it was negatively correlated with hand volume while there was no correlation with grip force (Raethjen et al, 2000).

The mechanical behaviour of fingers is possible with linear second order models. Many physical processes in nature and also technical processes can be described with differential equations. In a mechanical system the properties of the springs, dampers and mass determine response of the system. Such a system can be described by a transfer function. A transfer function relates an input signal, described by a differential equation, to an output system, which is also described by a differential equation. The transfer function is a fixed property of the system and condition for the transfer function is that the system is at rest at  $t=0$ , which means there is no potential or kinetic energy in the system. Laplace transformations are used to find the output of the system from its transfer function. The poles of the system reveal whether the system output is a stationary, damped and or amplified oscillation. From modelling the mechanical behaviour of the fingers using linear second order models, it was observed that with increasing finger grip force, the damping of force exerted on the mechanical finger system will also increase (Hajian and Howe, 1997 and Becker and Mote, 1990). However, this does not affect the frequencies of the force signal.

Based on the above, the observed frequency bands for subject 1 between 1Hz and 4Hz in Fig.7.17 are expected to originate from the arm, which establishes the pen tip motion. These frequencies (peaking at 2 and 3Hz) reflect the period of the spiral drawing motion. The frequencies around 5Hz reflect the hand motion. All frequencies above 5Hz are expected to originate from the fingers. The grade of difficulty of the task is believed to have an effect on the power spectral density, according to Van Galen (1990). With increasing motor demands a decrease of power was observed at the lower frequencies (1-4 Hz) of the spectrum and an

increase in the middle (9-12 Hz) of the spectrum (Van Galen, 1990). In addition, increasing the grip force that is exerted is also believed to impact the tremor frequency by causing damping of the frequencies.

The force modulation in some of the digits share a common frequency. These common frequencies should be considered as frequency bands rather than peaks. The following frequency bands are shared by digits. The frequencies at which both thumb and middle finger force are applied can be seen between 2-7 Hz (originating from the whole arm and hand); 11-22 Hz and 22-29Hz (originating from the fingers). The frequency bands at which both middle and index finger force are applied are (Fig.7.18b and Fig.7.18c): 2-7 Hz (originating from the whole arm and hand); 12-18Hz; 19-22Hz and 22-29Hz (originating from the fingers). In addition, the middle finger shows peak force modulation within the band at 24 Hz and the index finger shows modulation that peaks at 24.5Hz within the band, which are very close in value.

The Thumb and Index finger force both apply grip force at frequencies within the 2-9 Hz band (Fig.7.17a and Fig.7.17c) that originate from both the whole arm and hand. In addition, force modulation within the following bands is seen: 12-18Hz; 19-22Hz; 23-29Hz, which all originates from the fingers. There appear to be peaks of power at close modulation frequencies of 24 Hz (for the middle finger) and 24.5 (for the index finger). Two or three digits applying forces to the pen at the same frequencies may be a part of a strategy for controlling the pen grip by the fingers. Force modulation at frequencies that are close in value may also be an attempt to establish a synergy between the finger activities for pen gripping.

The force application by two digits may be in phase or there could be a constant phase lag (Rearick et al, 2002). Further analysis is required.

In addition, as the grip force spectra of thumb, middle and index finger that are presented here are from one spiral with 4 turns only that last less than 30 seconds, it is unclear if the power spectra presented here are representative for the subject's force modulation involved with spiral drawing. The peaks in the pattern could be due to lack of data, causing a noisy unsmoothed spectrum. In addition, it is not known if there is any tremor, which will show up as accentuated power at the tremor frequency. Therefore, the grip force frequency spectra were analysed for the drawing of a circle with 10 cycles and outer diameter  $d=12\text{mm}$ , which is the same

size as the outer diameter of the spiral that was assessed. The x,y-coordinates are shown in Fig. 7.18 and the corresponding thumb, middle and index finger force frequency spectra are shown in Fig. 7.19.

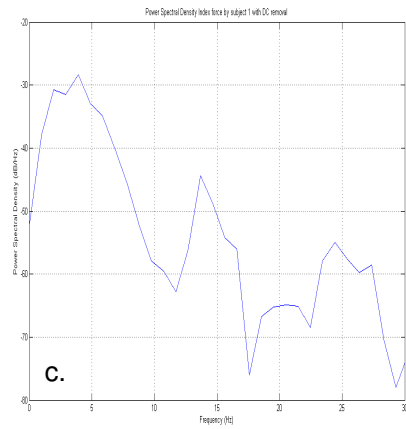
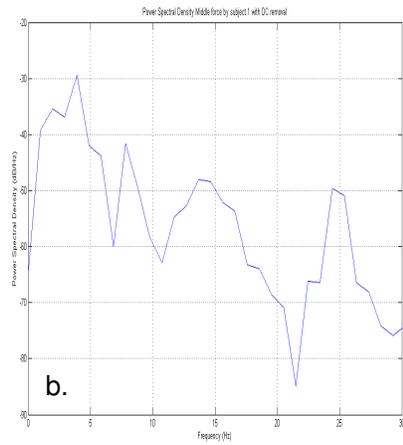
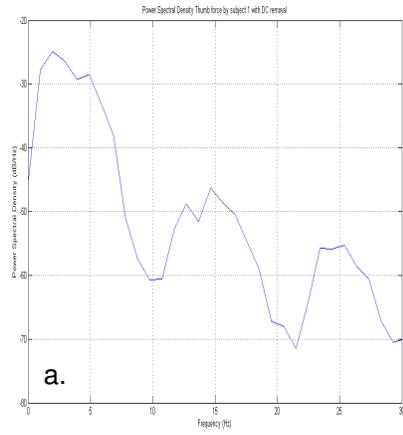


**Fig.7.17: Power spectral Density for Thumb, Index and Middle finger for spiral drawing by subject 1.**

**a: Thumb force;**

**b: Middle finger force;**

**c: Index finger force.**

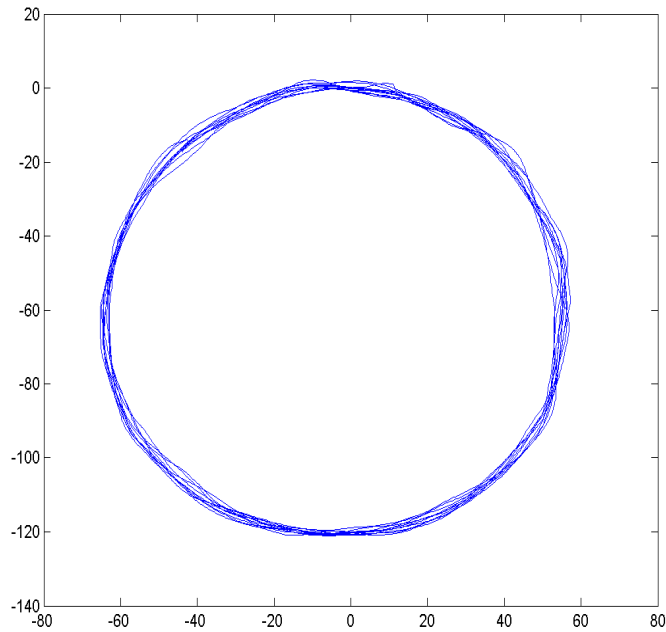


*Fig.7.18: x,y-coordinates for circle drawing (10 turns with  $d=12\text{mm}$ ) by subject 1.*

Fig.7.19 reveals that the force modulation in some of the digits share a common frequency. The frequency bands at which both thumb and middle finger force are applied are: 2-5 Hz (originating from the arm), 5-9 Hz (originating from the hand); 12-14 and 25-30 Hz (originating from the fingers). The frequencies bands at which both thumb and index finger force are applied are: 1-5 Hz (originating from the arm), 5-9 Hz (originating from the hand), 12-14 and 23-29 Hz (originating from the fingers). The frequency bands at which both middle and index finger force are applied are: 1-5 Hz (originating from the arm), 5-9, 12-14 and 23-29 Hz (originating from the fingers). As mentioned above, different digits sharing a common grip force modulation frequency may reveal a strategy to control the force.

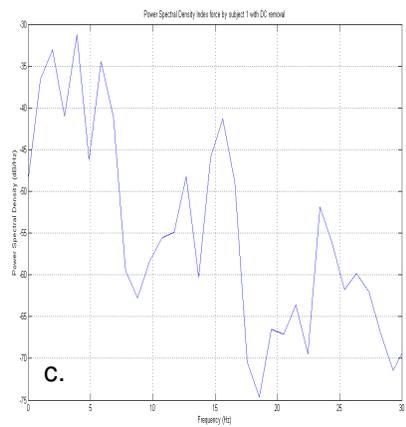
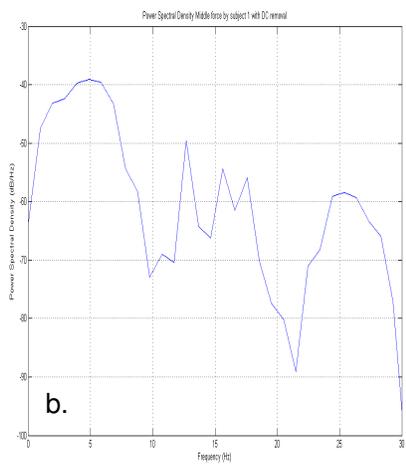
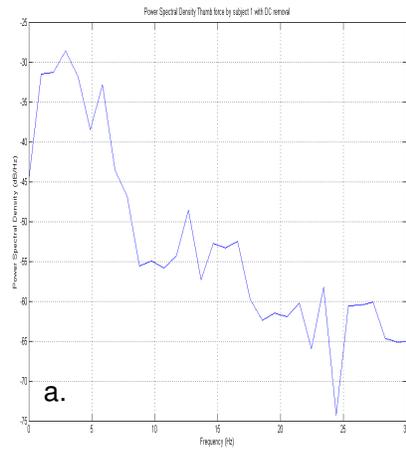


Fig.7.19: Power Spectral density (dB/Hz) for pen grip force during circle drawing (10 turns):

a.: Thumb force power spectrum

b.: Middle finger force power spectrum

c.: Index finger force spectrum

The data set for circle drawing was larger (10 cycles and drawing time of approximately 30 seconds) and therefore the frequency spectra for the circles can be regarded as more reliable than the frequency spectra that were found for spiral drawing. Interestingly, the following grip modulation frequencies that were observed for spiral drawing (Fig. 7.4 and spectra in Fig.7.17) are also seen for repetitive drawing of circles (Fig.7.18 and spectra in Fig.7.19). The thumb force shows peak modulation for both spiral and circle drawing at the following frequencies; 2, 14.5 and 25.5 Hz. The middle finger force patterns show peak modulation for both spiral and circle drawing at a frequency of 2 Hz. The index finger force shows peak modulation for spiral and line drawing at 2, 4 and 19.5 Hz. The spiral and circle drawing spectra also show peaks that are not exactly equal, but close in value. From the above it can be concluded that it is likely that the spiral drawing spectra are real peaks and the frequency spectra represent physiological processes, though more data collection and analysis is required to confirm this. The lower frequencies at 2 and 4Hz relate to rotational movement of the limb as mentioned above. The higher frequencies of 14.5, 19.5 and 25.5 are likely tremor frequencies.

The aim here is not to give an in depth analysis of frequencies observed in pen grip force modulation during spiral drawing. Instead it shows the potential of the grip measurement technique for advanced analysis. From background literature and further research on which specific changes that take place within the nervous system with different neuromotor impairments and development of a device for research into neuromotor impairments that incorporates grip force measurement, a platform for diagnostics may arise. Advanced analysis of frequency, amplitude and phase variations between force applications by digits along with advanced analysis techniques that allow to investigate the regulation of the nervous system's force output (e.g. described above as suggested by Lipsitz and Goldberger, 1992; Pincus and Goldberger, 1994; Vaillantcourt et al, 2001 and Rearick et al, 2002) need to be developed.

## 7.5.2 Spiral drawing by subject 2

### ***Kinematics***

Subject 2 also did not show any difficulties with drawing the spiral. Fig. 7.20 shows the result of spiral drawing (x,y-coordinates) by subject 4. Fig. 7.21 and 7.22 show the x- and y-coordinates as function of time for the shoulder, elbow and wrist joint and the pen tip. The pen tip and joint paths follow a smooth pattern.

From the x- and y-coordinates in Fig. 7.21 and Fig. 7.22 it may be concluded that spirals are produced by subject 4 by the superposition of oscillations in 2 orthogonal directions of the plane of motion. This was seen for subject 1 as well. Both amplitude and oscillation period increase over the course of the trial.

Fig.7.23 and Fig.7.24 illustrate the oscillations of the pen tip and joint paths in two dimensions (x,y-frame) and three dimensions (x,y,z-frame). The shoulder, elbow and wrist joint trajectories (Fig.7.21, 7.22, 7.23 and 7.24) are all oscillatory and originate from sinusoidal changes in orientation angles of shoulder, elbow and wrist joints.

As for subject 1, the sinusoidal changes in all three joints show fixed phase relations as may be seen from Fig.7.21, Fig.7.22, Fig.7.23 and Fig.7.24. Phase differences between the oscillation of the radius of the wrist joint and the elbow joint are seen, which are fixed and therefore remain constant throughout the trial.

The radius of the angular motion at the pen tip, wrist, elbow and shoulder joint and pen tip over the course of the 4 cycles is presented in Fig.7.25 to 7.28. The amplitude of the angular motion at the shoulder (Fig.7.28), elbow (Fig.7.27) and wrist (Fig.7.26) joints roughly scale with the size of the spiral in every cycle for subject 2. This is different from observation made by Lacquaniti et al (1987), who reported for the drawing of circles and elliptical figures that only the amplitude of the angular motion at the shoulder and elbow joints scale with the amplitude of the radius of the circle. The amplitude of the angular motion at the wrist was found not to scale with the amplitude of the radius of the circle, according to Lacquaniti (1987).

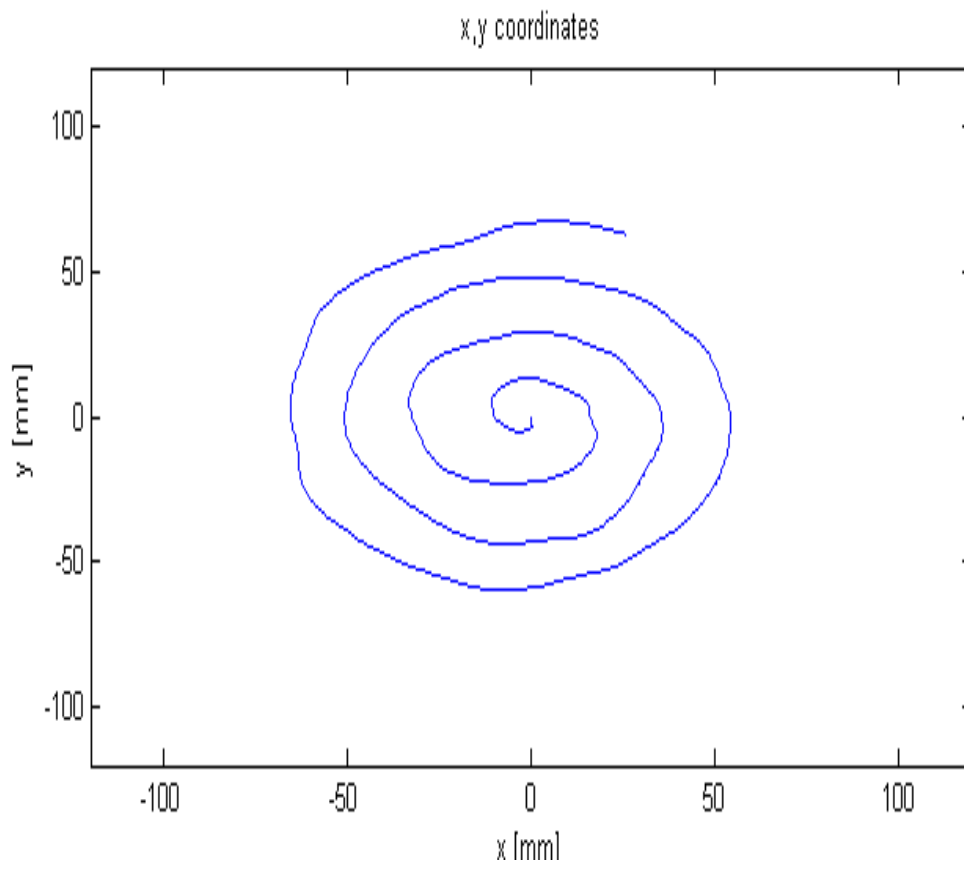


*Fig.7.20: Spiral drawing result: x,y-coordinates by subject 2.*

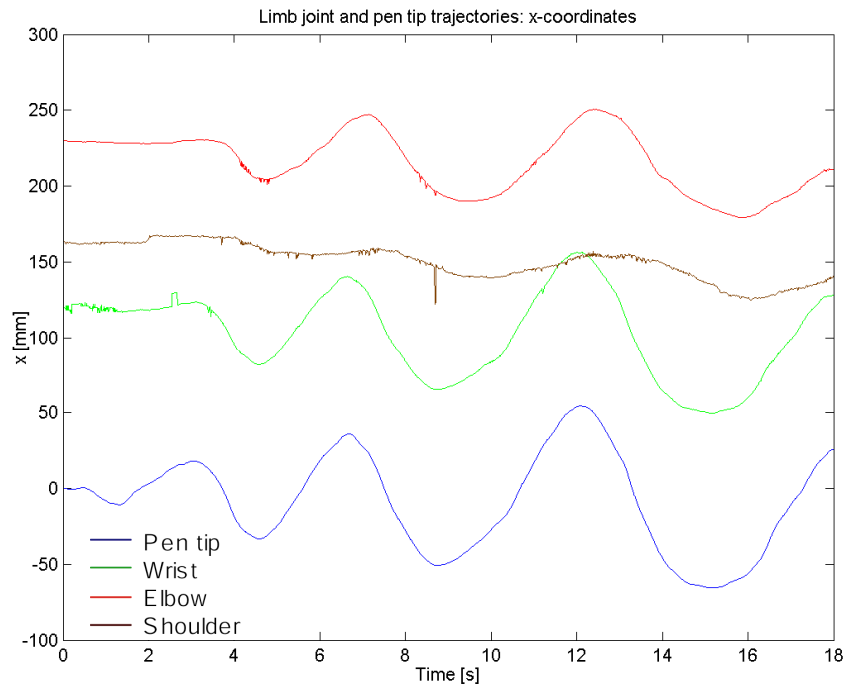


Fig.7.21: Spiral drawing kinematics: x-coordinates of pen tip and wrist, elbow and shoulder joints by subject 2.

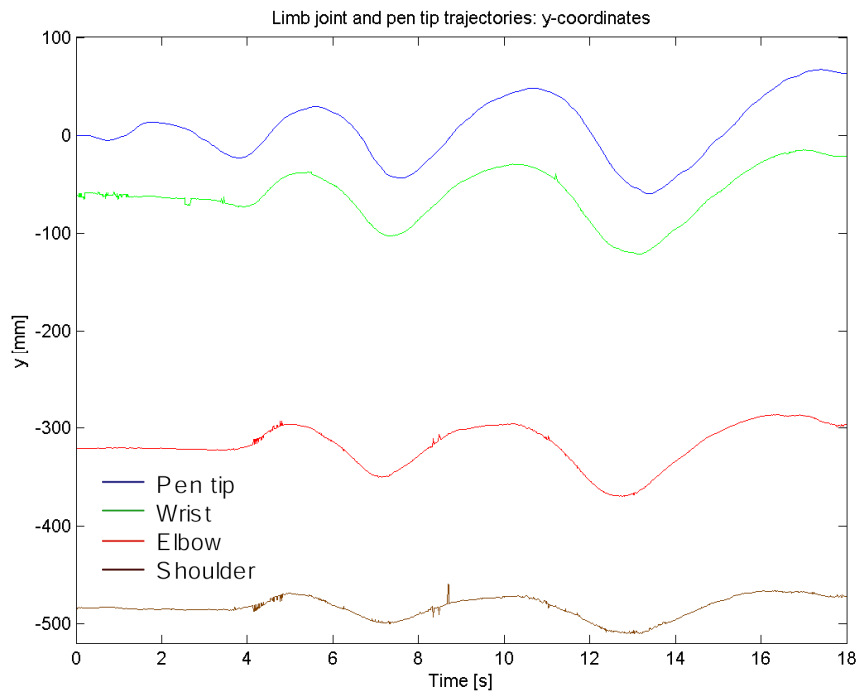


Fig.7.22: Spiral drawing kinematics: y-coordinates of pen tip and wrist, elbow and shoulder joints by subject 2.

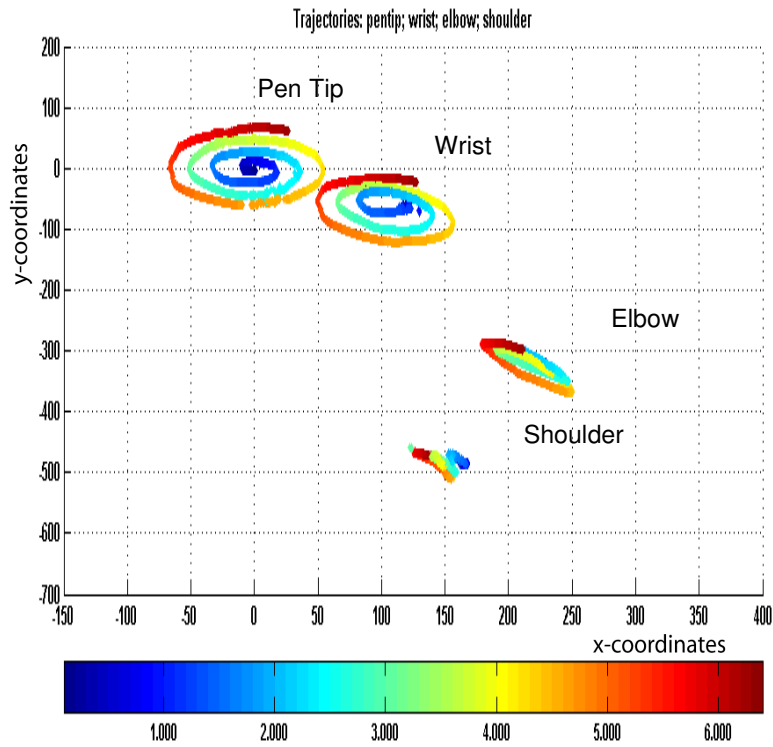


Fig.7.23: Pen tip and joint trajectories for subject 2.

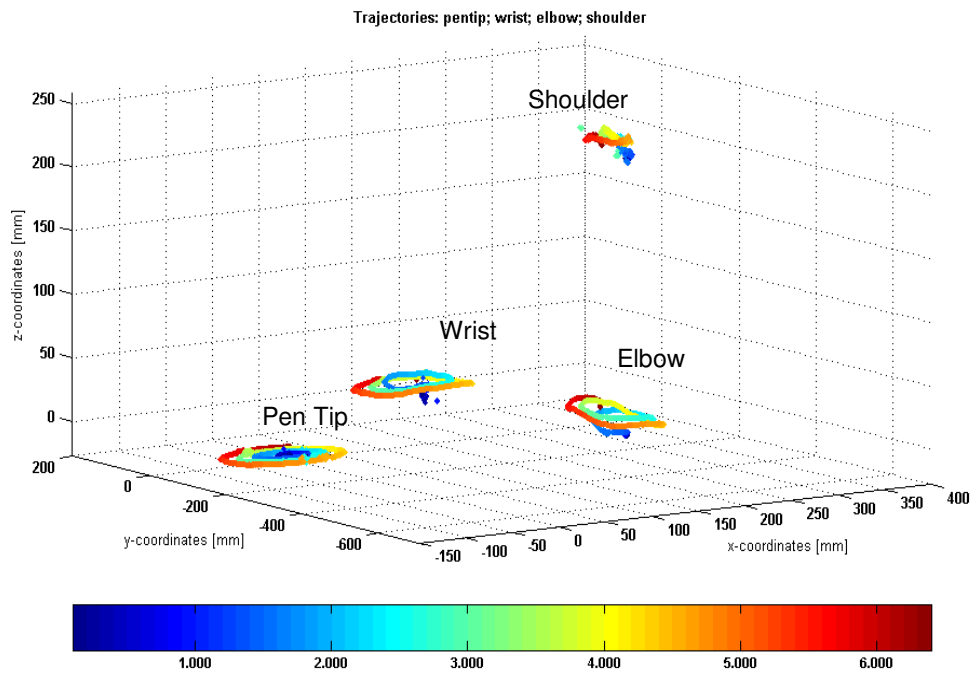


Fig.7.24: Pen tip and joint trajectories in three dimensions for subject 2.

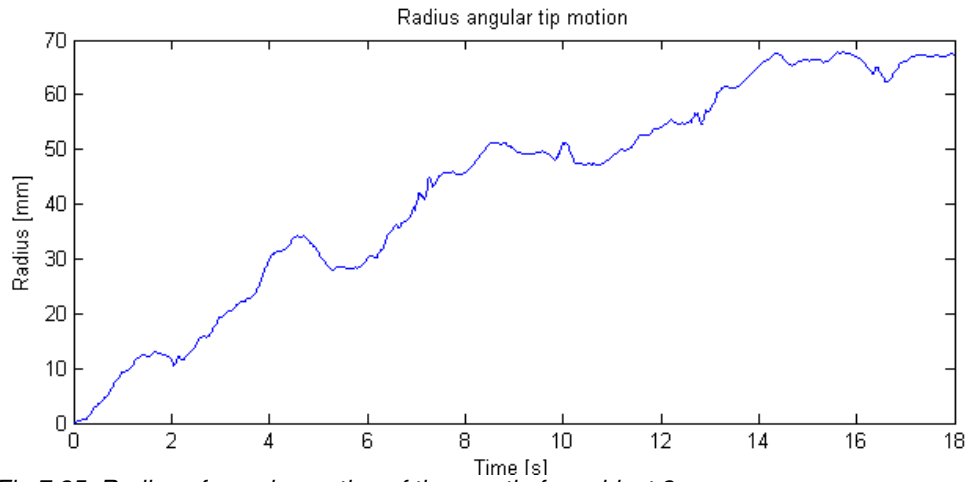


Fig.7.25: Radius of angular motion of the pen tip for subject 2.

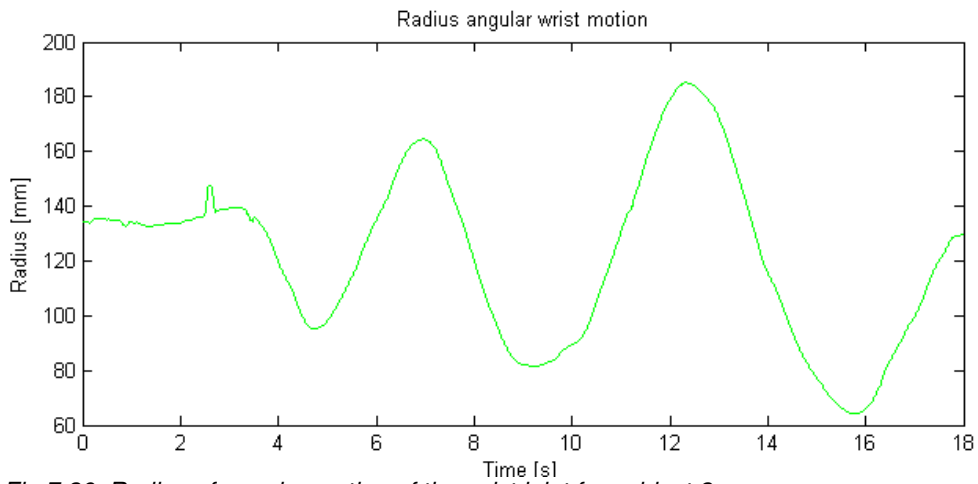


Fig.7.26: Radius of angular motion of the wrist joint for subject 2.

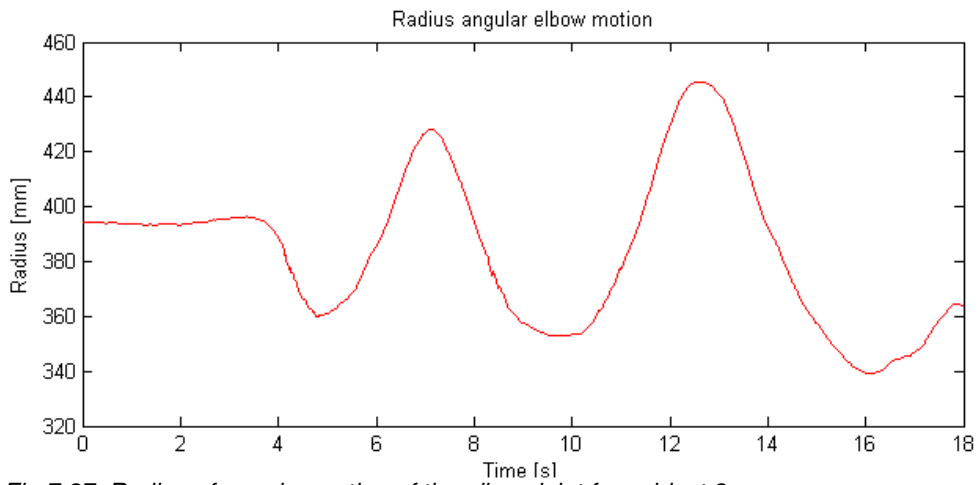
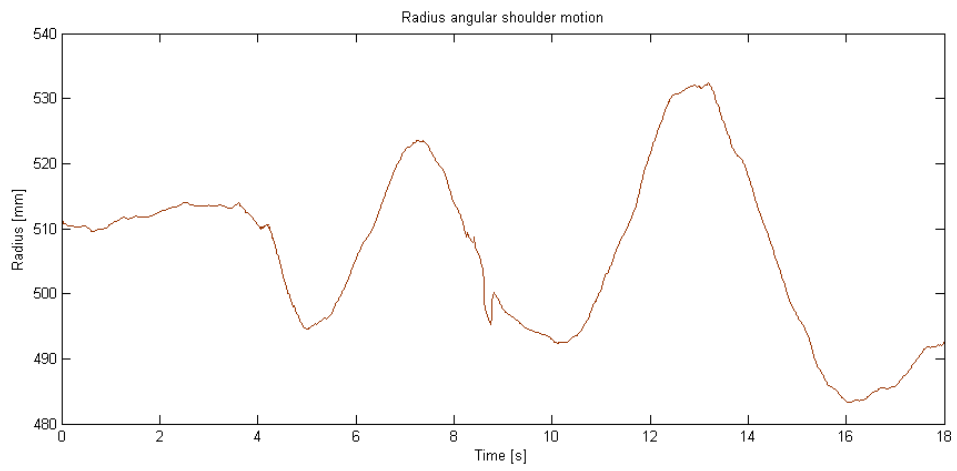


Fig.7.27: Radius of angular motion of the elbow joint for subject 2.



*Fig.7.28: Radius of angular motion of the shoulder joint for subject 2.*

### ***Pen grip force***

The grip forces applied by the fingers to the pen during spiral drawing by subject 2 are shown in Fig.7.29 and the simultaneous changes in x- and y-coordinates in Fig.7.30. While the x- and y-coordinates are increasing (until around the maximum value for x- and y-coordinates), the index finger force (green line in Fig.7.30) is increasing while the middle finger force (red line in Fig.7.30) is decreasing. Then the opposite happens: the middle finger force (red line in Fig.7.30) is increasing while the index finger force (green line in Fig.7.30) is decreasing. During the first half of this interval (between  $t=4s$  and  $t=8.5s$ ) the thumb force follows a pattern that is similar to the index finger. However, during the rest of the interval (from  $t=8.5s$  to  $t=13.5s$ ), the thumb force differs from the index finger force.

From Fig.7.30 no other consistent pattern of thumb, middle and index finger forces can be found than what was reported above for the period between  $t=4s$  and  $t=13.5s$ . During most of the first 6.4 seconds the resultant pen grip vector is directed in the negative y-direction (Fig.7.31), despite of the first two spiral turns being completed by moving the pen tip in both positive and negative y-direction. It can be concluded for this interval that the pen grip establishes a stable pen position and the limb joints must enable the pen tip movement to be executed.

During the last part of the trial from  $t=13.5s$  to  $t=18s$ , the variations in grip force are relatively small for the thumb, index and middle finger compared to the beginning of the trial. The resultant grip force from  $t=6.4$  seconds to  $t=18$  seconds follows the pen tip movement, but it is not in time with the tip movement (Fig.7.31). During the rest of the trial the forces do not relate to the pen tip movement as can be seen from the resultant pen grip forces in Fig.7.31 and as previously mentioned.

Overall, it can be concluded that not anywhere in the trial the pen tip movement is instigated by the pen grip forces. It rather seems to be a case of adapting the limb joint angles in synchrony to enable the execution of the pen tip motion while the fingers maintain a stable pen grip. Nevertheless, the pen grip is adaption in a fashion that reflects the pen tip movement, but that does not steer it.

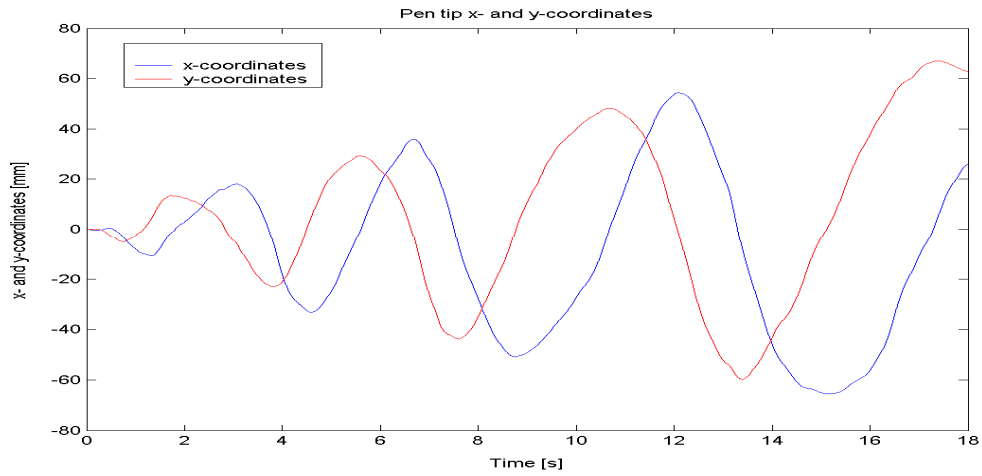


Fig.7.29: Pen tip x- and y-coordinates for spiral drawing by subject 2.

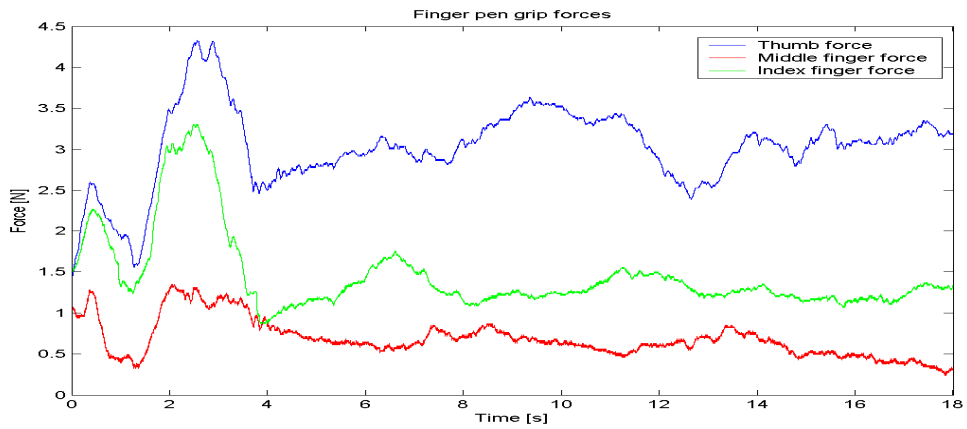


Fig.7.30: Pen tip finger forces for spiral drawing by subject 2.

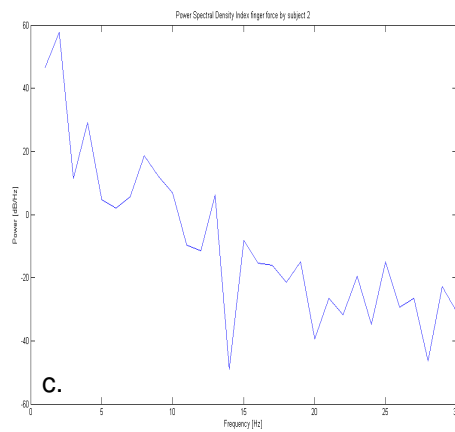
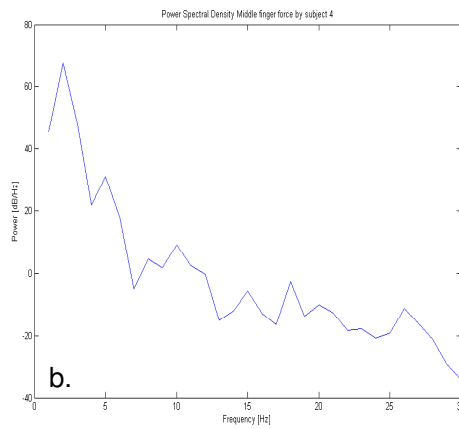
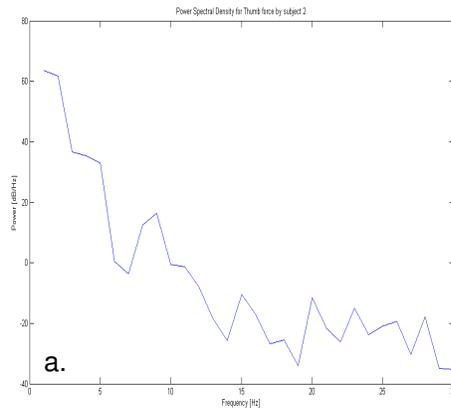


Fig.7.31: Resultant pen grip force for spiral drawing by subject 2.

### ***Frequency analysis***

For illustration purpose, the Power spectral density analysis for modulation of the thumb, index and middle finger force in the 0-30Hz frequency band by subject 2 are shown in Fig. 7.32. The vertical axis shows the power (dB/Hz) at the specific frequency in the force signal. The frequency bands with peaks reveal which frequencies are present strongest in the signal.

The force modulation in some of the digits share a common frequency. The frequency bands seen for both thumb and middle finger force are: 2-7Hz; 7-13Hz; 14-17Hz; 19-29Hz (Fig.7.32a and Fig.7.32b). The frequency bands for both middle and index finger force are applied are: 2-7Hz; 7-13Hz; 14-20Hz; 20-27Hz; 27-30Hz (Fig.7.33b and Fig.7.33c). The thumb and index finger force both apply grip force within the following frequency bands: 2-7Hz ; 7-12Hz; 14-19Hz; 20-22Hz; 22-24.5Hz; 24.5-27Hz and 27-29Hz (Fig.7.32a and Fig.7.32c). Two or three digits applying forces to the pen at the same frequencies, may be a part of a strategy for controlling the pen grip by the fingers. The force application by two digits may be in phase or there could be a constant phase lag (Rearick et al, 2002). Further analysis is required.



**Fig.7.32:** Power spectral Density for Thumb, Index and Middle finger for spiral drawing by subject 2.

**a:** Thumb force;

**b:** Middle finger force;

**c:** Index finger force.

### 7.5.3 Discussion: spiral drawing by subjects 1 and 2

#### ***The spiral drawing process***

Subject 1 and subject 2 were considered representative of the normal healthy population and both are seen to produce spirals by the superposition of oscillations in 2 orthogonal directions of the plane of motion, that are scaled in both orthogonal directions over time while the tip velocity remains constant (Fig.7.4, 7.5 and 7.6 for subject 1; Fig.7.18, 7.19 and 7.20 for subject 2).

Both amplitude and oscillation period were found to increase over the course of the trial. This is as one might expect, based on observations by Hollerback (1981); Lacquaniti et al (1983) and Soechting et al (1986) for circular and elliptical figures who reported superposition of approximately harmonic oscillations in 2 orthogonal directions of the plane of motion for drawing of circles and ellipses.

Soechting et al (1986) reported for drawing of ellipses and circles by the free arm in space that harmonic oscillations originate from sinusoidal changes in orientation angles of shoulder and elbow joints with fixed phase relations (Soechting et al, 1986). Lacquaniti et al (1987) observed that motion at the distal (wrist) joint was oscillatory as well, which is in concordance with the results observed here. However, Lacquaniti et al (1987) reported that only the amplitude of the angular motion at the shoulder and elbow joints scale roughly with the amplitude of the radius of the circle and that the amplitude of the angular motion at the wrist does not scale with the amplitude of the radius of the circle. For spiral drawing, on the contrary, from the radius of the angular tip motion, it was found that the amplitude of the angular motion at the wrist joint also scales with the size of the spiral cycle for both subjects 1 and 2.

This agrees with findings by Meulenbroek et al (1998), who state that during loop writing the wrist and elbow formed more stable coordination with pen-tip displacement dimensions than other joints within the arm and hand formed with the pen tip displacement. Interjoint coordination is most stable between the wrist and elbow. The elbow is coupled more closely to horizontal and vertical pen tip displacements than the index finger (Meulenbroek et al, 1998). This may be surprising as the prevailing view is that horizontal pen tip displacement are mapped onto wrist excursions and vertical pen tip displacements onto finger excursions (e.g. Bullock et al, 1993; Denier van der Gon et al, 1965; Edelman et al, 1987, Hollerback, 1981, Lelivelt et al, 1996, Vredenburg et al, 1971). In addition, pen-joint

coordination between horizontal pen-tip displacements and wrist excursions is found to be more stable than between vertical pen-tip displacements and finger excursions (Meulenbroek et al, 1998). In loop writing, within arm interjoint coordination is less stable than pen-joint coordination. Consequently, the task can not be described as a simple task in which the subjects only need to find a stable coordination of a single joint pair (Meulenbroek, 1998).

The changes of pen tip coordinates in y-direction was seen to precede the changes in the x-direction for both subjects. It may be hypothesised that this is part of a strategy adopted by the neuromuscular system to control and regulate the fine finger and limb movements involved with spiral drawing.

The results obtained in this study show for spiral drawing by subject 1 and subject 2 that the resultant grip force does not instigate the pen motion. It rather it seems to be a case of controlling the limb joint angles in synchrony to enable the execution of the pen tip motion. The fingers maintain a stable pen grip. For subject 2, it is seen in the second half of the trial that grip force is adapted in a fashion that reflects the pen tip motion, although the motion does not originate from the fingers.

The fine control of the finger joints seems to allow small adjustments to the pen tip motion, which became evident from Fig.7.6. The pen tip trajectory in Fig.7.6 is significantly smoother than the wrist joint trajectory. Results reported by Thomassen et al (1998) explain this further by showing that coordination between wrist and finger in loop writing is task-dependently adjusted, approximately once per second as subjects progress from left to right across the baseline of writing (Thomassen et al, 1998).

### ***Opportunity for tremor assessment***

The joint kinematics for spiral drawing by subject 1 were shown in Fig.7.4 to Fig.7.8. For this healthy subject smooth circular trajectories were seen for all limb joints. For subjects with impaired limb functioning due to e.g. limb stiffness, tremor or joint immobility the trajectories described by the limb joints will look differently. Particular the three-dimensional plots of pen and joint trajectories as in Fig.7.7, 7.8, 7.21 and 7.22 may be revealing and allow deficiencies in control to be localised. The analysis

of joint coordinates could be extended to enable quantification of range of mobility and tremor severity.

In addition, both finger tremor and tremor that originates from the hand and arm can be measured with the pen grip force transducer, although the validity of the method needs to be investigated further. More data collection and analysis is required.

Generally, the frequency of the tremor reveals its origin with the frequency bands 1-4Hz, 6-11Hz and 15-30 Hz relating to the resonance frequencies of the whole arm, the hand and the finger, respectively (Raethjen et al, 2000). The usefulness of tremor visualisation using motion analysis along with tremor measurement with the grip force transducer for tremor localisation also needs to be investigated further. Advanced methods for analysis of the regulation of force control by the nervous system need to be developed (e.g. as suggested by Lipsitz and Goldberger, 1992; Pincus and Goldberger, 1994; Vaillantcourt et al, 2001 and Rearick et al, 2002).

#### 7.5.4 Conclusion

The tests performed in this chapter shows that the novel comprehensive script analysis systems described in this theses allows to simultaneously look at action grip force modulation during spiral drawing, the joint kinematics and the corresponding drawing result. The sampled data is of high quality, which enables further analysis of script coordinates, three-dimensional joint movement and pen grip force control.

The results show that the pen tip motion is enabled by synergetic limb joint control, while the fingers ensure a stable pen grip to position the pen relative to the wrist joint. From the finger force control observed here for spiral drawing, it can be concluded that the fingers do not play an important role in directing the pen in vertical direction during circular pen motion. This is different from what was observed for line drawing and writing.

Development of analysis techniques for further assessment of the pen grip forces will allow assessing which specific changes take place in the neuromuscular system with handwriting deterioration due to aging or development of disease. Therefore, it is anticipated that the system will first of all find applications in research. Potentially, a set of quantifiable parameters may be defined that can be measured for

assessment of impairments. This may allow distinguishing between the regulation of the finger force control by the nervous system in healthy people and those with impaired function.

## **8 Handwriting and signature verification**

### **8.1 Introduction**

The fine motor control of distal joints within the biomechanical plant formed by hand and arm, typically allows the modulation of small (vertical) pen movements (Hollerback, 1981) and increases accuracy of the pen tip movement (Lacquaniti, 1987). As people's handwriting is very distinctive, one might expect someone's pen-hand interaction, resulting from the fine motor control of distal joints, to be characteristic for every individual. Pen-hand interaction could be measured as grip force. The aim of this chapter is to investigate whether there might be potential for measurement grip force to distinguish between genuine signature and an attempt to counterfeit one's signature.

The subjects included into the experiment are firstly described in section 8.2. Data was recorded for two different activities and the chapter is accordingly split into two parts. The first part was aimed at comparing x,y- and z-coordinates. The activity, results and signal processing for comparison of script of subjects and between subjects are described in 8.3. The second activity focussed on comparison of grip force along with x,y-coordinates and is described with results and signal processing in 8.4. The overall usefulness of comparing x,y- and z-coordinates for signature verification is discussed in the conclusion in section 8.5.

### **8.2 Subjects**

A total of seven healthy volunteers with good writing ability were tested. The results for four subjects will be presented here, which was considered to be sufficient for illustrative purpose of the potential. All four subjects were right hand dominant. Details of the four subjects, whose data will be compared in this chapter, are given in Table 8.1.

	Subject 1	Subject 2	Subject 3	Subject 4
<b>Ethnic origin</b>	Indian	Thai	white European	white European
<b>Gender</b>	male	female	female	male
<b>Age</b>	27	32	30	27

Table 8.1: Subjects that were included in the testing for signature verification.

### 8.3 Part I - Script comparison: methods for data analysis

#### 8.3.1 Activity: comparing x,y- and z-coordinates

The aim of the first activity was to assess if correlation of x,y- and z-coordinates (result of writing processes) allows comparison of signatures and what the effect of orientation angle of the signature is on its consistency.

Each subject's signature was repeated 10 times. The first trial was performed with the bottom of the tablet placed square with the table and between each of the following trials, the angle of the tablet relative to the table was increased with 10°. The last trial was performed with an angle of 90° between tablet and table. There was no time restriction to the task and subjects were not restricted to specific starting point or signature orientation on the tablet.

Fig 8.1 illustrates the procedure. The first signature (Fig.8.1a) and the last signature (Fig.8.1b) performed by subject 1 are shown. From the first trial (Fig.8.1a - with the bottom of the tablet placed square on the table) subject 1's signature is seen to naturally have an incline of 45 degrees compared to an horizontal line. The incline of the last trial (Fig.8.1b) differed 90 degrees from the first trial as a result of the tablet rotation over 90°.

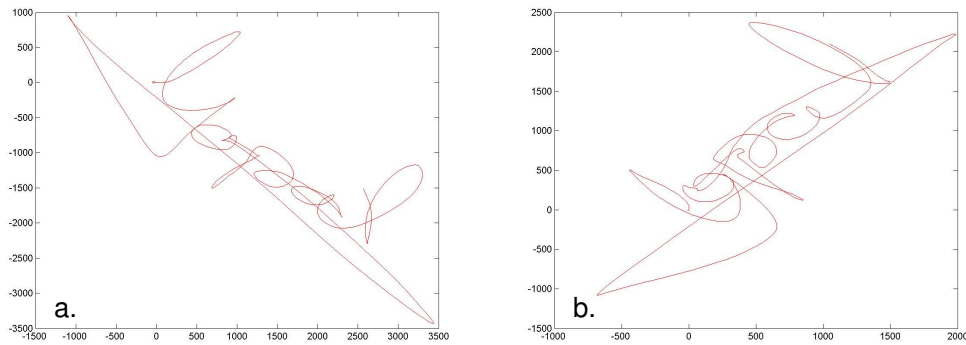


*Fig.8.1: x-and y-coordinates of signature by subject 1 for tablet orientation  $0^\circ$  (a.) and tablet orientation  $90^\circ$  compared to a horizontal line (b.).*

### 8.3.2 Data analysis: comparing x,y- and z-coordinates

A Matlab script was written that calculates correlation coefficients between x,y- and z-coordinates of signatures with different orientation angles. The first trial was performed with the bottom of the tablet placed square with the table. For each of the following trials the angle of the tablet relative to the table was increased with  $10^\circ$ . The last trial was performed with an angle of  $90^\circ$  between tablet and table. The script compensates for different tablet orientations, inclines of signature writing lines and different starting points by rotation and translation of coordinates as illustrated in Fig. 8.2. The manipulation by the script enables the start point of the signature to coincide with the origin (0,0) of the cartesian coordinate system and horizontal orientation of the signature.

The usefulness of the script was assessed by comparison of signatures produced by the same subject in section 8.3.2.1 and comparison of genuine signatures with attempts to counterfeit those signatures in 8.3.2.2.

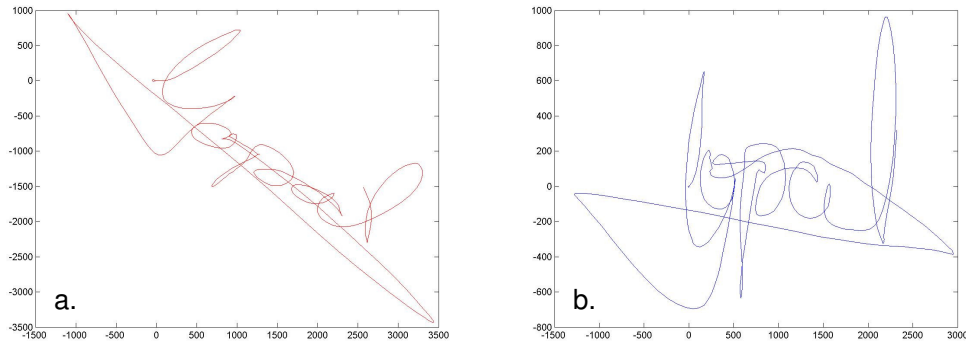


*Fig.8.2: x-and y-coordinates of subject 1's signature for tablet orientation  $0^\circ$  as recorded (a.) and after performing rotation and translating (b.).*

### 8.3.2.1 Comparison of signatures produced by one subject

The results of translation and rotation of signatures for subjects 1, 2 and 4 can be seen in Fig.8.3, Fig.8.4 and Fig.8.5 respectively, showing the original recording on the left and the result of translation and rotation to the right in an analogue fashion to Fig.8.2. The corresponding correlation coefficients between x-,y- and z-coordinates for each of the three subjects can be found in Table 8.2. The correlation of coordinates is represented in Table 8.2 by four values which are derived as follows. One signal is firstly correlated to the second signal and then correlated to itself, giving two results of which the latter one with correlation  $r=1$ . The same procedure is carried out for correlating the second signal to the first and to itself, giving the same correlation values, but in the opposite order.

#### ***z-Coordinates***

For subject 1 high correlations of the pen tip pressure values (z-coordinates) is seen between the first trial (incline  $=0^\circ$ ) and all other 8 trials. The correlation between the trial with a tablet incline of  $0^\circ$  and trial at incline of  $60^\circ$  is 60%. The correlation between the first trial (incline  $=0^\circ$ ) and all trials with other tablet orientations (Table 8.2.) is 70% or higher.

For subject 3 the correlation is over 90% between the first trial (incline =0°) and all trials with other tablet orientations (Table 8.2.)

For subject 4 the modulation in the z-axis (pressure) is not very consistent.

Correlations lower than 50% are seen. It can be concluded that tip pressure on its own might not be the best measure for checking authenticity of signatures.

### ***x,y-Coordinates***

The correlation coefficients for x- and y- coordinates between trials that are presented in Table 8.2 show that for each subject the signatures strongly resemble. In some cases one of the two axes do not strongly correlate, but it was never seen that both axis did not strongly correlate. It can be concluded that obtaining correlation factors between x- or y-coordinates of two recorded signatures might be a useful way for checking signatures for authenticity. However, comparing two single trials should be avoided as signatures differ and both x-coordinates and y-coordinates might occasionally not correlate despite of being produced by the same subject. Moreover, x- and y-coordinates could be traced by forgers or one could learn to reproduce some one else's signature, which in both cases would lead to high correlations between the coordinates of the authentic and copied signature.

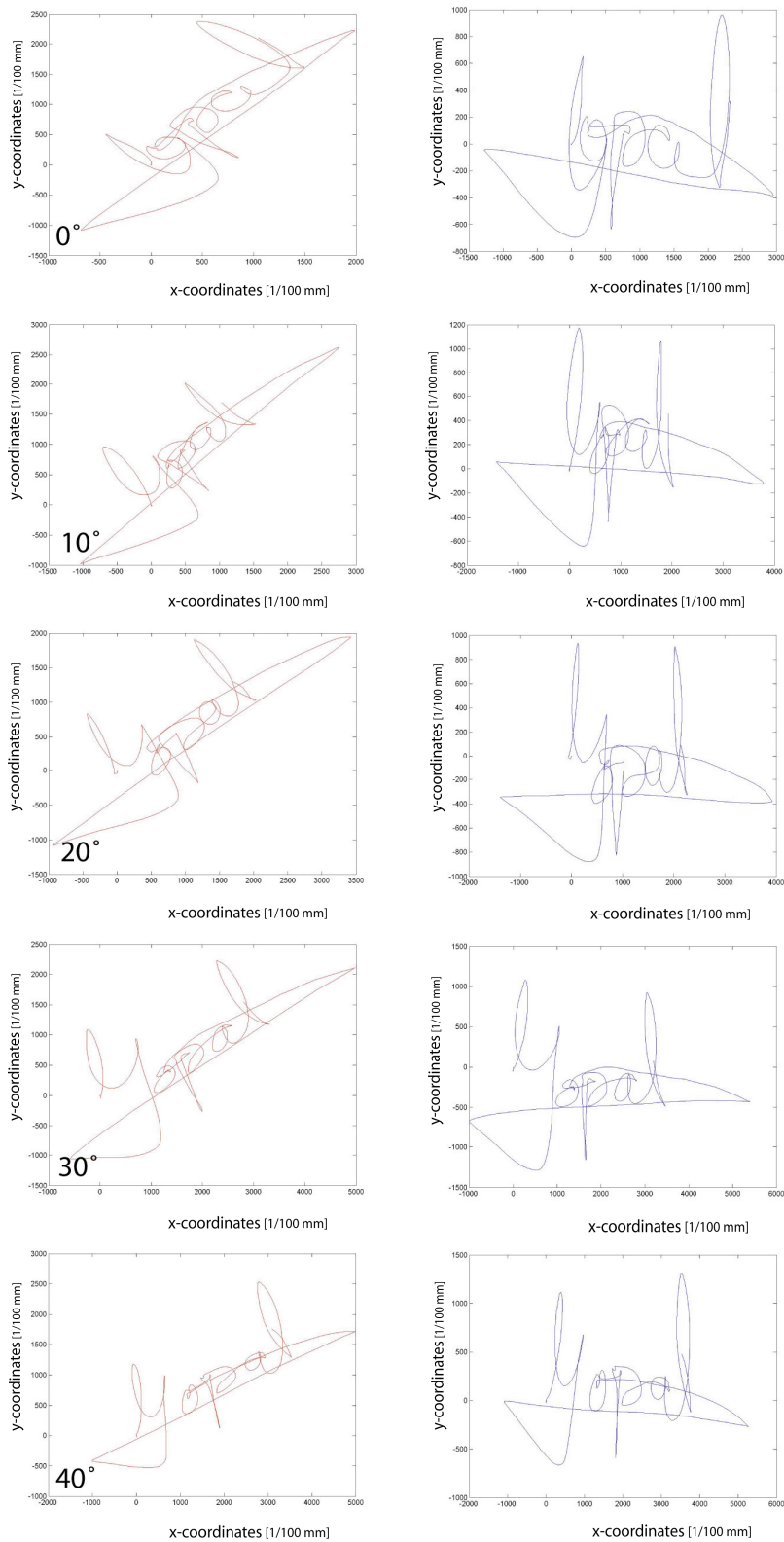


*Fig.8.3a: Rotation and translation of signatures written with incline angle of 0 - 40° by subject*

1.

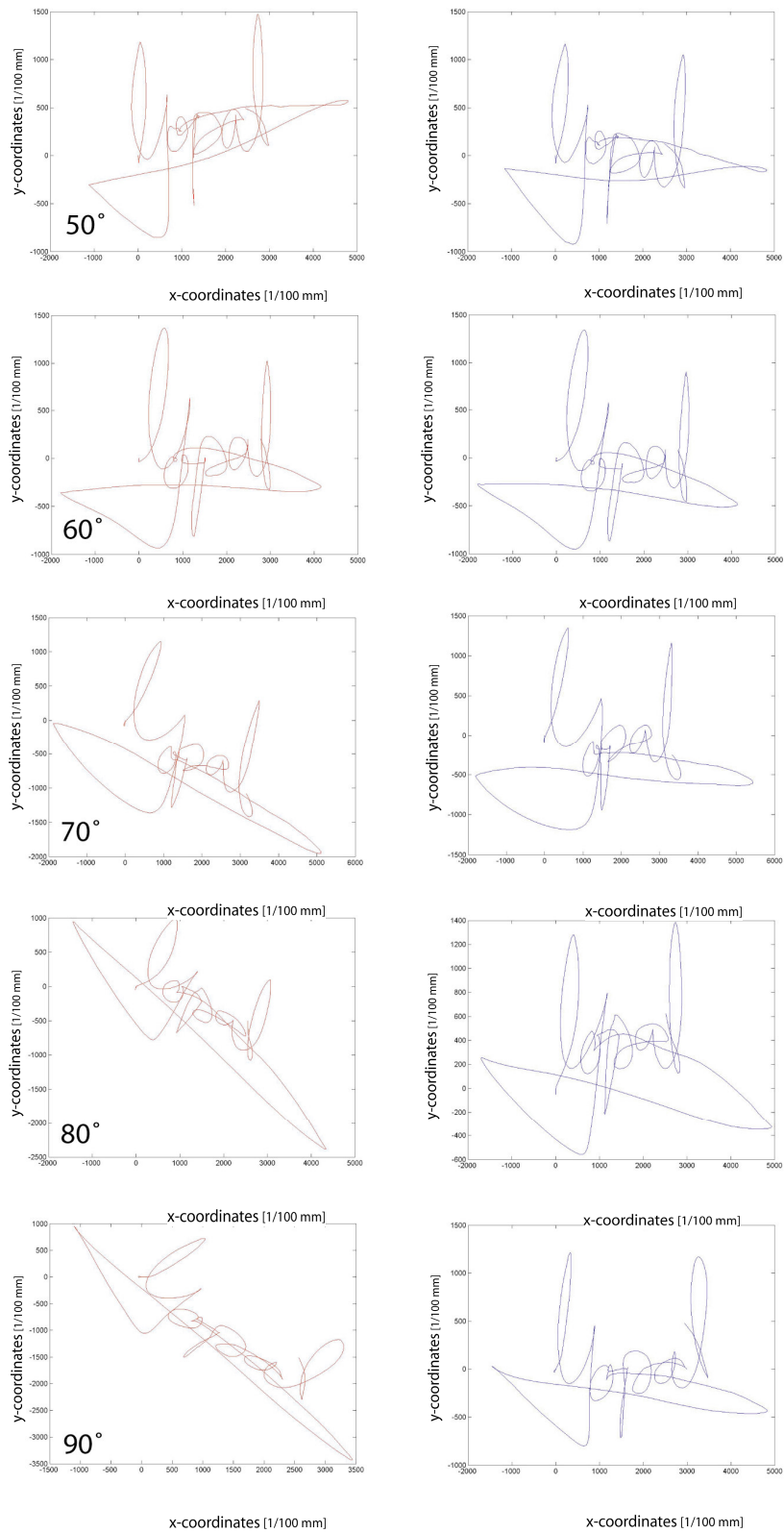


**Fig.8.3b:** Rotation and translation of signatures written with incline angle of 50 - 90 ° by subject 1.

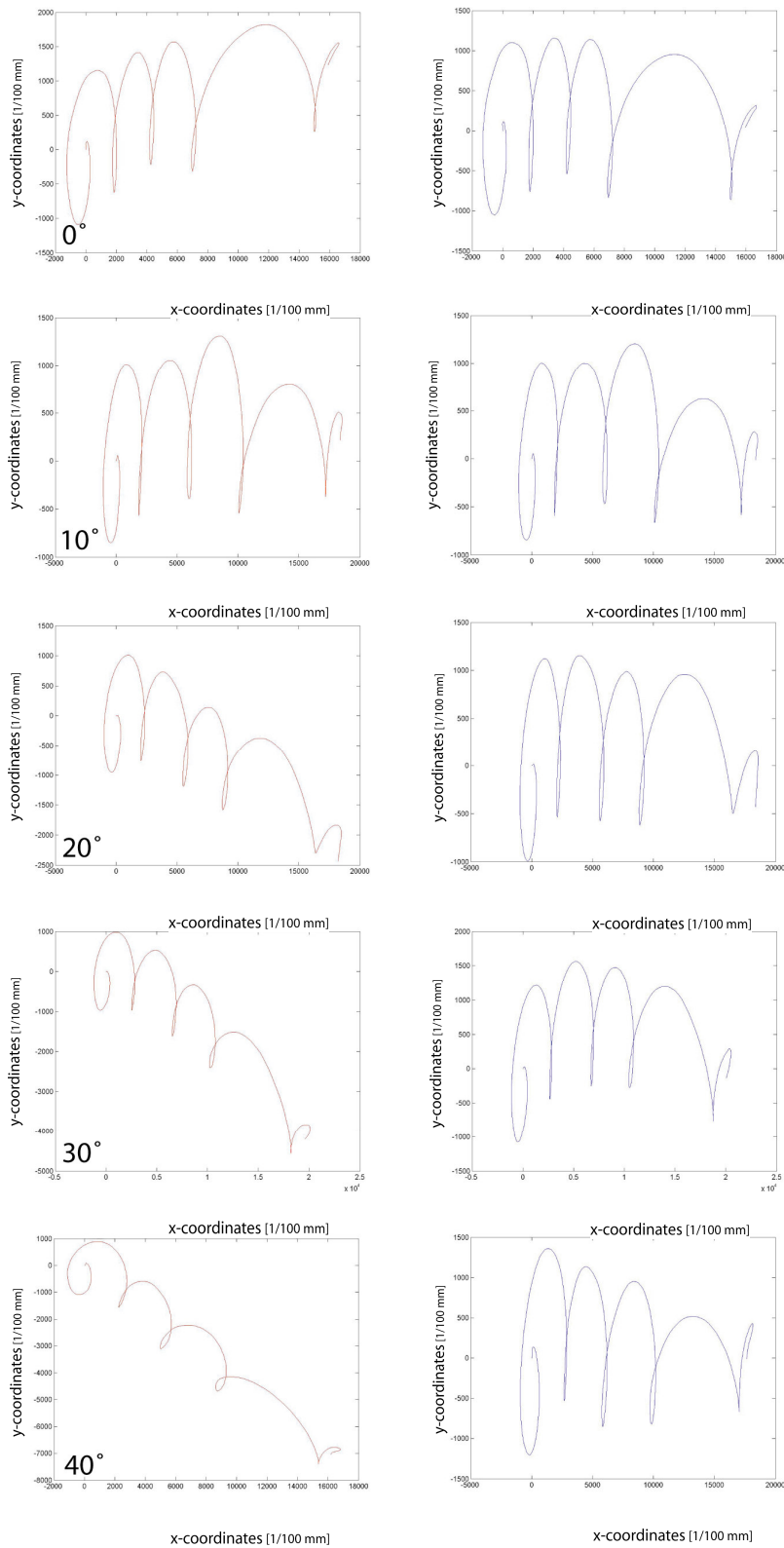


*Fig.8.4a: Rotation and translation of signatures written with incline angle of 10 -40 ° by subject 2.*

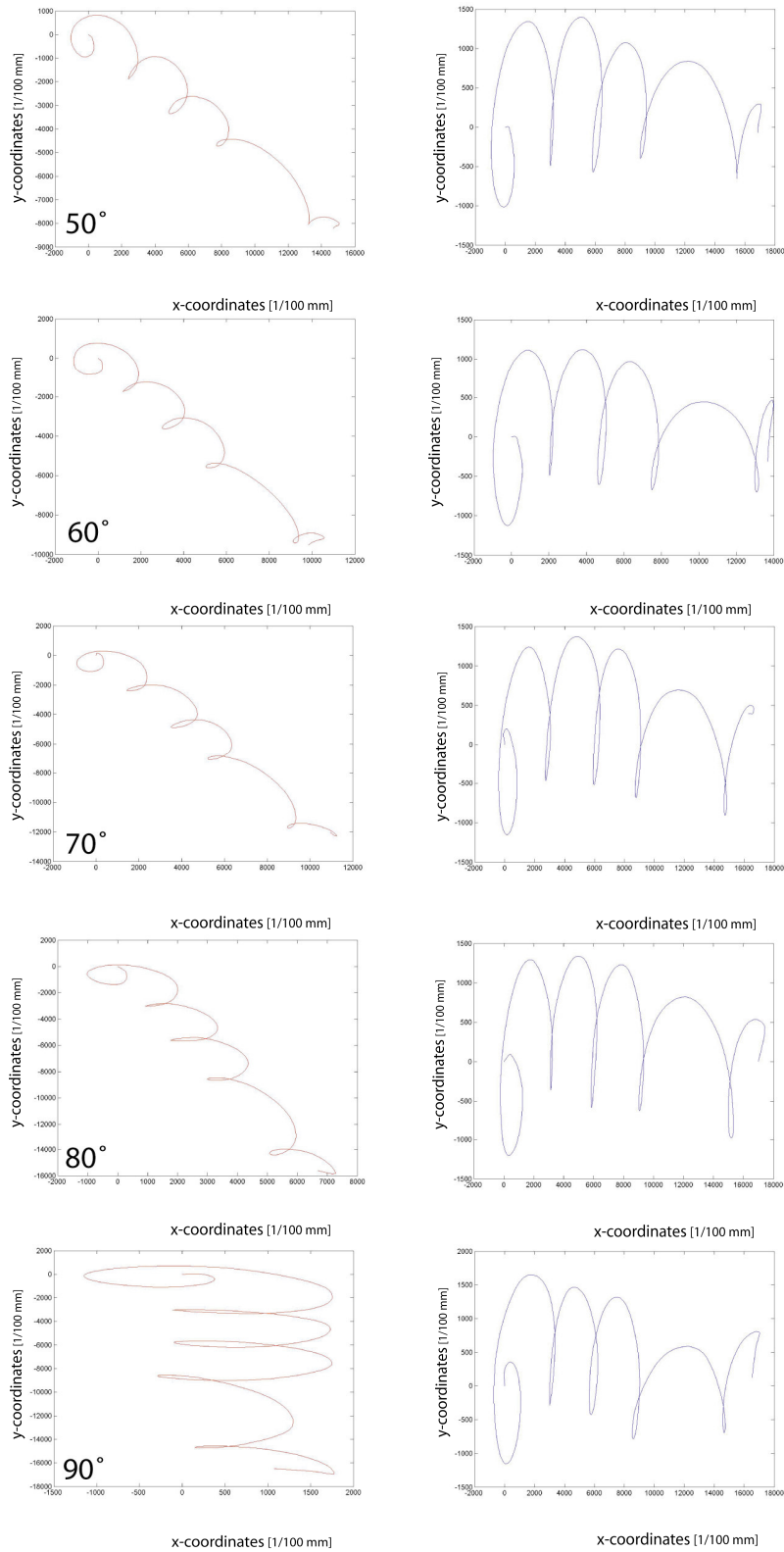


*Fig.8.4b: Rotation and translation of signatures written with incline angle of 50 -90° by subject 2.*

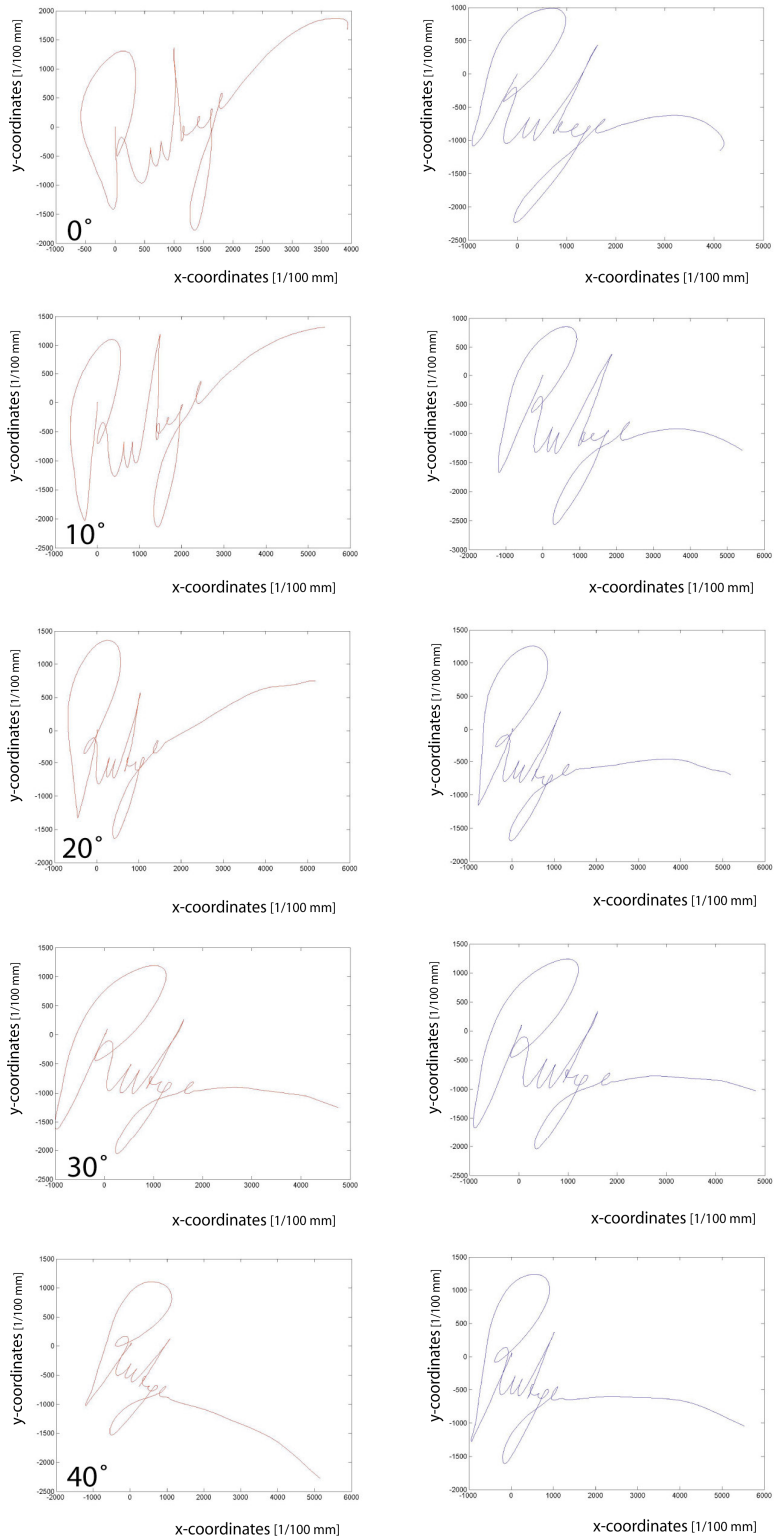


**Fig.8.5a:** Rotation and translation of signatures written with incline angle of 10 -40° by subject 4.

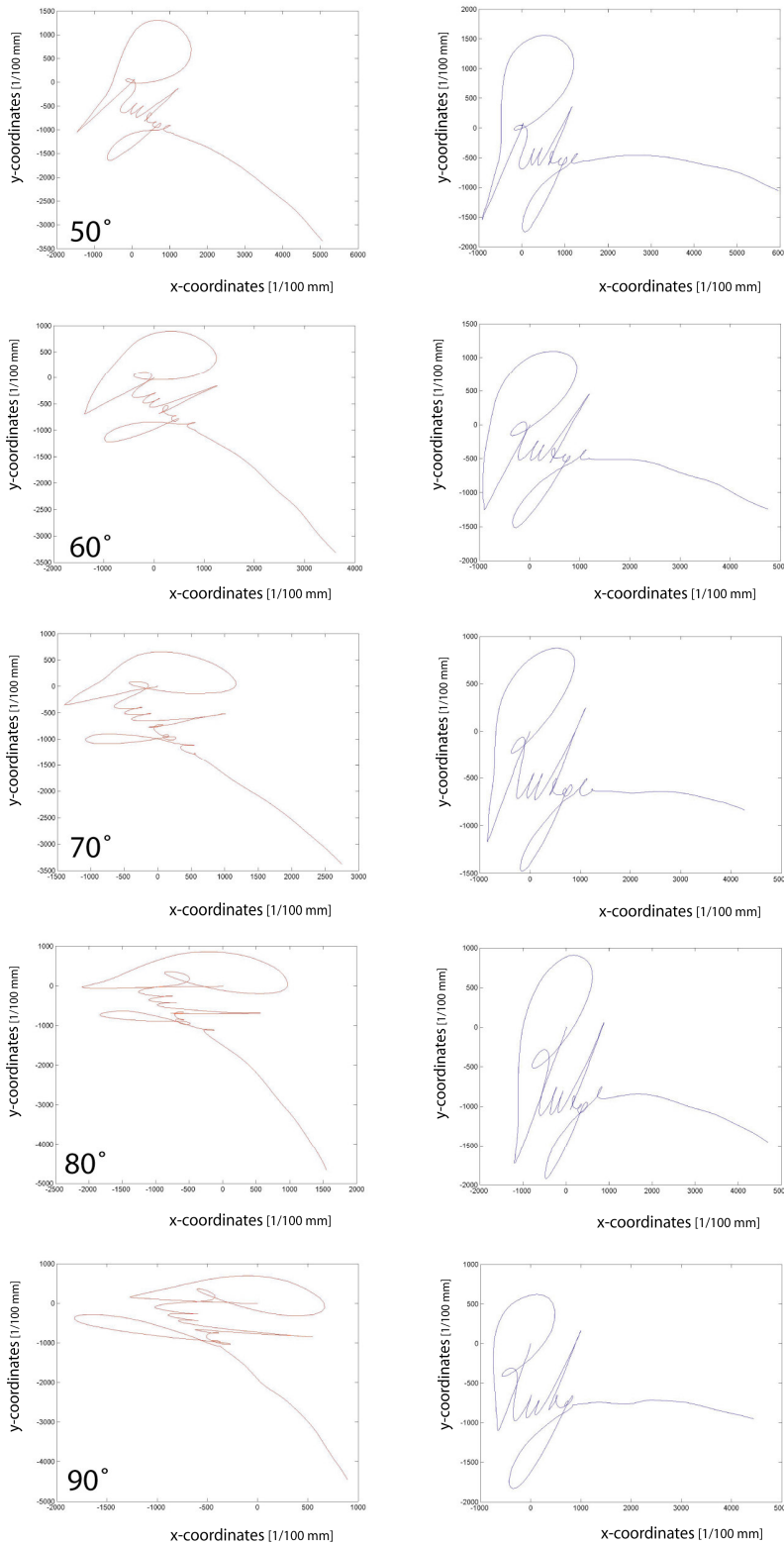


Fig.8.5b: Rotation and translation of signatures written with incline angle of 50 -90° by subject 4.

Subjects 1, 2 and 4: Correlation coefficient (x,y- and z-coordinates) of signatures with tablet orientation angles from 0° to 90°

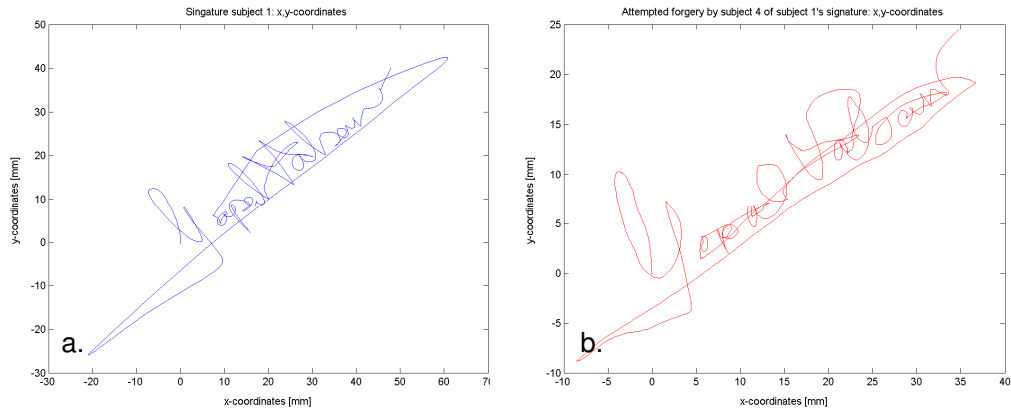
Subject 1			
incline=0°	incline=10°	incline=20°	incline=30°
rx =	1.0000 0.9370 0.9370 1.0000	1.0000 0.9438 0.9438 1.0000	1.0000 0.8702 0.8702 1.0000
ry =	1.0000 0.8563 0.8563 1.0000	1.0000 0.7970 0.7970 1.0000	1.0000 0.5604 0.5604 1.0000
rz =	1.0000 0.8923 0.8923 1.0000	1.0000 0.8613 0.8613 1.0000	1.0000 0.7627 0.7627 1.0000
	incline=40°	incline=50°	incline=60°
rx =	1.0000 0.8836 0.8836 1.0000	1.0000 0.8651 0.8651 1.0000	1.0000 0.9182 0.9182 1.0000
ry =	1.0000 0.5453 0.5453 1.0000	1.0000 0.4666 0.4666 1.0000	1.0000 0.4164 0.4164 1.0000
rz =	1.0000 0.7275 0.7275 1.0000	1.0000 0.6935 0.6935 1.0000	1.0000 0.5597 0.5597 1.0000
	incline=70°	incline=80°	incline=90°
rx =	1.0000 0.9472 0.9472 1.0000	1.0000 0.7272 0.7272 1.0000	1.0000 0.9527 0.9527 1.0000
ry =	1.0000 0.6162 0.6162 1.0000	1.0000 0.7437 0.7437 1.0000	1.0000 0.5336 0.5336 1.0000
rz =	1.0000 0.7968 0.7968 1.0000	1.0000 0.7522 0.7522 1.0000	1.0000 0.9600 0.9600 1.0000
Subject 3			
incline=0°	incline=10°	incline=20°	incline=30°
rx =	1.0000 0.9916 0.9916 1.0000	1.0000 0.9953 0.9953 1.0000	1.0000 0.9888 0.9888 1.0000
ry =	1.0000 0.8736 0.8736 1.0000	1.0000 0.7961 0.7961 1.0000	1.0000 0.6458 0.6458 1.0000
rz =	1.0000 0.9880 0.9880 1.0000	1.0000 0.9788 0.9788 1.0000	1.0000 0.9360 0.9360 1.0000
	incline=40°	incline=50°	incline=60°
rx =	1.0000 0.9907 0.9907 1.0000	1.0000 0.9832 0.9832 1.0000	1.0000 0.9882 0.9882 1.0000
ry =	1.0000 0.7929 0.7929 1.0000	1.0000 0.5636 0.5636 1.0000	1.0000 0.7351 0.7351 1.0000
rz =	1.0000 0.9541 0.9541 1.0000	1.0000 0.9845 0.9845 1.0000	1.0000 0.9557 0.9557 1.0000
	incline=70°	incline=80°	incline=90°
rx =	1.0000 0.9905 0.9905 1.0000	1.0000 0.9095 0.9095 1.0000	1.0000 0.9813 0.9813 1.0000
ry =	1.0000 0.8928 0.8928 1.0000	1.0000 0.4456 0.4456 1.0000	1.0000 0.7265 0.7265 1.0000
rz =	1.0000 0.9095 0.9095 1.0000	1.0000 0.9710 0.9710 1.0000	1.0000 0.9600 0.9600 1.0000
Subject 4			
incline=0°	incline=10°	incline=20°	incline=30°
rx =	1.0000 0.9550 0.9550 1.0000	1.0000 0.9401 0.9401 1.0000	1.0000 0.9495 0.9495 1.0000
ry =	1.0000 0.8668 0.8668 1.0000	1.0000 0.8542 0.8542 1.0000	1.0000 0.8045 0.8045 1.0000
rz =	1.0000 0.3547 0.3547 1.0000	1.0000 0.4034 0.4034 1.0000	1.0000 0.4562 0.4562 1.0000
	incline=40°	incline=50°	incline=60°
rx =	1.0000 0.9109 0.9109 1.0000	1.0000 0.8207 0.8207 1.0000	1.0000 0.9482 0.9482 1.0000
ry =	1.0000 0.7101 0.7101 1.0000	1.0000 0.0778 0.0778 1.0000	1.0000 0.8361 0.8361 1.0000
rz =	1.0000 0.5058 0.5058 1.0000	1.0000 0.3504 0.3504 1.0000	1.0000 0.6030 0.6030 1.0000
	incline=70°	incline=80°	incline=90°
rx =	1.0000 0.9173 0.9173 1.0000	1.0000 0.7284 0.7284 1.0000	1.0000 0.8971 0.8971 1.0000
ry =	1.0000 0.7284 0.7284 1.0000	1.0000 0.6697 0.6697 1.0000	1.0000 0.9162 0.9162 1.0000
rz =	1.0000 0.4617 0.4617 1.0000	1.0000 0.6129 0.6129 1.0000	1.0000 0.4238 0.4238 1.0000

Table 8.2: Correlation coefficient for x-,y- and z-coordinates after rotation and translation of signatures written with incline angle of 10 -90° by subject 1, 2 and 4.

### 8.3.2.2 Comparison of counterfeited to original signatures

#### **Comparing x,y-Coordinates**

A signature could be counterfeited by reproducing the x,y- coordinates, which will give high correlations between the coordinates of the authentic and the copied signature. An example is shown in Fig.8.6. Although the signatures differ in size, similarities in script can be recognised. The correlation between the trials is 30% for both x-coordinates and y-coordinates and 1% for z-coordinates. Normalisation of the original and forged signature to compensate for the difference in writing speed, could increase the correlation of z-coordinates up to 30%, but did not increase the correlation of the x- and y-coordinates.



*Fig.8.6: x,y-Coordinates:*

*a.: for subject 1' signature;*

*b.: for attempted forgery of subject 1' signature by subject 4.*

### ***Comparing pen tip velocity***

The Matlab script was extended with derivatives of the pen tip displacement. This was included since pen tip velocity reveals more about the writing process and may reflect the authenticity of a signature when the x,y- and -coordinates do not. Vertical (y-direction) pen tip velocity for two trials by subject 1 is shown in Fig.8.7a. The correlation coefficient between the two velocity profiles is 81%. Fig.8.7b shows the velocity profiles during two attempts to forge subject 1's signature and the two trials correlate for only 16%. Differences in tip velocity and consequent writing time between the two subjects can also be observed. The timing aspect of the well developed neuromuscular processes involved with normal signature writing seem reasonably consistent for one subject as one would expect. However, the timing (velocity) of processes involved with reproduction of someone else's signature are different from the original signature. In addition, the velocity of two attempts to forge someone else's signature are seen to be inconsistent

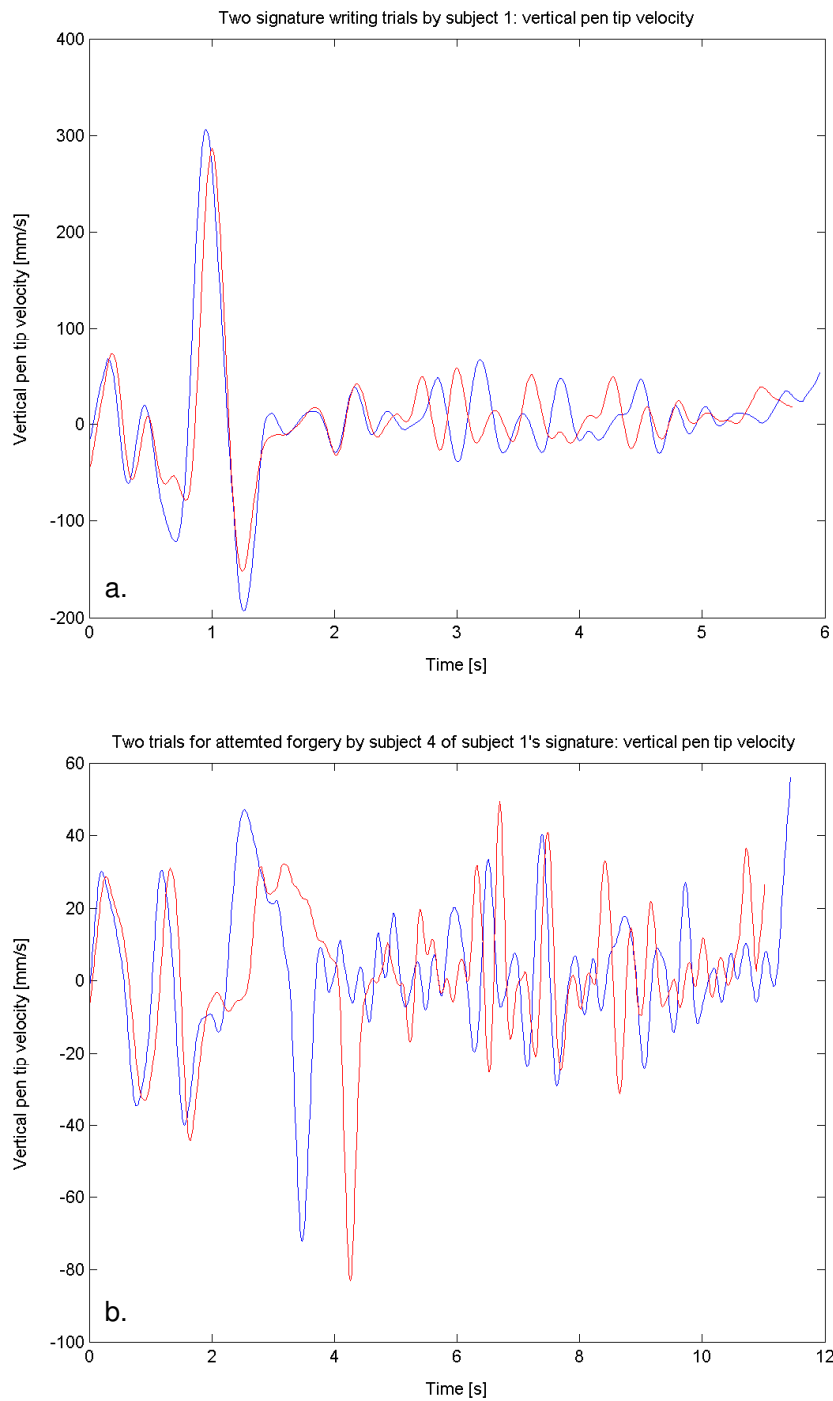


*Fig.8.7: Pen tip velocity profiles:*

*a: two trials performed by subject subject 1; correlation coefficient is  $r=0.81$ ;*

*b: two trials performed by subjet 4 attempting to counterfeit subject 1's signature; correlation coefficient  $r=0.16$ .*

The comparison between vertical pen tip velocity of a signature by subject 1 and an attempt to forge the signature by subject 4 is presented in Fig.8.8. There is no correlation between the two signals seen in Fig.8.8a. In fact the correlation coefficient has a low negative value, revealing that by chance the two signals have a partly opposite pattern. Normalising the two signals makes the profiles resemble stronger as seen in Fig.8.8b. As a result of normalisation, the correlation rises from  $r=-0.07$  to  $r=0.33$ .

It can be concluded that including analysis of pen tip velocity into a signature verification script may allow a more reliable judgement on the authenticity of a signature. However, one could still practice the writing speed in order to accurately simulate the pen tip movement in space and time. Therefore, there is a need for other signature verification techniques (not based on velocity) that give more insights in how the writing was produced. Pen tip velocity is just one measurable parameter that allows to measure the writing process and not just the result. The next section assesses the potential of measuring pen grip force as a representation of the pen-hand interaction during the writing process.

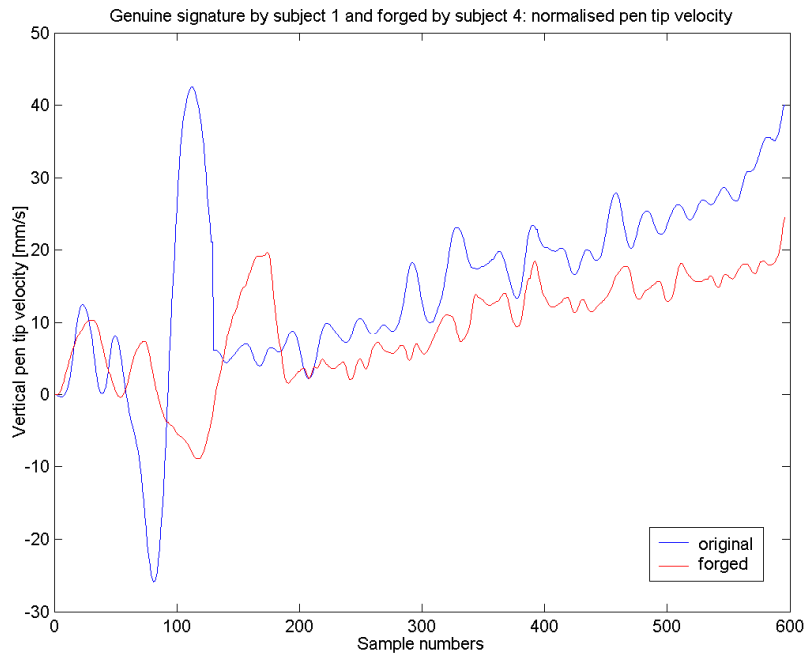
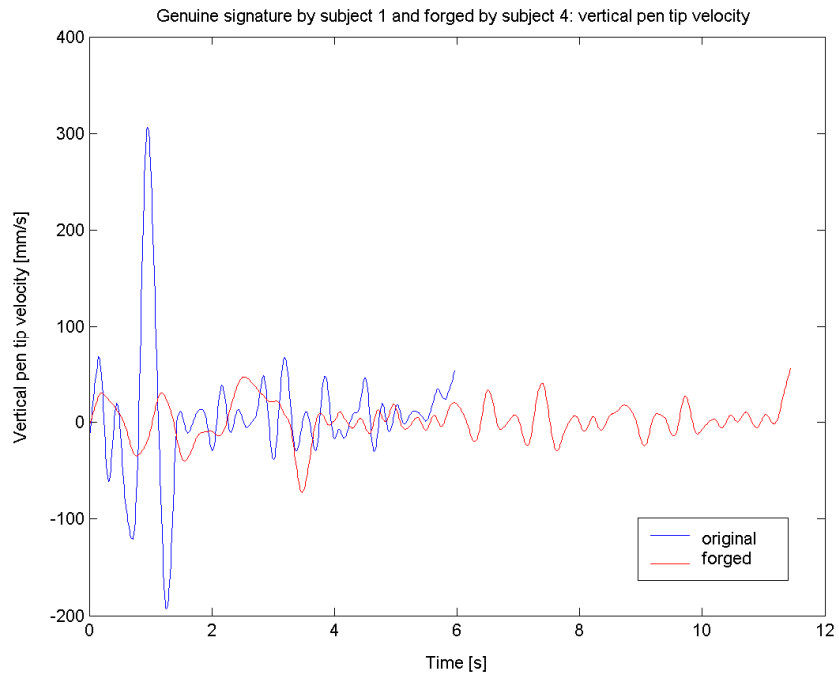


*Fig.8.8: Pen tip velocity profiles for subject 1's signature and attempt to counterfeit the signature by subject 4:*

*a: Pen tip velocity as function of time; correlation coefficient is  $r=-0.07$ ;*

*b: normalised pen tip velocity; correlation coefficient is  $r=0.33$ .*

## 8.4 Part II - Grip force comparison: methods for data analysis

### 8.4.1 Activity: comparing grip force

The second activity was performed to assess the consistency of individual finger grip forces that are applied to the pen during signature writing. Each subject repeated the signature twelve times. There was no time restriction to the task and subjects were not restricted to specific starting point or signature orientation on the tablet.

### 8.4.2 Data analysis: comparing grip force signals

#### 8.4.2.1 Pen grip characteristics: comparing signatures produced by one subject

For the assessment of authenticity of signatures, it is expected that the processes involved with producing signatures is more revealing than the final writing result as the comparison of writing velocity in paragraph 8.3.1 suggests. The pen-hand interaction, resulting from the fine motor control of distal joint muscles, plays an important role in the writing process. The pen-hand interaction can be measured as grip force. The grip force characteristics during signature writing are investigated here.

For illustration purpose Fig. 8.9 shows the Thumb, Index and Middle finger force patterns for the 12 signatures by subject 4. It is striking how the grip patterns resemble in all trials. In addition, the force values are seen to decrease from the first to the last trial. The correlation of finger force patterns between the 12 trials for subjects 1, 3 and 4 are presented in Table 8.3, Table 8.4 and Table 8.5, respectively. The average correlation between 12 trials for each finger is presented along with standard deviation in Table 8.6 for all three subjects. In addition, the correlation between trials for each of the three finger force patterns for subjects 3 is continuously seen to be higher than 80% (Table 8.4 and Table 8.6). For subject 4 there seems more variation and lower correlation coefficient with an average value of 70% can be seen (Table 8.5 and Table 8.6). For subject 1 the average correlation is below 50% for all three fingers (Table 8.3 and Table 8.6). However, comparing the

finger force patterns between trials for each subject reveals that the patterns of peaks and troughs are very similar. When low correlations are observed, they mostly seem to originate from differences in timing. This is illustrated in Fig.8.10 for two signatures by subject 1: despite of the Thumb, Index and Middle finger force patterns of trials 6 and 7 being very similar, they do not correlate for more than 1%. The reason is that from  $t=1.6$  seconds (sample number=1600) the force patterns are out of phase as a result of changes in the writing speed.

Fig.8.11 shows the grip force patterns in trial 7 and 9 by subject 4 for Thumb, Index and Middle finger forces with correlations of 32%, 41% and 54% respectively.

Although the same peaks and troughs can be recognized in both trials, the correlation is not any higher than 54%, which can be explained from the difference in writing velocity during the first part of the trials. The force pattern during the first 1.3 seconds of trial 7 can be recognised in trial 9, but is only taking around 0.6 seconds. The difference in writing velocity during the first part of the trials explains why the force patterns are out of phase.

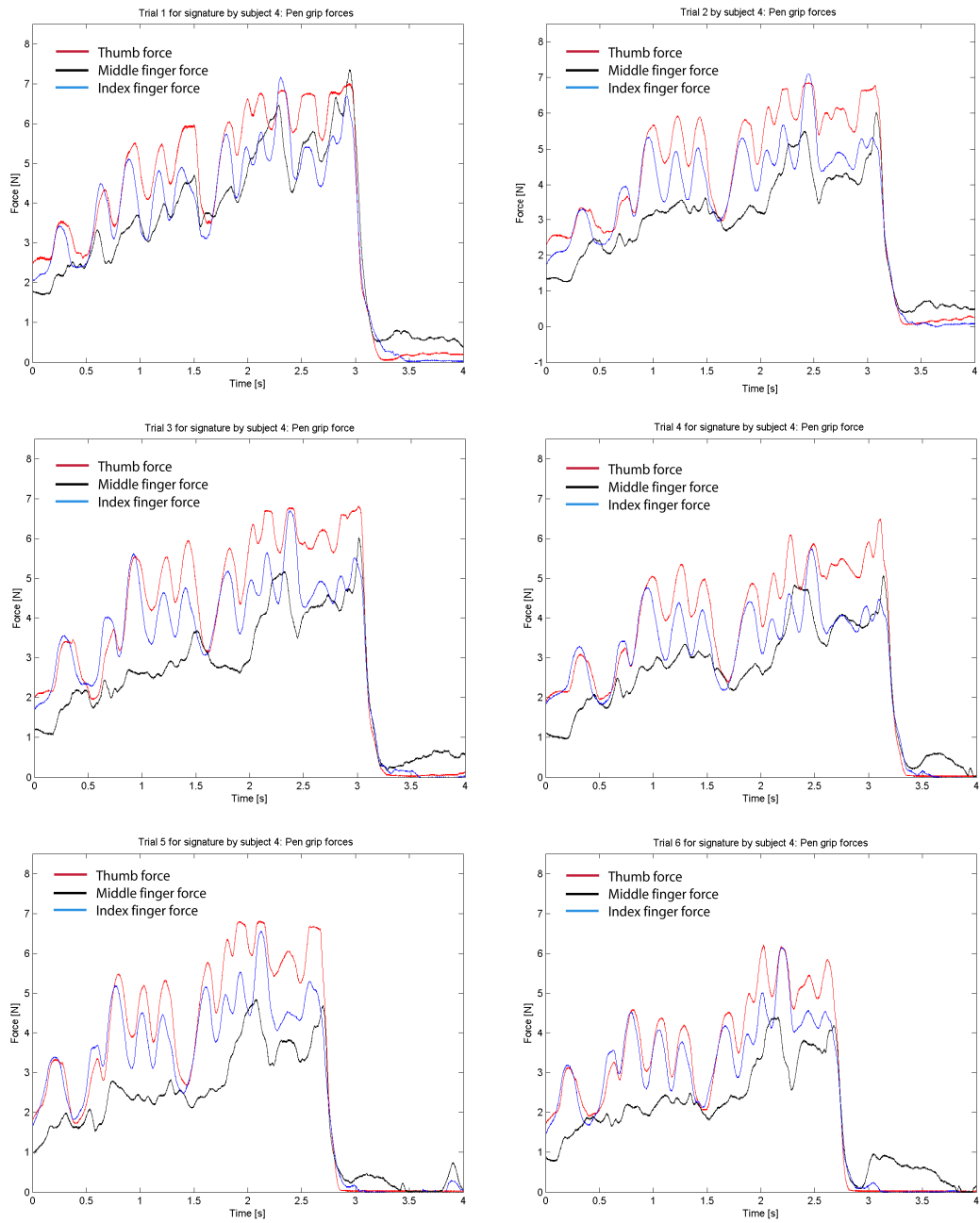


Fig.8.9a: Pen grip forces for signatures by subject 4: trials 1 to 6.

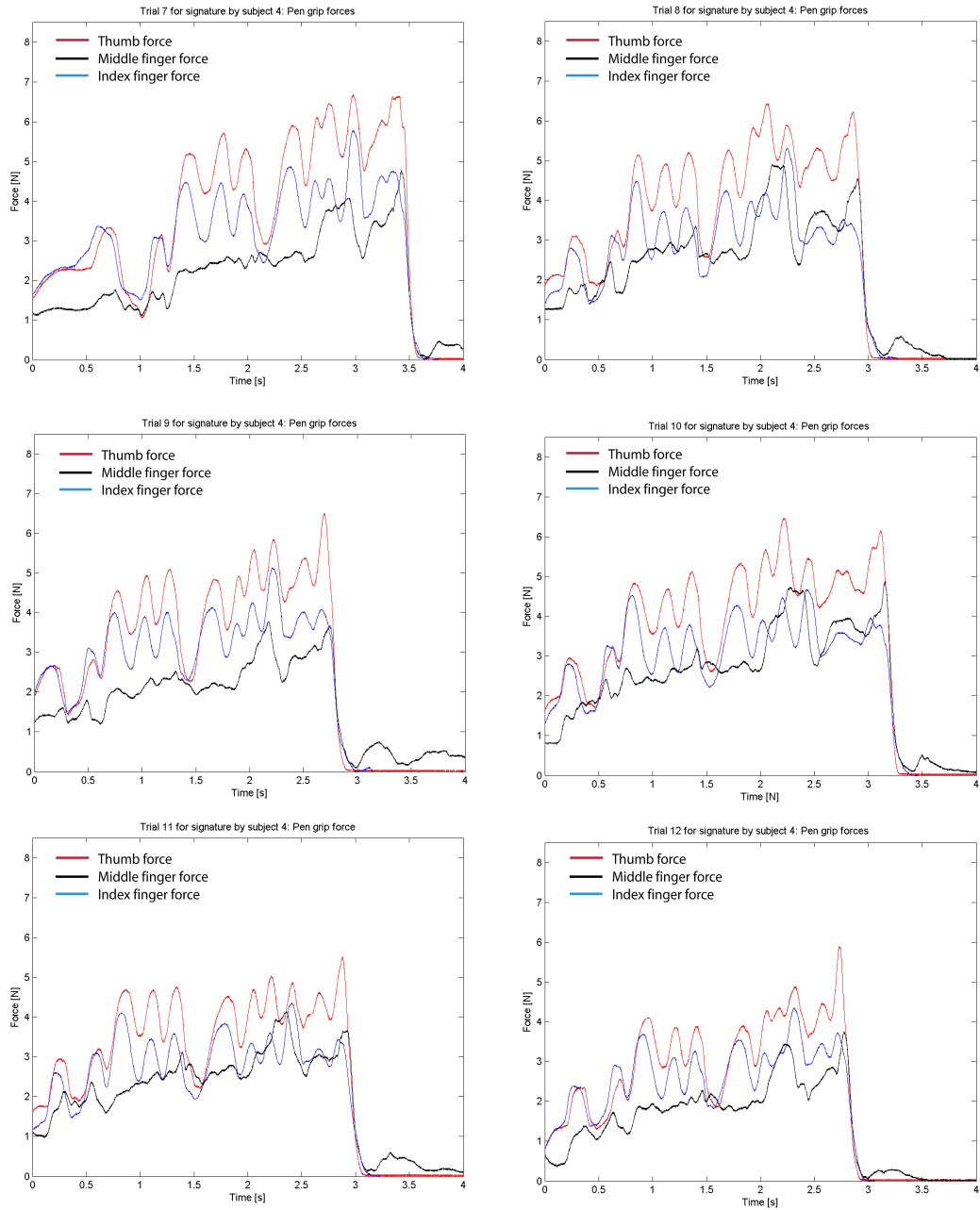


Fig.8.9b: Pen grip forces for signatures by subject 4: trials 7 to 12.

## Finger force correlations between 12 trials by subject 1

### Thumb

	1	2	3	4	5	6	7	8	9	10	11	12
1	0	0.455	0.633	0.393	0.325	0.183	0.625	0.409	0.343	0.334	0.394	0.349
2	0	0	0.268	0.345	0.239	-0.033	0.531	0.339	0.237	0.296	0.337	0.107
3	0	0	0	0.442	0.418	0.156	0.707	0.385	0.339	0.420	0.410	0.201
4	0	0	0	0	0.558	0.279	0.455	0.349	0.723	0.542	0.624	0.329
5	0	0	0	0	0	0.428	0.354	0.691	0.735	0.730	0.569	0.491
6	0	0	0	0	0	0	0.050	0.470	0.444	0.495	0.445	0.773
7	0	0	0	0	0	0	0	0.439	0.389	0.418	0.398	0.213
8	0	0	0	0	0	0	0	0	0.547	0.820	0.517	0.608
9	0	0	0	0	0	0	0	0	0	0.625	0.619	0.453
10	0	0	0	0	0	0	0	0	0	0	0.503	0.521
11	0	0	0	0	0	0	0	0	0	0	0	0.549
12	0	0	0	0	0	0	0	0	0	0	0	0

### Middle

	1	2	3	4	5	6	7	8	9	10	11	12
1	0	0.354	0.432	0.030	0.294	0.122	0.339	0.417	0.207	0.226	0.369	0.299
2	0	0	0.023	0.085	0.120	0.009	0.302	0.268	0.080	0.237	0.343	0.260
3	0	0	0	0.148	0.322	0.141	0.479	0.440	0.134	0.237	0.274	0.179
4	0	0	0	0	0.200	0.260	0.175	0.054	0.497	0.109	0.252	0.134
5	0	0	0	0	0	0.392	0.124	0.661	0.497	0.556	0.384	0.395
6	0	0	0	0	0	0	-0.077	0.462	0.304	0.306	0.286	0.615
7	0	0	0	0	0	0	0	0.304	0.079	0.274	0.269	0.095
8	0	0	0	0	0	0	0	0	0.238	0.622	0.433	0.548
9	0	0	0	0	0	0	0	0	0	0.187	0.434	0.235
10	0	0	0	0	0	0	0	0	0	0	0.249	0.373
11	0	0	0	0	0	0	0	0	0	0	0	0.466
12	0	0	0	0	0	0	0	0	0	0	0	0

### Index

	1	2	3	4	5	6	7	8	9	10	11	12
1	0	0.298	0.619	0.209	0.447	0.375	0.367	0.598	0.259	0.343	0.478	0.491
2	0	0	0.513	0.268	0.340	0.154	0.531	0.512	0.241	0.334	0.528	0.323
3	0	0	0	0.188	0.372	0.446	0.262	0.571	0.154	0.263	0.412	0.400
4	0	0	0	0	0.586	0.490	0.181	0.600	0.365	0.407	0.348	0.363
5	0	0	0	0	0	0.477	0.161	0.716	0.244	0.567	0.310	0.445
6	0	0	0	0	0	0	0.013	0.554	0.213	0.288	0.286	0.530
7	0	0	0	0	0	0	0	0.548	0.145	0.265	0.474	0.375
8	0	0	0	0	0	0	0	0	0.089	0.546	0.222	0.443
9	0	0	0	0	0	0	0	0	0	0.504	0.438	0.458
10	0	0	0	0	0	0	0	0	0	0	0.287	0.455
11	0	0	0	0	0	0	0	0	0	0	0	0.525
12	0	0	0	0	0	0	0	0	0	0	0	0

Table.8.3: Correlation coefficient between 12 signatures for Thumb, Index and Middle finger forces by subject 1.

## Finger force correlations between 12 trials by subject 3

### Thumb

	1	2	3	4	5	6	7	8	9	10	11	12
1	0	0.906	0.780	0.808	0.880	0.882	0.872	0.865	0.900	0.857	0.925	0.907
2	0	0	0.804	0.801	0.935	0.958	0.943	0.933	0.895	0.868	0.897	0.960
3	0	0	0	0.713	0.822	0.844	0.830	0.856	0.793	0.838	0.845	0.820
4	0	0	0	0	0.872	0.811	0.796	0.802	0.755	0.808	0.827	0.819
5	0	0	0	0	0	0.940	0.952	0.912	0.853	0.910	0.888	0.920
6	0	0	0	0	0	0	0.966	0.960	0.922	0.877	0.895	0.939
7	0	0	0	0	0	0	0	0.930	0.908	0.905	0.899	0.933
8	0	0	0	0	0	0	0	0	0.925	0.873	0.884	0.925
9	0	0	0	0	0	0	0	0	0	0.860	0.887	0.923
10	0	0	0	0	0	0	0	0	0	0	0.951	0.889
11	0	0	0	0	0	0	0	0	0	0	0	0.906
12	0	0	0	0	0	0	0	0	0	0	0	0

### Middle

	1	2	3	4	5	6	7	8	9	10	11	12
1	0	0.929	0.767	0.804	0.906	0.895	0.903	0.860	0.866	0.888	0.886	0.883
2	0	0	0.841	0.861	0.938	0.932	0.951	0.941	0.899	0.916	0.937	0.931
3	0	0	0	0.748	0.817	0.845	0.848	0.891	0.809	0.779	0.866	0.807
4	0	0	0	0	0.885	0.851	0.832	0.826	0.755	0.733	0.843	0.772
5	0	0	0	0	0	0.934	0.934	0.908	0.878	0.866	0.885	0.884
6	0	0	0	0	0	0	0.959	0.941	0.925	0.894	0.905	0.889
7	0	0	0	0	0	0	0	0.927	0.929	0.931	0.927	0.903
8	0	0	0	0	0	0	0	0	0.880	0.885	0.912	0.895
9	0	0	0	0	0	0	0	0	0	0.923	0.884	0.915
10	0	0	0	0	0	0	0	0	0	0	0.903	0.918
11	0	0	0	0	0	0	0	0	0	0	0	0.907
12	0	0	0	0	0	0	0	0	0	0	0	0

### Index

	1	2	3	4	5	6	7	8	9	10	11	12
1	0	0.906	0.752	0.734	0.874	0.852	0.871	0.833	0.806	0.807	0.795	0.831
2	0	0	0.730	0.792	0.888	0.821	0.828	0.802	0.788	0.824	0.835	0.833
3	0	0	0	0.679	0.721	0.736	0.744	0.730	0.734	0.696	0.788	0.701
4	0	0	0	0	0.787	0.797	0.757	0.752	0.689	0.709	0.794	0.717
5	0	0	0	0	0	0.780	0.790	0.740	0.741	0.784	0.796	0.778
6	0	0	0	0	0	0	0.844	0.814	0.828	0.817	0.841	0.842
7	0	0	0	0	0	0	0	0.817	0.824	0.824	0.873	0.831
8	0	0	0	0	0	0	0	0	0.887	0.860	0.896	0.866
9	0	0	0	0	0	0	0	0	0	0.826	0.833	0.833
10	0	0	0	0	0	0	0	0	0	0	0.904	0.901
11	0	0	0	0	0	0	0	0	0	0	0	0.888
12	0	0	0	0	0	0	0	0	0	0	0	0

Table.8.4: Correlation coefficient between 12 signatures for Thumb, Index and Middle finger forces by subject 3.

## Finger force correlations between 12 trials by subject 4

### Thumb

	1	2	3	4	5	6	7	8	9	10	11	12
1	0	0.916	0.777	0.918	0.779	0.884	0.366	0.613	0.971	0.520	0.862	0.823
2	0	0	0.860	0.829	0.694	0.970	0.432	0.693	0.879	0.609	0.940	0.933
3	0	0	0	0.713	0.562	0.864	0.525	0.770	0.755	0.685	0.908	0.910
4	0	0	0	0	0.827	0.798	0.283	0.520	0.927	0.435	0.791	0.759
5	0	0	0	0	0	0.625	0.278	0.394	0.766	0.345	0.667	0.588
6	0	0	0	0	0	0	0.410	0.681	0.853	0.589	0.945	0.941
7	0	0	0	0	0	0	0.000	0.740	0.324	0.900	0.424	0.412
8	0	0	0	0	0	0	0	0	0.581	0.864	0.689	0.698
9	0	0	0	0	0	0	0	0	0	0.486	0.820	0.807
10	0	0	0	0	0	0	0	0	0	0	0.614	0.615
11	0	0	0	0	0	0	0	0	0	0	0	0.944
12	0	0	0	0	0	0	0	0	0	0	0	0

### Middle

	1	2	3	4	5	6	7	8	9	10	11	12
1	0	0.890	0.753	0.906	0.753	0.860	0.377	0.642	0.977	0.463	0.863	0.824
2	0	0	0.833	0.829	0.707	0.965	0.425	0.702	0.880	0.579	0.924	0.921
3	0	0	0	0.668	0.514	0.848	0.563	0.750	0.754	0.664	0.901	0.890
4	0	0	0	0	0.836	0.767	0.292	0.487	0.896	0.360	0.822	0.770
5	0	0	0	0	0	0.614	0.228	0.385	0.757	0.290	0.666	0.608
6	0	0	0	0	0	0	0.488	0.724	0.839	0.651	0.930	0.944
7	0	0	0	0	0	0	0	0.758	0.409	0.929	0.442	0.416
8	0	0	0	0	0	0	0	0	0.646	0.832	0.693	0.674
9	0	0	0	0	0	0	0	0	0	0.481	0.851	0.797
10	0	0	0	0	0	0	0	0	0	0	0.608	0.604
11	0	0	0	0	0	0	0	0	0	0	0	0.972
12	0	0	0	0	0	0	0	0	0	0	0	0

### Index

	1	2	3	4	5	6	7	8	9	10	11	12
1	0	0.876	0.707	0.916	0.819	0.831	0.314	0.569	0.968	0.403	0.843	0.793
2	0	0	0.802	0.872	0.783	0.930	0.354	0.628	0.898	0.501	0.916	0.905
3	0	0	0	0.798	0.639	0.858	0.470	0.717	0.836	0.590	0.935	0.901
4	0	0	0	0	0.869	0.707	0.245	0.439	0.879	0.306	0.773	0.707
5	0	0	0	0	0	0.556	0.181	0.336	0.721	0.246	0.628	0.555
6	0	0	0	0	0	0	0.354	0.624	0.886	0.499	0.927	0.912
7	0	0	0	0	0	0	0	0.831	0.542	0.932	0.593	0.562
8	0	0	0	0	0	0	0	0	0.726	0.797	0.813	0.797
9	0	0	0	0	0	0	0	0	0	0.363	0.819	0.767
10	0	0	0	0	0	0	0	0	0	0	0.721	0.684
11	0	0	0	0	0	0	0	0	0	0	0	0.907
12	0	0	0	0	0	0	0	0	0	0	0	0

Table.8.5: Correlation coefficient between 12 signatures for Thumb, Index and Middle finger forces by subject 4.

	Subject 1			Subject 3			Subject 4		
	Thumb	Middle	Index	Thumb	Middle	Index	Thumb	Middle	Index
<b>Average correlation</b>	0.435	0.281	0.382	0.878	0.880	0.803	0.701	0.698	0.691
<b>Standard deviation</b>	0.174	0.161	0.148	0.056	0.053	0.058	0.195	0.194	0.219

Table 8.6: Average of correlation coefficient (and standard deviation) that were calculated between 12 trials for subjects 1, 3 and 4 and presented Tables 8.3, 8.4 and 8.5.

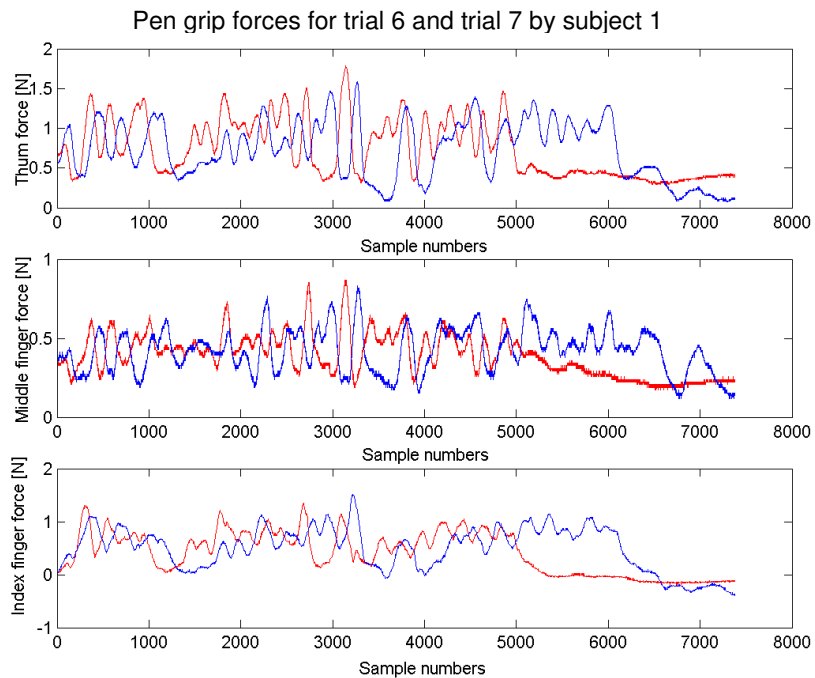
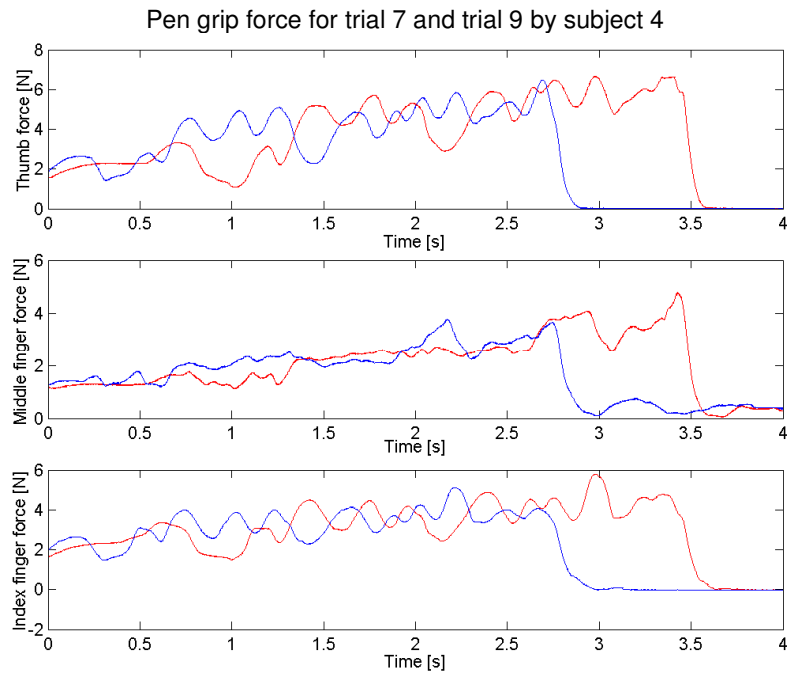


Fig. 8.10: Thumb, Index and Middle finger force patterns during trials 6 (red) and 7 (blue) of signature writing by subject 1. The finger patterns in both trials do not correlate.



*Fig. 8.11: Thumb, Index and Middle finger force patterns during trials 7 (red) and 9 (blue) of signature writing by subject 4. The Thumb, Index and Middle finger forces in both trials respectively correlate for 32%, 41% and 54%.*

#### 8.4.2.2 Summary: need for data analysis techniques for grip force assessment

Script x,y-coordinates and tip pressure were compared in 8.3. The results show that comparing script coordinates may be useful for signature verification, but not on its own. Script and signatures can be copied easily. Including the pen tip velocity seems useful as the timing reveals more about the writing process and is not limited to the resulting x,y-coordinates.

Further assessment of the process is possible by assessing the pen grip force, which allows to distinguish between genuine and couterfeited signatures as was seen in 8.4. The grip force patterns reveal the pen-hand interaction and are characteristic for individuals. The same peaks and troughs are seen. However, the timing of the writing activity and grip force peaks are variable. Therefore, a method is required that aligns the peaks and troughs to deal with the variability of time.

#### 8.4.2.3 Development data analysis techniques for comparing grip patterns

Matlab scripts were developed that compare the grip force patterns and allow to compensate for differences in timing so that the patterns become more identical whilst maintaining the individual's characteristic peaks and troughs in the force patterns. The methods are described below.

##### ***Normalisation***

The first option that was investigated, was aligning the peaks and troughs by normalisation of the force signals. To automate the process a simple Matlab script was written. For most trials by subjects 1 and 4 normalisation led to higher correlation. However, as an example the results of normalisation of the force pattern for subject 3 shown in Fig.8.12 makes clear that normalisation does not always improve the fit of two signals. Correlations after normalisation are:  $r_T=0.85$ ,  $r_M=0.87$  and  $r_I=0.73$  (for Thumb, Middle and Index finger force, respectively), whereas correlations before normalisation were:  $r_T=0.85$ ,  $r_M=0.87$  and  $r_I=0.79$  (for Thumb, Middle and Index finger force, respectively). It can be seen from Fig.8.12 also that over part of the trajectory the Thumb and Index finger force signals get stronger out of phase rather than in phase.

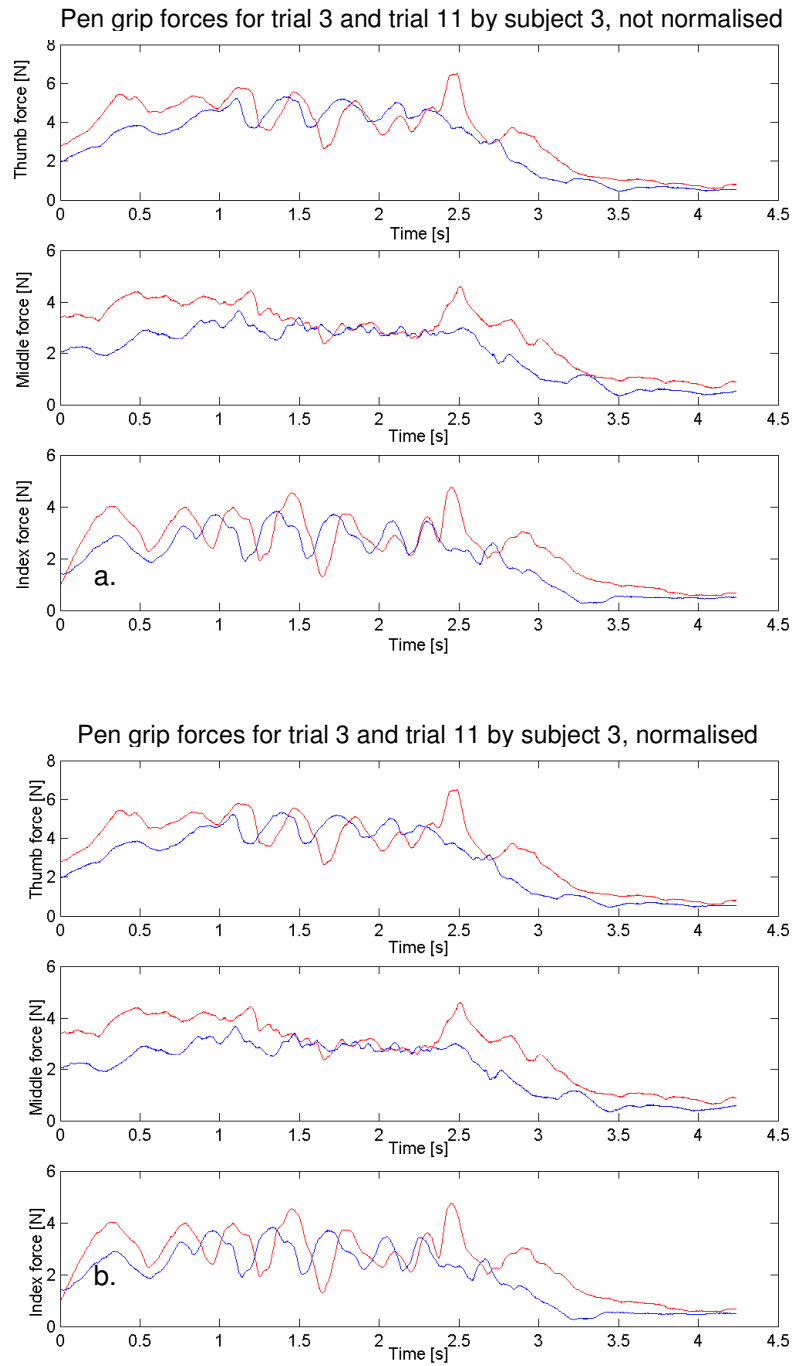


*Fig. 8.12: Thumb, Index and Middle finger force patterns during trials 3 (red) and 11 (blue) of signature writing by subject 3.*

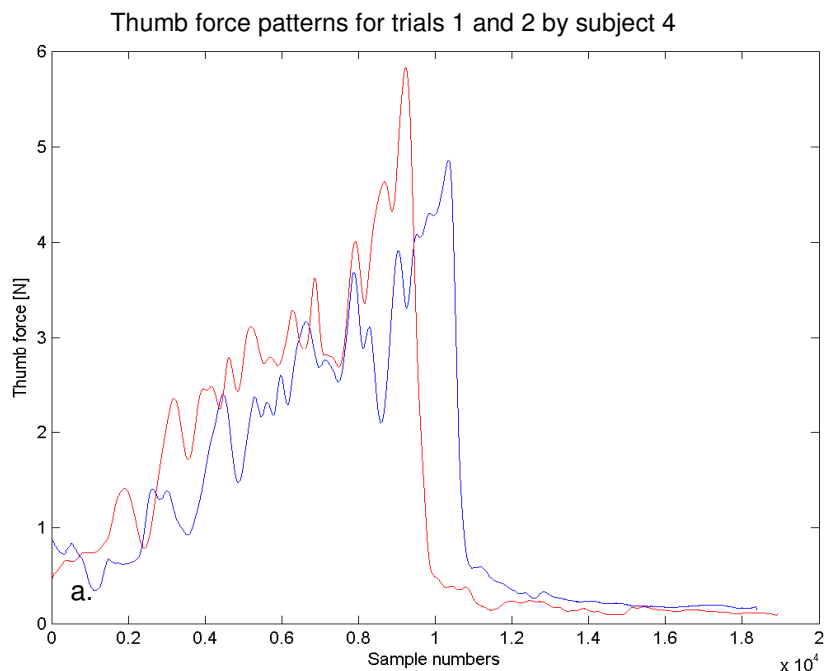
*a.: before normalisation, correlations coefficients:  $r_T=0.85$ ,  $r_M=0.87$  and  $r_I=0.79$ .*

*b.: after normalisation, correlations coefficients:  $r_T=0.85$ ,  $r_M=0.87$  and  $r_I=0.73$ .*

### **Position based segmentation for correlation**

A second technique that was developed for making the grip force patterns of two trials by one subject fit better was based on relating each sample of finger force in both trials to the actual writing coordinate (x,y). This allows both grip force patterns to be written as functions of the x,y-coordinates along the writing trajectory. Finger forces required to steer the pen tip over a certain trajectory in the x,y-plane during one trial can now be compared to finger forces applied to move the pen tip over the same trajectory in another trial. For each data point (coordinates x,y) in the first trial, the corresponding point in the second trial is found by searching for the coordinate values that are closest (using least squares calculation).

The grip force modulation of each trials for one subject's signature now correlates more strongly (Fig.8.13). However, no two signatures (x,y-coordinates) are perfectly identical and therefore sometimes the wrong point in the writing trajectory (x,y-coordinates sample) is addressed when searching in the second trial for the same x,y-coordinate values as was found in the first trial. In that case, the x,y-coordinate values of both trials that are compared do not correspond to the same pen tip trajectory. The consequence of this disadvantage of the technique on the finger force graph can be seen in Fig. 8.13 from the peaks and flattened part of the graph.



Thumb force patterns for trials 1 and 2 by subject 4, using position based correlation

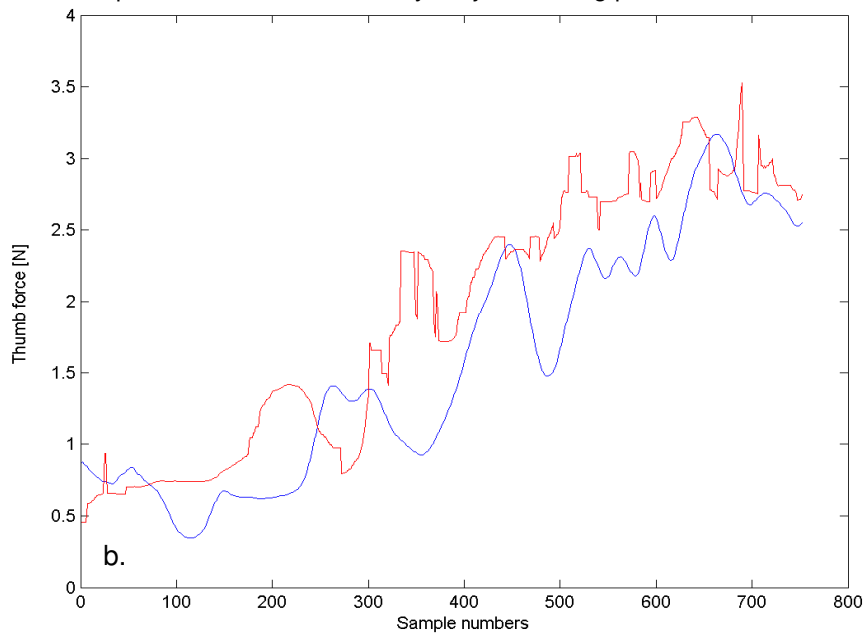


Fig. 8.13: Thumb force patterns during trial 1 (blue) and trial 2 (red) of signature writing by subject 4.

- a.: force patterns as recorded (without applying position based correlation), correlation coefficient:  $r_T=0.71$ .
- b.: force patterns after applying position based correlation. The force pattern of trial 2 (red) is resampled based on the comparing  $x,y$ -coordinates in both trials, correlation coefficient:  $r_T=0.89$ .

### ***Velocity and acceleration based segmentation for correlation***

The third technique for comparison of grip force patterns between trials, segmented the pattern based on pen tip velocity so that grip forces in specific segments of the signature writing trajectory can be compared.

Pen tip velocity during signature writing are characteristic for subjects as was illustrated in Fig.8.7. The pen tip velocity in the x,y-plane was calculated from the changes in x- and y-coordinates over time. Then, the pen tip acceleration was obtained by differentiating the pen tip velocity. The peaks in the pen velocity signal that coincide with zero pen tip acceleration could then be found and those instances that pen tip velocity reach peak values are used to segment the finger force patterns. The different segments of the force data files can be normalised or scaled relative to the writing speed in order to obtain a better fit of corresponding segments in different trials. Limitation to the usefulness of this technique was again variation of signature writing processes and resulting signatures for one subject. Variation in the number of points with zero pen tip acceleration led to comparison of force patterns in different phases in the writing process. Fig. 8.14 illustrates the variety in numbers of peaks in the pen tip velocity profiles.

A variation on segmenting the grip force pattern based on pen tip velocity, was segmenting the grip force pattern based on pen tip acceleration so that grip forces in specific segments of the signature writing trajectory can be compared. The pen tip acceleration signal obtained by differentiating the pen tip displacement twice gives a smoother pattern than the pen tip velocity pattern and takes out some of the differences between the two trials that are compared. Moreover, following Newton's law, the pen tip acceleration may be related directly to the pen grip force that is applied. This may be particularly relevant for vertical (y-direction) acceleration as the vertical pen tip movement originates mainly from the fingers. However, variation of signature writing processes and resulting signatures for one subject including variation in the pen tip acceleration, again led to comparison of force patterns in different phases in the writing process.

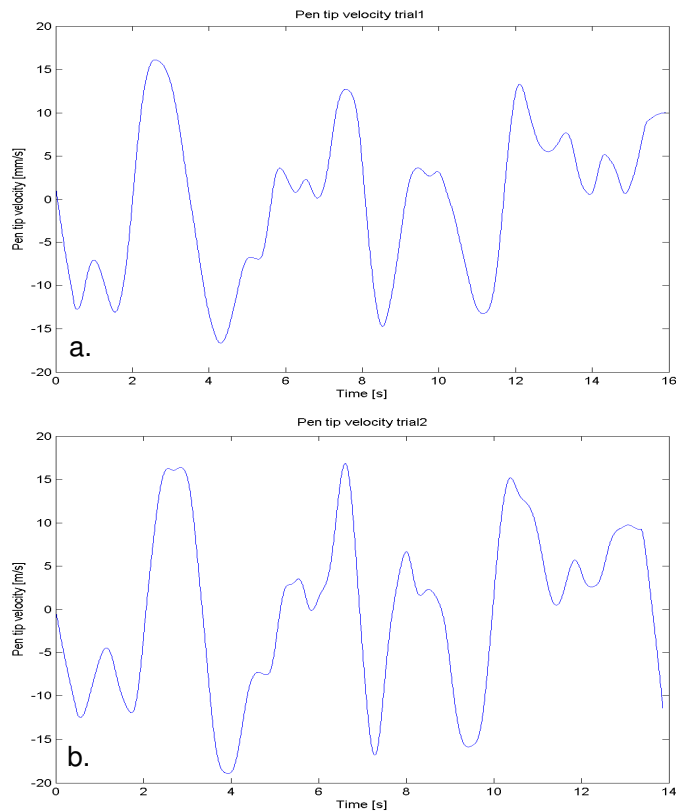


*Fig. 8.14: Pen tip velocity during two signature writing trials by subject 1. The number of peaks in a and b vary.*

### ***Grip pattern based segmentation for correlation***

The fourth technique made use of segmentation of grip force patterns based on the differentiated and twice differentiated grip force signal in an analogue fashion to segmentation of grip force patterns based on pen tip velocity and acceleration. Two different signature trials were compared by analysing segments of the finger force signals that are in the same phase of the signature writing process. This technique was successful for some trials, but had the same limitations as the other techniques described above. Variation of signature writing processes again led to comparison of force patterns in different phases in the writing process.

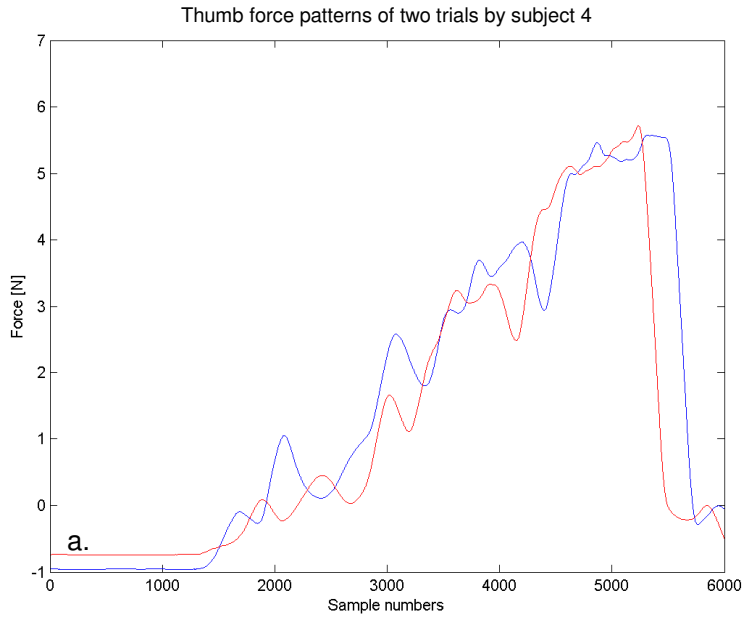
No two signature writing processes and resulting signatures seem to have enough similarity to allow segmentation based on the large changes of the pattern and comparing those segments after reducing the small variations within.

#### 8.4.2.4 Comparison of authentic and counterfeited signatures

The discussion so far has been on comparing signatures from the same subject and attempts to compensate for differences between trials. Fig. 8.15a shows the Thumb force during two trials performed by subject 4. The first (blue) trial is repeated in Fig.8.15b and the red graph is the Thumb force applied to the pen by subject 1 while trying to forge the first person's signature (by freehand drawing; not tracing). The graphs in Fig.8.15b were normalised for ease of comparison of the peaks as the time taken by subject 1 to reproduce subject 4's signature was twice the time taken for the original signature by subject 4.

The differences between force patterns of signatures produced by subject 4 are minimal: the peaks and troughs do not line up perfectly, but the patterns are very characteristic and the consequent correlation is high ( $r_{T,4}=0.96$ ). There is a much larger difference between the thumb force pattern for forging the signature by subject 1 and the original signature by subject 4. Consequently, the correlation is much lower ( $r_{T,1-4}=0.33$ ).

Similar result were observed for many comparisons between trials of one subject and subjects forging others' signatures. However, not all signatures by one person are identical and the force patterns vary as was shown above. Therefore, there is a challenge to further develop the techniques to eliminate the small differences between the grip force measurements of one subject (usually small peaks) without the data analysis technique altering the original signals to the extent that other subjects their signatures would become similar.



Original Thumb force pattern (subject 4) in blue and counterfeited pattern (subject1) in red

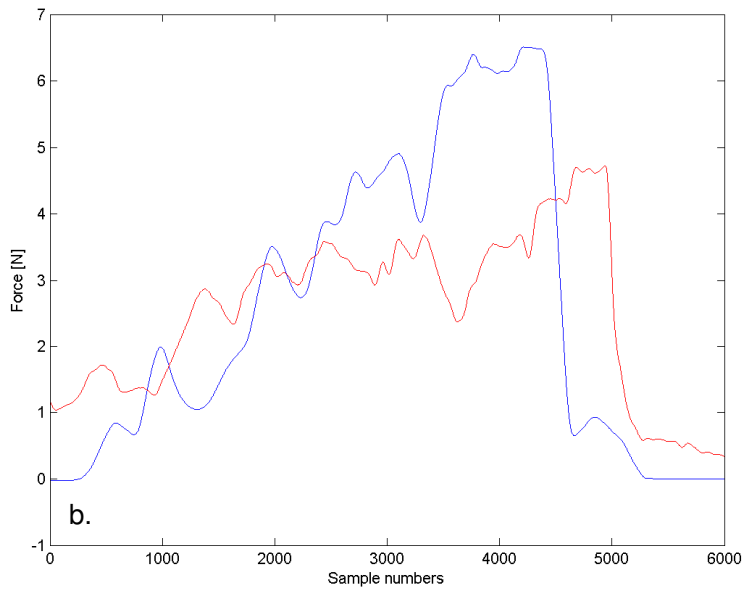


*Fig. 8.15: Thumb force patterns during two trials of signature writing:*

*a.: by subject 4:  $r_T=0.96$ .*

*b.: by subject 1 attempting to copy RCZ's signature:  $r_T=0.33$ .*

In addition, for most subjects it was seen that Thumb and Index finger forces showed a repeatable pattern and were therefore considered to be most characteristic. The Middle finger force showed more variation. However, for one

subject the Thumb and Middle finger force showed most repeatable characteristics, whereas the Index finger force varied.

It is assumed that measuring thumb force would be sufficient to study the interaction between pen and hand in order to distinguish between a genuine signature writing trial and attempt to unauthorised use someone's signature. This would allow a more compact pen design and pen size comparable to an ordinary ball point pen.

## **8.5 Conclusion**

Pen grip force during signature writing were investigated. Characteristics were seen in all four subjects their pen-hand interaction, resulting from the fine motor control of distal joints and which was measured as grip force. In addition to comparing x,y- and z-coordinates and derivatives of script, there is potential for finger force recording for the purpose of signature verification.

However, there are small variations between the grip force patterns for each subject and the patterns are never identical. As the grip force patterns of two identical looking signatures produced by one subject were out of phase during part of the trial, the role of time had to be addressed. In addition, variation in force values was observed between trials.

It is important to note here that although the signature writing process is often perceived as an automated process, the variation reveals that the computations for pen grip control is continuously adapted during the writing process. Therefore, there is a challenge to further develop the techniques to eliminate the differences in timing between the grip force measurements of one subject (usually small peaks) without the data analysis technique altering the original signals to the extent that other subjects their signatures would become similar. What is needed is a statistical representation of the actual variability in signature writing on which individual samples are compared.

The initial approach taken was attempting to segment the grip patterns based on specific characteristics of one subject's signature that are present in all trials (e.g. using velocity/acceleration based correlation). The individual segments of patterns could then be modified to eliminate the minor differences between the segments within trials. The modified segments could be compared between subjects.

The usefulness of the method was demonstrated. However, at current stage it has not been possible yet to reliably adjust the differences in timing between signatures for all subjects.

In addition, the Thumb force was seen to be characteristic for every subject, which suggests that measuring and comparing force application by the thumb on the pen would be sufficient.

The usefulness of a range of other processing techniques should be investigated for decomposition and minor altering of the grip force patterns. This procedure may enable to assess the specifics of the patterns and enable minor altering, which could make grip force patterns of the same subject resemble stronger, while patterns of a counterfeited signature produced by someone else will resemble less.

In particular the following techniques could be useful. Empirical Mode Decomposition (EMD) is frequently used in vibration analysis of bearing machine parts for failure detection and could possibly decompose the grip force patterns in order to differentiate between signatures produced by different subjects.

Finite Impulse Response (FIR) filtering may be useful to alter the amplitude and phase of force signals to make it fit a second signal produced by the same subject without losing the characteristic features. Alternatively, dynamic time warping, which is used to align oscillations of recorded speech when words are spoken with different speed, may be used. The force signals could also be decomposed using wavelets. These and other techniques should be investigated further.

## 9 Conclusion and discussion

The system for advanced research into writing and drawing and suggestions for further development will firstly be discussed in 9.1. The discussion then continues with a summary of the research outcomes in 9.2. The discussion continues in 9.3 with recommendations for further research.

### 9.1 System limitations and recommendations

From the background literature study it was concluded that an overall assessment of handwriting or drawing should include the following biomechanical aspects that vary with time:

- script kinematics (x- and y-coordinates) and derivatives;
- pen tip pressure;
- pen-hand interaction, including pen grip force;
- limb and upper body kinematics.

Consequently, the first objective was to develop a novel pen-like grip force measurement device to study the pen-hand interaction, combined with a script digitiser and motion analysis. The system is evaluated below.

Two previous studies were reviewed in chapter 2 that attempted to measure the variations in grip force associated with writing tasks (Herrick et al, 1961; Chau et al, 2006), but a limitation to both systems was that they did not include measurement of kinematic biomechanical aspects of handwriting. Therefore, the systems did not provide a platform for extended development of theories on biomechanics and motor control in handwriting. In addition, there were accuracy issues with both systems that lead to limitations to their usefulness to study pen grip modulation.

The pen developed by Herrick et al (1961) sensed finger forces applied to barrels, equipped with strain gauges, and pressure variations were recorded on standard EEG paper. The proposed measurement technique could involve significant error. Only limited resolution was obtained from manually measuring deviation of pressure from the baseline on EEG paper. In addition, inaccuracies originated from the calibration method.

The pen grip measurement system by Chau et al (2006), based on the F-scan system enabled comparing of different types of pen grip between subjects. However, it was not a reliable method for comparing pen grip force distributions and its relation to script production and investigating pressure ranges. Inaccuracies originated from the F-socket sensors and calibration techniques if the measurements are not taken within a close approximation of time. Analysis of grip force modulation was not carried out. An evaluation of the system that was developed in this project and recommendations for future developments follow in 9.1.1 and 9.1.2, respectively.

### 9.1.1 System evaluation

#### ***Grip measuring pen***

The pen grip measurement device enabled measurement of individual *thumb, index and middle finger pressure* while holding the pen in tripod grip - with thumb in opposition to index and middle finger.

Despite of the larger size and higher weight than an ordinary ball point pen, the handling of the grip measuring pen was reported comfortable to use. The centre of gravity of the pen was 80 mm from the tip, which is just above the ring of the grip measuring element and which enabled easy handling. Consequently, balancing the pen during movement was found easier than for some of the larger fountain pens that have the centre of gravity within the top half of the pen.

Due to manufacturing inaccuracies of the lower pen half, the load stop to limit the maximum applicable force varied for the three beams ( $F_{\max, \text{beam } 1}$ : 6.4N,  $F_{\max, \text{beam } 2}$ : 10N and  $F_{\max, \text{beam } 3}$ : 7.5N). However, the transducer output did not saturate in practice for any of the subjects included and it can be concluded that the measureable force range was sufficient for normal handwriting. Nevertheless, for the next prototype, it is recommended to increase the range of pressure measurement. A range up to 50N will still enable accurate measurement for patients that may apply excessive force.

A linear regression analysis revealed a linear transducer response and gave calibration factors for each beam. The R-square and adjusted R-Square values

higher than 0.999 show that the linear model fits the data well. RMSE values lower than 0.1 is another proof for a good fit of the linear model for each of the beams. No hysteresis can be seen.

In addition, predicted force values with the linear regression model with a 95% confidence differed only +/-1% from the actual measured nominal force value (+/- 0.05 N at 5N load). No cross talk was seen.

However, the finger positioning on the transducer beams is not fixed, which may lead to inaccuracies as follows. Although it is generally assumed that during normal handwriting the finger positioning does not change (Latash et al, 2003), slight variation of pen grip during pen motion may occur. Consequently, the bending moment around the gauging area will vary and this will induce inaccuracies. With the nominal point of force application being 30 mm away from the top of the gauging area and the assumption that the variation of finger positioning is not larger than +/- 3 mm, inaccuracies up to 10% may occur. It is recommended for the next prototype to use miniature force sensors that measure the exact force, independent of the point of force applications. Alternatively, transducer beams, equipped with two strain gauge bridges should be used on each beam to measure the bending moments in two places on the beams with known distance in between. The bending moments  $M_a$  and  $M_b$  are experienced by the gauges at distances of respectively  $a$  and  $b$  from the point of application:

$$M_a = Fx_a \text{ and } M_b = Fx_b \quad \Rightarrow \quad M_a - M_b = F(a-b)$$

Since the distance  $(a-b)$  between the gages is known, the force  $F$  on each beam can be derived. Using two strain gauge bridges for each beam and each bridge using 4 wires, a total of 24 wires is required for a pen with three beams. The 24 wires make the pen harder to handle and therefore this option was rejected in the pilot study.

The pen tip pressure was recorded from the stylus of the Wacom Intuos2 tablet, which was integrated with the strain gauge transducer pen. During testing it was found that the pen tip pressure recordings saturated. In addition, it is known that the pen tip pressure with resolution of 1024 pressure levels is uncalibrated. As the relation between the pen tip pressure and vertical reaction force between tablet and pen tip varies, dependent on the pen tip inclination angle as explained in section 3.2.1, the tip recording cannot be accurately calibrated.

The maximum sampling frequency that Spike2 program and the 1401 DAC analogue to digital converter allow was 166kHz. The maximum sampling frequency used for sampling finger grip forces was 1kHz, which gave more than sufficient frequency resolution for investigating the frequency of grip modulation. Sampling at higher frequencies would have been possible, but this would have unnecessarily increased the amount of data and in some cases the data might have required additional filtering to eliminate the smallest force variations.

Synchronisation of grip force recording by the 1401 ADC, combined with Spike2 software, and script recording by ScriptAlyzer was enabled through event markers that were sent from ScriptAlyzer to the 1401 ADC, when the pen tip made contact with the tablet. Pen-tablet contact was registered in the ScriptAlyzer software by an increase in pen tip force (z-coordinates) on the tablet, which triggered the script recording. When pen-tablet contact occurred, simultaneously a synchronisation pulse was sent to the 1401ADC and Spike2 software. The Spike2 script enables the 1401 ADC to send a pulse to the Vicon motion analysis system to trigger the motion recording to start. The described synchronisation was found to be reliable and the synchronisation procedure did not hinder the subjects in their experiment.

In conclusion, the grip measuring pen provided ergonomic pen-hand interaction that despite of the triangular arranged gripping area is comparable with an ordinary pen and it enabled high accuracy force measurement.

### ***Sampling script***

ScriptAlyzer software provided a convenient interface with the Wacom Intuos2 digitiser tablet. Script was sampled at frequency of 100Hz, which was sufficiently high to allow accurate recording and analysis of derivatives. Higher sampling frequencies would lead to unnecessary large amounts of recorded data.

Issues with ScriptAlyzer software did not allow the simplest and most convenient from of synchronisation of ScriptAlyzer and grip force measurement with Spike2. When sending a trigger pulse on start-recording-signal from ScriptAlyzer (through parallel port) to the ADC and Spike2 to trigger force measurement, ScriptAlyzer starts counting and recording only if there is pen-tablet contact. Therefore, synchronisation required trigger pulses from ScriptAlyzer on both first contact (to start sampling) and second tablet contact (to mark the start of writing tasks). This is explained in detail in paragraph 4.3.5 and Fig.4.13.

The accuracy of sampling x- and y-coordinates with the Wacom Intuos2 is  $\pm 0.50$  mm as specified by Wacom.

A problem was observed with the timing of the ScriptAlyzer program, which is dependent on the Windows operating system of the host computer. Pen tip coordinates sampled with ScriptAlyzer were seen to be out of phase over part of the trajectory with Vicon pen tip recordings, although equal in value (an example can be found in Fig.4.14). Therefore, the sampled ScriptAlyzer x,y- and z-coordinates were compared to the Vicon coordinates for every trial and if required, the ScriptAlyzer coordinates were shifted to compensate for phase lag to ensure that the start and stop of both signals were always synchronised. While this enabled synchronisation of the start of ScriptAlyzer and Vicon recordings, both recordings were on some occasions observed to be out of phase with a difference of up to 0.2 seconds over part of the trajectory.

### ***Motion analysis***

Kinematics of the limb and upper body were sampled with the Oxford Metrics Vicon motion capture system with eight Charge-Coupled Device (CCD) cameras at a frequency of 120Hz. The setup as presented in 4.3.4.6 is recommended for handwriting motion capture. For a successful motion capture in such a small volume, accurate camera alignment and system calibration were found to be crucial. The accuracy of the dynamic calibration is determined by inspection of the calibration residual (calibration units in mm), which is defined as the angular error (radians) by which a ray from the calibrated camera misses the reference marker multiplied by mean distance from camera to the reference markers. The average calibration residual for all cameras was 0.184, corresponding to the average distance between a reconstructed point and the rays used for its reconstruction of 0.362mm. It was concluded that the calibration results for the setup allows motion capture with an accuracy of  $\pm 0.5$ mm. This equals the accuracy of the script digitiser tablet ( $\pm 0.50$ mm) and it was perceived as sufficient to do all required analysis. However, despite of high calibration results, the motion analysis accuracy may not be guaranteed. This is firstly because markers that are in close approximation may not always be distinguished over the whole writing trajectory and secondly markers can be obscured by the fingers. This is the reason why the Vicon pen tip recordings are less accurate and therefore appear less smooth than the digitised script.

Nevertheless, the Vicon pen tip recordings clearly reveal the trajectory and the correct timing. For analysis of pen tip trajectories the digitiser recordings were used.

### ***Conclusion pen system***

From the above review of the developed system and the two existing devices, it can be concluded that the set of equipment will fill the current deficiency of technology for advanced research into handwriting and the gap in literature. Sufficient accuracy was achieved and the system will contribute to gaining better understanding of the overall neuromuscular and biomechanical processes involved in producing handwriting or drawing. However, there is still room for improvement. Recommendations follow below in 9.1.2.

#### 9.1.2 Recommendations for further system development

##### ***Measuring the fourth pen contact point***

The main coordination of the pen tip originates from exertion of forces at the pad of the thumb, pad of the index finger and the lateral surface of the distal phalanx of the middle finger. Nevertheless, a fourth contact point at the proximal portion of the hand (between metacarpophalangeal MCP joints of the thumb and the index finger or at the proximal phalange of the index finger) fulfills a role in maintaining the pen balance as well. Measurement of pressure at the fourth contact point was not incorporated at this stage. The ideal system would incorporate pen grip force measurement at all four contact points with the pen.

Therefore, a fourth prototype pen for investigating handwriting and drawing should be equipped with a fourth barrel for measuring pressure at the proximal portion of the hand.

### ***Measuring bending moments along with forces***

The ideal system, which incorporates force measurement at all four contact points between hand and pen, allows measurement of both forces and moments in finger synergies, as suggested by Latash et al (2003). Extending the pen with facilities to measure moments as well as forces, will enable to test speculations on controlling of pen balance by the neuromuscular system (Latash, 2003). However, this extension requires to equip the pen with double the amount of strain gauges and wires than the prototype pen that was used in this project. This was a problem as the required small pen size does not accommodate for 24 wires internally. In addition, the 24 wires that connect the pen to the strain gauge amplifier will constrain the pen movement. With sufficient funding and appropriate manufacturing facilities these two problems could be resolved. The problem with pen size and internal wiring could be resolved by using advanced cnc production methods combined that allows placement of a printed circuit that contains the wiring. Ideally the chip and wiring would be integrated into one circuit. The problems with movement constriction of the pen due to wiring could be resolved by making the pen wireless and powering the circuit with a small internal battery, combined with an integrated controller chip for analogue to digital conversion and sending the values to a host computer.

These two suggested further improvements of the prototype pen will first of all increase its abilities as a research tool as it allows to record both finger forces and moments that are required to balance the pen to verify Latash' speculations (2003) on grip force and moment control during handwriting. Moreover, the accuracy of the force measurement will improve. Bending moments that are measured by strain gauges at two locations along each bending beam with known distance between the gauges, allow to derive the exact force applied to the barrels as explained in 3.4.1. This improves accuracy compared to the current approach of using the calibration curve to relate bridge voltage output (resulting from the strain in the gauges) directly to force in order to derive the force value. With the current approach the point of force application during pen grip might differ a few millimeters from the point of force application during calibration, which induces slight inaccuracies, although it does not hinder to study grip force variations.

Alternatively, a pen could be designed around three off-the-shelf six-axes force and torque sensors that enable to measure both force and moment at the thumb, index and middle finger the same time (e.g. FT-NANO 17-TWE-R1.8). However, the

sensors itself are very costly (well over £4k) and requires embedded OEM system development, which will also drastically increase the costs. Another disadvantage is the large transducer size, which does not leave enough space within the pen body for integration with the Wacom printed circuit for sampling script.

### ***Improved range and accuracy force measurement***

Although the strain gauge transducers performed well in terms of linearity (R-square and adjusted R-Square values higher than 0.999; RMSE < 0.1) and no hysteresis and cross talk could be seen, varying finger positioning on the transducer beams may induce inaccuracies. With varying finger positioning the bending moment around the gauging area will vary and this will induce inaccuracies. With the nominal point of force application being 30 mm away from the top of the gauging area and the assumption that the variation of finger positioning is not larger than +/-3 mm, inaccuracies up to 10% may occur.

It is recommended to equip transducer beams with two strain gauge bridges on each beam to measure the bending moments in two places on the beams with known distance in between as described above (Measuring bending moments along with forces). The bending moments  $M_a$  and  $M_b$  are experienced by the gauges at distances of respectively  $a$  and  $b$  from the point of application:

$$M_a = Fx_a \text{ and } M_b = Fx_b \quad \Rightarrow \quad M_a - M_b = F(a-b)$$

Since the distance  $(a-b)$  between the gages is known, the force  $F$  on each beam can be derived.

Due to manufacturing inaccuracies of the lower pen half, the maximum beam deflection at maximum applicable force, varied for the three beams ( $F_{\max, \text{beam 1}}: 6.4\text{N}$ ,  $F_{\max, \text{beam 2}}: 10\text{N}$  and  $F_{\max, \text{beam 3}}: 7.5\text{N}$ ). It is recommended to measure forces in the range up to 50N without imposed geometric constraints due to inaccurate manufacturing. This will still enable to accurately measure forces in patients that may apply excessive force.

### ***Measuring pen tip force***

The pen tip pressure recordings with the stylus of the Wacom Intuos2 tablet, which was integrated with the strain gauge transducer pen, was uncalibrated and was found to saturate. Calibration of the pressure levels recorded with the Wacom pen is not possible. The relation between the pen tip pressure and vertical reaction force between tablet and pen tip varies, dependent on the pen tip inclination angle as explained in section 3.2.1. It is recommended to include a pen tip force transducer for accurate measurement of pen tip force without saturation.

### ***Resolving timing problem with script recording***

The timing problem with the ScriptAlyzer software were addressed in this project doing a simple tasks as line drawing by shifting the individual cycles of the recording and using the Vicon pen tip recordings to reveal the right timing. The Vicon and digitiser recordings were seen to follow the same trajecory and the correct timing (the Vicon pen tip recordings being less accurate and appearing less smooth than the digitiser tablet recordings). For more complicated tasks the timing cannot be resolved easily and remains an issue, although it did not affect the data analysis in this project.

The limited time available for this project lead to the choice for commercial ready to use software, but developing a software application for sampling x,y-coordinates and tip pressure seems the way forward. It is recommended to firstly develop a simple application for recording script with similar or higher quality digitiser as the Wacom Intuos2. This should be run on a stand alone device using embedded system technology to ensure correct timing.

A next generation software could be developed that also includes features for recording other handwriting mechanics: tip pressure and pen grip forces as well as x,y-coordinates. The script recordings could be exported and analysed in Matlab. Alternatively, the recording could take place in Matlab with real time visualization, which could be compiled to an executable file that works outside the Matlab environment on any PC.

Alternatively, Labview could be used. It is possible to collect the data directly from the digitizer hardware into LabView and avoid using the standard Wintab digitizer drivers. This option was previously investigated and requires a Wacom tablet with USB connection instead of the parallel port connection that was used in this project. In addition, to capture the USB digitizer data directly in Labview a National Instruments USB ADC for Labview is required and Labview needs instructions regarding the Vendor ID (VID) and Product ID (PID) of the tablet device. Labview procedures need to be written to extract the x,y-coordinates and pressure data. This approach should enable synchronizing the data streams in time as Labview will give time referenced data for the USB data as well as the A/D force data. There is still a slight timing uncertainty since the USB data is transported across a frame oriented bus, but it is a fixed transport delay that remains constant for a given session. For example, the digitizer data arrives 8ms after it was recorded on the hardware. Another challenge of the method is the entire removal of the Wacom drivers. This may not be easy as Windows likes to keep cached copies of the data associating which driver is bound to which hardware and these bindings need to get changed so that the Labview drivers are associated with the Wacom hardware. After having completed these steps, Labview is ready to receive raw data from the digitizer from which x,y-coordinates and tip pressure can get parsed out. The C-code from public Linux drivers for Wacom tablets explain this parsing. Documentation is available from Wacom and LCS/Telegraphics. This cannot be established without input from Wacom developers and will be a time consuming and expensive option despite of using standard components. An alternative to a standard digitiser would be developing a new system for recording pen tip motion. Although there are realistic opportunities, this will be time consuming and more costly. Despite this and the challenge to obtain the required accuracy and repeatability, it will significantly simplify the interfacing with software for recording and synchronisation with the pen grip force recording.

### ***Extended motion analysis***

Motion capture was combined with the novel Matlab code that was developed to enable a three dimensional graphical presentation of the arm joints and pen tip to be constructed. Finger joints during pen grip were not visualised nor investigated yet,

but might reveal more on the involvement of pen-hand interaction during line drawing as reported in chapter 5 in addition to measuring the pen grip forces. In addition, angles between limb segments and finger segments were not analysed, although the developed Vicon Body builder code allows to output them. Another opportunity towards further explaining the coordination of line segment drawing, reported in chapter 5, would be assessing the movements in joint space by calculating the following limb segment angles. The required angles are (according to Klein Breteler et al, 1998): elbow angle (between upper arm and forearm), shoulder elevation (between saggital projection of the upper arm and a vector pointing forward through the trunk) and (shoulder) azimuth (between projection of the upperarm in the horizontal plane and the forward writing direction).

## **9.2 Research outcomes**

### **9.2.1 Proximal and distal muscle control: Fingers enables vertical (y-)motion**

Grip force applied by thumb, index and middle finger was found to be directly related to pen movement in the y-direction of the tablet and less so for writing and drawing in the x-direction of the tablet.

This was clearly seen from the line drawing task in chapter 5, where the processes for line drawing towards 12 and 6 o'clock targets were compared with line drawing towards the 3 and 9 o'clock target positions. The finger grip forces while drawing lines in the y-direction of the tablet were seen to be more repeatable and predictable than while drawing lines in the x-direction. In general, the pen tip movements in the positive or negative y-direction are caused by up and down going finger movements relative to the hand. Linear wrist motion in the y-direction is also observed, but the wrist excursions in the y-direction are shorter than in the x-direction. In contrast, horizontal progression of the pen originates from wrist, elbow and shoulder movements.

These outcomes are evidence for what had previously been assumed for normal handwriting (Van der Gon, 1965; Edelman S, 1987; Hollerbach, 1981). These assumptions on contributions of proximal and distal muscle groups to handwriting and drawing movements were quantified and confirmed here for line drawing for the first time. Earlier assumptions on pen-hand coordination and the contributions of finger and arm joints in relation to pen tip movement direction had not been

evaluated and no empirical and experimental evidence has been collected to describe the process (Meulenbroek, 1998) as no equipment existed that enabled to test any hypotheses.

In chapter 6 it was concluded that (in general) the pen tip movements in the y-direction of the tablet during writing are caused by up and down translations of finger movements relative to the hand. Comparison of graphs of thumb, middle and index finger forces with vertical pen tip motion (y-coordinates) reveals that for at least part of the writing trials, the finger force modulation does relate to vertical tip motion (e.g. Fig.6.36 and Fig.6.37). However, the writing process is more complicated and the contribution of fingers and limb to the overall pen tip motion during normal handwriting still needs further investigation. Suggestions for further research are made in section 9.3.2.

The results in chapter 7 show for spiral drawing by two subjects that the fingers ensure a stable pen grip to position the pen relative to the wrist joint. From the finger force control observed for spiral drawing, it can be concluded that the fingers do not play an important role in directing the pen in vertical direction to establish circular pen motion. This is different from what was observed for line drawing and writing. In addition, the changes of pen tip coordinates in y-direction were seen to precede the changes in the x-direction for both subjects. It is hypothesized that this is part of a strategy adopted by the neuromuscular system to control and regulate the fine finger and limb movements involved with spiral drawing and suggests a form of task specificity in pen control. However, more data needs to be collected to investigate if this is a general finding or not.

### 9.2.2 Control of wrist rotation during horizontal line drawing

The writing velocity and deviation from the ideal line straight line was investigated in chapter 5 and differences between subjects were observed. Wrist rotation was seen for all trials by both subjects when producing horizontal lines. It may be hypothesised that wrist rotation is required with the production of horizontal lines without excessive deviation. Excessive line curvature by subject 1 to the 9 o'clock target is seen while limited wrist rotation occurs. This is in agreement with findings by Morasso (1981) and Cruse and Brüwer (1987), who found that curved paths are adopted to simplify the tasks of the control requirements to draw a straight line.

In addition, the pen orientation angle (between the triangular pen cross section and the writing line) tends to increase with lateral progression as was seen in chapter 6 (e.g. Fig.6.40 and Fig.6.41). The most plausible explanation is that lateral pen tip motion is established by rotational motions around the limb joints (Some shoulder rotation, particular elbow rotation and combined rotation and translation of the wrist (e.g. Fig.6.42 and 6.43).

### 9.2.3 Anticipatory grip actions

For line drawing (chapter 5) anticipatory grip actions are frequently seen: an increase or decrease in finger force values before the start of a trial or when reaching a particular point in the cycle. For example, peak forces are seen to stabilise the pen grip just before initiation of the pen motion (e.g. 12 and 3 o'clock target by subject 1). Another example of anticipatory action is that for line drawing towards the 12 o'clock target (subject 2), a dip in thumb force is seen in every cycle before reaching the maximum y-value.

Anticipatory grip actions are associated with feed forward predictive control mechanisms (Blakemore et al, 1998). In the background section (2.2.2) the assumption was made that for finger grip modulation during normal handwriting both pro-active grip force modulation tasks (initiated small pen tip movement executed by fingers) and reactive grip force modulation tasks (e.g. respond to inertia effects) are essential. The anticipatory grip actions observed confirm feed forward processing, resulting in pro-active grip actions. This implies that internal representation of the physical object properties are crucial, for feed forward predictive neural control mechanisms in pro-active grip modulation tasks (Blakemore et al, 1998). No previous reference to pro-active and reactive grip phenomena during handwriting was found in literature.

In addition, force modulation by individual fingers seems to fulfil a role in coordinating the synergies between fingers that enable executing the pen motion. For example for vertical line drawing (y-direction) to the 6 and 12 o'clock targets, the changes in index finger force values shown by subject 1 precede changes in thumb and middle finger force values. For horizontal targets (x- direction; 3 and 9 o'clock), adaptations in thumb force precede adaptations by index and middle fingers for subject 2.

#### 9.2.4 Redundancy and flexibility of continuous neuromuscular control

In chapter 5 it was observed that even relatively simple tasks, such as line drawing, involve proximal and distal muscle groups. Subject 2's strategy is very repeatable for attempting to produce similar straight lines of the pen tip: the trajectories of Shoulder, Elbow, and Wrist are very similar among cycles. Subject 1, however, uses more variable trajectories of Shoulder, Elbow, and Wrist among cycles in one trial, but nevertheless produces similar approximately straight lines for every cycle. The redundancy in controlling the different limb joints was highlighted: the neuromuscular system's flexibility enables different kinematics to result in the same drawing output.

From an in-depth comparison of the biomechanical aspects of handwriting in (chapter 6), including joint trajectories, pen finger grip and script, it was concluded that no two trials performed by one subject share an identical writing process, not even when the writing results are (nearly) identical. Based upon the resultant grip patterns, it was concluded that the way the pen and hand interact differs when the same word is produced within a sentence. No direct relation was found between tablet position and the writing process, the duration of the writing task and or resulting script for any of the subjects. This confirmed again that the neuromuscular control apparatus is highly adaptive, allowing the production of a nearly equal end result, but by means of different mechanical and therefore neuromuscular activities for controlling joint torques.

#### 9.2.5 Pen grip and signature verification

Pen tip x,y-coordinates and derivatives (velocity/acceleration) and pen grip force during signature writing were investigated. The grip forces applied to the pen represent the fine motor control of distal joints that enable pen control. It was found that the pen-hand interaction was characteristic for all four subjects and there is potential for finger force recording for the purpose of signature verification. However, it appears that pen grip control is continuously adapted during the writing process and small variations between the grip force patterns for each subject exist. The grip force patterns produced by one subject differ in amplitude, frequency and phase and signature writing is not an automated task. The thumb force was seen to be characteristic for every subject and it is hypothesised that comparing thumb force on the pen would be sufficient for applications in signature verification. One reason

for this is the role of the thumb in generating upward pen motion as was seen in the line drawing experiment. Preliminary steps have been made by applying signal processing techniques for signature verification based on grip force patterns.

### **9.3 Recommendations for further research**

Recommendation for further research will be detailed in this section. The different point of interest will be discussed individually and are arranged below according to the experimental chapters 5 to 8.

#### **9.3.1 Line drawing - Chapter 5**

##### ***Controlling of wrist rotation during horizontal line drawing***

The writing velocity and deviation from the ideal line straight line was investigated in chapter 5 for two subjects and differences between the subjects were observed. Wrist rotation was seen for all trials by both subjects with the production of horizontal lines. It may be hypothesised that Wrist rotation is required with the production of horizontal lines without excessive deviation. In fact, excessive line curvature by subject 1 to the 9 o'clock target is seen, which is expected to originate from limited Wrist rotation. This also agrees with findings by Morasso (1981) and Cruse and Brüwer (1987), who found that curved paths are adopted to simplify the tasks of the control system to draw a straight line.

The next questions would be whether 1) there is a superimposed control centre that (globally) controls the timing of the individual muscles during the line drawing movement with the calculations of actual path and of incremental angle changes (by distal effectors) being carried out on the local level; or 2) both the form of the path and muscle activation is done on the global level (Hollerbach et al, 1986). One might argue that in the latter case, the problem of redundancy is ignored, but further research using the uncontrolled manifold hypothesis (UCM) may lead to an answer. The UCM offers a framework to explain synergies that are active in motion control and which originate centrally (Latash, 2002; 2003). However, controlling of local parameters, such as the finger kinetics and kinematics, may happen distally.

It could be hypothesised that the CNS uses joint angles as one of the parameters following an UCM-like approach to address redundancy in the effector system of arm, hand and fingers to produce a line by controlling joint angles and finger forces and moments applied to the pen. Although UCM has so far only been used as a general theoretical framework for kinetics and kinematics, the theories could be extended to physiological parameters, such as muscle activation patterns and patterns of neural signals associated with motor tasks, according to Latash (2002). A start could be made by assessing the consistency of joint angles in the arm and fingers for a large sample group, which could indicate that the nervous system holds the requirement to control the joint angles during the line drawing tasks. The marker set that was used during data collection already includes finger joint markers as described in 4.3.4.5. In addition, the bodybuilder script that was developed already enables to export the angles between segments.

### ***Finger pressure***

For both subject 1 and subject 2, grip force applied by thumb, index and middle finger was directly related to pen movement in the y-direction of the tablet, while that relation seems less obvious for writing and drawing in the x-direction of the tablet. The finger grip forces while drawing lines in the y-direction of the tablet were seen to be more repeatable and predictable than while drawing lines in the x-direction. In general, the pen tip movements in the positive or negative y-direction are caused by up and down going finger movements relative to the hand. There is also wrist motion involved, but the wrist excursions in the y-direction are shorter than in the x-direction. The horizontal progression of the hand originates from wrist, elbow and shoulder movements. This corresponds to what was reported for normal handwriting (Van der Gon, 1965; Edelman S, 1987; Hollerbach, 1981). However, these assumptions on contributions of proximal and distal muscle groups to handwriting and drawing movements were quantified and confirmed here for line drawing for the first time. Earlier assumptions on pen-hand coordination and the contributions of finger and arm joints in relation to pen tip movement direction had not been evaluated and no empirical evidence existed (Meulenbroek, 1998). The contribution of both fingers and limb to the overall pen tip motion during normal handwriting should also be investigated further and a start was made in chapter 6. In

addition to investigating the finger forces applied to the pen, the actual finger movement could also be investigated. The marker set that was used during all data collection already included light reflecting markers mounted onto the fingers as explained in 4.3.4.5. Therefore, finger joint motion could be analysed.

In addition, there has not been any data available in literature on grip force ranges during drawing tasks. The force values of the three fingers differs between the subjects and overall, the finger forces are lower for subject 2 than for subject 1. Data from a large group of subjects should be collected to provide reference to average grip force values during handwriting for future studies into handwriting and comparison of healthy subjects with impaired subjects.

For vertical line production for target positions 12 and 6 o'clock for both subjects, a very similar force pattern was observed for the two trials of each subject. Only the force value differed, dependent on the movement direction. The same finger synergies could be active in both vertical trials for one subject. Latash' uncontrolled manifold (UCM) hypothesis may be valid, which is a concept that explains how the CNS deals with the problem of redundancy by controlling particular parameters, such as force and moment. Latash reports that his theory could not be proven yet as a tool that enabled to measure grip forces and also moments on the pen did not exist. The novel set of equipment enables to assess Latash' UCM in a set of additional experiments to proof if such synergies for force control exist.

It is possible that different finger synergies are active in different subjects. For example, subject 1 was seen to steer the pen in vertical direction by in the first place controlling the Index finger force level, whereas subject 2 was seen to steer in vertical direction by controlling force levels of both Index finger and Thumb to the same extent.

### ***Joint trajectories***

Subject 2's strategy is very constant for attempting to produce similar straight lines of the pen tip: the trajectories of shoulder, elbow, and wrist are very similar among cycles. Subject 1, however, uses more variable trajectories of shoulder, elbow, and wrist among cycles in one trial, but nevertheless produces similar approximately

straight lines for every cycle. The redundancy in controlling the different limb joints also was highlighted: the neuromuscular system's flexibility enables different kinematics to result in the same drawing output.

The variability within a larger sample group should be investigated further to firstly report the different combinations of limb joint motion that result in the same line drawing. This may also shine light on the processes behind the movement.

A start towards further explaining the observed joint motion during line drawing would be to further assess the movements in joint space. Following Klein Breteler et al (1998), the movements in joint space could be investigated by calculating the angles between the limb segments and plotting them combined in one graph. Klein Breteler et al (1998) performed this for reaching movements, but the same graphical presentation of angles could be used for drawing. The angles of interest are: the elbow angle (between upper arm and forearm), shoulder elevation (between sagittal projection of the upper arm and a vector pointing forward through the trunk) and shoulder azimuth (between projection of the upperarm in the horizontal plane and the forward writing direction). The bodybuilder script that was written for the system to enable joint coordinate calculation and visualisation experiment already also enables to export of the angles between the different limb segments.

### 9.3.2 Writing activity - Chapter 6

From an in-depth comparison of the biomechanical aspects of handwriting for the three subjects, including joint trajectories, pen finger grip and script, it was concluded that no two trials performed by one subject share an identical writing process, not even when the writing results are (nearly) identical. Once again, this confirmed that the neuromuscular control apparatus is highly adaptive and works in a coordinated fashion that allows the production of a nearly equal end result, but by means of different mechanical and therefore neuromuscular processes.

No direct relation was found between tablet position and the writing process, duration of the writing and the resulting script for any of the subjects.

In general, the pen tip movements in the y-direction of the tablet during writing are caused by up and down translations of finger movements relative to the hand. This was confirmed and quantified for the first time in chapter 5 on line drawing and is evidence for assumptions made by Van der Gon (1965), Edelman (1987) and

Hollerbach (1981) for drawing and handwriting. Comparison of graphs of thumb, middle and index finger forces with vertical pen tip motion (y-coordinates) reveals that for at least part of the writing trials, the finger force modulation does relate to vertical tip motion (e.g. Fig.6.36 and Fig.6.37). However, the writing process is more complicated and the contribution of both fingers and limb to the overall pen tip motion during normal handwriting still needs further investigation. The correlation between the pen tip y-coordinates (vertical tip motion) and the direction of forces applied by thumb, index and middle finger could be assessed by means of a simple algorithm. This should be carried out for a large sample group of e.g. 50 subjects. One might suggest that for subject 2 the differences between force patterns relate more directly to the differences in produced script. For subject 2, a stronger similarity is seen in limb activities to establish lateral progression in every trial than for subjects 1 and 5. It could be hypothesised that as a result of the more constant lateral movement (compared to subject 1 and 2), less adaption of pen positioning by the fingers is required. Pen incline, pen orientation and differences in produced script should then relate more directly to the small differences in force pattern in each trial. However, these thoughts remain speculations at the present time. The effect off repetitiveness of the writing process on grip force application needs to be studied in more detail.

It was concluded that for all three subjects, based on the resultant grip patterns, that the way the pen and hand interact differs when the same word is produced within a sentence.

In addition, the pen orientation angle (between the triangular pen cross section and the writing line) tends to increase with lateral progression (e.g. Fig.6.40 and Fig.6.41). The most plausible explanation is that lateral pen tip motion is established by rotational motions around the limb joints (Some shoulder rotation, particular elbow rotation and combined rotation and translation of the wrist (e.g. Fig.6.42 and 6.43). The joint motion could be further investigated. The movements can be assessed in joint space as previously done by Klein Breteler et al (1998) and described above for further analysis of linedrawing in chapter 5.

In addition, there has not been any data available in literature on grip force ranges during handwriting tasks. Table 6.10 provides some initial data for 4 subjects, showing average force values for thumb, middle and index finger between 0.5 and

5N. Data from a large group of subjects should be collected to provide reference to average grip force values during handwriting for future studies into handwriting and comparison of healthy subjects with impaired subjects.

### 9.3.3 Spiral drawing - Chapter 7

The results for the subjects included in the experiments on spiral drawing in chapter 7 show that the the fingers ensure a stable pen grip to position the pen relative to the wrist joint. From the finger force control observed for spiral drawing, it can be concluded that the fingers do not play an important role in directing the pen in vertical direction to establish circular pen motion. This is different from what was observed for line drawing and writing.

In addition, the changes of pen tip coordinates in y-direction were seen to precede the changes in the x-direction for both subjects. At this stage, it is not known if what is described above is part of a strategy adopted by the neuromuscular system to control and regulate the fine finger and limb movements involved with spiral drawing. However, this could be hypothesised. Collecting and analysing more data could also make clear if this is a general tendency adopted by many people or if this is just the case for the subjects included in this experiment only.

Development of analysis techniques for further assessment of the pen grip forces will allow assessing which specific changes take place in the neuromuscular system with handwriting deterioration due to aging or development of disease. Pen grip force measurement along with recording of pen tip force and writing and drawing coordinates will specifically enable the investigation of tremor. It was reported that for PD there seems to be a renewed interest in action tremor assessment (Aly et al, 2007; Rudzńska et al, 2007; Saunders-Pullman et al, 2008). However, normally rest tremor is seen in PD and action tremor in more advanced and progressed stages of PD. This form of tremor is particularly disabling as it interferes with reaching and grasping actions. Although the new system enables an investigation of action tremor, it is not clear if there is any use for investigating PD due to the disabling nature of obvious action tremor in PD.

Potentially, a set of quantifiable parameters may be defined that will help to distinguish between the regulation of the finger force control by the nervous system in healthy people and those with impaired function.

### 9.3.4 Handwriting and signature verification Chapter 8

Pen tip x,y-coordinates and derivatives (velocity/acceleration) and pen grip force during signature writing were investigated. The grip forces applied to the pen represent the fine motor control of distal joints that enable pen control. It was found that the pen-hand interaction was characteristic for all four subjects and there is potential for finger force recording for the purpose of signature verification. However, it appears that pen grip control is continuously adapted during the writing process and small variations between the grip force patterns for each subject exist. The grip force patterns produced by one subject differ in amplitude, frequency and phase and signature writing is not an automated task. The thumb force was seen to be characteristic for every subject and it is hypothesised that comparing thumb force on the pen would be sufficient for applications in signature verification.

It was required to develop analysis techniques for comparing signature samples for signature verification as variations between the grip force patterns for each subject exist. The initially approach was to attempt segmenting the grip patterns based on specific characteristics of one subject's signature that are present in all trials (e.g. using velocity/acceleration based correlation). The individual segments of patterns could then be modified to eliminate the minor differences between the segments within trials. The modified segments could be compared between subjects. It remains a challenge to further develop the techniques to eliminate the differences in timing and force values between the grip force measurements of one subject (usually small peaks). The grip force signals require processing without the data analysis technique altering the original signals to the extent that other subjects their signatures would become similar. Several techniques will be briefly discussed below.

Finite impulse response (FIR) Filtering will be useful to adapt the amplitude and phase of signal to make it resemble the second signal more without altering the signal too much from the original.

In addition, empirical mode decomposition (EMD) technique could be implemented with Matlab to assess oscillation frequencies of the grip force signals (e.g. Zhou et al, 2008). EMD has many applications in vibration analysis of bearing machine parts

for failure detection. EMD could be used to compare oscillation frequencies of different signatures. Using EMD, any given time series data is firstly composed into a set of simple oscillatory functions by the repeated application of a nonlinear iterative procedure. Then time-dependent amplitudes and frequencies of the simple oscillatory functions are defined using a Hilbert transform.

Alternatively, wavelets, which are frequently used in image analysis, could be used to assess the grip force patterns. Wavelet transforms can be used to decompose and analyse the signals and this process could be automatised with Matlab (e.g. Brittain et al, 2007). This type of analysis has already been used for comparing x,y-coordinate data from different subjects for signature verification (e.g. Deng et al, 1992; Vergara et al, 2002) and could also be applied to grip force patterns.

Another potentially useful method is dynamic time warping, which is frequently used to align oscillations of recorded speech when words are spoken with different speed. Dynamic time warping was recently also applied in signature verification (Jayadevan, 2009). The technique could possibly also be applied to decomposing the grip force patterns. Basic Matlab codes that enable analysis using dynamic time warping are available and they could be customised for grip force signals and signature verification.

## Bibliography

Abbs JH, Winstein CJ, 1990, Functional contributions of rapid and automatic sensory-based adjustments to motor output. In: Jeannerod M (Ed.), *Attention and Performance XIII: Motor representation and control*, LEA, Hillsdale, NJ.

Abend W, Bizzi E, Morasso P, 1982, Human arm trajectory formation. *Brain* 105: 331-348.

Aly N.M., Playfer J.R., Smith S.L., Halliday D.M., *A Novel computer-based technique for the assessment of tremor in Parkinson's Disease*, Age and aging, June 1, 2007.

Alberts JL, Tresilian JR, and Stelmach GE, 1998, The coordination and phasing of a bilateral prehension task, *Brain* 121: 725–742.

Andrews JG, Youm Y., 1979, A biomechanical investigation of wrist kinematics, *J. Biomechanics* 12: 83-93.

Arbib, M.A., 1990, Programs, schemas, and neural networks for control of hand movements, Beyond the RS framework. In: Jeannerod, M. (Ed.), *Attention and Performance XIII: Motor Representation and control*. LEA, Hillsdale, NJ, pp. 111±138.

Augurelle, Anne-Sophie, Allan M. Smith, Thierry Lejeune, and Jean-Louis Thonnard, Importance of Cutaneous Feedback in Maintaining a Secure Grip During Manipulation of Hand-Held Objects, *J Neurophysiol* 89: 665–671, 2002.

Bain PG, Findley LJ, *Assessing tremor severity*, Smith-Gordon and Company Limited, 1993, ISBN 1-85463-099-7.

Baur B., Fuerholzer W., Jasper I., Marquardt C., Hermsdoerfer J., *Effects of Modified Penn Grip and Handwriting Training on Writer's Cramp*, 2009, *Arch Phys Med Rehabil* Vol (90).

Benecke, R., J. C. Rothwell, J. P. R. Dick, B. L. Day, and C. D. Marsden. 1986. Performance of simultaneous movements in patients with Parkinson's disease. *Brain* 109: 739–757.

Bernstein, N., *The coordination and regulation of movements*, 1967, London: Pergamon.

Birznieks I, Burstedt MKO, Edin BB, Johansson RS, 1998, Mechanisms for force adjustments to unpredictable frictional changes at individual digits during two-fingered manipulation. *Journal of Neurophysiology* 80: 1989-2002.

Blakemore SJ, Goodbody SJ, Wolpert DM (1998) Predicting the consequences of our own actions: the role of sensorimotor context estimation. *J Neurosci* 18:7511–7518.

Brittain J.S., Halliday D.M., Conway B.A. and Nielsen J.B., 2007, Single-Trial Multiwavelet Coherence in Application to Neurophysiological Time Series, *IEEE Transaction on biomedical engineering*, Vol. 54 (5).

Brown P, Corcos DM, Rothwell JC. *Does Parkinsonian action tremor contribute to muscle weakness in Parkinson's disease?* *Brain* 1997;120:401-408.

Bullock D, Grossberg S, Guenther F, 1993, A self-organising neural model of motor equivalent reaching and tool use by a multijoint arm. *J. Cogn Neuroscience* (in press).

Burstedt MKO, Birznieks I, Edin BB, Johansson RS, 1997a, Control of forces applied by individual fingers engaged in restraint of an active object, *Journal of Neurophysiology* 78: 117-128.

Burstedt MK, Edin BB, Johansson RS, 1997b, Coordination of fingertip forces during human manipulation can emerge from independent neural networks controlling each engaged digit. *Exp Brain Res* 117:67–79.

- Burstedt MK, Flanagan JR, Johansson RS (1999) Control of grasp stability in humans under different frictional conditions during multidigit manipulation. *J Neurophysiol* 82:2393–2405.
- Cappozzo A., Catani F., Della Croce U.D., Leardini A., 1995, Position and orientation in space of bones during movement: anatomical frame definition and determination. *Clinical Biomechanics* 10(4): 171-178.
- Chau T., Ji J. Tam C., Schwellnus H., A novel instrument for quantifying grip activity during handwriting, *Arch Phys Med Rehabil*, vol 87, November 2006, pp.1542-1547.
- Cole KJ and Abbs JH, 1988, Grip force adjustments evoked by load force perturbations of a grasped object, *Journal of Neurophysiology* 60 : 1513-1522.
- Cole KJ and Johansson RS, 1993, Friction at the digit-object interface scales the sensorimotor transformation for grip responses to pulling loads, *Experimental Brain Research* 95: 523-532.
- Da Silva A.V., De Freitas, D.S., *Wavelet-based Compared to Function-based On-line Signature Verification*, 2002
- DeLong, M. R., M. D. Crutcher, and A. P. Georgopoulos. 1985. Primate globus pallidus and subthalamic nucleus: Functional organisation. *J. Neurophysiol.* 53: 530–543.
- Deng P.S. , Liao H.M. , Wen Ho C. and Tyan H., *Wavelet-based Off-line Signature Verification*, 1992.
- Denier Van der Gon J.J., Thuring J. Ph., *The guiding of human writing movements*, 1965. *Kybernetik* 2: 145-148.
- Delwaide PJ and Gonce M, 1989, Parkinson's disease and movement disorders, *Williams & Wilkins*, Chapter 8: Pathophysiology of Parkinson's Signs.
- Dooijes EH, 1983, Analysis of handwriting movements, *Acta Psych* 54: 99-114.

Dounskaia N, Van Gemmert AW, Stelmach GE, 2000, Interjoint coordination during handwriting-like movements, *Experimental Brain Research*, 735: 127-140.

Edelman, S., Flash, T., 1987, A model of handwriting, *Biological Cybernetics* 57: 25-36.

Edin BB, Westling G, Johansson RS (1992) Independent control of human finger-tip forces at individual digits during precision lifting. *J Physiol (Lond)* 450:547–564.

Eichhorn T., Arnold G., Mai N., Gasser T., Oertel, W.H., 1994, Disturbance in the execution of automated handwriting movements. A sensitive marker for early Parkinsonism. *Movement Disorders* 9: 121.

Elble R.J., R., Brilliant M., Leffler K., Quantification of essential tremor in writing and drawing. *Mov. Disorder*, 11: 70-78, 1996.

Elble R.J., Sinha R., Higgins C., Quantification of tremor with a digitizing tablet. *J.Neuroscience Methods*, 32: 193-198, 1990.

Emery P., The optimal management of early rheumatoid disease: the key to preventing disability, 1994. *British Journal of Rheumatology* 33:765-768.

Fahn S, Elton R.L., UPDRS Development committee, United Parkinson's Disease Rating Scale. In: Fahn S., Marsden C.D., Calne D.B., Goldstein M., eds. *Recent Developments in Parkinson's Disease*. Florham Park, NJ: Macmillan; 1987:153-163

Fellows, S. J., J. Noth, and M. Schwarz. 1998. Precision grip and Parkinson's disease. *Brain* 121: 1771–1784.

Fergenbaum M, Hadcock L., Severson J., Morin E., Bryant T., Reed S., Abdoli M., Tara T., 2003, Pressure measurement applications for humans, School of Rehabilitation, Queens University, Ontario, Canada.

Flanagan, J. R., M. K. O. Burstedt, and R. S. Johansson. 1999. Control of fingertip forces in multidigit manipulation. *J. Neurophysiol.* 81: 1706–1717.

Flanagan JR and Wing AM, 1997a, The role of internal models in motion planning and control: evidence for grip force adjustments during movements of hand-held loads. *Journal of Neuroscience* 17: 1519-1528.

Flanagan JR and Wing AM, 1997b, Effects of surface texture and grip force on the discrimination of hand-held loads, *Percept Psychophysiology* 59: 111-118.

Flanagan JR, Tresilian J, Wing AM (1993) Coupling of grip force and load force during arm movements with grasped objects. *Neurosci Lett* 152:53–56.

Flanagan JR, Tresilian JR (1994) Grip-load force coupling: a general control strategy for transporting objects. *J Exp Psychol Hum Percept Perform* 20:944–957.

Flash T, Sejnowski TJ, 2001, Computational approaches to motor control, *Current opinion in neurobiology* 11(6): 655-662.

Forsberg, H., P. E. Ingvarsson, N. Iwaskai, R. S. Johansson, and A. M. Gordon. 2000. Action tremor during object manipulation in Parkinson's disease. *Mov. Disord.* 15(2): 244–254.

Gielen C, Vrijenhoek EJ, Flash T, Neggers S: Arm position constraints during pointing and reaching in 3-D space. *J Neurophysiol* 1997, 78:660-673.

Goodwin AW, Jenmalm P, Johansson RS (1998) Control of grip force when tilting objects: effect of curvature of grasped surfaces and applied tangential torque. *J Neurosci* 18:10724–10734.

Gordon, A. M., P. E. Ingvarsson, and H. Forssberg. 1997. Anticipatory control of manipulative forces in Parkinson's disease. *Exp. Neurol.* 145: 477–488.

Gottschalk L.A., Serota H.M., Goldzieher Roman, K., Handwriting in rheumatoid arthritics, 1949, XI(6): 354-360.

Grea H, Desmurget M: Prablanc C: Postural invariance in threedimensional reaching and grasping movements. *Exp Brain Res* 2000, 134:155-162.

Greve D, Grossberg S, Guenther F, Bullock D, 1992, Neural representations for sensory-motor control. I Head-centered 3-D target positions from opponent eye commands. *Acta Psychol* 82: 115-138.

Gross C.M., Llod J.D., Tabler R.E., 1996, Ergonomic evaluation of five writing instruments, Center for product ergonomics, College of public health, University of South Florida.

Harris T.L., Rarick G.L., 1959, The relation between handwriting pressure and legibility in children and adults. *Journal of experimental education* 26: 151-178.

Herrick V.E., Otto W., 1961, Pressure on point and barrel of a writing instrument, *Journal of experimental education* 30(2): 215-230.

Hogan N, Bizzi E, Mussa-Ivaldi FA, Flash T, 1987, Controlling multijoint motor behavior, *Exerc Sport Sci Rev.* 15:153-90.

Hollerbach J.M., *An oscillation theory of handwriting*, 1981. *Biological Cybernetics* 39: 139-156.

Hooke W., Park Jaebum, Shim J.K., *The forces behind the words: Development of the Kinetic Pen*, 2008, *J.Biomech* 41: 2060-2064.

- Ingvarsson PE, Gordon AM and Forssberg H, 1997, Coordination of manipulative forces in Parkinson's disease. *Exp.Neurol.* 145: 489–501.
- Jankovic, J. Kapadia A.S., Functional decline in Parkinson disease, 2001. *Arch. Neurol.* 58 (10): 1611-1615.
- Jayadevan R., Kolhe S.R., Pradeep M. P., 2009, Dynamic Time Warping Based Static Hand Printed Signature Verification, *Journal of Pattern Recognition Research* 1: 52-65
- Jenhalm P, Goodwin AW and Johansson RS, 1998, Control of grasp stability when humans lift objects with different surface curvatures. *J Neurophysiol* 79: 1643–1652.
- Jenmalm and Johansson RS, 1997, Visual and somatosensory information about object shape control manipulative finger tip forces. *J Neurosci* 17: 4486–4499.
- Jenhalm P, Dahlstedt S, Johansson RS, 2000, Visual and tactile information about object-curvature control fingertip forces and grasp kinematics in human dexterous Manipulation, *Journal Neurophysiology* 84: 2984-2997,
- Johansson RS (1996) Sensory control of dexterous manipulation in humans. In: *Hand and brain: the neurophysiology and psychology of hand movements.* (Wing AM, Haggard P, Flanagan JR, eds), pp 381–414. San Diego: Academic.
- Johansson RS, 1998, Sensory input and control of grip. In: *Sensory guidance of movement.* Novartis Foundation symposium 218, pp 45-59, Chichester, UK, Wiley.
- Johansson RS, Cole KJ, 1992a, Sensory-motor coordination during grasping and manipulative actions. *Curr Opin Neurobiol* 2:815–823.
- Johansson RS, Cole KJ (1994) Grasp stability during manipulative actions. *Can J Physiol Pharmacol* 72:511–524.

Johansson RS, Westling G, 1984a, Roles of glabrous skin receptors and sensorimotor memory in automatic control of precision grip when lifting rougher or more slippery objects. *Exp Brain Res* 56:550–564.

Johansson RS and Westling G, 1987, Signals in tactile afferents from the fingers eliciting adaptive motor responses during precision grip, *Exp Brain Res* 66:141-154.

Johansson RS, Westling G, 1988a, Coordinated isometric muscle commands adequately and erroneously programmed for the weight during lifting task with precision grip. *Exp Brain Res* 71:59–71.

Johansson RS, Westling G, 1988b, Programmed and triggered actions to rapid load changes during precision grip. *Exp Brain Res* 71:72–86.

Johansson RS, Riso R, Häger C, Bäckström L. Somatosensory control of precision grip during unpredictable pulling loads. I. Changes in load force amplitude. *Experimental Brain Research*. 1992c; 89:181–191.

Johansson RS, Häger-Ross C, Riso R, 1992b, Somatosensory control of precision grip during unpredictable pulling loads. II. Changes in load force rate. *Exp Brain Res* 89:192–203.

Johansson RS, Häger-Ross C, Bäckstrom L, 1992c, Somatosensory Control of precision grip during unpredictable pulling loads. III. Impairments during digital anesthesia. *Exp Brain Res* 89:204–213.

Johansson RS, Lemon RN, Westling G (1994) Time-varying enhancement of human cortical excitability mediated by cutaneous inputs during precision grip. *J Physiol (Lond)* 481:761–775.

Johansson RS, Bäcklin JL, Burstedt MK (1999) Control of grasp stability during pronation and supination movements. *Exp Brain Res* 128:20–30

Keele, S.W., 1981. Behavioral analysis of movement. In: Brooks V.B. (Ed.), Handbook of Physiology, Section I. The Nervous System, Vol. II. Motor Control, Pt. 2 American Physiological Society, Baltimore, pp. 1391±1414.

Keele, S.W., Summers, J.J., 1976. The structure of motor programs. In: Stelmach, G.E. (Ed.), Motor, Control: Issues and Trends. Academic Press, New York: pp. 109±141.

Kimber TE, Brophy BP, Thompson PD, 1998, An update on Parkinson's disease, Modern Medicine of Australia, September, pp. 21-31.

Kinoshita H, Bäckström L, Flanagan JR, Johansson RS, 1997, Tangential torque effects on the control of grip force when holding objects with precision grip, Journal of Neurophysiology 78: 1619-1630.

Klein Breteler MD, Meulenbroek RGJ, Gielen SCAM, 1998, Geometric features of workspace and joint-space paths of 3D reaching movements, Acta Psychologica 100:37-53.

Kraus P.H., Lemke M.R., Reichmann H., *Kinetic tremor in Parkinson's Disease - an underrated symptom*, J.Neural Transm, 2006.

Kunesch E., Binkofski F., Freund H.J., 1989, Invariant temporal characteristics of manipulative hand movements. Exp.Brain. Research 78: 539-546.

Lacquaniti F, Terzuolo C., Viviani, P. 1983, The law relating the kinematic and figural aspects of drawing movements. Acta Psychol. 54: 115-130.

Lacquaniti F, Ferrigno G, Pedotti A, Soechting JP & Terzuolo C., 1987, Changes in spatial scale in drawing and handwriting: kinematic contributions by proximal and distal joints. Journal of Neuroscience 7(3):819-828.

Lance JW, Schwab RS, Peterson EA. Action tremor and the cogwheel phenomenon in Parkinson's disease. Brain 1963;86:95±110.

- Lashley, K.S., 1951. The problem of serial order in behavior. In: Je.ress, L.A. (Ed.), Cerebral mechanisms in behavior, Wiley, New York, pp. 122±137.
- Latash ML, 1996, How does our brain make its choices? In: Latash ML & Turvey MT (Eds.), Dexterity and its development, pp.277-304, Mahwah NJ: Erlbaum Publisher.
- Latash M.L., Scholz J.P., Schoener G., Motor control strategies revealed in the structure of motor variability. Exerc. Sport Sci.Rev., Vol 30 (1), pp 26-31, 2002
- Latash ML, Danion F, Scholtz JF, Zatsiorsky VM, Schöner G., 2003, Approaches to analysis of handwriting as a task of coordinating a redundant motor system, Human Movement Science 22: 153-171.
- Lipsitz LA, Goldberger AL. Loss of 'complexity' and aging: potential applications of fractals and chaos theory to senescence. J Am Med Assoc 1992;267:1806±1809.
- Liu X., Aziz T.Z., Niall R.C., Rowe J., Alusi S.H., Bain P.G., Stein J.F., 2000, Frequency analysis of involuntary movements during wrist tracking: a way to identify ms patients with tremor who benefit from thalamotomy. Stereotact. Funct. Neurosurg. 74 (2000) 53-62.
- Liu X., Miall R.C., Aziz T.Z., Palace J.A., Stein J.F., 1999, Distal versus proximal arm tremor in multiple sclerosis assessed by visually guided tracking tasks. J. Neurosci. Methods 90 (1999) 157-169.
- Luo Z.P., Berglund L.J., An K.N., 1998, Validation of F-scan pressure sensor system: a technical note. J Rehab.Res.Devel. 35: 186-191.
- Martini F.H., Ober W.C., Garrison C.W., Welch K., Hutchings R.T., Fundamentals of anatomy and physiology, 2001, Prentice Hall, Fifth edition, Chapter 9: Articulations, p.265.

Macefield VG, Häger-Ross C and Johansson RS, 1996, Control of grip force during restraint of an object held between finger and thumb: responses of cutaneous afferents from the digits. *Exp. Brain Res.* 108: 155–171.

Merton P.A., 1972, How we control the contraction of our muscles, *Scientific American* 226: 30-37.

Meulenbroek R.G.J., Rosenbaum D.A., Thomassen A.J., Schomaker L.R., Limb-segment selection in drawing behaviour, *Exp. Psychol.* 46A (1993) 273-299.

Meulenbroek RGJ, Thomassen JWM, Van Lieshout PHHM, Swinnen SP, 1998, The stability of pen-joint and interjoint coordination in loop writing, *Acta Psychologica* 100: 55-70.

Modugno N., Nakamura Y., Bestmann S., Curra A., Berardelli A., Rothwell J., Neurophysiological investigations in patients with primary writing tremor, 2002. *Mov Disord.* 2002 17(6): 1336-1340.

Morasso P, 1981, Spatial control of arm movements, *Exp. Brain Res* 42:223-227.

Morin E.L., Bryant J.T., Reid S.A., Whiteside R.A., 2000, Calibration issues of Tekscan system for human pressure assessment. Paper presented at the RTO HFM Specialists Meeting on Soldier Mobility: Innovations in load carriage system design and evaluation, Held in Kingston, Canada 27-29 June 200 and published in RTO MP-056.

Morosso P, 1986, Trajectory formation. In.: Morasso P, Tagliasco V (eds), *Human movement understanding*, North-Holland, Amsterdam.

Morosso P, Mussa-Ivaldi FA 1982, Trajectory formation and handwriting: a computational model. *Biol Cybern* 45:131-142.

Morosso P, Mussa-Ivaldi FA, Ruggiero C, 1983, How a discontinuous mechanism can produce a continuous pattern in trajectory formation and handwriting. *Acta Psychol.* 54: 83-98.

Muller, F., and Abbs J.H., 1990, *Precision grip in Parkinsonian patients. Adv. Neurol.* 53: 191–195.

Mussa Ivaldi, FA, Morasso P, Zaccaria R, 1989, Kinematic networks, A distributed model for representing and regularising motor redundancy, *Biological Cybernetics*, 60: 1-16.

Nakazawa N, Ikeura R and Inooka H, 2000, Characteristics of human fingertips in the shearing direction. *Biol Cybern* 82: 207–214.

Nicolopoulos C.S., Anderson E.G., Solomonidis S.E., Giannoudis P.V., 2000, Evaluation of the gait analysis FSCAN pressure system: clinical tool or toy? *The foot* 10: 124-130.

Ohki Y, Edin BB, Johansson RS, Predictions specify reactive control of individual digits in manipulation, *J Neuroscience*, January 15, 2002, 22(2):600–610

Ohki et al. • Object Behavior and Reactive Finger Response *J. Neurosci.*, January 15, 2002, 22(2):600–610 609

Panicker J.N., Pal P.K., 2003, Clinical features, assessment and treatment of essential tremor, *Journal Assoc Physicians India* 51: 276-279.

Pawluk DT and Howe RD, 1999, Dynamic lumped element response of the human fingerpad. *J Biomech Eng* 121: 178–183.

Pincus SM, Goldberger AL. *Physiological time-series analysis: what does regularity quantify?* *Am J Physiol* 1994;266:H1643±H1656.

Pincus SM. *Approximate entropy as a measure of system complexity.* *Proc Natl Acad Sci USA* 1991;88:2297±2301.

Plamondon R, 1989, Handwriting control:a functional model, In: Cotterill RMJ (ed), *Models of brain function.* University Press, Cambridge.

- Plamondon R, 1992, A model-based segmentation framework for computer processing of handwriting. Proceedings of the 11th International Conference on Pattern Recognition, IEEE Computer Society Press, Los Alamitos, California, pp. 303-307.
- Plamondon R, Guerfali W, 1998, The 2/3 power law: When and why?, *Acta psychologica* 100: 85:96.
- Pollak P, Benabid AL, Krack P, Deep brain stimulation. In: Jankovich J, Tolosa E, eds. *Parkinson's Disease and Movement Disorders*. 3rd ed. Baltimore, Md: Williams & Wilkins; 1998:1085-1101.
- Raibert M.H., 1977, Motor control and learning by the state-space model, Technical Report AI-M-351, Massachusetts Institute of Technology, NTIS AD-A026-960.
- Rearick MP and Santello M, 2002, Force synergies for multifingered grasping: Effect of predictability in object center of mass and handedness. *Exp. Brain Res.* 144: 38–49.
- Reilmann, R., A. M. Gordon, and H. Henningsen. 2001. Initiation and development of fingertip forces during whole-hand grasping. *Exp. Brain Res.* 140: 443–452.
- Sara Rosenblum, Patrice L. Weiss and Shula Parush, 2004, Handwriting evaluation for developmental dysgraphia: Process versus product, *Reading and Writing*, 2004, 17(5), 433-458.
- Rudzińska M., Izvorski A., Banaszkiwicz K., Bukowczan, Marona M., Szczudlik A., Quantitative tremor measurement with computerized analysis of spiral drawing *Neurologia i Neurochirurgia Polska* 2007 (41), 6: 510-516.
- Sang-Wook L., Zhang X., 2005, Development and evaluation of an optimization-based model for power-grip posture prediction. *J. Biomech.*38:1591-1597.

Sanguineti V, 1998, Can non-linear muscle dynamics explain the smoothness of handwriting movements?., *Acta Psychologica*, (100) pp.154-159.

Santello M and Soechting JF 2000, Force synergies for Multi-fingered grasping, *Exp. Brain Res.* 133: 457–467.

Serian ER, Mockensturm E, Mote CD JR, and Rempel D, 1998, A structural model of the forced compression of the fingertip pulp. *J Biomech* 31: 639–646, 1998.

Saunders-Pullman S., Derby C., Stanly K., Floyd A., Bressman S., Lipton R., Deligtisch A., Severt L., Yu Q., Kurtis M., Pullman S., Validity of spiral analysis in early Parkinso's Disease, *Mov.Disorder* 23(4): 531-537, 2008.

Schillings JJ, Meulenbroek GJ, Thomassen AJWM, Functional properties of graphic workspace: assessment by means of a 3D geometric arm model, 1998, *Acta Psychologica* 100: 97-115.

Schmidt R., Disselhorst-Klug C., Silny J., Rau G., 1999, A marker-based measurement procedure for unconstrained wrist and elbow motions. *Journal biomechanics* 32: 615-621.

Schomaker, L.R.B., & Van Galen G.P.(1996). *Computer modeling of handwriting*. In A.F.J. Dijkstra, & K.J.M.J. De Smedt (Eds.), *Computational psycholinguistics: AI and connectionist models of human language processing* (pp. 386-420). London: Taylor & Francis.

Schomaker L, Thomassen A., Teulings HL, 1989, A computational model of cursive handwriting. In: Plamondon R, Suen CY, Simner ML (eds), *Computer recognition and human production of handwriting*. World Scientific, Singapore, pp. 153-177.

Serina ER, Mote CD JR, and Rempel D, 1997, Force response of the fingertip pulp to repeated compression-effects of loading rate, loading angle and anthropometry. *J Biomech* 30: 1035–1040.

Siebner H.R., Limmer C., Peinemann A., Bartenstein P., Drzezga A., Conrad B., Brain correlates of fast and slow handwriting in humans: A PET-performance correlation analysis. *European Journal of Neuroscience* 14: 726-736,

Sharp J.T., Wolfe F., Mitchell D.M., Bloch D.A., The progression of erosion and joint space narrowing scores in rheumatoid arthritis during the first twenty-five years of disease, 1991. *Arthritis Rheum* 34:660-668.

Sih B.L., 2001, Modeling for military operational medicine scientific and technical objectives (improving accuracy of the F-scan sensor. Final report Contract no. DAMD17-00-1-0031. JAYCOR, San Diego, CA.

Soechting J, Buneo C, Hermann U, Flanders M: Moving effortlessly in three dimensions: does Donders' law apply to arm movement? *J Neurosci* 1995,15:6271-6280.

Srinivasan MA, Surface deflection of primate fingertip under line load, *J Biomech* 20: 343–349, 1989.

Srinivasan MA and Dandekar K, 1996, An investigation of the mechanics of tactile sense using two-dimensional models of the primate fingertip, *J Biomech Eng* 118: 48–55.

Stelmach, G. E., and U. Castiello. 1992. Functional force control in Parkinson's patients. In *Tutorials of Motor Behavior* (G. E. Stelmach and J. Requin, Eds.), pp. 401–423. Elsevier, Amsterdam.

Stroeve S, 1998, Neuromuscular control model of the arm including feedback and feedforward components, *Acta Psychol (Amst)*, 100(1-2):117-31.

Teulings HL, Thomassen A, Galen GP van, 1986, Invariant handwriting: the information contained in a motor program. In: Kao HS, Galen GP van, Hoosain R (eds), *Graphonomics contemporary research in handwriting*. Elsevier, Amsterdam, pp 305-315.

Teulings HL, Schomaker LRB, 1993, Invariant properties between stroke features in handwriting, *Acta Psychologica* 82: 69-88.

Teulings, H-L., J. L. Contreras-Vidal, G. E. Stelmach, and C. H. Adler. 1997. Parkinsonism reduces coordination of fingers, wrist, and arm fine motor control. *Exp. Neurol.* 146: 159–170.

Thomassen, AJWM, Meulenbroek, RGJ, 1993. Effects of manipulating horizontal progression in handwriting, *Acta Psychologica* 82, 329-352.

Thomassen AJWM, Meulenbroek RGJ, 1998, low-frequency periodicity in the coordination of progressive handwriting, *Acta Psychologica* 100:133-144.

Thomassen AJW, Schomaker L.R.B., 1986. Between-letter context effects in handwriting trajectories. In: Kao HSR, Van Galen GP, Hoosain R (eds.), *Graphonomics: Contemporary research in handwriting*, Elsevier Amsterdam, pp. 253±272.

Thomassen AJWM, Teulings HL, 1985, Time, size and shape in handwriting: Exploring spatiotemporal relationships at different levels. In: Michon JA, Jackson JL (Eds.), *Time, mind and behavior*, Springer, Berlin, pp. 253±263.

Turvey MT, 1990, Coordination, *American psychology*, 45: 938-953.

Vaillancourt, D. E., and K. M. Newell. 2000. *The dynamics of resting and postural tremor in Parkinson's disease*. *Clin Neurophysiol* 2000b;111:2042±2052.

Vaillancourt, D. E., A. B. Slifkin, and K. M. Newell. 2001. Regularity of force tremor in Parkinson's disease. *Clin. Neurophysiol.*

Valero-Cuevas, *Muscle coordination of the human index finger*, 1997. PhD dissertation Stanford University, p.35.

- Van Den Heuvel C, Van Galen GP, Teulings HL, Van Gemmert AWA, 1998, Axial pen force increases with processing demands in handwriting, *Acta Psychologica* 100 (1/2): 145-160.
- Van der Horst-Bruinsma I.E., Speyer I., Visser H., Breedveld F.C., Hazes J.M.W., Diagnosis and course of early-onset arthritis: results of a special early arthritis clinic compared to routine patient care, 1998. *British Journal of Rheumatology* 37:1084-108.
- Van Galen G.P., 1990, Phonological and motoric demands in handwriting: evidence for discrete transmission of information, *Acta Psychologica* 74: 259-275
- Van Galen, G.P., 1991. Handwriting: Issues for a psychomotor theory. *Human Movement Science* 10, 165-191.
- Van Galen, G. P., Portier, S. J., Smits- Engelsman, B. C. M., & Shoemaker, L. R. B., 1993, Neuromotor noise and poor handwriting in children. *Acta Psychologica* 82, 161-178.
- Van Galen G.P., Morasso P.G., 1998, Neuromotor control in handwriting and drawing: introduction and overview, *Acta Psych.* 100:1-7.
- Van Galen GP, Weber JF, On-line size control in handwriting demonstrates the continuous nature of motor programs, 1998, *Acta Psychologica* 100: 195-216.
- Van Gemmert A.W., Teulings H.L., Stelmach G.E., The influence of mental and motor load on handwriting movements in Parkinsonian patients, 1998. *Acta psych* 100: 161-175.
- Van Gemmert A.W., Teulings H.L., Contreras-Vidal J.L., Stelmach G.E., Parkinson's disease and the control of size and speed in handwriting, 1999. *Neuropsychologia* 37 (6): 685-694.
- Van Sommers P., 1984, *Drawing and cognition: descriptive and experimental studies of graphic production processes*. Cambridge: University Press.

Vinter A., Gras P., Spatial features of angular drawing movements in Parkinson's disease patients, 1998, *Acta Psych* 100: 177-193.

Walton J., Handwriting changes due to aging and Parkinson's syndrome, 1997. *Forensic Science International* 88: 197-214.

Wang S., Bain P.G., Aziz T.Z., Liu X., The direction of oscillation in spiral drawings can be used to differentiate distal and proximal arm tremor, 2005. *Neuroscience Letters* 384: 188-192.

Wing AM, 1980, The height of handwriting, *Acta Psychologica*, 46: 141-151.

Wing AM (1996) Anticipatory control of grip force in rapid arm movements. In: *Hand and brain: neurophysiology and psychology of hand movement* (Wing AM, Haggard P, Flanagan JR, eds), pp 301–324. San Diego: Academic.

Wing AM, Lederman SJ (1998) Anticipating load torques produced by voluntary movements. *J Exp Psychol Hum Percept Perform* 24:1571–1581.

Winnstein CJ, Merians AS, Sullivan KJ, 1999, Motor learning after unilateral brain damage. *Neurophysiologica* 37: 975-987.

Wright CE, 1990, Generalised motor programs: Reexamining claims of effector independence in writing. In: Jeannerod M (Ed.), *Attention and Performance XIII: Motor Representation and control*. LEA Hillsdale, NJ, pp. 294±320.

Wright CE, 1993, Evaluating the special role of time in the control of handwriting, *Acta Psychologica* 82: 5-52.

Woodburn J., Helliwell P.S., 1996, Observations on the FSCAN in-shoe pressure measuring system, *In-Vivo Pressure Measurement: Scientific, Commercial and Clinical Aspects Seminar*, Crewe & Alsager faculty, 3-4 April, Manchester UK.

Wu GE, Frans C.T., Veeger H.E.J., Makhsous M., Van Roy P., Anglin C, Nagels J., Karduna A.R., McQuade K., Wang X., Werner F.W., Buchholz B., 2005, ISB recommendation on definition of joint coordinate system of various joints for the reporting of human joint motion - Part II: shoulder, elbow, wrist and hand. *Journ Biomech* 38: 981-992.

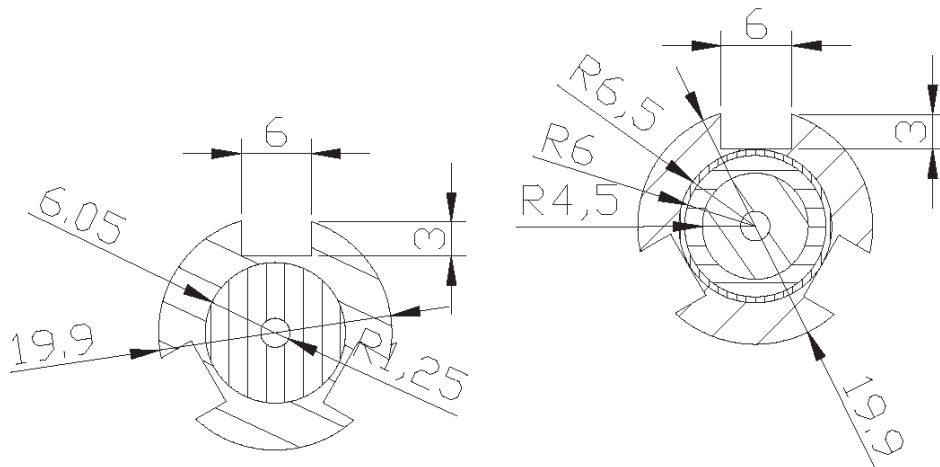
Zatskiorsky VM, 1999, *Kinematics of Human Movement*. Champaign, IL: Human Kinematics.

Zhang X., Sang-Wook L., Braido P., 2003, Determining finger segmental centers of rotation in flexion-extension based on surface marker measurement. *J.Biomech.* 36: 1097-1102.

Zirh A., Reich S.G., Dougherty P.M., Lenz F.A., 1999, Stereotactic thalamotomy in the treatment of essential tremor of the upper extremity: reassessment including a blinded measure of outcome, *Journal of Neurology/Neurosurgery/Physiatry* 66: 772-775

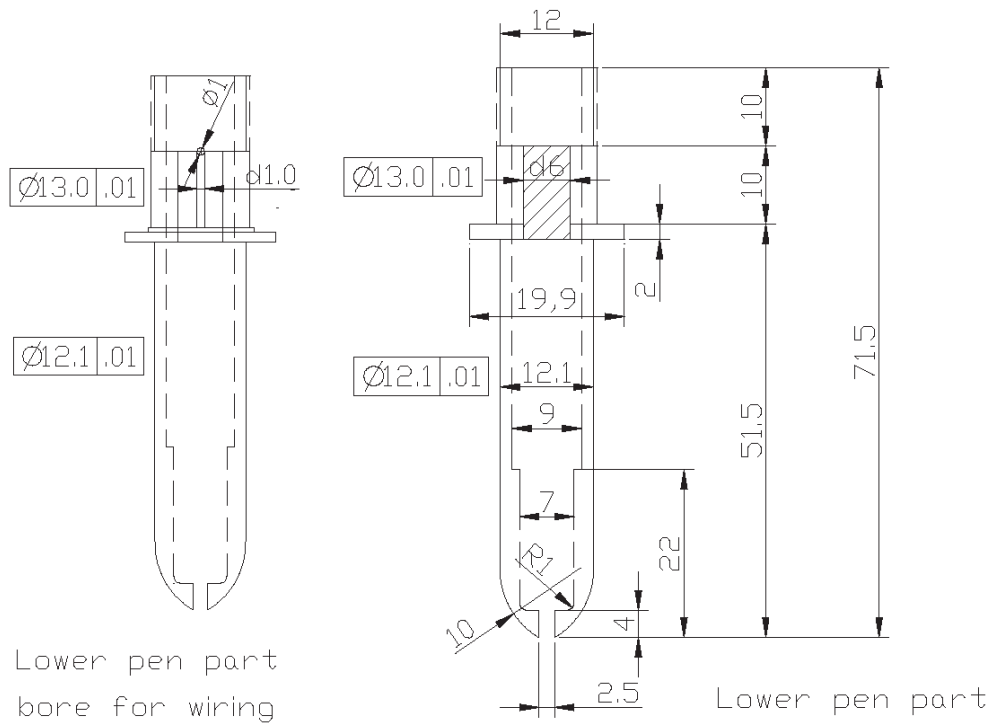
Zhou Z., Cai P., 2008, Weighing axle weight of moving vehicle based on empirical mode decomposition, *J Shanghai Univ (Engl Ed)* 12(1): 76–79

## Appendix 1A Design drawings of lower pen half



Bottom view  
lower pen part

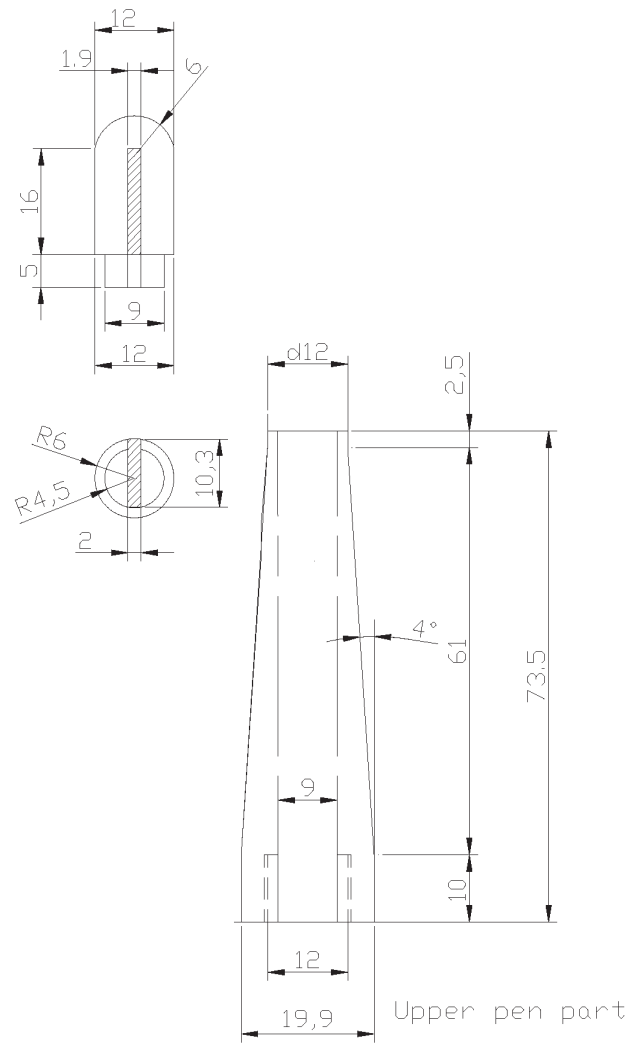
Top view  
lower pen part



Lower pen part  
bore for wiring

Lower pen part

# Appendix 1B Design drawings of upper pen part



## Appendix 2A Properties HE30 (AlSi1MgMn)

27 Jan. 2006 12:22

Al-Cu AND AL-Si IN ALLOYS

Ver. 920

85-2: 1994

**Table 29. Alloy EN AW-6082 (AlSi1MgMn)**

Temper	Specified thickness		$R_{p0.2}$		$R_{m0.2}$		Elongation, min.		Bend Radii <sup>1)</sup>		Hardness HB <sup>3)</sup>	
	mm		MPa		MPa		%					
	over	up to	min.	max.	min.	max.	$A_{50 \text{ mm}}$	A	180°	90°		
O	≥ 0,4	1,5		150		85	14			1,0r	0,5r	40
	1,5	3,0		150		85	15			1,0r	1,0r	40
	3,0	6,0		150		85	15				1,5r	40
	6,0	12,5		150		85	17				2,5r	40
	12,5	25,0		155				15				40
T4	≥ 0,4	1,5	205		110		12			3,0r	1,5r	58
T451	1,5	3,0	205		110		14			3,0r	2,0r	58
	3,0	6,0	205		110		15				3,0r	58
	6,0	12,5	205		110		14				4,0r	58
T451	12,5	40,0	205		110			13				58
	40,0	80,0	205		110			12				58
T42	≥ 0,4	1,5	205		95		12			1,5r		67
	1,5	3,0	205		95		14			2,0r		67
	3,0	6,0	205		95		16			3,0r		67
	6,0	12,5	205		95		14			4,0r		67
	12,5	40,0	205		95			13				67
	40,0	80,0	205		95			12				67
T6	≥ 0,4	1,5	310		260		6			2,5r		94
	1,5	3,0	310		260		7			3,5r		94
	3,0	6,0	310		260		10			4,5r		94
	6,0	12,5	300		255		9			5,0r		91
	T651	12,5	60,0	295		240			8			
60,0		100,0	295		240			7				89
100,0		150,0	275		240			6				84
150,0		175,0	275		230			4				83
T61	≥ 0,4	1,5	280		205		10			2,0r		82
	1,5	3,0	280		205		11			2,5r		82
	3,0	6,0	280		205		11			4,0r		82
	6,0	12,5	280		205		13			5,0r		82
T6151	12,5	60,0	275		200			12				81
	60,0	100,0	275		200			10				81
	100,0	150,0	275		200			9				81
	150,0	175,0	275		200			8				81

<sup>1)</sup> For information only.

<sup>2)</sup> Appreciably smaller cold bend radii can be achieved immediately after solution heat-treatment.

## Appendix 2B Tensile test HE30 (AlSi1MgMn) T6

A tensile test was carried out to obtain stress-strain curves to check the material properties supplied by the manufacturer. The stress-strain curves reveal the linear elastic range in which Hooke's law yields: where there will be a linear relation between stress and strain. The end of the elastic range should be at  $\sigma \geq 260 \text{ Mpa}$  and above that plastic deformation will set in.

### Test

A total of 8 specimens were tested. From the original material used to machine the transducer beams, 4 specimens could be machined with a diameter  $d=3\text{mm}$  (Fig.1a). From another rod from the same supplier, 2 specimens according to the European Standard EN 10 002-1 for tensile testing of metallic materials were machined (Fig.1b) with a diameter  $d=5\text{mm}$ . From this rod 2 specimens were also machined that had the same size ( $d=3\text{mm}$ ) as the 4 specimens of the original beam material (Fig.1b).

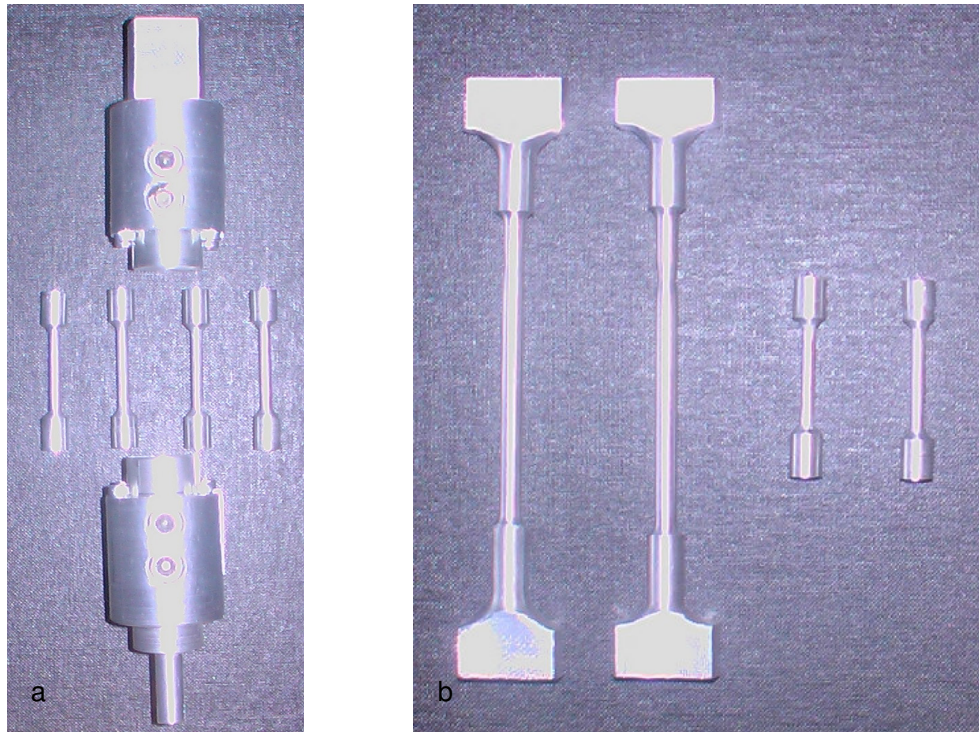


Fig 1: Tensile test specimen:

1a: Specimens beam material (4x) with  $d=3\text{mm}$  and collets;

1b: Specimens (2x) according to EN 10 002-1 with  $d=5\text{mm}$  and specimens (2x) with  $d=3\text{mm}$ .

In order to mount the small specimens with  $d=3\text{mm}$  in the testing machine, collets were designed that could be clamped in the testing machine (Fig.1a).

### Results

The test results can be found in Fig.2 and Fig.3 for respectively the material from which the transducer beams were machined and the new material. From Fig.3 linear elastic behaviour can be seen up to stresses of  $\sigma=250\text{Mpa}$  for specimen 2 and for the other specimens the linear elastic range extends up to  $\sigma=300\text{Mpa}$ .

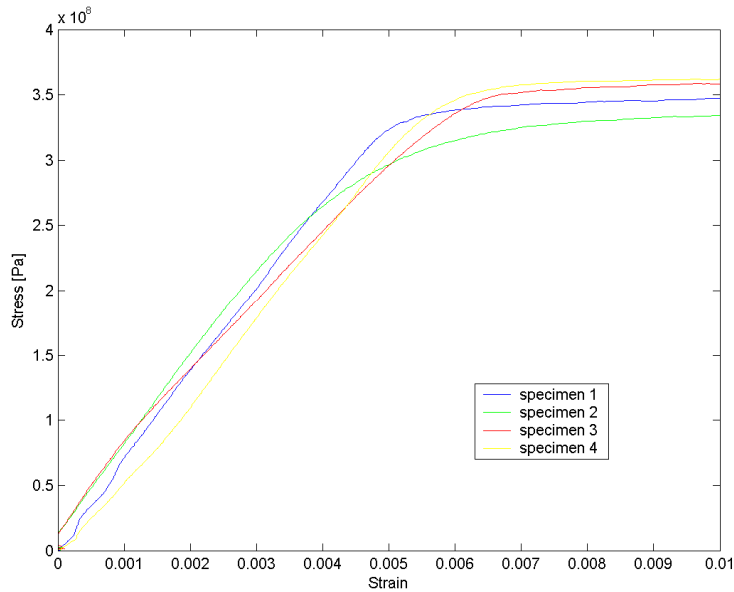
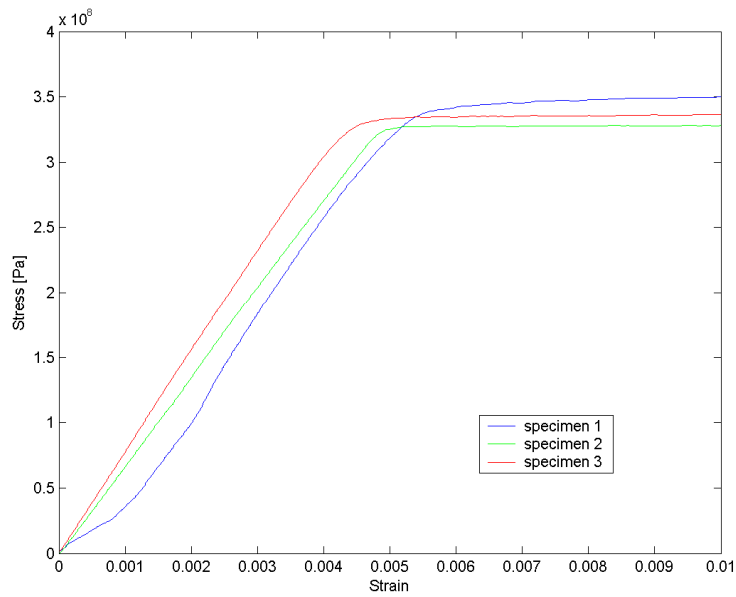


Fig.2: Stress-strain curve for specimens of beam material.

The stress-strain curves of the specimens 1 and 2 (designed according to European Standard EN 10 002-1) show linear elastic behaviour of the material well over stresses of  $\sigma=300\text{Mpa}$ .

Specimen 3 in Fig.3 shows non-linear behaviour, which is a result of setting of the test specimen in the collet and after which, it shows linear behaviour. Specimen 4 is left out for that reason.



*Fig.3: Stress-strain curve for specimens of new material.*

### **Conclusion**

For design safety calculation of the beams, a maximum allowable stress of  $\sigma=250\text{Mpa}$  and a safety margin of 30% was taken into account and therefore the beam-ring construction will never be exposed to any stress higher than 175Pa. The stress  $\sigma=175\text{Mpa}$  to which the beams are exposed is well within the linear elastic range.

## Appendix 3 Transducer beam dimensioning

The transducer beams are dimensioned based on the following requirements:

- Force measurement in range of 0-10N;
- Maximum allowable stress in transducer beams, machined from HE30 (AlSi1MgMn):  $\sigma_{\max} = 250\text{Mpa}$  (specified by supplier Richard Austin and Tensile test carried out, see appendix 2A );
- Maximum strain to avoid aging of strain gauges (Hannah R.L., Reed S.E., 1992):  $\epsilon_{\max} = 1500\mu\epsilon$ .

*The maximum allowable force applicable at contact area of each beam is limited by beam deflection.*

$$\sigma = My / I = PLy / I \Rightarrow P_{\max} = \sigma_{\max} \cdot I / (y \cdot L)$$

$$L = 3.0 \cdot 10^{-2} \text{ m (for nominal point of contact)}$$

$$y = 9.0 \cdot 10^{-4} \text{ m}$$

$$I = 1/12 \cdot b \cdot h^3 = 1/12 \cdot (0.05 \cdot 10^{-3}) \cdot (1.8 \cdot 10^{-3})^3 = 2.43 \cdot 10^{-12}$$

$$\Rightarrow P_{\max} = 22.5\text{N};$$

$$\text{introducing safeting margin of 30\%} \Rightarrow P_{\text{allowable}} = 15.8\text{N}$$

*The maximum allowable beam deflection is limited by strain in gauges.*

The construction of POM pen and aluminium ring-beam-piece are dimensioned so that the pen shaft limits the beam deflection to  $\delta_{\max} = 0.46\text{mm}$  when a force of  $P = 10\text{N}$  is applied. The maximum strain ( $\epsilon_{\max}$ ) for  $P = 10\text{N}$  does not exceed  $1500\mu\epsilon$ . Seldomly, it might occur that a subject would handle the transducer so that force is applied at the outermost edge of the beams, which is 5mm further from the nominal point of contact. In such a case, the stress might equal  $1540\mu\epsilon$  with a force application of 10N. This rare occasion, will not decrease the lifetime of the gauges.

# Appendix 4 MC SILI-E 0.15 wire specifications



Multi-Contact

---

**Litzenleitungen mit dünnwandiger Isolierung**

**Silivolt®-E**

Höchst flexible, basisisolierte Litzenleitung. Feinstrährtige, sauerstofffreie Cu-Litze, blankweich, kurzschlagverseilt. Typen ... SN mit verzinneten Drähtchen.

**Multistrand Wires with Thin-Walled Insulation**

Highly flexible base-insulated stranded wire. Super-fine wire, oxygen-free Cu strand, bright-soft, tightly twisted. Typen ... SN with tinned wire strands.

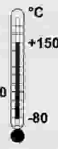
**Câbles multi-brins à isolation simple**

Câble extra-souple à isolation simple. Brins de cuivre électrolytique très fins, à pas de câblage court. Modèles ... SN avec des brins étamés.



**Silicon Silicone** Seite Page 25



- ☞ bis +300°C kurzzeitig (LötKolbenberührung) up to +300°C temporarily (Contact with soldering iron) jusqu'à +300°C (momentanément, contact du fer à souder)
- ☞ bis +250°C mehrstündig up to +250°C for several hours jusqu'à +250°C (pendant plusieurs heures)
- ☞ AWM 3525  Nicht verzinnnte Typen bis +60°C UL-approbiert als Messlitze Non-tinned types up to +60°C UL-approved as test lead wire Modèles non étamés jusqu'à +60°C : Approuvés UL en tant que câbles pour cordons de mesure
- ☞ AWM 3670  Verzinnnte Typen ...SN bis +105°C UL-approbiert als Messlitze Tinned types ...SN up to +105°C UL-approved as test lead wire Modèles étamés jusqu'à +105°C : approuvés UL en tant que câbles pour cordons de mesure

**Typische Anwendung**

Interne Verdrahtung sehr beweglicher Bauteile und Baugruppen bei thermisch hoher Belastung. Höchst flexible Verbindungsleitungen im Laborbereich, wenn mit kleinen Spannungen gearbeitet wird.

**Typical Application**

Internal wiring of very mobile components and assemblies under high thermal stress. Super flexible connecting leads for low-voltage applications in the laboratory field.

**Applications**

Câblage intérieur de pièces ou de montages mobiles soumis à des contraintes thermiques élevées. Cordons de liaison extra-souples dans le domaine Labo (utilisation en basse tension).

Silivolt® -E	Nennquerschnitt Nominal cross section Section nominale	Litzenaufbau Strand design Composition de l'âme	Kupfergewicht Copper weight Masse de l'âme	Leiterdurchmesser Conductor diameter Diamètre sur âme	Isolierwandstärke Thickness insulation wall Épaisseur d'isolation	Aussendurchmesser Outer diameter Diamètre sur isolant	Nennspannung Nominal voltage Tension nominale	Prüfspannung Test voltage Tension d'essai	Nennstrom Nominal current Intensité nominale	UL	Standard-Farben** Standard colours** Couleurs standards**	Bestellnummer Order No. N° de Cde
SILI-E 0,15	0,15 / 26	39 x 0,07	1,4	0,50	0,25	1,0	150	2 000	6		21 - 27, 29	61.7550-*
SILI-E 0,25	0,25 / 23	66 x 0,07	2,3	0,65	0,50	1,7	300	2 000	9		21 - 27, 29	61.7551-*
SILI-E 0,50	0,50 / 20	129 x 0,07	4,5	0,90	0,70	2,3	300	2 000	10		21 - 27, 29	61.7552-*
SILI-E 0,50 SN	0,50 / 20	129 x 0,07	4,5	0,90	0,70	2,3	300	2 000	10		21 - 23	61.7532-*
SILI-E 0,75	0,75 / 18	196 x 0,07	6,9	1,25	0,70	2,7	600	2 500	15		20 - 27, 29	61.7553-*
SILI-E 1,0	1,0 / 17	259 x 0,07	9,1	1,4	0,80	3,0	600	2 500	19		20 - 27, 29	61.7554-*
SILI-E 1,0 SN	1,0 / 17	259 x 0,07	9,1	1,4	0,80	3,0	600	2 500	19		21 - 23	61.7534-*
SILI-E 1,5	1,5 / 15	392 x 0,07	14	1,7	0,85	3,4	600	2 500	24		20 - 27, 29	61.7555-*
SILI-E 2,5	2,5 / 13	651 x 0,07	24	2,4	0,75	3,9	600	2 500	32		20 - 27, 29	61.7556-*
SILI-E 2,5 SN	2,5 / 13	651 x 0,07	24	2,4	0,75	3,9	600	2 500	32		21 - 23	61.7537-*

*Code Farben Couleurs	20 grün-gelb green-yellow vert-jaune	21 schwarz black noir	22 rot red rouge	23 blau blue bleu	24 gelb yellow jaune	25 grün green vert	26 violett violet violet	27 braun brown marron	28 grau grey gris	29 weiss white blanc	30 orange orange	33 transparent transparent transparent
** Nicht aufgeführte Farben auf Anfrage   Other colours on request!   Autres couleurs sur demande!												